Strain and Tool Development
for the Production of Industrially Relevant
Compounds with *Corynebacterium glutamicum*

Inaugural dissertation

submitted to
the Faculty of Mathematics and Natural Sciences
of the Heinrich Heine University Düsseldorf

presented by

M.Sc. Maike Kortmann

born in Münster

Jülich, June 20

Results described in this dissertation have been published in the following original articles:

Kortmann, M., Kuhl, V., Klaffl, S., Bott, M. (2015) A chromosomally encoded T7 RNA polymerase-dependent gene expression system for *Corynebacterium glutamicum*: construction and comparative evaluation at the single-cell level. Microbial Biotechnology 8:253–265.[1]

Kortmann M., Mack C., Baumgart M., Bott M. (2019) Pyruvate carboxylase variants enabling improved lysine production from glucose identified by biosensor-based high-throughput fluorescence-activated cell sorting screening. ACS Synthetic Biology 8:274-281.

Kortmann, M., Baumgart, M., Bott, M. (2019) Pyruvate carboxylase from *Corynebacterium glutamicum*: purification and characterization. Applied Microbiology and Biotechnology 103:6571-6580.

List of Patent applications:

Kortmann, M., Baumgart, M., Bott, M.: Pyruvatcarboxylase und für die Pyruvatcarboxylase kodierende DNA, Plasmid enthalten die DNA, sowie Mikroorganismus zur Produktion und Verfahren zur Herstellung von Produkten, deren Biosynthese Oxalacetat als Vorstufe beinhaltet, Chromosom und Screeningverfahren. Registration Date 11.05.2017, Pub. No. WO/2018/206024, PCT/DE2018/000108.

Kortmann, M., Baumgart, M., Bott, M.: Pyruvatcarboxylase und für die Pyruvatcarboxylase kodierende DNA, Plasmid enthalten die DNA, sowie Mikroorganismus zur Produktion und Verfahren zur Herstellung von Produkten, deren Biosynthese Oxalacetat als Vorstufe beinhaltet und Chromosom. Registration Date 18.05.2017, Pub. No. WO/2018/210359, PCT/DE2018/000107.

Kortmann, M., Baumgart, M., Bott, M.: Pyruvatcarboxylase und für die Pyruvatcarboxylase kodierende DNA, Plasmid enthalten die DNA, sowie Mikroorganismus zur Produktion und Verfahren zur Herstellung von Produkten, deren Biosynthese Oxalacetat als Vorstufe beinhaltet und Chromosom. Registration Date 18.05.2017, Pub. No. WO/2018/210358, PCT/DE2018/000104.

---

[1] Some results of this publication were obtained in the master thesis of Maike Kortmann (*Entwicklung von Werkzeugen zur Überexpression von Genen in Corynebacterium,* performed at the Institute of Bio- and Geosciences, IBG-1: Biotechnology, Forschungszentrum Jülich, submitted to the Faculty of Mathematics and Natural Sciences of the University of Rostock, 2013).

Abbreviations

Δ	deletion
ACC	acetyl-CoA carboxylase
AMP	adenosine monophosphate
ADP	adenosine diphosphate
ATc	anhydrotetracycline
ATCC	American Type Culture Collection
ATP	adenosine triphosphate
a.u.	arbitrary units
BC	biotin carboxylase domain
BCCP	biotin carboxyl carrier protein
bp	base pairs
BHI	Brain Heart Infusion
CoA	coenzyme A
CT	carboxyl transferase domain
Da	Dalton
eYFP	enhanced yellow fluorescent protein
FACS	fluorescence-activated cell sorting
GFP	green fluorescent protein
GRAS	generally regarded as safe
GTP	guanosine triphosphate
HPLC	high performance liquid chromatography
IPTG	isopropyl-β-D-thiogalactopyranoside
LysC	aspartate kinase
K_i	inhibitor constant
K_m	Michaelis constant
M	molar (mol/l)
MNP	multiple nucleotide polymorphism
M_r	molecular weight
NADP(H)	nicotinamide adenine dinucleotide phosphate, oxidized/reduced
OAA	oxaloacetate
OD600	optical density at 600 nm
P	promoter
PCx	pyruvate carboxylase
PEP	phosphoenolpyruvate
PEPCx	PEP carboxylase
PPP	pentose phosphate pathway
PT	PCx tetramerization (or allosteric) domain
PTS	phosphoenolpyruvate-dependent phosphotransferase system
PYK	pyruvate kinase
RNAP	RNA polymerase
rpm	revolutions per minute
SDS	sodium dodecyl sulfate
SNP	single nucleotide polymorphism
TAT	twin arginine translocation
TCA	tricarboxylic acid
TCE	total cell extract
TF	transcription factor
TY	tryptone-yeast extract
vol/vol	volume per volume
wt	wild-type
wt/vol	weight per volume

Further abbreviations not included in this section are according to international standards, as, for example listed in the author guidelines of the *FEBS Journal.*

Content

1 Summary

1.1 Summary English

Corynebacterium glutamicum is one of the most important model organisms in white biotechnology for the industrial production of numerous amino acids, most notably L-glutamate and L-lysine, but also of other metabolites and proteins. In order to further expand possible applications of this organism for the conversion of renewable feedstocks into industrially relevant compounds, two different approaches of strain engineering of *C. glutamicum* were addressed in the present thesis.

In the first part of this work, a new expression system based on a chromosomally encoded T7 RNA polymerase and a plasmid-based T7 promoter was established and characterized in *C. glutamicum*. For this purpose, the T7 RNA polymerase (gene *1*) was integrated into the prophage-free strain *C. glutamicum* MB001 under the control of the IPTG-inducible *lac*UV5 promoter, resulting in strain MB001(DE3). In addition, the expression plasmids pMKEx1 and pMKEx2 were constructed into which a target gen can be cloned under control of the T7 promoter and, if necessary, can be fused to a polyhistidine-tag or a Strep-tag. The T7 expression system was evaluated with the reporter gene *eyfp* and compared to the well-established pEKEx2 system, which is based on the *tac* promotor. The basal expression of the T7 system was lower than that of the pEKEx2 system. The specific fluorescence of eYFP increased 450-fold after maximal induction of the T7 system with 250 µM IPTG and was 3.5-fold higher than the specific eYFP fluorescence obtained after maximal *eyfp* expression with the pEKEx2 system. Furthermore, it was shown that proteins such as pyruvate kinase or secretory GFP proteins can also be successfully produced in higher amounts with the T7 system than with the pEKEx2 system.

In the second part of this work, a genetically encoded biosensor for the cytoplasmic lysine concentration was used to screen for mutated variants of pyruvate carboxylase (PCx), which enabled an improved L-lysine production. PCx catalyzes the ATP-dependent carboxylation from pyruvate to oxaloacetate and plays an important role as anaplerotic enzyme. It replenishes the tricarboxylic acid cycle during growth on sugars when intermediates have been removed from the cycle by branching metabolic pathways. This reaction is for example of great importance for L-lysine production and it has already been shown that overexpression of the *pyc* gene as well as the mutation P458S in PCx lead to an increased L-lysine yield in *C. glutamicum*. In order to find further advantageous mutations for lysine production, a plasmid-based library with mutated *pyc* variants was generated in this work using error-prone PCR. Out of this library, two PCx variants could be isolated with the help of the lysine biosensor pSenLys-Spec and FACS-based high-throughput screening, which showed an increased lysine formation compared to the strain with wild-type PCx. The variants PCx$^{T343A, I1012S}$ and PCx^{T132A} enabled an increase of the lysine titer by 9% and 19%, respectively, after plasmid-based overexpression of the respective genes in the strain DM1868Δ*pyc*/pSenLys-Spec. When the mutations were introduced one by one into the genome of the lysine-producing strain DM1868, the variant PCx^{T132A} produced 7% more lysine and PCx^{T343A} 15% more lysine compared to strain DM1868 encoding wild-type PCx.

In previous studies, PCx activity of *C. glutamicum* could only be measured with permeabilized cells. For a more detailed characterization, conditions were established that enabled the measurement of PCx activity in cell-free extracts and the isolation of the enzyme in active form. For purified PCx, K_m values of 3.8 mM for pyruvate, 0.6 mM for ATP, and 13.3 mM for bicarbonate were determined. ADP and aspartate inhibited PCx activity with K_i values of 1.5 mM and 9.3 mM, respectively. Initial characterization of the variants PCx^{T132A} and PCx^{T343A} revealed that their activity was not inhibited up to aspartate concentrations of approx. 7.5 mM. The K_i values of 13.2 mM for PCx^{T132A} and 10.8 mM for PCx^{T343A} were higher than for wild-type PCx and provide an explanation for the increased lysine production obtained with these variants in *C. glutamicum*.

1.2 Summary German

Corynebacterium glutamicum ist einer der wichtigsten Modellorganismus in der Weißen Biotechnologie und wird zur industriellen Produktion zahlreicher Aminosäuren, insbesondere von L-Glutamat und L-Lysin, aber auch weiterer Metaboliten und Proteinen eingesetzt. Um die Einsatzmöglichkeiten dieses Organismus für die Umwandlung von nachwachsenden Rohstoffen in industriell relevante Verbindungen weiter auszubauen, wurden in der vorliegenden Arbeit zwei verschiedene Ansätze des *Strain Engineering* von *C. glutamicum* behandelt.

Im ersten Teil der Arbeit wurde ein neues Expressionssystem basierend auf einer chromosomal codierten T7-RNA-Polymerase und einem Plasmid-basierten T7-Promoter in *C. glutamicum* etabliert und charakterisiert. Dafür wurde das T7 RNA-Polymerase-Gen (gene *1*) unter Kontrolle des IPTG-induzierbaren *lac*UV5 Promotors in den Prophagen-freien Stamm *C. glutamicum* MB001 integriert, was im Stamm MB001(DE3) resultierte. Zusätzlich wurden die Expressionsplasmide pMKEx1 und pMKEx2 konstruiert, in die Zielgene unter Kontrolle des T7-Promoters kloniert und bei Bedarf mit einem Polyhistidin-Tag oder einem Strep-Tag fusioniert werden können. Das T7-Expressionssystem wurde zunächst mit dem Reportergen *eyfp* im Vergleich zum pEKEx2-System getestet, welches auf dem *tac* Promoter basiert. Hierbei wurde eine niedrigere Basalexpression des T7 Systems im Vergleich zum etablierten pEKEx2-System festgestellt. Die spezifische Fluoreszenz von eYFP stieg nach maximaler Induktion des T7-Systems mit 250 µM IPTG um das 450-fache und war 3,5-fach höher als die spezifische eYFP-Fluoreszenz, die nach maximaler *eyfp*-Expression mit dem pEKEx2-System erhalten wurde. Weiterhin konnte gezeigt werden, dass auch Proteine wie die Pyruvat-Kinase oder sekretorische GFP-Proteine in höheren Mengen als mit dem pEKEx2-System produziert werden können.

Im zweiten Teil dieser Arbeit wurde ein genetisch kodierter Biosensor für die cytoplasmatische Lysin-Konzentration verwendet, um nach Enzym-Varianten der Pyruvat-Carboxylase (PCx) zu screenen, die eine verbesserte L-Lysin-Produktion ermöglichen. PCx katalysiert die ATP-abhängige Carboxylierung von Pyruvat zu Oxalacetat und spielt eine wichtige Rolle als anaplerotisches Enzym. Es füllt den Tricarbonsäurezyklus während des Wachstums auf Zuckern wieder auf, wenn Zwischenprodukte durch abzweigende Stoffwechselwege aus dem Zyklus entfernt worden sind. Diese Reaktion ist z.B. für die L-Lysin-Produktion von großer Bedeutung und es konnte bereits gezeigt werden, dass eine Überexpression des *pyc*-Gens sowie die Mutation P458S in PCx zu einer erhöhten L-Lysin-Ausbeute in *C. glutamicum* führen. Um weitere vorteilhafte Mutationen für die Lysin-Produktion zu finden, wurde in dieser Arbeit eine Plasmid-basierte Bibliothek mit mutierten *pyc*-Varianten mittels Error Prone-PCR generiert. Aus dieser konnten im Anschluss mit Hilfe des Lysin-Biosensors pSenLys-Spec und FACS-basiertem Hochdurchsatz-Screening zwei PCx-Varianten isoliert werden, die eine gesteigerte Lysin-Bildung im Vergleich zum Stamm mit der Wildtyp-PCx zeigten. Die Varianten $PCx^{T343A, I1012S}$ und PCx^{T132A} ermöglichten eine Erhöhung des Lysin-Titers um 9% und 19% nach Plasmid-basierter Überexpression der entsprechenden Gene im Stamm DM1868Δ*pyc*/pSenLys-Spec. Wurden die Mutationen einzeln in das Genom des Lysin-Produzenten DM1868 eingebracht, konnte mit der Variante PCx^{T132A} 7% mehr Lysin produziert werden, mit PCx^{T343A} 15% mehr im Vergleich zum Stamm DM1868 mit Wildtyp-PCx.

In früheren Studien konnte die PCx-Aktivität von *C. glutamicum* nur mit permeabilisierten Zellen gemessen werden. Für eine detailliertere Charakterisierung wurden Bedingungen geschaffen, die die Messung der PCx-Aktivität in zellfreien Extrakten und die Isolierung des Enzyms in aktiver Form ermöglichten. Für die gereinigte PCx wurden so K_m-Werte von 3,8 mM für Pyruvat, 0,6 mM für ATP und 13,3 mM für Bicarbonat bestimmt. ADP und Aspartat hemmten die PCx-Aktivität mit K_i-Werten von 1,5 mM bzw. 9,3 mM. Eine erste Charakterisierung der Varianten PCx^{T132A} und PCx^{T343A} ergab, dass ihre Aktivitäten bis zu einer Aspartat-Konzentration von ca. 7,5 mM nicht gehemmt waren. Die K_i Werte waren mit 13,2 mM für PCx^{T132A} und 10,8 mM für PCx^{T343A} entsprechend höher und liefern damit eine erste Erklärung für die erhöhte Lysin-Produktion, die mit diesen Varianten in *C. glutamicum* erzielt wurden. Für PCx^{I1012S} konnten keine signifikanten Unterschiede der gemessenen kinetischen Parameter im Vergleich zu Wildtyp-PCx beobachtet werden.

2 Introduction

2.1 Microbial biotechnology and metabolic engineering

In times of food and resource scarcity, a fundamental change in the industry towards more environment-friendly solutions is required. Although fossil resources, in particular mineral oil, are still the most important raw materials for the chemical industry, a switch towards a sustainable biotechnology is in progress. As a consequence, the white biotechnology is presently getting more and more important to enable low-energy and low-cost production of valuable compounds by living microorganisms, which can be grown on renewable feedstocks (Becker and Wittmann, 2015; Erickson et al., 2012). Whereas in former times, microorganisms were used unconsciously in fermentation processes of food and beverage for example (Cavalieri et al., 2003; Vitorino and Bessa, 2017), nowadays they are exploited purposefully to synthesize a wide range of different products of commercial interest, like nutrients, polymers, solvents or pharmaceuticals in a stereo-, regio- and chemo-selective manner (Becker and Wittmann, 2015; Demain and Adrio, 2008). However, production by microorganisms as isolated from nature is often low and a scale-up not always meaningful due to high nutritional requirements, pathogenicity or other limitations. To overcome these limitations and to improve product titers, the performance of the producer strains has to be optimized. In former times, random mutagenesis of the whole genome followed by screening steps were often performed to isolate mutants with improved production. This approach does not require a deeper knowledge of the metabolic pathways and the regulatory processes of the production host (Nakayama et al., 1978; Pfefferle et al., 2003; Rowlands, 1984). However, it led to strains with numerous mutations of unknown function, which also could hamper growth or stress tolerance for example. With the development of recombinant DNA techniques, rational optimization of producer strains by metabolic engineering was established, which involves precise alterations of the metabolic network to improve production. For example, the supply of precursors and cofactors required for production of a certain metabolite can be increased, formation of by-products reduced or eliminated, and higher carbon fluxes into the desired biosynthesis pathways accomplished (Ikeda et al., 2006; Pickens et al., 2011; Sahm et al., 2000). Moreover, (over)expression of heterologous genes or even entire pathways from organisms which are difficult to cultivate, enable an extension of the natural product range (Becker and Wittmann, 2015; Pickens et al., 2011). Today, the most important microorganisms in white biotechnology are, inter alia, *Escherichia coli*, *Saccharomyces cerevisiae*, and *Corynebacterium glutamicum* (Becker and Wittmann, 2015; Demain and Adrio, 2008). Whereas *E. coli* and *S. cerevisiae* are used for the production of pharmaceuticals (Walsh, 2018), biofuels (Peralta-Yahya et al., 2012) or other chemicals (Jang et al., 2012), *C. glutamicum* has been mainly used for the production of L-amino acids (Wendisch et al., 2014). However, in recent years *C. glutamicum* was shown to

be an excellent production host for a wide range of other products, too. Therefore, the characteristics that make *C. glutamicum* particularly interesting for industry are described in more detail below.

2.2 *Corynebacterium glutamicum* - an industrial production workhorse

In the late 1950's, *C. glutamicum* was discovered by Kinoshita et al. due to its ability to secrete glutamate under biotin-limiting conditions (Kinoshita et al., 1957). It was characterized to be a biotin-auxotrophic, non-sporulating and facultative anaerobic bacterium (Nishimura et al., 2007; Michel et al. 2015), belonging to the phylum of Actinobacteria, which are characterized by a high GC-content and a positive gram-staining (Ventura et al., 2007). It is closely related to the human pathogenic species *Corynebacterium diphtheriae*, but also to *Mycobacterium tuberculosis* and *Mycobacterium leprae* (Gao and Gupta, 2012). Because *C. glutamicum* itself is an apathogenic organism and possesses a generally regarded as safe (GRAS) status, it is often used as a model organism for the order *Corynebacteriales*. But the main focus of research was directed on its ability to produce large amounts of different amino acids. Most notably is the production of over three million tons of L-glutamate and more than two million tons of the food additive L-lysine per year (Ajinomoto Co., 2016; Eggeling and Bott; 2015; Sanchez et al., 2018).

In order to produce these amino acids efficiently, strains were initially optimized by random mutagenesis and screening and later by metabolic engineering. A big leap forward was achieved in 2003, when the complete genome of the type strain *C. glutamicum* ATCC13032 was sequenced (Ikeda and Nakagawa, 2003; Kalinowski et al., 2003). Since then, deep knowledge of the metabolism and regulatory network of *C. glutamicum* was obtained (Becker and Wittmann, 2012) and a broad spectrum of tools for genetic and metabolic engineering developed (Baritugo et al., 2018; Kogure and Inui, 2018; Nesvera and Patek, 2011). As a result, *C. glutamicum* is today one of the most important producers of industrially relevant compounds. In addition to the above mentioned L-lysine and L-glutamate, *C. glutamicum* is also used to produce other amino acids (Wendisch et al., 2016; Stäbler et al., 2011; Vogt et al. 2014; Vogt et al. 2015), organic acids (Wieschalka et al., 2013), diamines (Nguyen et al., 2015) or alcohols (Niimi et al., 2011; Blombach et al. 2011; Siebert and Wendisch, 2015) for example. Apart from the mentioned products, the portfolio of compounds produced by *C. glutamicum* is constantly increasing.

The fact that *C. glutamicum* has become an established platform organism for the biotech industry is not least due to several advantageous properties, which appear to be suitable for the production of valuable substances. An important factor for the industry is the use of cost-

effective and renewable substrates, especially for large-scale fermentation. *C. glutamicum* already has a wide-ranging natural substrate spectrum and cultivation is possible on a huge variety of different carbon sources like D-glucose, acetate, lactate but also organic acids and alcohols (Arndt et al., 2008; Bäumchen et al., 2007; Stansen et al., 2005). Nowadays, a broad research area focuses on the extension of this substrate spectrum, taking agricultural waste streams into account (Mussatto et al., 2012). Thus, engineered *C. glutamicum* strains are now also able to grow on further interesting substrates like glycerol (Rittmann et al., 2008), xylose (Buschke et al., 2013), or cellobiose (Kotrba et al., 2003). Unlike other bacteria, *C. glutamicum* can also utilize several carbon sources simultaneously, leading to higher production rates, as the organism is able overcome possible limitations in sugar metabolism by transcriptional regulation of metabolic pathways (Blombach and Seibold, 2010; Krause et al., 2010). Another important characteristic for the successful industrial scale cultivation of *C. glutamicum* is that this organism is extremely robust against varying substrate and oxygen supply, as it is often the case in large fermenters (Käß et al. 2014) as well as its ability to grow to very high cell densities with growth rates of up to $\mu = 0.6$ h^{-1} in minimal medium with 4% (wt/vol) D-glucose (Graf et al., 2019; Unthan et al., 2014).

Besides its use as a production host of various bio-chemicals, *C. glutamicum* has been increasingly established for recombinant protein production in recent years (Lee and Kim, 2018). In this context, the great potential of the organism is not only due to the above-mentioned properties for cultivation, but it also exhibits other advantageous physiological characteristics for efficient (recombinant) protein production. One of it is its ability to efficiently secrete proteins into the extracellular medium. For this, more than 108 functional signal sequences were identified for the secretion via the Sec- or twin arginine translocation (TAT)-secretion system in *C. glutamicum* (Freudl, 2017; Watanabe et al., 2009). The production of secreted proteins has several advantages over intracellular production, such as rapid and simplified downstream processing, because the cells do not have to be disrupted for protein purification and there is a lower concentration of other proteins outside the cell. The oxidative milieu of the extracellular medium is also favorable for the formation of disulphide bonds, which are important for the correct folding and the associated stability of many proteins (Freudl, 2018). Finally, unlike many other soil bacteria *C. glutamicum* shows only a low protease activity and thus enables high product yields (Lee and Kim, 2018; Yukawa et al., 2007).

All these points make *C. glutamicum* an important organism for the industry. Nevertheless, despite the great progress in recent years, there is still the need to expand the corynebacterial toolbox e. g. with strong expression systems for a sufficient protein production.

## 2.3 Expression systems for overproduction of homologous and heterologous proteins in *C. glutamicum*

The groundwork for the use of *C. glutamicum* as a host for the expression of homologous and heterologous genes was laid by the discovery of 24 endogenous plasmids and the associated research and development of different cloning and expression strategies in this organism (Miwa et al., 1985; Santamaría et al., 1984; Tauch et al., 2003). Today, most vectors are based on the plasmids pBL1 (Santamaría et al., 1984) and pCG1 (Ozaki et al., 1984), which are both replicated via the rolling-circle mechanism (Archer and Sinskey, 1993; Fernandez-Gonzalez et al., 1994). One of the best characterized plasmids of the pCG1 family is called pGA1 (Sonnen et al., 1991). It encodes a RepA primase, which is necessary to initiate the replication of the plasmid (Lei et al., 2002), in addition, the genes *per* and *aes* were identified to be important for the replication of pGA1as well. Whereas the protein encoded by *per* has a positive influence on the copy number of the plasmid (Nesvera et al., 1997), *aes* encodes an effector, which is important for the segregational stability of the plasmid and influences the stable maintenance of the plasmid in the cell (Venkova et al., 2001).

Based on the named plasmids, heterologous gene expression was already successfully established in *C. glutamicum* (Freudl, 2017; Lee and Kim, 2018). For example, a nuclease of *Staphylococcus aureus* (Liebl et al., 1992), the protease subtilisin from *Bacillus subtilis* (Billman-Jacobe et al., 1995) or human epidermal growth factor, which was subsequently secreted into the extracellular medium, could be expressed in *C. glutamicum* (Date et al., 2006). Thereby, genes are cloned under control of a promoter derived from *E. coli* for most of these applications. A well-established expression system is the pEKEx2 plasmid (Eikmanns et al., 1991). Here, the target gene is under control of the *tac* promoter (P_{tac}), which is repressed by LacI in the absence of the inducer IPTG. The expression of *lacI* in turn is controlled by the promoter *lacI^q* (q stands here for quantity), which carries a mutation in its -35 sequence, thereby allowing a 10-fold higher expression of the *lacI* gene (Calos, 1978). Nevertheless, this system shows a relatively high basal expression of the target gene even in the absence of IPTG (Patek et al., 2003). Therefore, another plasmid-based expression system was developed for *C. glutamicum*, which is based on the TetR system (Lausberg et al., 2012). Here, the target gene is cloned under control of the tetracycline-inducible *tet* promoter (Kamionka et al., 2006). Furthermore, the repressor TetR is encoded on this plasmid as well and is constitutively expressed by the native promoter of the *gap* gene (cg1791) encoding glyceraldehyde 3-phosphate dehydrogenase from *C. glutamicum* to prevent the expression of the target gene. This system has a much lower basal expression of the target gene in comparison to pEKEx2, but its expression strength is also considerably lower (Lausberg et al., 2012). Accordingly, no expression system is available for *C. glutamicum* up till now, which enables a tight control of the basal expression in the absence of an inducer, but promotes a high expression level after induction.

2.3.1 T7 RNA polymerase-dependent gene expression systems

In 1985, a T7 RNA polymerase (T7 RNAP)-dependent gene expression system was developed by Tabor and Richardson, which enabled a controlled expression of target genes in *Escherichia coli* (Tabor and Richardson, 1985). It is based on the monomeric polymerase of bacteriophage T7, which is able to transcribe DNA about 5-times faster in comparison to the RNA polymerase from *E. coli* (Chamberlin and Ring, 1973). Because of its high activity, processivity and promoter specificity, almost all resources of the cell are used to produce the protein of interest upon induction. As a result, the target gene product can constitute up to 50% of the total protein amount in the cell (Studier and Moffatt, 1986; Tabor and Richardson, 1985). During the 1980's, the T7 system was refined by Studier und Moffatt. By placing the gene of T7 RNAP, gene *1*, under control of the *lac*UV5 promoter ($P_{lac\,UV5}$), the expression of target genes was now inducible by addition of IPTG (Studier and Moffatt, 1986). The construct was placed on the λ-lysogen DE3, which was integrated into the genome of *E. coli* BL21, resulting in strain *E. coli* BL21(DE3). Moreover, for a tight repression of the system in the absence of the inducer IPTG, a constitutively expressed *lacI* gene encoding the LacI repressor as well as the operator sequences O_1-O_3 are also located on the λ-DE3-sequence.
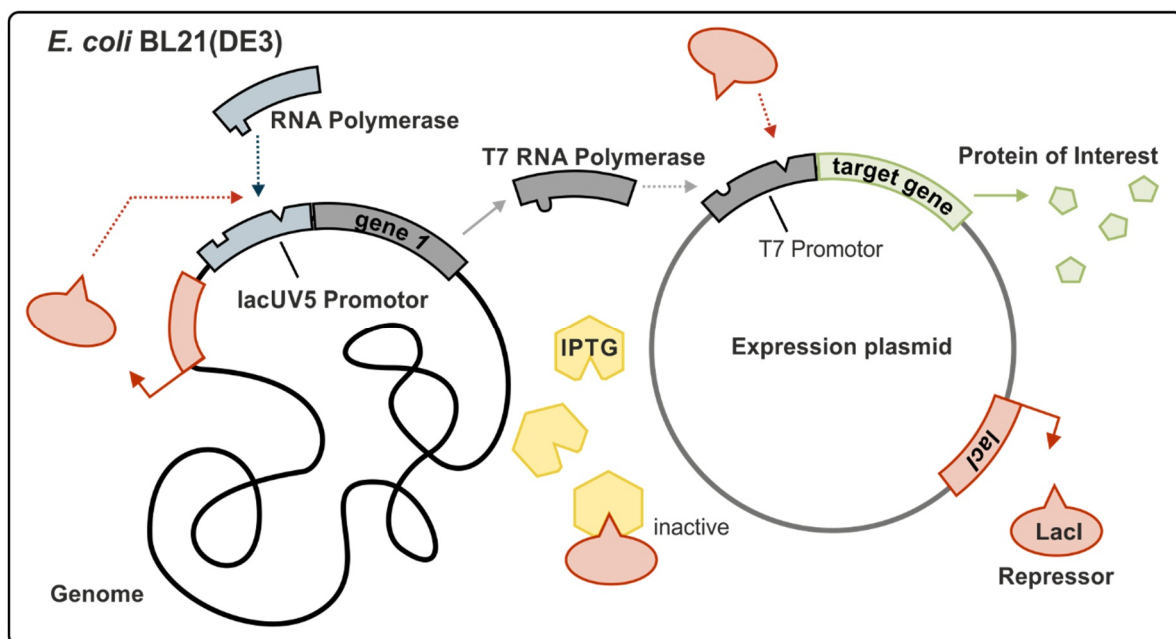
Figure 1 Schematic presentation of the T7 expression system in *E. coli* BL21(DE3). The gene of T7 RNAP, gene *1*, is chromosomally encoded under control the promoter P_{lacUV5}. If no IPTG is added to the cell, the repressor LacI, which is constitutively synthesized, binds to the operator sequence of $P_{lac\,UV5}$ and P_{T7lac}. As a consequence, the expression of gene *1* and the target gene is repressed, because no RNA polymerase can bind to the promoter sequences anymore. When IPTG is added to the cell, it binds the repressor, which in turn is not able to bind to the Lac operator sequences anymore. As a result, gene *1* is expressed by the host RNAP and the synthesized T7 RNAP binds to P_{T7} on the expression plasmid and promotes the expression of the target gene. For reasons of simplification, only one binding site of the operator is shown in the genome of *E. coli* BL21(DE3).

To be able to transcribe the target gene by T7 RNAP it has to be under control of the T7 promoter P_{T7}. This promoter does not naturally occur in *E. coli* and is highly selectively recognized by T7 RNAP only (Chamberlin and Ring, 1973). Both, P_{T7} and the target gene controlled by this promoter are located on an expression plasmid, which is transferred into *E. coli* BL21(DE3). Nevertheless, even with the chromosomal copy of *lacI* in the λ-DE3 region a low basal transcription of T7 RNAP occurs (Studier and Moffatt, 1986). Therefore, various T7-based expression plasmids, like the well-established pET vectors, harbor a constitutively expressed *lacI* gene to increase the LacI concentration. In addition, a LacI-operator sequence is cloned downstream of P_{T7} to ensure a tight repression of target gene expression in the absence of IPTG, even at high copy numbers of the T7 expression plasmid (Dubendorff and Studier, 1991). The operating principle of the expression system is shown schematically in Figure 1. In the absence of IPTG, *lacI* is constitutively expressed by the RNAP of *E. coli*. The repressor is then able to bind two of the three operator sequences simultaneously (Kania and Brown, 1976). Operator sequences 2 and 3 are also called pseudo-operator sequences, because their affinity for LacI is relatively low compared to O_1 and they only have a marginal effect on the repression of $P_{lac\,UV5}$ (Fried and Crothers, 1981; Pfahl et al., 1979). However, if LacI binds to O_1, a loop is formed between O_1 and the second operator sequence, which prevents the binding of RNA polymerase to the promoter (Bell and Lewis, 2000; Oehler et al., 1990). As a consequence, gene *1* is not transcribed, no T7 RNAP is produced and the target gene under control of P_{T7} will not be expressed. After addition of IPTG, the inducer forms a complex with LacI, in which the inducer promotes a conformation of LacI with lower binding affinity towards the operator. The LacI-IPTG complex thereupon does not bind to the DNA anymore, and expression of the target gene is possible (Daber et al., 2007). Because of high production rates and easy handling, the T7 RNAP-dependent expression system has already been established in several other organisms, like *Rhodobacter capsulatus* (Katzke et al., 2010)*, Bacillus megaterium* (Gamer et al., 2009) or *Lactococcus lactis* (Wells et al., 1993).

2.4 The PEP–pyruvate–oxaloacetate node in *C. glutamicum*

Because of the importance of *C. glutamicum* for the industrial production of amino acids and other metabolites, its central metabolism has been studied extensively. Of special interest is the tricarboxylic acid (TCA) cycle, since it has a major role in energy production by complete oxidation of acetyl-coenzyme A (acetyl-CoA) to CO_2 (Bott, 2007). Moreover, the intermediates of the cycle are interesting products for the industry itself, like succinate for example (Litsanov et al., 2012; Wang et al., 2017). They serve as precursors for the production of a huge variety of different compounds like organic acids, diamines, diols and most notably for the production of amino acids of the glutamate and aspartate family. Since intermediates like 2-oxoglutarate and oxaloacetate (OAA) are withdrawn for biosynthetic processes, the TCA cycle has to be replenished with so-called anaplerotic reactions (from the Greek ἀνά= 'up' and πληρόω= 'to fill'). In this context, the phosphoenolpyruvate (PEP)-pyruvate-OAA node is of special interest. At this node *C. glutamicum* is able to regulate and balance the carbon fluxes between glycolysis/gluconeogenesis and the TCA cycle. The PEP-pyruvate-OAA node of *C. glutamicum* comprises five enzymes which ensure the mutual conversion of C_3- and C_4-intermediates (Sauer and Eikmanns, 2005).

Three enzymes are present, which are catalyzing the decarboxylation of OAA or malate to PEP and pyruvate (Figure 2): The first one is the PEP carboxykinase (PEPCk), which catalyzes the GTP-dependent decarboxylation of OAA to form PEP and CO_2. Although the reaction is generally reversible and could thus contribute to anaplerosis, the formation of OAA is strongly inhibited under physiological conditions by ATP. Therefore, its main function is attributed to gluconeogenesis (Jetten et al., 1994; Riedel et al., 2001). A second enzyme called malic enzyme (MalE) was found in *C. glutamicum* to catalyze the reversible decarboxylation of malate to form pyruvate and CO_2. During this reaction $NADP^+$ is reduced to NADPH (Gourdon et al., 2000). The carboxylation of pyruvate with this enzyme shows a fivefold lower maximal velocity compared to the decarboxylation reaction, pointing out that decarboxylation is the main reaction of this enzyme under physiological conditions (Gourdon et al., 2000). The third enzyme is oxaloacetate decarboxylase (ODx). ODx performs the irreversible decarboxylation of OAA to pyruvate (Jetten and Sinskey, 1995; Klaffl and Eikmanns, 2010). Even if ODx could in principle catalyze the first reaction of gluconeogenesis, its involvement in this pathway can almost be excluded. Analyses of a PEPCk negative mutant grown on acetate or L-lactate as sole carbon source suggest that no PEP synthetase exists in *C. glutamicum*, which would be necessary for the subsequent conversion of pyruvate to PEP. Therefore, the main function of ODx in *C. glutamicum* remains further unknown (Klaffl and Eikmanns, 2010; Riedel et al., 2001).
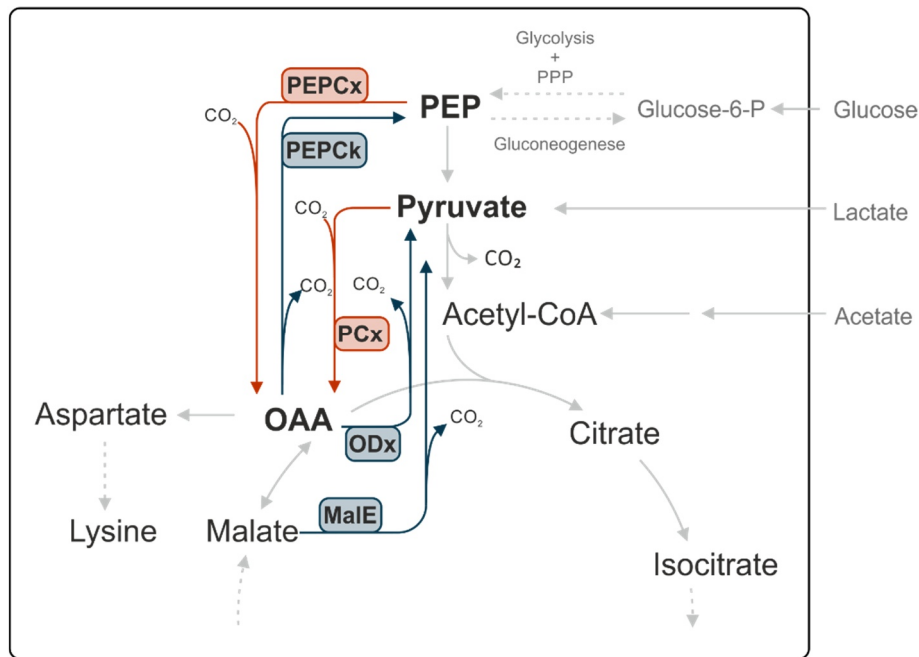
Figure 2 The PEP–pyruvate–OAA node in *C. glutamicum*. Dotted arrows include several reaction steps, whereas solid arrows represent single reactions. Anaplerotic reactions and enzymes are shown with red arrows and boxes. Blue arrows and boxes indicate decarboxylation reactions and enzymes of the PEP-pyruvate-OAA node. Additional reactions which are relevant for lysine production and growth are shown in grey. Abbreviations: PEPCx – PEP carboxylase; PEPCk – PEP carboxykinase; PCx – pyruvate carboxylase; ODx – OAA decarboxylase; MalE – malic enzyme.

Unlike many other organisms, *C. glutamicum* possess two C_3-carboxylating enzymes, PEP carboxylase (PEPCx) and pyruvate carboxylase (PCx). PEPCx catalyzes the carboxylation of PEP to form OAA (Eikmanns et al., 1989; Mori and Shiio, 1985). Kinetic characterization of this enzyme revealed a specific activity of 0.6 µmol min^{-1} mg^{-1} in cell-free extracts of *C. glutamicum*. Higher activities were determined in the presence of acetyl-CoA and fructose 1,6-bisphosphate, whereas aspartate, citrate, malate, succinate and 2-oxogluterate inhibited the enzyme (Eikmanns et al., 1989; Mori and Shiio, 1985). The regulatory properties of PEPCx and its high specific activity suggest a major role of the enzyme in anaplerosis under glycolytic conditions and consequently in the production of amino acids derived from the TCA cycle. Nevertheless, since the deletion of the *ppc* gene encoding PEPCx had no effects on growth and lysine production, a second enzyme was predicted to be present in *C. glutamicum* (Cremer et al., 1991; Gubler and et al., 1994; Peters-Wendisch et al., 1993; Tosaka et al., 1979). With ^{13}C-nuclear magnetic resonance (^{13}C-NMR) and gas chromatography-mass spectrometry analysis as well as $H^{13}CO_3$–labelling experiments, PCx was found to be the second enzyme (Park et al., 1997; Peters-Wendisch et al., 1996). In vivo flux analysis revealed that both enzymes, PCx as well as PEPCx, are active in cells growing on glucose. However, the PCx reaction contributes with more than 90% to OAA synthesis from C_3 precursors, whereas

PEPCx contributes only 10% (Petersen et al., 2000). Since a mutant of *C. glutamicum* lacking both the *ppc* gene for PEPCx and the *pyc* gene for PCx is not able to grow on carbohydrates, one can assume that no further enzymes exist in this organism for OAA synthesis via C_3 carboxylation (Peters-Wendisch et al., 1998).

2.4.1   The pyruvate carboxylase

PCx is a ubiquitously present enzyme in bacteria, archaea and eukaryotic cells as well (Jitrapakdee et al., 2008). Two major classes of PCxs are known, which differ in their structural organization. In the $\alpha_4\beta_4$ form, PCx consists of two polypeptides with a mass of $\sim$55 kDa (α) and $\sim$70 kDa (β) (Jitrapakdee et al., 2008). This type is mostly found in archaea, like *Methanococcus* sp., but also in some bacteria like *Pseudomonas* spp. or *Azotobacter* sp. In contrast, the α_4 form is composed of a single polypeptide with a mass of about $\sim$130 kDa (Jitrapakdee et al., 2008). This α_4 type PCx is more widespread, e.g. in fungi, vertebrates and invertebrates, and in most bacteria such as *C. glutamicum.* For both types, each subunit consists of an N-terminal biotin carboxylase domain (BC), a carboxyl transferase domain (CT), an allosteric or tetramerization domain (PT) and a C-terminal biotin carboxyl carrier protein domain (BCCP) (Attwood, 1995).

The overall reaction of PCx can be divided into two steps (Attwood, 1995; Menefee and Zeczycki, 2014):

$$\text{enzyme-biotin} + \text{MgATP} + \text{HCO}_3^- \rightarrow \text{enzyme-biotin-CO}_2 + \text{MgADP} + P_i$$

$$\text{enzyme-biotin-CO}_2\text{-} + \text{pyruvate} \rightarrow \text{enzyme-biotin} + \text{oxaloacetate}$$
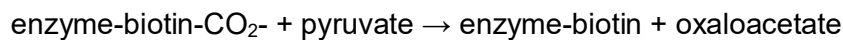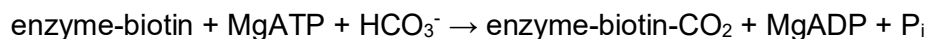
In *C. glutamicum*, PCx (EC 6.4.1.1) was characterized as a polypeptide of 1140 amino acids with a calculated mass of 123 kDa (Peters-Wendisch et al., 1998). Sequence analysis revealed 76% amino acid similarity to PCx of *M. tuberculosis* and over 60% similarity to the PCx enzymes of *Rhizobium etli*, *Bacillus stearothermophilus* or humans (Peters-Wendisch et al., 1998). These results underline the high level of conservation of the enzyme even across different kingdoms. The conserved sequence motif of the biotin binding site M-K-M was found in the corynebacterial PCx at position 1105-1107, with biotin bound covalently to the central lysine residue (Peters-Wendisch et al., 1998).

PCx activity from *C. glutamicum* was dependent on pyruvate, MgATP and HCO_3^- (Peters-Wendisch et al., 1997). Aspartate and ADP inhibited the enzyme with K_i values of about 15 mM and 2.6 mM, respectively (Koffas et al., 2002; Peters-Wendisch et al., 1997). But whereas other PCxs of the α_4-type are activated by acetyl-CoA to different degrees (Adina-Zada et al., 2012), PCx from *C. glutamicum* seemed to be inhibited by this effector with a K_i of 0.11 mM (Peters-Wendisch et al., 1997). Probably because of the high instability of PCx from *C. glutamicum*, its activity could only be measured in permeabilized cells and purification of an active

enzyme was impossible up till now (Koffas et al., 2002; Peters-Wendisch et al., 1997; Uy et al., 1999).

The role of PCx of *C. glutamicum* for amino acid production and growth on different carbon sources has been thoroughly analyzed. It was shown that PCx is dispensable for growth in minimal medium containing glucose or acetate as sole carbon source. In contrast, a PCx-deficient *C. glutamicum* strain was not able to grow on lactate as sole carbon source and its function cannot be replaced by PEPCx in this case (Peters-Wendisch et al., 1998; Peters-Wendisch et al., 1997). This phenotype of the PCx-negative mutant also indicates the absence of a PEP synthase, which together with PEPCx would have been able to bypass the reaction of the PCx and thus enable growth on lactate (Peters-Wendisch et al., 1998). Regarding the production of amino acids derived from the TCA cycle, it was found that PCx takes over the main function in anaplerosis compared to PEPCx. Concerning glutamate production, the deletion or overexpression of PEPCx had almost no effect on the production of the amino acid, whereas a PCx-negative mutant showed a reduced production of about 40% (Delaunay et al., 1999; Peters-Wendisch et al., 2001). On the other hand, overexpression of *pyc* caused a proportional increase in glutamate production as well as an increase of more than 150% in homoserine production (Peters-Wendisch et al., 2001). Moreover, PCx was shown to be an important enzyme for the production of lysine, which is derived from OAA. An increased flux from pyruvate to OAA caused by overexpression of *pyc* increased L-lysine production by about 50% in *C. glutamicum*, whereas the deletion of *pyc* caused a decrease in lysine production by about 60% (Peters-Wendisch et al., 2001). In summary, these results demonstrate the importance of PCx for optimization of *C. glutamicum* strains producing metabolites derived from the TCA cycle.

2.4.2   L-Lysine production with *C. glutamicum*

L-Lysine is an essential amino acid that is mainly used as an additive in animal feed, to ensure a low-cost production of swine and poultry. By adding lysine to the feed, the nutritional requirements of the animals can be better met and restrictions in the protein source can be overcome. This allows the use of a more cost-effective protein source that contains naturally lower levels of lysine, such as corn instead of soy, without restrictions in the fattening (Eggeling and Sahm, 1999). In addition, the excretion of nitrogen, which would otherwise pollute the environment, can be reduced by supplementation of the feed with lysine. Today, more than 2,200,000 tons/year L-lysine are produced in fermentation processes mostly by *C. glutamicum* with a market volume of more than €1.22 billion and an annual growth of ~7% (Eggeling and Bott, 2015). For a competitive large-scale production of L-lysine, it is particularly important to reduce production costs through the efficient use of the carbon source, reduced energy consumption

and minimized waste production. Therefore, in addition to the optimization of the manufacturing process, e.g. by improved cultivation strategies and downstream processing, also strain optimization of *C. glutamicum* is of essential importance for industrial research (Kelle et al., 2005). The first strains used for lysine production were already available in in the early 60's and were derived by random mutagenesis and subsequent strain selection (Kinoshita et al., 1961; Nakayama et al., 1978; Pfefferle et al., 2003). These approaches strongly improved L-lysine production by *C. glutamicum* and strains were already able to accumulate more than 100 g l^{-1} L-lysine-HCl with conversion yields up to 50% (Ikeda, 2003; Leuchtenberger, 1996). Hundreds of mutations can be found in those strains, but their effect on L-lysine production is known for only a few of them. Additionally, these strains are often auxotrophic for e.g. L-homoserine or L-leucine and show a low stress tolerance and delayed growth (Kelle et al., 2005; Ohnishi et al., 2002). Nowadays, research is focused on the construction of minimally mutated strains, to exclude those unintended effects for L-lysine production. The profound understanding of L-lysine biosynthesis and its regulation in *C. glutamicum* that is required for rational strain optimization was gained by analyzing its proteome (Schaffer et al., 2001), the fluxome (Wittmann et al., 2004), the metabolome (Drysch et al. 2003; Bolten et al., 2007) and also the transcriptome (Wendisch, 2003). Improvements in L-lysine production with *C. glutamicum* are now focused on the downregulation of competing pathways, increasing the sugar uptake as well as precursor and cofactor supply, like OAA and NADPH, respectively, and introducing feedback-resistant enzymes to overcome limiting reactions in the pathway (Eggeling and Bott, 2015; Kelle et al., 2005).

A key enzyme for improved L-lysine production is the aspartate kinase LysC, which catalyzes the first step in the biosynthesis of L-lysine and other amino acids of the aspartate family, like L-threonine and L-methionine (Figure 3). This enzyme is strongly feedback-inhibited by lysine and threonine in the wild-type and its deregulation is considered to be one of the most important steps towards increased L-lysine production in *C. glutamicum* (Cremer et al., 1991). Up to now, more than 20 different amino acid mutations are known in LysC that alter its allosteric regulation causing an increased L-lysine production, like the commonly used mutation T311I (Ohnishi et al. 2002; Chen et al., 2011; Schendzielorz et al., 2014). Another relevant mutation for L-lysine production is associated to the homoserine dehydrogenase Hom, V59A, causing a decreased activity of the enzyme (Ohnishi et al. 2002; Figure 3). By that, L-threonine synthesis is reduced and in turn the carbon flux gets redirected into L-lysine biosynthesis. An increased flux through the lysine biosynthetic pathway can also be achieved by overexpressing genes of the metabolic pathway itself, such as *dapB*, *ddh* or *lysA,* (Becker et al. 2011; Figure 3). Since for the production of one mole L-lysine four moles of NADPH are required, sufficient availability of the cofactor NADPH is essential for lysine overproduction.
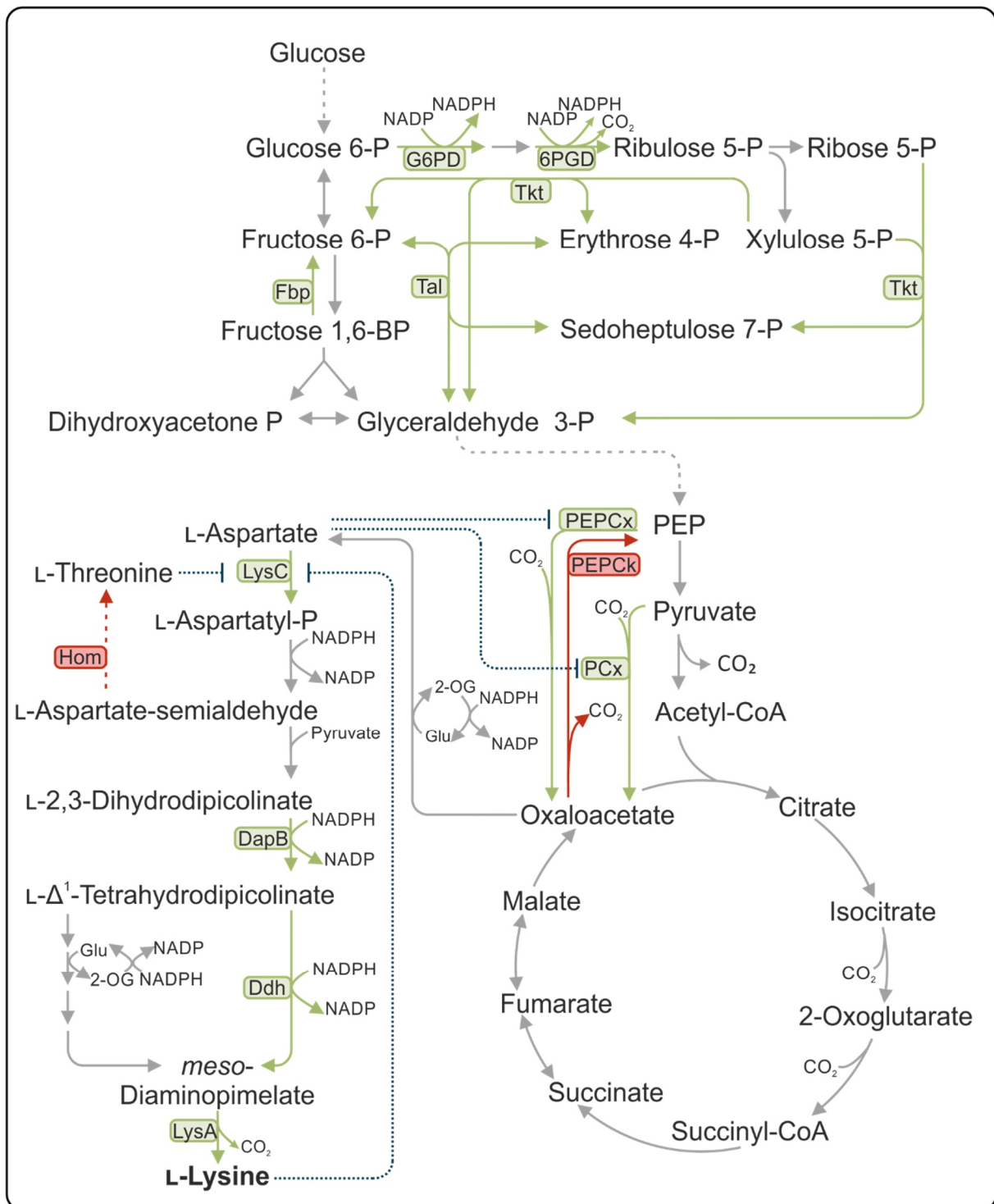
Figure 3 L-Lysine biosynthesis pathway and central metabolism of *C. glutamicum*. Examples of deleted or downregulated enzymes causing an increased L-lysine production are marked in red. Enzymes, which increased activities caused by mutations or overexpression, leading to a higher L-lysine production are marked in green. Additionally, feedback inhibition of enzymes of the lysine biosynthesis pathway are shown by dotted lines marked in dark blue. Enzyme abbreviations: DapB – dihydrodipicolinate reductase; Ddh – diaminopimelate dehydrogenase; Fbp – fructose 1,6-bisphosphatase; G6PD – glucose 6-phosphate dehydrogenase; Hom – homoserine dehydrogenase; LysA – diaminopimelate decarboxylase; LysC – aspartate kinase; 6PGD – 6-phosphogluconate dehydrogenase; PCx – pyruvate carboxylase; PEPCx – PEP carboxylase; PEPCk – PEP carboxykinase; Tal – transaldolase; Tkt – transketolase. Metabolite abbreviations: Glu - L-glutamate; 2-OG – 2-oxoglutarate; NADP(H) – nicotinamide adenine dinucleotide phosphate (oxidized/reduced state); PEP – phosphoenolpyruvate.

In this context, the pentose phosphate pathway (PPP) has been identified as a main pathway for the regeneration of this cofactor and different strategies have been developed to force an increased metabolic flux through the PPP (Becker et al. 2005). This includes the overexpression of the *fbp* gene, coding for fructose 1,6-bisphosphatase (Becker et al., 2005) as well as overexpression of the *tkt* operon, encoding the glucose 6-phosphate dehydrogenase (G6PD), transaldolase (Tal), transketolase (Tkt) and 6-phosphate dehydrogenase (6PGD) (Becker et al., 2011). Additionally, a S361F mutation in 6PGD releases the enzyme from feedback inhibition of different intracellular metabolites, like fructose 1,6-bisphosphate, ATP and NADPH (Ohnishi et al., 2005). Moreover, it was shown, that an increased precursor supply of OAA and aspartate has a positive effect on the lysine production rate in *C. glutamicum*. For instance, a deregulated PEPCx, caused by the mutation N917G, resulted in a significantly improved lysine production of almost 37% compared to the wild-type PEPCx (Chen et al., 2014). The deletion of PEPCk, catalyzing the counter-reaction from OAA to PEP caused an increase in lysine production as well, whereas the overexpression of the corresponding gene had the opposite effect and lysine production was reduced (Petersen et al., 2001). The second C_3-carboxylating enzyme, PCx, is also an important target for metabolic engineering in lysine-producing *C. glutamicum* strains. As mentioned already before, by overexpressing the *pyc* gene, L-lysine production was increased by almost 50% due to an increase of the precursor OAA (Peters-Wendisch et al., 2001). Moreover, the mutation P458S was also found to increase the carbon flux towards OAA when introduced into PCx and by that enabling a higher lysine production (Ohnishi et al., 2002), however, the effect of the mutation on the PCx has not yet been further characterized.

2.5 Sensor-based enzyme optimization in *C. glutamicum*

Metabolic engineering of bacterial production strains has clearly become a driving momentum in recent years. However, the growing demand for better and more efficient production strains of a constantly growing product range also requires better and, above all, faster screening methods. Especially screening techniques for producer strains of small molecules that do not cause a specific phenotype have so far proven to be laborious, since the production of the desired compound could only be determined in low- to medium-throughput screening procedures using chromatography or mass spectrometry for example (Dietrich et al., 2010; Zhang et al., 2015). Even though this method is suitable for rational strain engineering, in which e.g. selected amino acids are mutated with a predicted effect on the activity of a certain enzyme and only a smaller number of strains have to be tested for a higher production rate (Chen et al., 2011), most of the known useful mutations were (so far) unpredictable and were discovered by undirected mutagenesis. For example, the lysine-producing strain *C. glutamicum* B-6 was

constructed from the wild-type strain ATCC13032 by several rounds of random mutagenesis and subsequent selection steps (Hirao et al., 1989). But not until 10 years after the publication of this strain the mutations primarily responsible for the increased L-lysine production were identified, including the mutation T311I in the aspartate kinase LysC, P458S in the PCx and V59A in the homoserine dehydrogenase Hom (Ohnishi et al., 2002). However, even strains in which several known beneficial mutations have been combined by metabolic engineering processes can hardly compete with classical production strains in terms of lysine production.
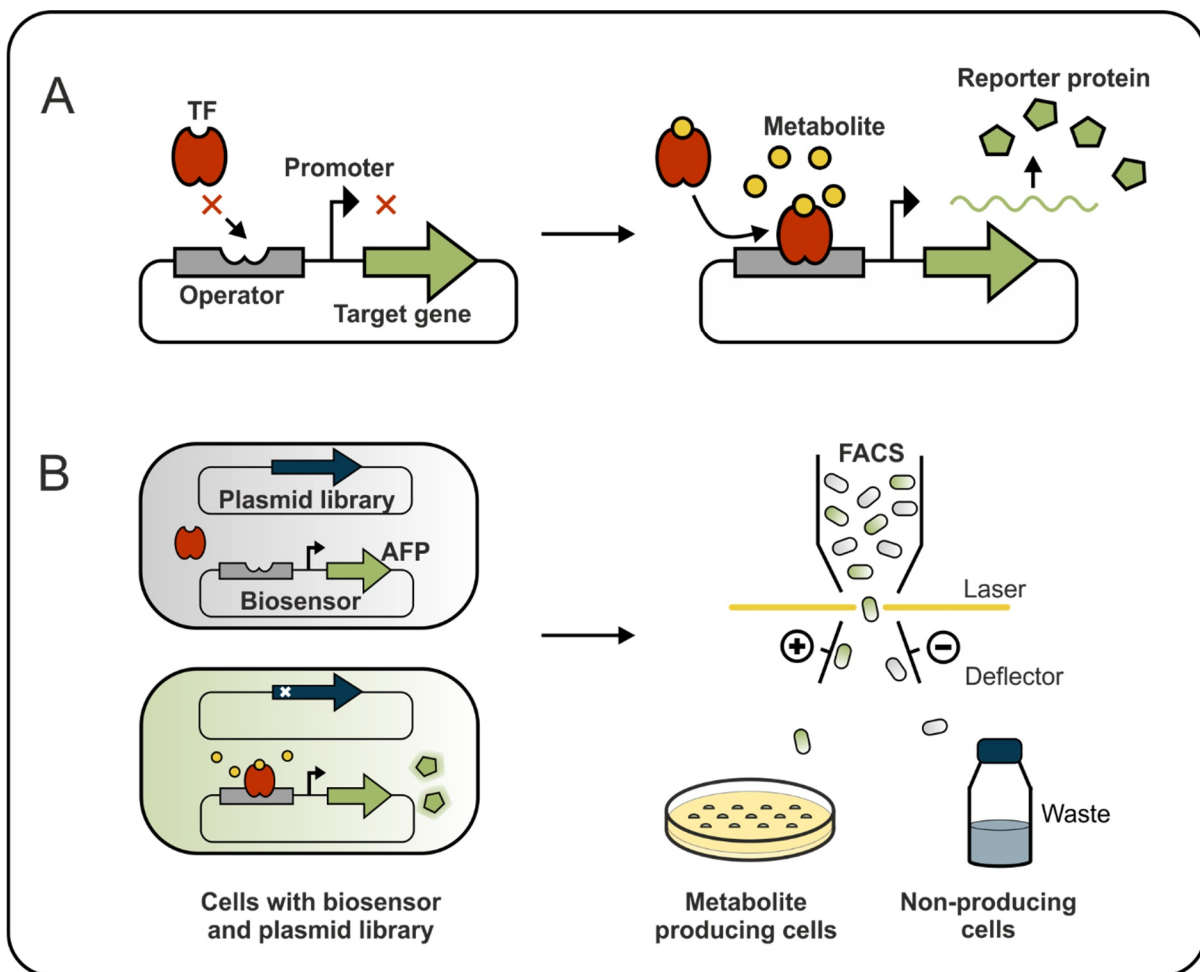
Figure 4 Principle and application of transcription factor-based biosensors. (A) Upon sensing increased levels of a specific metabolite, the transcription factor (TF) binds to the operator sequence of its target promoter and thereupon regulating its transcriptional activity. By placing a gene encoding a reporter protein with an optical or biochemical output under control of the regulated promoter, the metabolite concentration is coupled to this output and can be easily visualized. (B) Transcription factor-based biosensors can be used in high-throughput approaches using FACS to screen large enzyme libraries for variants enabling increased metabolite formation. For this purpose, a (plasmid-based) mutant library of the target gene is generated and subsequently transferred into cells equipped with a biosensor encoding an autofluorescent protein (AFP) like eYFP under control of the TF-regulated promotor. If an enzyme variant of the mutant library then enables an increased metabolite production in the cell, the fluorescence of the cell also increases. Subsequently, the fluorescence of each cell can be measured and quantified individually with FACS analysis and cells showing a higher fluorescence and hence increased metabolite production can be directly selected for further analysis, e.g. sorted directly on agar plates.

Likewise, the strain, in which all three mutants mentioned above were combined, showed a lower lysine accumulation of about 16% compared to strain B-6 (Ohnishi et al., 2002).

Therefore, a new approach for high-throughput screening has been developed, in which genetically encoded biosensors are used in combination with fluorescence-activated cell sorting (FACS) to screen millions of cells individually for their production of a desired metabolite *in vivo* within a very short time (Binder et al., 2012; Mustafi et al., 2015). For this purpose, the desired intracellular metabolite formation is directly converted into an easily detectable and measurable output like a fluorescence signal by using transcription factor-based biosensors (Figure 4A). In general, transcription factors are important for the cell to adapt gene expression at the transcriptional level to certain stimuli such as (intracellular) concentrations of small molecules, but also inorganic ions or physical quantities like pH or temperature. The sensor pSenLys, for instance, is based on the transcriptional regulator LysG, which senses increased intracellular concentrations of the basic amino acids L-arginine, L-histidine and L-lysine (Bellmann et al., 2001; Binder et al., 2012). Naturally, LysG activates the transcription of the lysine exporter gene *lysE* when the cytoplasmic concentrations of lysine, arginine or histidine reach high levels (Bellmann et al., 2001), but in case of pSenLys the promotor of *lysE* is fused to the *eyfp* gene encoding enhance yellow fluorescent protein eYFP (Binder et al., 2012). Thereby, increased intracellular concentrations of basic amino acids cause an increased synthesis of eYFP and thus an increased fluorescence of the cell. The fluorescence of single cells can be measured and quantified by fluorescence-activated cell sorting (FACS) analysis, which enables analysis of up to 10,000 cells per second (Figure 4B). The sensor pSenLys has already been used successfully to screen a library of *C. glutamicum* cells obtained by genome-wide random chemical mutagenesis for mutants with increased lysine production (Binder et al., 2012). Besides mutations in known target genes, the approach also led to the discovery of previously unknown mutations that enable lysine overproduction, such as MurE[G81E] and MurE[L121F]. MurE is an essential protein for murein biosynthesis that uses *meso*-diaminopimelate, which is also the precursor of lysine, as substrate (Binder et al., 2012). Presumably the G81E and L121F mutations cause a decreased activity of MurE. In another approach, pSenLys was used in a gene-directed approach to isolate feedback-resistant variants of the key enzymes of lysine, arginine, and histidine biosynthesis, i.e. aspartate kinase (LysC), N-acetyl-glutamate kinase (ArgB), and ATP phosphoribosyltransferase (HisG) (Schendzielorz et al., 2014). In the case of LysC, 11 variants were isolated in just one screening step, which were able to produce comparable or even two-fold higher amounts of L-lysine compared to the known feedback-resistant variant LysC[T311I] (Schendzielorz et al., 2014). Other successful screening approaches with transcriptional biosensors in *C. glutamicum* targeted for example increased production of

L-valine (Mahr et al., 2015; Mustafi et al., 2012; Mustafi et al., 2014) or L-serine (Zhang et al., 2018). These results clearly emphasize the power and potential of this screening method.

2.6 Aims of this thesis

In this thesis, two very different topics were addressed to further expand and increase the potential of *Corynebacterium glutamicum* in white biotechnology. The first part of this work aimed at the establishment of a T7 RNA polymerase-based gene expression system in *C. glutamicum*. Despite the enormous potential of *C. glutamicum* for the expression of homologous and heterologous genes, there is still no strong and tightly controlled expression system available. Due to the excellent properties of the T7 expression system and its successful transfer from *E. coli* into various other bacteria, it was considered as a very attractive system to be established also in *C. glutamicum*. For this purpose, *C. glutamicum* MB001 (Baumgart et al., 2013) should be used as parent strain for genomic integration of the key genetic elements of the T7 system from λDE3. In strain MB001 the three prophages CGP1-3 have been deleted, which caused an increased *eyfp* expression up to 40% compared to the wild-type strain ATCC13032 (Baumgart et al., 2013). This effect might be due to the fact that the genes of a restriction modification system located within the prophage CGP3 have been removed, resulting in a higher copy number of plasmids in strain MB001. Besides the T7-RNAP-encoding *C. glutamicum* strain, suitable expression vectors with the T7 promoter should to be constructed. Finally, the system should be characterized by expression of several target genes and compared to established expression systems.

The second part of this thesis is focused on the enzyme PCx. For *C. glutamicum* it was shown that PCx is a very important anaplerotic enzyme and a bottleneck for the production of various intermediates of the TCA cycle and of metabolites derived from the TCA cycle, such as L-glutamate and L-lysine. Therefore, PCx represents a highly interesting target for metabolic engineering (Peters-Wendisch et al., 2001). The first goal was to find improved variants of PCx that enable an increased production of L-lysine in *C. glutamicum*. Until now, it was believed that there is no selectable phenotype for improved PCx variants (Ohnishi et al., 2002). With the establishment of the genetically encoded lysine biosensor pSenLys (Binder et al., 2012), a tool became available that might allow the high throughput-screening for improved PCx variants, as such variants should lead to improved lysine production. To test this idea, a plasmid-based *pyc* mutant library was constructed by error-prone PCR, transferred into a suitable pSenLys-carrying reporter strain of *C. glutamicum* and then screened by FACS for single cells showing increased fluorescence. In order to be able to characterize the isolated PCx variants in more detail afterwards, a suitable enzyme assay was required. Until now, the activity of PCx and the influence of different effectors on it could only been determined with permeabilized

cells and discontinuous assays (Peters-Wendisch et al., 1998; Uy et al., 1999), due to the lability of the enzyme. Therefore, conditions and methods should be developed in this thesis that stabilize the enzyme and enable the measurement of PCx activity in cell-free extracts and purification of the enzyme.

3   Results

In this doctoral thesis the overarching theme was to optimize *C. glutamicum* for the production of industrially relevant compounds from renewable carbon sources. In the first part of this thesis a new expression system based on T7 RNA polymerase was constructed and characterized. The results are presented in one original publication. In the second part, pyruvate carboxylase (PCx) was optimized for L-lysine production and then characterized in more detail. The results were described in two original publications.

The first publication "A chromosomally encoded T7 RNA polymerase-dependent gene expression system for *Corynebacterium glutamicum*: construction and comparative evaluation at the single-cell level" describes the construction and characterization of a T7 RNA polymerase-based expression system in *C. glutamicum*. For this purpose, gene *1* encoding T7 RNA polymerase was integrated into the genome of the prophage-free strain *C. glutamicum* MB001 under control of the *lac*UV5 promoter. For characterization of the system, different target genes were then cloned into the newly constructed expression vector pMKEx2 under control of the T7 promoter. After addition of IPTG, T7 RNA polymerase is synthesized and in turn selectively enables the expression of the target gene upon binding to the T7 promotor. The properties of the system were initially analyzed by the expression of the reporter gene *eyfp*. A 3.5-fold higher specific eYFP fluorescence could be obtained with the T7 system in comparison to the established pEKEx2 system. Cells in which *eyfp* was expressed via the T7 system also showed a highly uniform population with more than 99% of all cells showing a high fluorescence. At the same time, a lower basal expression in the non-induced state was observed with the T7 system compared to pEKEx2. The functionality of the T7 system was further underlined by the expression of the pyruvate kinase gene (*pyk*). After induction with 250 µM IPTG, pyruvate kinase activity of cell-free extracts of *C. glutamicum* MB001(DE3) with pMKEx2-*pyk* increased about 50-fold.

In the second publication "Pyruvate carboxylase variants enabling improved lysine production from glucose identified by biosensor-based high-throughput fluorescence-activated cell sorting screening" a *pyc* mutant library was prepared via error-prone PCR and screened for variants which enable a higher L-lysine production in *C. glutamicum* DM1868Δ*pyc*. Lysine production was analyzed at the single cell level via the lysine biosensor pSenLys-Spec using FACS. Finally, two enzyme variants were found to cause higher lysine production. After plasmid-based expression of *pyc*$^{T343A; I1012S}$, *C. glutamicum* DM1868Δ*pyc* was able to produce about 9% more lysine compared to the strain expressing wild-type *pyc*. The second variant identified was PCx^{T132A}, which caused an increase in lysine production of about 19% after plasmid-based expression. Subsequently, each of the mutations T343A and T132A could be successfully integrated into the genome of *C. glutamicum* DM1868. Lysine production of strains DM1868

pyc[T132A] and DM1868 *pyc*[T343A] was increased about 7% and 15%, respectively, compared to the parental strain DM1868.

In the third publication "Pyruvate carboxylase from *Corynebacterium glutamicum*: purification and characterization" conditions were identified that enabled stabilization, activity measurements in cell-free extracts, and purification of the labile PCx of *C. glutamicum*. Purification of PCx was achieved by avidin affinity chromatography and gel filtration. After that, V_{max} values between 20 and 25 µmol min^{-1} mg^{-1} of PCx were determined in a coupled enzyme assay with malate dehydrogenase. K_m values of 3.76 mM for pyruvate and of 0.61 mM for ATP were measured. For bicarbonate concentrations ≤5 mM, no activity of PCx could be measured. At higher bicarbonate concentrations, half-maximal activity of PCx was determined at 13.25 mM. As previously shown in enzyme assays with permeabilized cells, PCx activity is inhibited by ADP and aspartate with apparent K_i values of 1.5 mM and 9.3 mM, respectively. Acetyl-CoA, however, showed only a weak inhibitory effect on PCx activity up to a concentration of approx. 50 µM, which was even reversed at higher concentrations. This result differs from previously reported data obtained with permeabilized cells.

3.1 A chromosomally encoded T7 RNA polymerase-dependent gene expression system for *Corynebacterium glutamicum*: construction and comparative evaluation at the single-cell level.

Kortmann M., Kuhl V., Klaffl S., Bott M.*

IBG-1: Biotechnology, Forschungszentrum Jülich, Jülich, Germany

*Corresponding author

MBo and SK designed the study and planned the experiments. Experimental work was performed by MK and VK. MK constructed *C. glutamicum* MB001(DE3) and all plasmids. Biolector® experiments, FACS and microscopy experiments, SDS-PAGE and pyruvate kinase enzyme assays were performed by MK and VK. MK prepared the figures. MK and MBo wrote the manuscript.

MK: Maike Kortmann, VK: Vanessa Kuhl, SK: Simon Klaffl, MBo: Michael Bott

Overall contribution MK: 50%

microbial biotechnology

Open Access

A chromosomally encoded T7 RNA polymerase-dependent gene expression system for *Corynebacterium glutamicum*: construction and comparative evaluation at the single-cell level

Maike Kortmann, Vanessa Kuhl, Simon Klaffl and Michael Bott*
Institute of Bio- and Geosciences, IBG-1: Biotechnology, Forschungszentrum Jülich, Jülich D-52425, Germany.

Summary

Corynebacterium glutamicum **has become a favourite model organism in white biotechnology. Nevertheless, only few systems for the regulatable (over)expression of homologous and heterologous genes are currently available, all of which are based on the endogenous RNA polymerase. In this study, we developed an isopropyl-β-D-1-thiogalactopyranosid (IPTG)-inducible T7 expression system in the prophage-free strain** ***C. glutamicum*** **MB001. For this purpose, part of the DE3 region of** ***Escherichia coli*** **BL21(DE3) including the T7 RNA polymerase gene** ***1*** **under control of the** ***lac*****UV5 promoter was integrated into the chromosome, resulting in strain MB001(DE3). Furthermore, the expression vector pMKEx2 was constructed allowing cloning of target genes under the control of the T7*lac* promoter. The properties of the system were evaluated using** ***eyfp*** **as heterologous target gene. Without induction, the system was tightly repressed, resulting in a very low specific eYFP fluorescence (= fluorescence per cell density). After maximal induction with IPTG, the specific fluorescence increased 450-fold compared with the uninduced state and was about 3.5 times higher than in control strains expressing** ***eyfp*** **under control of the IPTG-induced** ***tac*** **promoter with the endogenous RNA polymerase. Flow cytometry revealed that T7-based** ***eyfp*** **expression resulted in a highly uniform population, with 99% of all cells showing high fluorescence. Besides** ***eyfp*****, the functionality of the corynebacterial T7 expression system was also successfully demonstrated by overexpression of the** ***C. glutamicum pyk*** **gene for pyruvate kinase, which led to an increase of the specific activity from 2.6 to 135 U mg^{-1}. It thus presents an efficient new tool for protein overproduction, metabolic engineering and synthetic biology approaches with** ***C. glutamicum*****.**

Introduction

The recombinant production of proteins is a highly important issue in industrial biotechnology as well as in scientific research. Many different expression systems have been established in various eukaryotic and prokaryotic organisms (Demain and Vaishnav, 2009). Due to their easy handling and well-established genetic tools, bacteria are broadly used to express heterologous and homologous genes (Baneyx, 1999; Terpe, 2006; Chen, 2012). One of the most popular and commonly used systems for high-level protein production in *Escherichia coli* is the T7 expression system developed by Studier and Moffatt (1986). It is based on the RNA polymerase (RNAP) of bacteriophage T7, which shows a number of beneficial properties: (i) single-subunit enzyme in contrast to multi-subunit bacterial RNAP, (ii) high processivity, (iii) high specificity towards the T7 promoter, (iv) independence of auxiliary transcription factors, (v) production of very long transcripts, and (vi) termination only by class I and class II termination signals that differ significantly from bacterial transcription termination sites (Chamberlin and Ring, 1973; Macdonald *et al.*, 1994; Lyakhov *et al.*, 1998). Expression hosts like *E. coli* BL21(DE3) carry a single copy of gene *1* for T7 RNAP located chromosomally on a λDE3 lysogen (Studier and Moffatt, 1986). In strain *E. coli* BL21(DE3), transcription of gene *1* is controlled by a *lac*UV5 promoter, allowing repression by LacI and induction with isopropyl-β-D-1-thiogalactopyranoside (IPTG). The expression of desired target genes is controlled by the T7 promoter, which is usually present on a suitable expression vector. To minimize basal transcription, a LacI binding site can be introduced in front of the target gene, placing both gene *1* and the target gene under the control of the LacI repressor (Dubendorff and Studier, 1991). The characteristics of the T7 RNAP-dependent expression system permit a very efficient and exclusive expression of

2   *M. Kortmann, V. Kuhl, S. Klaffl and M. Bott*

genes under control of the strong T7 promoter. Due to its favourable properties, the T7 RNAP-based expression system has also been established in a variety of other bacteria, such as *Pseudomonas aeruginosa* (Brunschwig and Darzins, 1992), *Pseudomonas putida* (Herrero *et al.*, 1993), *Ralstonia eutropha* (Barnard *et al.*, 2004), *Bacillus megaterium* (Gamer *et al.*, 2009), *Streptomyces lividans* (Lussier *et al.*, 2010), *Rhodobacter capsulatus* (Katzke *et al.*, 2010; Arvani *et al.*, 2012) and *Corynebacterium acetoacidophilum* (Equbal *et al.*, 2013).

Corynebacterium glutamicum is a Gram-positive soil bacterium of the order *Corynebacteriales* and serves in industry as the major host for production of amino acids, with L-glutamate and L-lysine being the most important ones. Efficient strains are available also for the synthesis of a variety of other amino acids, for example L-leucine (Vogt *et al.*, 2013), L-serine (Stolz *et al.*, 2007) or D-serine (Stäbler *et al.*, 2011). Furthermore, a variety of other commercially interesting metabolites can be produced with *C. glutamicum* (Becker and Wittmann, 2012), such as organic acids (Wendisch *et al.*, 2006; Okino *et al.*, 2008; Litsanov *et al.*, 2012a,b; Wieschalka *et al.*, 2013), diamines (Mimitsuka *et al.*, 2007; Kind and Wittmann, 2011; Schneider and Wendisch, 2011) or alcohols (Inui *et al.*, 2004; Smith *et al.*, 2010; Blombach *et al.*, 2011; Yamamoto *et al.*, 2013). Despite its complex cell envelope (Bansal-Mutalik and Nikaido, 2011; Marchand *et al.*, 2012; Laneelle *et al.*, 2013), *C. glutamicum* is also an efficient host for the secretory production of heterologous proteins (see Kikuchi *et al.*, 2008; Scheele *et al.*, 2013; Matsuda *et al.*, 2014; and references therein). Based on the broad spectrum of products and its robustness in large-scale production processes, *C. glutamicum* has become a platform and model organism in industrial biotechnology (Eggeling and Bott, 2005; Burkovski, 2008; Yukawa and Inui, 2013).

The development of production strains often requires the controlled expression of target genes or operons. All currently available systems for controlling gene expression in *C. glutamicum* are based on transcription by the endogenous RNA polymerase (Kirchner and Tauch, 2003; Eggeling and Reyes, 2005; Nesvera and Patek, 2011; Patek *et al.*, 2013). In this study, we constructed an IPTG-inducible expression system in *C. glutamicum* that is based on T7 RNAP. We characterized the properties of this system with the *eyfp* gene for enhanced yellow fluorescent protein (Perez-Jimenez *et al.*, 2006), which allows for analysing population heterogeneity by flow cytometry, and the homologous *pyk* gene for pyruvate kinase as a test case for overproduction of a cytosolic enzyme. The results obtained show that the T7 system allows very efficient and controllable protein overproduction in *C. glutamicum* to levels that outperform currently available systems.

Results and discussion

Construction of a T7 RNAP-dependent expression system for *C. glutamicum*

In this study, a T7 RNAP-dependent expression system was developed for *C. glutamicum* based on a chromosomally encoded T7 RNAP and a vector in which the target gene was placed under the control of a T7 promoter. For regulatable chromosomal expression of the T7 RNAP gene *1*, a 4.47 kb fragment (sequence is shown Fig. S1) was amplified by polymerase chain reaction (PCR) from the genome of *E. coli* BL21(DE3) (Table 1) with oligonucleotides DE3-for and DE3-rev (Table 2) that contains the repressor gene *lacI* under the control of its native promoter, *lacZα*, and T7 gene *1*, the latter two under the control of the *lac*UV5 promoter, including three LacI operator sites O1-O3 (Fig. 1A). The fragment was used to construct plasmid pK18*mobsacB*-DE3 (Table 1), in which the DE3 insert is flanked by adjacent 800 bp regions covering the genes cg1121 (encoding a permease of the major facilitator superfamily) and cg1122 (encoding a putative secreted protein) and their downstream regions (Fig. 1A). Via homologous recombination (Niebisch and Bott, 2001), the DE fragment was integrated into the intergenic region of cg1121-cg1122 within the genome of *C. glutamicum* MB001 (NC_022040.1), a prophage-free derivative of the type strain ATCC 13032, which showed a higher expression level for eYFP than the parent strain (Baumgart *et al.*, 2013b). The insertion site is located 340 bp downstream of the cg1121 stop codon. Kanamycin-sensitive and sucrose-resistant clones were checked by PCR and sequence analysis for the correct chromosomal insertion of the DE fragment and the generated strain was named *C. glutamicum* MB001(DE3).

For exclusive transcription by T7 RNAP, the target gene has to be under control of a T7 promoter. Therefore, a suitable expression vector was constructed based on the shuttle vector pJC1, which contains the pHM1519 replicon for *C. glutamicum* and the pACYC177 replicon for *E. coli* (Cremer *et al.*, 1990). In order to provide unique restriction sites for BamHI, XbaI and SalI in the multiple cloning site (MCS) to be inserted, the corresponding restriction sites in the backbone sequence of pJC1 were deleted in advance. For this purpose, pJC1 was digested with BamHI and SalI, the resulting 5′-overhangs filled in with Klenow polymerase and re-circularized via blunt end ligation, resulting in pJC1ΔBXS. A 1.97 kb fragment of plasmid pET52b(+) containing *lacI*, the T7 promoter, the *lac* operator and the downstream MCS was amplified with the oligonucleotides pETEx-for and pETEx-rev and inserted into the unique PstI restriction site of pJC1ΔBXS. After insertion of the expression cassette, an NcoI restriction site in the pJC1 backbone was removed by exchanging a single base (CCATGG → CCATAG). The resulting

Table 1. Bacterial strains and plasmids used in this study**.**

Strain or plasmid	Relevant characteristics	Source
Strain		
E. coli BL21(DE3)	F⁻ *ompT hsdSB*(r$_B$⁻ m$_B$⁻) *gal dcm* (*lcIts857 ind1 Sam7 nin5 lac*UV5-T7 gene *1*)	(Studier and Moffatt, 1986)
E. coli DH5α	F⁻ φ80*lacZ*ΔM15 Δ(*lacZYA-argF*)U169 *recA*1 *endA*1 *hsdR*17(rk⁻, mk⁺) *phoA supE*44 *thi*-1 *gyrA*96 *relA*1 λ⁻	Invitrogen
C. glutamicum MB001	Type strain ATCC 13032 with deletion of prophages CGP1 (cg1507-cg1524), CGP2 (cg1746-cg1752), and CGP3 (cg1890-cg2071)	(Baumgart *et al.*, 2013b)
C. glutamicum MB001(DE3)	MB001 derivative with chromosomally encoded T7 gene *1* (cg1122-P$_{lacI}$-*lacI*-P$_{lacUV5}$ −*lacZ*α-T7 gene *1*-cg1121)	This study
Plasmid		
pEKEx2	Kan^R; *C. glutamicum*/*E. coli* shuttle vector for regulated gene expression (P$_{tac}$, *lacI*^{q}, pBL1 *oriV$_{Cg}$*, pUC18 *oriV$_{Ec}$*)	(Eikmanns *et al.*, 1991)
pEKEx2-*eyfp*	Kan^R; expression plasmid carrying the *eyfp* gene under the control of the *tac* promoter	(Hentschel *et al.*, 2013)
pET-52b(+)	Amp^R; *E. coli* vector for expression of target genes under control of the T7 promoter (pBR322 *ori$_{Ec}$*, P$_{T7}$, *lacI*)	Novagen
pJC1	Kan^R; *E. coli*/*C. glutamicum* shuttle vector (pHM1519 *ori$_{Cg}$*, pACYC177 *ori$_{Ec}$*);	(Cremer *et al.*, 1990)
pJC1-*venus*-term	Kan^R; pJC1 derivative containing *venus* gene and additional terminators	(Baumgart *et al.*, 2013a)
pJC1ΔBXS	Kan^R; pJC1 derivative lacking BamHI, XbaI, and SalI restriction sites	This study
pJC1-P$_{tac}$-*eyfp*	Kan^R; pJC1 derivative containing the *eyfp* gene under the control of the P$_{tac}$	This study
pK18*mobsacB*	Kan^R; vector for allelic exchange in *C. glutamicum* (oriT oriV$_{Ec}$ *sacB lacZ*α)	(Schäfer *et al.*, 1994)
pK18*mobsacB*-DE3	Kan^R; pK18*mobsacB* derivative containing the 4.5 kb λDE3 region (P$_{lacI}$, *lacI*, P$_{lacUV5}$, gene *1*) from *E. coli* BL21(DE3) flanked by two 800-bp DNA regions for homologous recombination into the intergenic region of cg1121 and cg1122	This study
pMKEx2	Kan^R; *E. coli*/*C. glutamicum* shuttle vector based on pJC1 for expression of target genes under control of the T7 promoter (P$_{lacI}$, *lacI*, P$_{T7}$, *lacO1*, N-term. Strep•tag II, MCS, C-term. His•tag, pHM1519 *ori$_{Cg}$*; pACYC177 *ori$_{Ec}$*)	This study
pMKEx2-*eyfp*	Kan^R; pMKEx2 derivative containing the *eyfp* gene under control of P$_{T7}$	This study
pMKEx2-*pyk*	Kan^R; pMKEx2 derivative with the *C. glutamicum pyk* gene under control of P$_{T7}$	This study

expression vector was named pMKEx2 (GenBank accession number KM658503) and allows fusion of the target protein either with an N-terminal Streptag II or with a C-terminal decahistidine tag (Fig. 1B).

Characterization of T7 RNAP-dependent expression system in C. glutamicum *with the heterologous target protein eYFP and comparison with* P$_{tac}$-*based expression*

To analyse the functionality and efficiency of the newly constructed T7 expression system in *C. glutamicum*, the heterologous model protein eYFP (Perez-Jimenez *et al.*, 2006) was used as target, as it allows easy detection also at the single-cell level by fluorescence microscopy and fluorescence-activated cell sorting (FACS). The *eyfp* gene was amplified from the plasmid pEKEx2-*eyfp* (Hentschel *et al.*, 2013) with oligonucleotides eYFP-for and eYFP-rev and cloned as NcoI-BamHI fragment into pMKEx2 under transcriptional control of the T7 promoter. The resulting plasmid pMKEx2-*eyfp* was transferred into *C. glutamicum* MB001(DE3), and for control purposes into *C. glutamicum* MB001. The synthesis of eYFP by strain MB001(DE3)/pMKEx2-*eyfp* was compared with strain MB001/pEKEx2-*eyfp*. The well-established expression vector pEKEx2 permits expression of target genes under control of the IPTG-inducible *tac* promoter by the endogenous RNA polymerase (Eikmanns *et al.*, 1991).

The strains were cultivated in CGXII minimal medium with 4% (wt/vol) glucose using a BioLector system

Table 2. Oligonucleotides used in this study**.**

Name	Sequence (5′→3′)	Restriction sites
DE3-for	CCGCTCGAGAACTGCGCAACTCGTGAAAGG	XhoI
DE3-rev	CGGAATTCGTTACGCGAACGCGAAGTC	EcoRI
pETEx-for	AACTGCAGGGAGCTGACTGGGTTGAAGG	PstI
pETEx-rev	AACTGCAGCTTAATGCGCCGCTACAGGG	PstI
pEKEx-for	GGAATTCCATATGTCGCTCAAGCCTTCGTCACTG	NdeI
pEKEx-rev	GGACTAGTTTATCTAGACTTGTACAGCTCGTCCATG	SpeI
eYFP-for	CATGCCATGGACAATAACGATCTCTTTCAGGCATCAC	NcoI
eYFP-rev	CGGGATCCTCAGCCCGCGAGCACC	BamHI
PykCg-for	CGGGATCCGGCGTGGATAGACGAACTAAG	BamHI
PykCg-rev	TGTACAGACACCACGTACAGTGTCAACGC	BsrGI

4   *M. Kortmann, V. Kuhl, S. Klaffl and M. Bott*
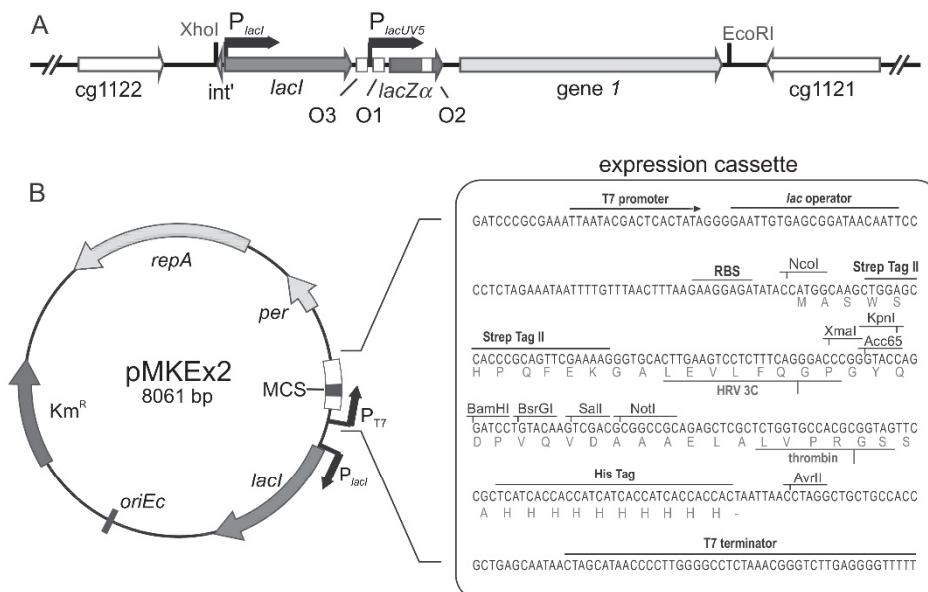
Fig. 1. A. genomic region of *C. glutamicum* MB001(DE3) carrying the DE3 insertion. A 4.5 kb DNA fragment was amplified from chromosomal DNA of *E. coli* BL21(DE3) and inserted into the intergenic region of cg1121-cg1122 of MB001(DE3). The fragment contains *lacI*, *lacZα* and T7 gene *1*, the latter two under the transcriptional control of the *lac*UV5 promoter and its three LacI operator sites O1-O3. B. Map of the expression plasmid pMKEx2, which is based on pJC1 and an expression cassette from pET52b. The region between the T7 promoter and the T7 terminator is shown in detail.

(Fig. S2) in the presence of 0, 5, 10, 15, 25, 50, 100 and 250 µM IPTG and expression of the target gene was determined by measuring the specific eYFP fluorescence (Fig. 2). For strain MB001/pMKEx2-*eyfp*, which lacks T7 RNAP, only background specific fluorescence was observed (< 0.001). In the case of strain MB001(DE3)/pMKEx2-*eyfp*, specific fluorescence was very low in 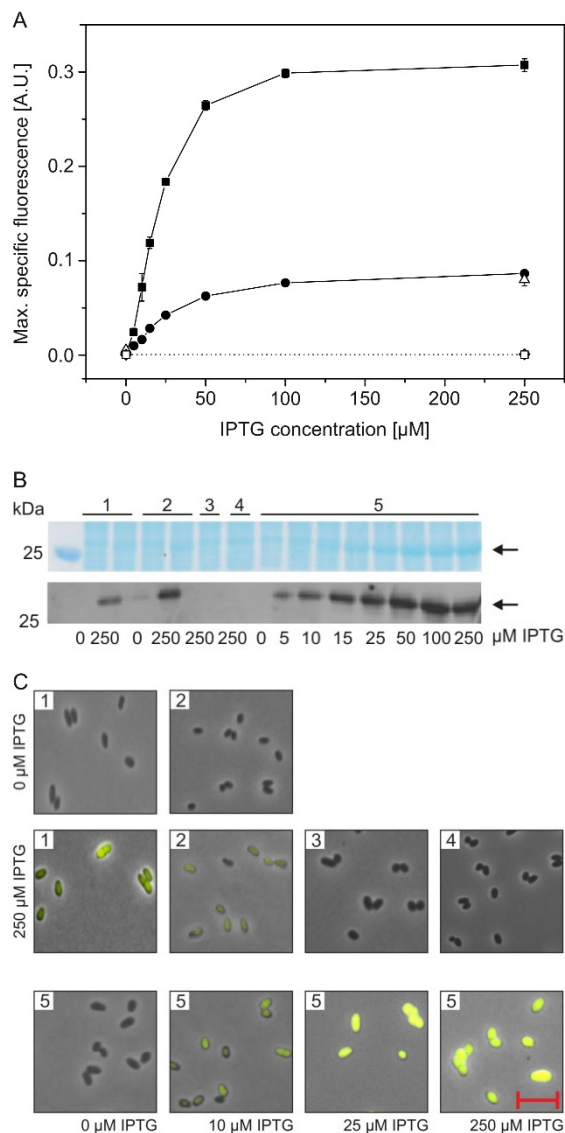the absence of IPTG (< 0.001), but increased up 0.30 when the medium was supplemented with 100 µM IPTG. These results demonstrate that the T7 promoter is not recognized by the corynebacterial RNAP, whereas specific and efficient expression occurs in the presence of T7 RNAP. In the case of strain MB001/pEKEx2-*eyfp*, the specific fluorescence in the absence of IPTG (0.001) was 1.6-fold higher than in the case of MB001(DE3)/pMKEx2-*eyfp* and increased up to 0.08 in the presence of 100 µM IPTG (Fig. 2). Thus, the T7 system shows a slightly lower expression level in the absence of IPTG and an up to fourfold higher maximal expression level in the presence of IPTG compared with pEKEx2-based expression of *eyfp*. Half-maximal specific fluorescence was obtained with 20 µM IPTG for strain MB001(DE3)/pMKEx2-*eyfp* and with 31 µM IPTG for strain MB001(DE3)/pEKEx2-*eypf*.

To exclude an influence of the different replication mechanisms of pMKEx2 and pEKEx2, the specific eYFP fluorescence was also determined in *C. glutamicum* MB001(DE3) transformed with plasmid pJC1-P$_{tac}$-*eyfp*. This plasmid contains the same replicon as pMKEx2 and the expression cassette of pEKEx2 (for construction see *Experimental procedures*). The results obtained with MB001/pJC1-P$_{tac}$-*eyfp* were comparable to that of MB001/pEKEx2-*eyfp*, indicating that the difference to T7-based *eyfp* expression is not caused by the different replicons, but by the use of different RNAPs and promoters (Fig. 2).

To further characterize the T7 expression system in *C. glutamicum*, the four strains described above were analysed by SDS-PAGE, Western blotting and fluorescence microscopy. The Coomassie-stained SDS-polyacrylamide gel and more clearly the Western blot with anti-green-fluorescent protein (GFP) antiserum shown in Fig. 2B qualitatively confirmed the results of the specific fluorescence measurements described above. In the case of strains MB001/pEKEx2-*eyfp* and MB001(DE3)/pMKEx2-*eyfp*, no distinct band with a size of 27 kDa (calculated mass of eYFP) was visible in cells grown in the absence of IPTG, whereas a faint band was visible in the case of strain MB001/pJC1-P$_{tac}$-*eyfp*. When cultivated in the presence of 250 µM IPTG, the 27 kDa eYFP protein band was clearly visible in strains MB001/pEKEx2-*eyfp*, MB001/pJC1-P$_{tac}$-*eyfp* and pMB001(DE3)/pMKEx2-*eyfp*. For the latter strain, the intensity of the eYFP band continuously increased when the IPTG concentration was

Fig. 2. Comparison of eYFP synthesis in *C. glutamicum* with the newly constructed T7-based expression system and the pEKEx2 system using the *tac* promoter and the endogenous RNAP. The strains MB001/pEKEx2-*eyfp* (●/1), MB001/pJC1-P$_{tac}$-*eyfp* (∆/2), MB001(DE3)/pMKEx2 (◊/3), MB001/pMKEx2-*eyfp* (□/4) and MB001(DE3)/pMKEx2-*eyfp* (■/5) were grown aerobically in CGXII minimal medium with 4% (wt/vol) glucose using a Biolector system at 30°C and 1200 r.p.m. Target gene expression was induced 2 h after inoculation by addition of 0–250 µM IPTG.
A. 25 h after starting the cultivation, the maximal specific eYFP fluorescence (ratio of fluorescence emission at 532 nm and backscatter value at 620 nm) was determined. Mean values of at least three independent experiments and standard deviations are shown.
B. For protein analysis, cells were disrupted by beat-beating and equivalent amounts of total protein (10 µg) of the cell-free extracts were subjected to SDS-PAGE and visualized by staining with Coomassie Brilliant Blue. In addition, eYFP was detected by Western blotting with an polyclonal anti-GFP antibody. The arrows indicate the predicted size of 27.2 kDa for eYFP.
C. Cells were analysed by fluorescence microscopy and images were taken with an exposure time of 40 ms. The red bar represents a length of 5 µm.

Characterization of T7 RNAP-dependent expression system in C. glutamicum *with the heterologous target protein eYFP and comparison with P$_{tac}$-based expression at the single-cell level*

Flow cytometry was used to analyse *eyfp* expression at the single-cell level, allowing the detection of population heterogeneity (Figs 3 and S3). The gate used to define background fluorescence was set with *C. glutamicum* MB001(DE3)/pMKEx2, with 100% of the analysed cells falling into this gate (Fig. 3A). In the case of strain MB001/pEKEx2-*eyfp* (Fig. 3B), 7% of the cells cultivated in the absence of IPTG showed fluorescence above background, with an average intensity of 1.0×10^2, confirming the leakiness of the *tac* promoter used. When cultivated in the presence of 5, 10, 15, 25, 50, 100 and 250 µM IPTG, MB001/pEKEx2-*eyfp* cells formed subpopulations (Fig. 3E and Fig. S3A and C). At 250 µM IPTG, 19.5% of the cells showed a high average fluorescence signal of 2.63×10^4, whereas 78.5% of the cells had only a weak average fluorescence signal of 7.80×10^3, and 2% of the cells possessed only background fluorescence. The overall averaged fluorescence signal of MB001/pEKEx2-*eyfp* cells including all subpopulations was 1.13×10^4.

In the case of strain MB001/pJC1-P$_{tac}$-*eyfp* (Fig. 3C), which was only analysed after cultivation without and with 250 µM IPTG, more than 99% of the cells cultivated in the presence of 250 µM IPTG showed high fluorescence, with an average signal intensity of 7.38×10^3 and formed a homogenous population. But also in the absence of IPTG, about 90% of the cells showed a low fluorescence signal of 4.4×10^2 above background, confirming the results of the Western blot shown in Fig. 2B. As pEKEx2-*eyfp* and pJC1-P$_{tac}$-*eyfp* possess identical target gene expression determinants, the differences observed by flow cytometry presumably result from the different replicons. The vector

raised from 5 µM to 100 µM. The eYFP bands of MB001/pEKEx2-*eyfp* and MB001/pJC1-P$_{tac}$-*eyfp* in the presence of 250 µM IPTG were much fainter than those of strain MB001(DE3)/pMKEx2-*eyfp* in the presence of 50, 100 and 250 µM IPTG. As expected, no eYFP band was visible in the negative control strains MB001(DE3)/pMKEx2 and MB001/pMKEx2-*eyfp* in the presence of 250 µM IPTG. The fluorescence microscopy images shown in Fig. 2C were also in agreement with the results of the specific fluorescence measurements, the SDS polyacrylamide gels and the Western blots, with the most strongly fluorescent cells being those of strain MB001(DE3)/pMKEx2-*eyfp* cultivated in the presence of 250 µM IPTG.

6   *M. Kortmann, V. Kuhl, S. Klaffl and M. Bott*

Fig. 3. Analysis of heterologous eYFP production in the *C. glutamicum* strains MB001/pMKEx2-*eyfp* (A), MB001/pEKEx2-*eyfp* (B), MB001/pJC1-P*tac*-*eyfp* (C) and MB001(DE3)/pMKEx2-*eyfp* (D) at the single-cell level. The strains were cultivated for 24 h at 30°C in CGXII minimal medium with 4% (wt/vol) glucose using a Biolector system. Induction of *eyfp* expression was triggered by adding 250 μM IPTG to the cultures after 2 h. Pseudo-coloured dot plots from flow cytometry analysis (excitation at 488 nm, emission at 533 nm) of at least 100 000 cells of each strain displaying the eYFP fluorescence signal against the forward scatter signal (FSC) are shown. The gate used to define non-fluorescent cells was set with *C. glutamicum* MB001(DE3)/pMKEx2 with 100% of the cells falling into this gate (data not shown). The number inside the blot indicates the percentage of cells inside this gate. Panel E shows a histogram of the strains MB001/pEKEx2-*eyfp* (red) and MB001(DE3)/pMKEx2-*eyfp* (green). The number of cells is plotted against the eYFP fluorescence intensity. The dotted peaks show the measurement of the uninduced culture, the continuous line the cultures grown in the presence of 250 μM IPTG. The orange peak represents the background set with strain MB001(DE3)/pMKEx2.

pEKEx2 (Eikmanns *et al.*, 1991) contains the replicon from plasmid pBL1 (Santamaria *et al.*, 1984), whereas pJC1 (Cremer *et al.*, 1990) contains the replicon from plasmid pHM1519 (Miwa *et al.*, 1984), which presumably is identical with the one from plasmids pCG1 (Ozaki *et al.*, 1984), pSR1 (Yoshihama *et al.*, 1985) and pCG100 (Trautwetter and Blanco, 1991), as described previously (Nešvera and Pátek, 2008). Both replicons mediate replication in the rolling circle mode, but the pBL1 replicons belong to pIJ101/pJV1 family, whereas the pHM1519 replicon belongs to pNG2 family (Pátek and Nešvera, 2013). The copy number of pBL1 and similar plasmids

was estimated to be between 10 and 30 copies per chromosome (Miwa *et al.*, 1984; Santamaria *et al.*, 1984), and that of pCG100 was also reported to be about 30 copies per chromosome (Trautwetter and Blanco, 1991). Apparently, the pNM1519 replicon is more stable than the pBL1 replicon, at least in the case of the expression vectors used in our study.

In the case of strain MB001(DE3)/pMKEx2-*eyfp* (Fig. 3D), less than 1% of the cells cultivated in the absence of IPTG showed fluorescence slightly above background. The fluorescence of cells cultivated in the presence of 5, 10, 15, 25, 50, 100 and 250 μM IPTG is

shown in Fig. S3B and D. In the presence of 250 IPTG, 99.5% of the cells formed a very homogenous population, with an average fluorescence signal of about 5.22×10^4. Compared with *C. glutamicum* MB001/pEKEx2-*eyfp* and MB001/pJC1-P$_{tac}$-*eyfp*, the T7-based system showed a 4.6-fold and 7.1-fold higher eYFP signal after induction with 250 μM IPTG, respectively, whereas the signal in the uninduced state of the cells was at least 1.8-fold lower. These results confirm that the *C. glutamicum* T7 expression system allows tight repression of target gene expression in the absence of inducer, and a very uniform and strong expression level in the presence of inducer.

Comparison of T7 RNAP-dependent expression of eyfp *in* C. glutamicum *and* E. coli

To compare the T7 RNAP-dependent expression system of *C. glutamicum* MB001(DE3) with the well-established *E. coli* BL21(DE3) system, the production of eYFP was analysed in both strains transformed with pMKEx2-*eyfp* and cultivated in 2xTY medium supplemented with different IPTG concentrations using the BioLector system (Fig. 4). The specific fluorescence of the culture in the absence of IPTG was lower for *C. glutamicum* MB001(DE3)/pMKEx2-*eyfp* (< 0.001) than for *E. coli* BL21(DE3)/pMKEx2-*eyfp* (0.003). The negative controls *C. glutamicum* MB001/pMKEx2-*eyfp* and *E. coli* BL21(DE3)/pMKEx2 showed only background fluorescence independent of the absence and presence of 250 μM IPTG (Fig. 4A). For *C. glutamicum* MB001(DE3)/ pMKEx2-*eyfp* and *E. coli* BL21(DE3)/pMKEx2-*eyfp*, comparable maximal values of 0.26 ± 0.005 and 0.25 ± 0.002 were recorded for the specific eYFP fluorescence, but at different IPTG concentrations of 250 μM and 50 μM, respectively (Fig. 4A). Half-maximal specific fluorescence was obtained with 31 μM IPTG for strain MB001(DE3)/ pMKEx2-*eyfp* and with 11 μM IPTG for strain BL21(DE3)/ pMKEx2-*eypf*. This difference is probably due to the presence of lactose permease in *E. coli*, which presumably is involved in IPTG uptake and allows *E. coli* to obtain higher intracellular IPTG concentrations than a strain lacking *lacY* (Fernandez-Castane *et al.*, 2012). In contrast to *E. coli*, *C. glutamicum* is unable to grow on lactose, but is able to do so when harbouring the *E. coli lac* operon, including *lacY*, which is essential for lactose uptake (Brabetz *et al.*, 1991; 1993).

Fluorescence microscopy (Fig. 4B) revealed that in the case of strain *E. coli* BL21(DE3)/pMKEx2-*eyfp* and *C. glutamicum* MB001(DE3)/pMKEx2-*eyfp*, almost all cells were fluorescent when cultivated in the presence of 250 μM IPTG. Whereas fluorescence was equally distributed over the entire cell in the case of the *C. glutamicum* strain, the majority of poles appeared non-fluorescent in the case of *E. coli* strain. The images taken at 10 and

25 μM IPTG confirm the results shown in Fig. 4A that *E. coli* requires lower IPTG concentrations for maximal expression.

Fluorescence-activated cell sorting analysis of cells of *E. coli* BL21(DE3)/pMKEx2-*eyfp* and *C. glutamicum* MB001(DE3)/pMKEx2-*eyfp* cultivated with 0, 10, 25 and 250 μM IPTG are depicted in Figs 4C and S4. Of the *E. coli* cells, 92% cultivated with 250 μM IPTG revealed an increased fluorescence, with an average signal intensity of 5.2×10^4. In the case of *C. glutamicum*, more than 99% of the cells cultivated with 250 IPTG showed an increased fluorescence, with an average signal intensity of 2.8×10^4. In contrast to the *E. coli* cells, the *C. glutamicum* cells formed a much more homogeneous population. When calculating the average fluorescence intensity of all analysed cells, the value for *C. glutamicum* MB001(DE3)/pMKEx2-*eyfp* (2.8×10^4) was 1.8 times lower than the one for *E. coli* BL21(DE3)/pMKEx2-*eyfp* (5.0×10^4). The FACS analysis of the strains cultivated in the absence of IPTG confirmed a lower basal *eyfp* expression in the *C. glutamicum* strain compared with the *E. coli* strain. Of the *E. coli* BL21(DE3)/pMKEx2-*eyfp* population, 1.4% showed an eYFP fluorescence above background, but none of the *C. glutamicum* MB001(DE3)/pMKEx2-*eyfp* cells.

T7 RNAP-dependent overproduction of pyruvate kinase in C. glutamicum *and* E. coli

As an alternative target protein for analysing the properties of the newly established T7 expression system for *C. glutamicum*, we tested pyruvate kinase of *C. glutamicum*, which catalyses the conversion of phosphoenolpyruvate (PEP) and ADP to pyruvate and ATP. *Corynebacterium glutamicum* possesses a single *pyk* gene for pyruvate kinase (Gubler *et al.*, 1994), which was amplified by PCR from chromosomal DNA of *C. glutamicum* MB001 with the oligonucleotides Pyk-for and Pyk-rev and cloned into pMKEx2 using BamHI and BsrGI restriction sites. The resulting plasmid pMKEx2-*pyk* was transferred into *C. glutamicum* MB001(DE3) and *E. coli* BL21(DE3), and the overproduction of pyruvate kinase was analysed by measuring the specific activity in crude extract.

The results presented in Table 3 show that the expression of the *pyk* gene on plasmid pMKEx2-*pyk* in the absence of IPTG led to a small increase of the endogenous pyruvate kinase activity of 0.5 U mg^{-1} in the case of *C. glutamicum* MB001(DE3) and of 0.9 U mg^{-1} in the case of *E. coli* BL21(DE3). When cultivated in the presence of 250 μM IPTG, the pyruvate kinase activity increased more than 40-fold to 135 U mg^{-1} in *C. glutamicum* carrying pMKEx2-*pyk* and 14-fold in *E. coli* carrying pMKEx2-*pyk*. In agreement with these data, SDS-PAGE of the cell

8   *M. Kortmann, V. Kuhl, S. Klaffl and M. Bott*
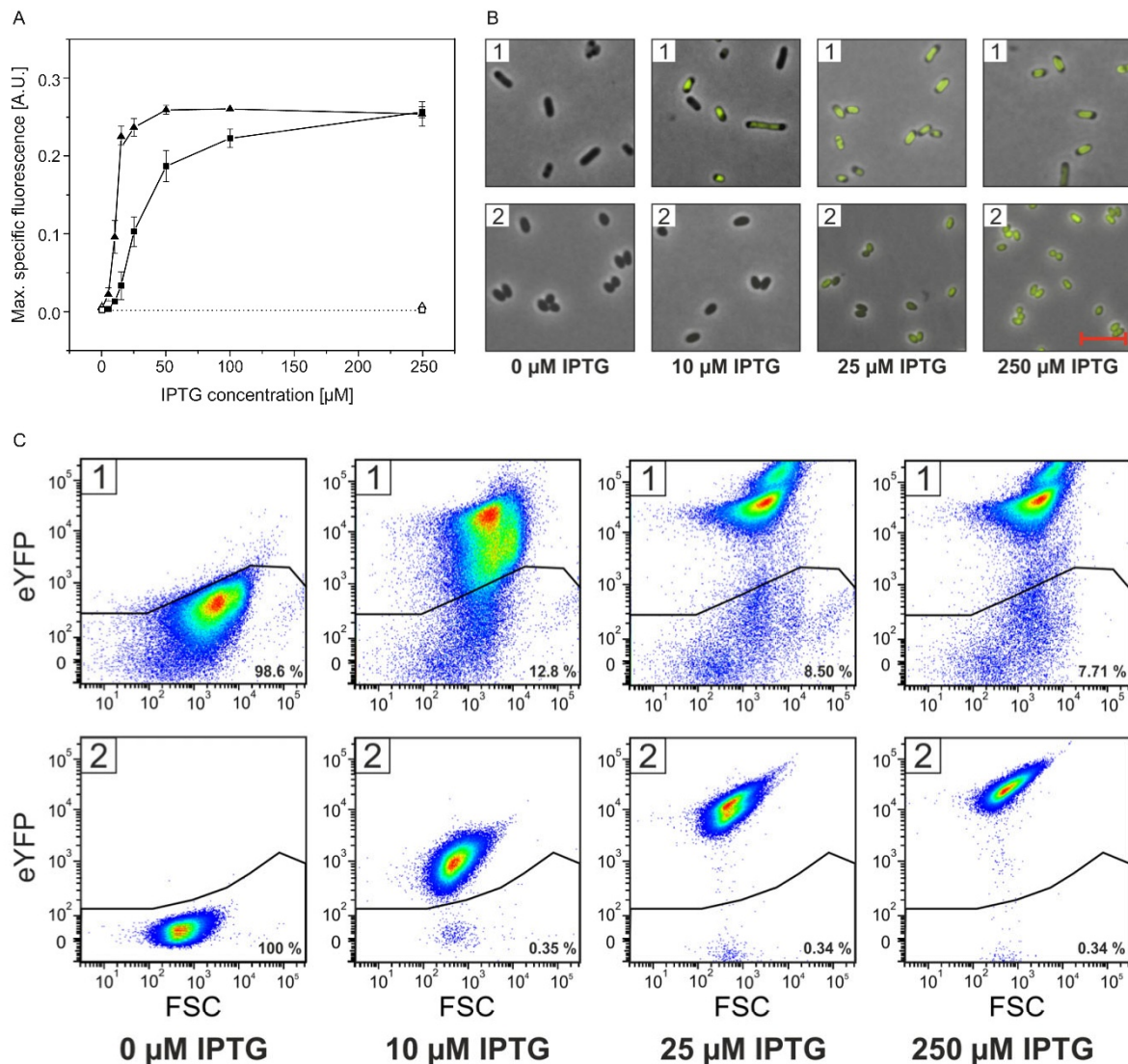
Fig. 4. T7 RNAP-dependent expression of *eyfp* in *C. glutamicum* and *E. coli*. The strains *C. glutamicum* MB001/pMKEx2-*eyfp* (□),
C. glutamicum MB001(DE3)/pMKEx2-*eyfp* (■), *E. coli* BL21(DE3)/pMKEx2 (△) and *E. coli* BL21(DE3)/pMKEx2-*eyfp* (▲) were cultivated for
24 h aerobically in 2xTY medium using a BioLector system at 1200 r.p.m. and either 30°C (*C. glutamicum*) or 37°C (*E. coli*). Gene expression
was induced 2 h after starting the cultivation by addition of 0–250 μM IPTG.
A. After 24 h, the maximal specific eYFP fluorescence was determined (ratio of fluorescence emission at 532 nm and backscatter value at
620 nm). Mean values and standard deviations of at least three independent replicates are shown.
B. Fluorescence microscopy images of *E. coli* BL21(DE3)/pMKEx2-*eyfp* (1) and *C. glutamicum* MB001(DE3)/pMKEx2-*eyfp* (2) cultivated with
different IPTG concentrations. Images were taken with an exposure time of 40 ms. The red bar represents a length of 5 μm.
C. Flow cytometry analysis of *E. coli* BL21(DE3)/pMKEx2-*eyfp* (1) and *C. glutamicum* MB001(DE3)/pMKEx2-*eyfp* (2) cultivated with different
IPTG concentrations. Pseudo-coloured dot plots of eYFP fluorescence versus forward scatter are shown.

extracts revealed a higher pyruvate kinase protein level in
C. glutamicum compared with *E. coli* (Fig. 5). The more
efficient overproduction of pyruvate kinase in the homolo-
gous host compared with *E. coli* might be due to a more
efficient translation caused by differences in codon usage
between the two species.

Concluding remarks

In this study, a T7 RNAP-based expression system
was developed for *C. glutamicum*. It is based on strain
MB001(DE3), in which gene *1* encoding T7 RNAP is
chromosomally encoded under control of the *lac*UV5

**Table 3.** Pyruvate kinase activity of different overexpression strains.

Strain	Plasmid	Pyruvate kinase activity (U/mg) − IPTG	Increase (x-fold)[a]	Pyruvate kinase activity (U/mg) + 250 μM IPTG	Increase (x-fold)[b]
C. glutamicum MB001(DE3)	pMKEx2	n.d.	n.a.	2.6 ± 0.7	n.a.
C. glutamicum MB001(DE3)	pMKEx2-*pyk*	3.1 ± 0.2	1.2	135 ± 14	43.6
E. coli BL21(DE3)	pMKEx2	n.d.	n.a.	0.6 ± 0.1	n.a.
E. coli BL21(DE3)	pMKEx2-*pyk*	1.5 ± 0.2	2.8	20.9 ± 7.1	13.9

Specific activity was measured in crude extracts of cells harvested 4 h after addition or non-addition of IPTG. Mean values and standard deviations of at least three independent measurements are shown. n.d., not determined; n.a., not applicable.
a. pMKEx2-*pyk* −IPTG versus pMKEx2 +IPTG.
b. pMKEx2-*pyk* −IPTG versus +IPTG.

promoter, and the expression vector pMKEx2 carrying the T7*lac* promoter. Thus, both gene *1* and the target gene are repressed by LacI. Using *eyfp* as target gene, the new system allowed tightly IPTG-regulatable gene expression to levels that were about four times higher than those obtained with expression vectors using the *tac* promoter and the endogenous RNA polymerase. It thus probably represents the strongest overexpression system currently available for *C. glutamicum*. A particular feature of the new system was revealed by flow cytometry: IPTG induction led to the formation of very homogeneous populations, in which about 99% of the cells showed high expression of the target protein. Half-maximal induction was obtained with IPTG concentrations between 20 and 30 μM, depending on the medium used. The T7 RNAP-based system can be useful for the overproduction of proteins for subsequent purification, but also for metabolic engineering studies in which strong overproduction of certain genes is required.
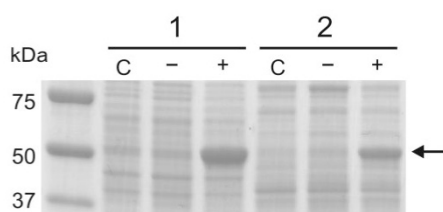
Fig. 5. Coomassie-stained SDS-polyacrylamide gel for analysing overproduction of pyruvate kinase in *C. glutamicum* MB001(DE3)/pMKEx2-*pyk* (1) and *E. coli* BL21(DE3)/pMKEx2-*pyk* (2). The strains were cultivated in M9 medium with 2% (wt/vol) glucose (*E. coli*) or in CGXII medium with 4% (wt/vol) glucose (*C. glutamicum*). Strains labelled with '−' were grown without IPTG, whereas strains labelled '+' were supplemented with 250 μM IPTG when the cultures had reached an OD$_{600}$ of 2. When the cultures had reached an OD$_{600}$ of 5, cells were harvested and used for preparation of cell extracts. Ten microgram total protein of these extracts were subjected to SDS-PAGE. The samples labelled with 'C' represent control strains, either *C. glutamicum* MB001(DE3)/pMKEx2 (1) or *E. coli* BL21(DE3)/pMKEx2 (2), that were cultivated in the presence of 250 μM IPTG. The arrow indicates the predicted size for *C. glutamicum* pyruvate kinase (54.4 kDa).

Experimental procedures

Bacterial strains, plasmids and growth conditions

All bacterial strains and plasmids used in this study are listed in Table 1. *Escherichia coli* was grown at 37°C in a complex tryptone-yeast extract medium (2xTY) or in M9 minimal medium with 4% (wt/vol) glucose (Sambrook and Russell, 2001). *Corynebacterium glutamicum* was routinely cultivated at 30°C in 2xTY medium or in defined CGXII minimal medium with 4% (wt/vol) glucose (Keilhauer *et al.*, 1993). If necessary, the media were supplemented with 50 mg l^{-1} kanamycin for *E. coli* and 25 mg l^{-1} kanamycin for *C. glutamicum*. *Escherichia coli* DH5α was used for plasmid construction, *E. coli* BL21(DE3) and *C. glutamicum* MB001(DE3) for overproduction of recombinant proteins. Cultures were inoculated to an optical density at 600 nm (OD$_{600}$) of 1, and target gene induction was triggered by adding 0–250 μM IPTG to the culture at an OD$_{600}$ of 2. To analyse *eyfp* expression, cells were grown as 800 μl cultures in 48-well microtitre plates (Flowerplates, m2p-labs, Baesweiler, Germany) at 80% humidity and 1200 r.p.m. using a BioLector system (m2p-labs, Baesweiler, Germany), which allows isochronal measurement of cell growth as backscattering light intensity at a wavelength of 620 nm and of eYFP fluorescence (ex/em 510/532 nm). For the overproduction of pyruvate kinase, all strains were cultivated at 120 r.p.m. and the required temperature in baffled 500 ml shake flasks with 50 ml CGXII or M9 medium, respectively.

Recombinant DNA techniques

Standard DNA and cloning techniques were performed as described (Sambrook and Russell, 2001). Oligonucleotides were purchased from Eurofins MWG Operon (Ebersberg, Germany). Restriction enzymes (New England Biolabs, Frankfurt, Germany), shrimp alkaline phosphatase and Klenow fragment (both Thermo Scientific, Schwerte, Germany) were used according to the recommendations of the supplier. Introduction of a single point mutation in a pJC1 derivative was performed with the QuikChange Lightning Kit (Agilent Technologies, Waldbronn, Germany). Plasmid DNA of *E. coli* was isolated with QIAprep Spin Miniprep Kit (Qiagen, Hilden, Germany). Plasmid isolation from *C. glutamicum* was carried out with the same kit, but cells were pre-incubated in buffer P1 supplemented with 15 mg ml^{-1} (wt/vol) lysozyme for 2 h at 30°C. Purification of

10   *M. Kortmann, V. Kuhl, S. Klaffl and M. Bott*

DNA fragments from agarose gels was done using the QIAex gel elution kit (Qiagen). RbCl-competent *E. coli* cells were transformed with plasmid DNA by the heat-shock method of Hanahan (1983), and *C. glutamicum* cells were transformed with plasmid DNA by electroporation as described previously (Tauch *et al.*, 2002).

For the construction of plasmid pJC1-P$_{tac}$-*eyfp*, the plasmid pJC1-venus-term (Baumgart *et al.*, 2013a) was cut by NdeI and SalI to obtain a 6.58 kb fragment containing the same backbone (kanamycin resistance cassette, pCG1 replicon for *C. glutamicum*, pACYC177 replicon for *E. coli*) as pMKEx2. The expression cassette from plasmid pEKEx2-*eyfp* was amplified with oligonucleotides pEKEx-for and pEKEx-rev to obtain a 2.31 kb fragment containing the target gene *eyfp* under transcriptional control of the *tac* promoter and the *lacI* gene. After digestion with NdeI and SalI, this fragment was ligated with the 6.58 kb fragment from pJC1-venus-term to obtain pJC1-P$_{tac}$-*eyfp*.

Protein analysis

Recombinant protein production was analysed by SDS-PAGE. Cells were harvested by centrifugation and washed twice with lysis buffer (10 mM Tris-HCl, pH 8.0, 25 mM MgCl$_2$, 200 mM NaCl). Afterwards, *C. glutamicum* and *E. coli* cells were disintegrated by beat beating using a Precellys 24 device (Peqlab Biotechnologie, Erlangen, Germany). Intact cells and cell debris were sedimented by centrifugation (13 000 *g*, 20 min), and the supernatant was used further. The concentration of intracellular proteins was determined with the BCA assay (BC Assay Protein Quantitation Kit, Uptima, Interchim, Montlucon, France) as described (Smith *et al.*, 1985). Electrophoretic separation of proteins on SDS-polyacrylamide gels was performed by a standard procedure (Laemmli, 1970), and the gels were stained with Coomassie Brilliant Blue G-250 dye or used further for Western blot analysis. Immunological detection of eYFP was performed by using a polyclonal anti-GFP antibody (ab290, Abcam, Cambridge, UK) and a Cy5-conjugated goat-anti-rabbit antibody (GE Healthcare). Visualization and recording of fluorescent bands were performed using a Typhoon scanner (GE Healthcare) and the programme IMAGEQUANT TL 7.0.

Fluorescence microscopy

For fluorescence microscopy, cells were fixed on soft-agarose coated glass slides. Images were taken on a Zeiss Axioplan 2 imaging microscope that was equipped with an AxioCam MRm camera and a Plan-Apochromat 100×, 1.40 Oil Ph3 immersion objective. Digital images were acquired and analysed with the AXIOVISION 4.6 software (Zeiss, Göttingen, Germany).

Flow cytometry

Cells were grown under appropriate conditions in a BioLector system, harvested after 24 h and diluted to an OD$_{600}$ below 0.1 with sterile phosphate-buffered saline (37 mM NaCl, 2.7 mM KaCl, 10 mM Na$_2$HPO$_4$, 1.8 mM KH$_2$PO$_4$, pH 7.4). Expression of *eyfp* was analysed using a FACS ARIA II high-speed cell sorter (BD Biosciences, Franklin Lakes, NJ, USA) and the BD DIVA 6.1.3 software by measuring the eYFP fluorescence of single cells with an excitation wavelength of 488 nm and an emission wavelength of 533 ± 15 nm at a sample pressure of 70 psi. A threshold was set to exclude non-bacterial particles on the basis of forward versus side scatter area. There were 100 000 cells analysed for each measurement with a flow rate of 2000–4000 cells/s.

Pyruvate kinase assay

Pyruvate kinase activity was determined spectrophotometrically using a coupled enzymatic assay with L-lactate dehydrogenase. The rate of NADH consumption was measured using an Infinite 200 PRO reader (Tecan, Männedorf, Switzerland) as the decrease of NADH absorbance at 340 nm ($\varepsilon_{NADH} = 6.22$ mM^{-1} cm^{-1}). The assay mixture contained 100 mM Tris-HCl buffer (pH 7.3), 15 mM MgCl$_2$, 1 mM ADP, 0.4 mM NADH, 5 U L-lactate dehydrogenase from pig heart, and 10 or 20 µl of cell extract (corresponding to 0.1–0.2 mg protein) in a total volume of 150 µl. The reaction was started by addition of 12 mM PEP. One unit of pyruvate kinase activity is defined as the amount of enzyme that converted 1 µmol of PEP to pyruvate per minute.

Conflict of interest

None declared.

References

Arvani, S., Markert, A., Loeschcke, A., Jaeger, K.E., and Drepper, T. (2012) A T7 RNA polymerase-based toolkit for the concerted expression of clustered genes. *J Biotechnol* **159:** 162–171.

Baneyx, F. (1999) Recombinant protein expression in *Escherichia coli*. *Curr Opin Biotechnol* **10:** 411–421.

Bansal-Mutalik, R., and Nikaido, H. (2011) Quantitative lipid composition of cell envelopes of *Corynebacterium glutamicum* elucidated through reverse micelle extraction. *Proc Natl Acad Sci USA* **108:** 15360–15365.

Barnard, G.C., Henderson, G.E., Srinivasan, S., and Gerngross, T.U. (2004) High level recombinant protein expression in *Ralstonia eutropha* using T7 RNA polymerase based amplification. *Protein Expr Purif* **38:** 264–271.

Baumgart, M., Luder, K., Grover, S., Gätgens, C., Besra, G.S., and Frunzke, J. (2013a) IpsA, a novel LacI-type regulator, is required for inositol-derived lipid formation in Corynebacteria and Mycobacteria. *BMC Biol* **11:** 122.

Baumgart, M., Unthan, S., Rückert, C., Sivalingam, J., Grünberger, A., Kalinowski, J., *et al.* (2013b) Construction of a prophage-free variant of *Corynebacterium glutamicum* ATCC 13032 for use as a platform strain for basic research and industrial biotechnology. *Appl Environ Microbiol* **79:** 6006–6015.

Becker, J., and Wittmann, C. (2012) Bio-based production of chemicals, materials and fuels -*Corynebacterium glutamicum* as versatile cell factory. *Curr Opin Biotechnol* **23:** 631–640.

Blombach, B., Riester, T., Wieschalka, S., Ziert, C., Youn, J.W., Wendisch, V.F., and Eikmanns, B.J. (2011) *Corynebacterium glutamicum* tailored for efficient isobutanol production. *Appl Environ Microbiol* **77:** 3300–3310.

Brabetz, W., Liebl, W., and Schleifer, K.H. (1991) Studies on the utilization of lactose by *Corynebacterium glutamicum*, bearing the lactose operon of *Escherichia coli*. *Arch Microbiol* **155:** 607–612.

Brabetz, W., Liebl, W., and Schleifer, K.H. (1993) Lactose permease of *Escherichia coli* catalyzes active beta-galactoside transport in a gram-positive bacterium. *J Bacteriol* **175:** 7488–7491.

Brunschwig, E., and Darzins, A. (1992) A two-component T7 system for the overexpression of genes in *Pseudomonas aeruginosa*. *Gene* **111:** 35–41.

Burkovski, A. (ed.) (2008) *Corynebacteria: Genomics and Molecular Biology*. Norfolk, UK: Caister Academic Press.

Chamberlin, M., and Ring, J. (1973) Characterization of T7-specific ribonucleic acid polymerase: I. General properties of the enzymatic reaction and the template specificity of the enzyme. *J Biol Chem* **248:** 2235–2244.

Chen, R. (2012) Bacterial expression systems for recombinant protein production: *E. coli* and beyond. *Biotechnol Adv* **30:** 1102–1107.

Cremer, J., Eggeling, L., and Sahm, H. (1990) Cloning the *dapA dapB* cluster of the lysine-secreting bacterium *Corynebacterium glutamicum*. *Mol Gen Genet* **220:** 478–480.

Demain, A.L., and Vaishnav, P. (2009) Production of recombinant proteins by microbes and higher organisms. *Biotechnol Adv* **27:** 297–306.

Dubendorff, J.W., and Studier, F.W. (1991) Controlling basal expression in an inducible T7 expression system by blocking the target T7 promoter with *lac* repressor. *J Mol Biol* **219:** 45–59.

Eggeling, L., and Bott, M. (eds) (2005) *Handbook of Corynebacterium glutamicum*. Boca Raton, FL, USA: CRC Press, Taylor and Francis Group.

Eggeling, L., and Reyes, O. (2005) Experiments. In *Handbook of Corynebacterium Glutamicum.* Eggeling, L., and Bott, M. (eds). Boca Raton, FL, USA: CRC Press, Taylor and Francis Group, pp. 535–566.

Eikmanns, B.J., Kleinertz, E., Liebl, W., and Sahm, H. (1991) A family of *Corynebacterium glutamicum/Escherichia coli* shuttle vectors for cloning, controlled gene expression, and promoter probing. *Gene* **102:** 93–98.

Equbal, M.J., Srivastava, P., Agarwal, G.P., and Deb, J.K. (2013) Novel expression system for *Corynebacterium acetoacidophilum* and *Escherichia coli* based on the T7 RNA polymerase-dependent promoter. *Appl Microbiol Biotechnol* **97:** 7755–7766.

Fernandez-Castane, A., Vine, C.E., Caminal, G., and Lopez-Santin, J. (2012) Evidencing the role of lactose permease in IPTG uptake by *Escherichia coli* in fed-batch high cell density cultures. *J Biotechnol* **157:** 391–398.

Gamer, M., Frode, D., Biedendieck, R., Stammen, S., and Jahn, D. (2009) A T7 RNA polymerase-dependent gene expression system for *Bacillus megaterium*. *Appl Microbiol Biotechnol* **82:** 1195–1203.

Gubler, M., Jetten, M., Lee, S.H., and Sinskey, A.J. (1994) Cloning of the pyruvate kinase gene (*pyk*) of *Corynebacterium glutamicum* and site-specific inactivation of *pyk* in a lysine-producing *Corynebacterium lactofermentum* strain. *Appl Environ Microbiol* **60:** 2494–2500.

Hanahan, D. (1983) Studies on transformation of *Escherichia coli* with plasmids. *J Mol Biol* **166:** 557–580.

Hentschel, E., Will, C., Mustafi, N., Burkovski, A., Rehm, N., and Frunzke, J. (2013) Destabilized eYFP variants for dynamic gene expression studies in *Corynebacterium glutamicum*. *Microb Biotechnol* **6:** 196–201.

Herrero, M., de Lorenzo, V., Ensley, B., and Timmis, K.N. (1993) A T7 RNA polymerase-based system for the construction of *Pseudomonas* strains with phenotypes dependent on TOL-meta pathway effectors. *Gene* **134:** 103–106.

Inui, M., Kawaguchi, H., Murakami, S., Vertes, A.A., and Yukawa, H. (2004) Metabolic engineering of *Corynebacterium glutamicum* for fuel ethanol production under oxygen-deprivation conditions. *J Mol Microbiol Biotechnol* **8:** 243–254.

Katzke, N., Arvani, S., Bergmann, R., Circolone, F., Markert, A., Svensson, V., *et al.* (2010) A novel T7 RNA polymerase dependent expression system for high-level protein production in the phototrophic bacterium *Rhodobacter capsulatus*. *Protein Expr Purif* **69:** 137–146.

Keilhauer, C., Eggeling, L., and Sahm, H. (1993) Isoleucine synthesis in *Corynebacterium glutamicum*: molecular analysis of the *ilvB-ilvN-ilvC* operon. *J Bacteriol* **175:** 5595–5603.

Kikuchi, Y., Itaya, H., Date, M., Matsui, K., and Wu, L.F. (2008) Production of *Chryseobacterium proteolyticum* protein-glutaminase using the twin-arginine translocation pathway in *Corynebacterium glutamicum*. *Appl Microbiol Biotechnol* **78:** 67–74.

Kind, S., and Wittmann, C. (2011) Bio-based production of the platform chemical 1,5-diaminopentane. *Appl Microbiol Biotechnol* **91:** 1287–1296.

Kirchner, O., and Tauch, A. (2003) Tools for genetic engineering in the amino acid-producing bacterium *Corynebacterium glutamicum*. *J Biotechnol* **104:** 287–299.

Laemmli, U.K. (1970) Cleavage of structural proteins during the assembly of the head of bacteriophage T4. *Nature* **227:** 680–685.

Laneelle, M.A., Tropis, M., and Daffe, M. (2013) Current knowledge on mycolic acids in *Corynebacterium glutamicum* and their relevance for biotechnological processes. *Appl Microbiol Biotechnol* **97:** 9923–9930.

Litsanov, B., Brocker, M., and Bott, M. (2012a) Toward homosuccinate fermentation: metabolic engineering of *Corynebacterium glutamicum* for anaerobic production of

12   *M. Kortmann, V. Kuhl, S. Klaffl and M. Bott*

succinate from glucose and formate. *Appl Environ Microbiol* **78:** 3325–3337.

Litsanov, B., Kabus, A., Brocker, M., and Bott, M. (2012b) Efficient aerobic succinate production from glucose in minimal medium with *Corynebacterium glutamicum*. *Microb Biotechnol* **5:** 116–128.

Lussier, F.X., Denis, F., and Shareck, F. (2010) Adaptation of the highly productive T7 expression system to *Streptomyces lividans*. *Appl Environ Microbiol* **76:** 967–970.

Lyakhov, D.L., He, B., Zhang, X., Studier, F.W., Dunn, J.J., and McAllister, W.T. (1998) Pausing and termination by bacteriophage T7 RNA polymerase. *J Mol Biol* **280:** 201–213.

Macdonald, L.E., Durbin, R.K., Dunn, J.J., and McAllister, W.T. (1994) Characterization of two types of termination signal for bacteriophage T7 RNA polymerase. *J Mol Biol* **238:** 145–158.

Marchand, C.H., Salmeron, C., Bou Raad, R., Meniche, X., Chami, M., Masi, M., *et al.* (2012) Biochemical disclosure of the mycolate outer membrane of *Corynebacterium glutamicum*. *J Bacteriol* **194:** 587–597.

Matsuda, Y., Itaya, H., Kitahara, Y., Theresia, N.M., Kutukova, E.A., Yomantas, Y.A., *et al.* (2014) Double mutation of cell wall proteins CspB and PBP1a increases secretion of the antibody Fab fragment from *Corynebacterium glutamicum*. *Microb Cell Fact* **13:** 56.

Mimitsuka, T., Sawai, H., Hatsu, M., and Yamada, K. (2007) Metabolic engineering of *Corynebacterium glutamicum* for cadaverine fermentation. *Biosci Biotechnol Biochem* **71:** 2130–2135.

Miwa, K., Matsui, H., Terabe, M., Nakamori, S., Sano, K., and Momose, H. (1984) Cryptic plasmids in glutamic acid-producing bacteria. *Agric Biol Chem* **48:** 2901–2903.

Nešvera, J., and Pátek, M. (2008) Plasmids and promoters in corynebacteria and their applications. In *Corynebacteria: Genomics and Molecular Biology*. Burkovski, A. (ed.). Norfolk, UK: Caister Academic Press, pp. 111–154.

Nesvera, J., and Patek, M. (2011) Tools for genetic manipulations in *Corynebacterium glutamicum* and their applications. *Appl Microbiol Biotechnol* **90:** 1641–1654.

Niebisch, A., and Bott, M. (2001) Molecular analysis of the cytochrome bc_1-aa_3 branch of the *Corynebacterium glutamicum* respiratory chain containing an unusual diheme cytochrome c_1. *Arch Microbiol* **175:** 282–294.

Okino, S., Noburyu, R., Suda, M., Jojima, T., Inui, M., and Yukawa, H. (2008) An efficient succinic acid production process in a metabolically engineered *Corynebacterium glutamicum* strain. *Appl Microbiol Biotechnol* **81:** 459–464.

Ozaki, A., Katsumata, R., Oka, T., and Furuya, A. (1984) Functional expression of the genes of *Escherichia coli* in gram-positive *Corynebacterium glutamicum*. *Mol Gen Genet* **196:** 175–178.

Pátek, M., and Nešvera, J. (2013) Promoters and plasmid vectors of *Corynebacterium glutamicum*. In *Corynebacterium Glutamicum: Biology and Biotechnology*. Yukawa, H., and Inui, M. (eds). Berlin, Heidelberg, Germany: Springer-Verlag, pp. 51–88.

Patek, M., Holatko, J., Busche, T., Kalinowski, J., and Nesvera, J. (2013) *Corynebacterium glutamicum* promoters: a practical approach. *Microb Biotechnol* **6:** 103–117.

Perez-Jimenez, R., Garcia-Manyes, S., Ainavarapu, S.R., and Fernandez, J.M. (2006) Mechanical unfolding pathways of the enhanced yellow fluorescent protein revealed by single molecule force spectroscopy. *J Biol Chem* **281:** 40010–40014.

Sambrook, J., and Russell, D. (2001) *Molecular Cloning: A Laboratory Manual*. Cold Spring Harbor, NY, USA: Cold Spring Harbor Laboratory Press.

Santamaria, R., Gil, J.A., Mesas, J.M., and Martin, J.F. (1984) Characterization of an endogenous plasmid and development of cloning vectors and a transformation system in *Brevibacterium lactofermentum*. *J Gen Microbiol* **130:** 2237–2246.

Schäfer, A., Tauch, A., Jäger, W., Kalinowski, J., Thierbach, G., and Pühler, A. (1994) Small mobilizable multipurpose cloning vectors derived from the *Escherichia coli* plasmids pK18 and pK19 – selection of defined deletions in the chromosome of *Corynebacterium glutamicum*. *Gene* **145:** 69–73.

Scheele, S., Oertel, D., Bongaerts, J., Evers, S., Hellmuth, H., Maurer, K.H., *et al.* (2013) Secretory production of an FAD cofactor-containing cytosolic enzyme (sorbitol-xylitol oxidase from *Streptomyces coelicolor*) using the twin-arginine translocation (Tat) pathway of *Corynebacterium glutamicum*. *Microb Biotechnol* **6:** 202–206.

Schneider, J., and Wendisch, V.F. (2011) Biotechnological production of polyamines by bacteria: recent achievements and future perspectives. *Appl Microbiol Biotechnol* **91:** 17–30.

Smith, K.M., Cho, K.M., and Liao, J.C. (2010) Engineering *Corynebacterium glutamicum* for isobutanol production. *Appl Microbiol Biotechnol* **87:** 1045–1055.

Smith, P.K., Krohn, R.I., Hermanson, G.T., Mallia, A.K., Gartner, F.H., Provenzano, M.D., *et al.* (1985) Measurement of protein using bicinchoninic acid. *Anal Biochem* **150:** 76–85.

Stäbler, N., Oikawa, T., Bott, M., and Eggeling, L. (2011) *Corynebacterium glutamicum* as a host for synthesis and export of D-amino acids. *J Bacteriol* **193:** 1702–1709.

Stolz, M., Peters-Wendisch, P., Etterich, H., Gerharz, T., Faurie, R., Sahm, H., *et al.* (2007) Reduced folate supply as a key to enhanced L-serine production by *Corynebacterium glutamicum*. *Appl Environ Microbiol* **73:** 750–755.

Studier, F.W., and Moffatt, B.A. (1986) Use of bacteriophage T7 RNA polymerase to direct selective high-level expression of cloned genes. *J Mol Biol* **189:** 113–130.

Tauch, A., Kirchner, O., Löffler, B., Gotker, S., Pühler, A., and Kalinowski, J. (2002) Efficient electrotransformation of *Corynebacterium diphtheriae* with a mini-replicon derived from the *Corynebacterium glutamicum* plasmid pGA1. *Curr Microbiol* **45:** 362–367.

Terpe, K. (2006) Overview of bacterial expression systems for heterologous protein production: from molecular and biochemical fundamentals to commercial systems. *Appl Microbiol Biotechnol* **72:** 211–222.

Trautwetter, A., and Blanco, C. (1991) Structural organization of the *Corynebacterium glutamicum* plasmid pCG100. *J Gen Microbiol* **137:** 2093–2101.

Vogt, M., Haas, S., Klaffl, S., Polen, T., Eggeling, L., van Ooyen, J., and Bott, M. (2013) Pushing product formation

to its limit: metabolic engineering of *Corynebacterium glutamicum* for L-leucine overproduction. *Metab Eng* **22:** 40–52.

Wendisch, V.F., Bott, M., and Eikmanns, B.J. (2006) Metabolic engineering of *Escherichia coli* and *Corynebacterium glutamicum* for biotechnological production of organic acids and amino acids. *Curr Opin Microbiol* **9:** 268–274.

Wieschalka, S., Blombach, B., Bott, M., and Eikmanns, B.J. (2013) Bio-based production of organic acids with *Corynebacterium glutamicum. Microb Biotechnol* **6:** 87–102.

Yamamoto, S., Suda, M., Niimi, S., Inui, M., and Yukawa, H. (2013) Strain optimization for efficient isobutanol production using *Corynebacterium glutamicum* under oxygen deprivation. *Biotechnol Bioeng* **110:** 2938–2948.

Yoshihama, M., Higashiro, K., Rao, E.A., Akedo, M., Shanabruch, W.G., Follettie, M.T., *et al.* (1985) Cloning vector system for *Corynebacterium glutamicum. J Bacteriol* **162:** 591–597.

Yukawa, H., and Inui, M. (eds) (2013) *Corynebacterium glutamicum: Biology and Biotechnology.* Heidelberg, Germany: Springer.

Supporting information

Additional Supporting Information may be found in the online version of this article at the publisher's web-site:

Fig. S1. Sequence of the 4,46 kb fragment amplified from the genome of *E. coli* BL21(DE3) and inserted into the intergenic region of cg1122-cg1121 of *C. glutamicum* MB001. 70 bp and 85 bp of the flanking *C. glutamicum* genome region are also shown with a grey background. The XhoI and EcoRI restriction sites used for cloning are shown in bold.

Fig. S2. Growth of *C. glutamicum* MB001/pEKEx2-*eyfp* (A) and *C. glutamicum* MB001(DE3)/pMKEx2-*eyfp* (B). The strains were inoculated to an OD600 of 1 and cultivated for 24 h at 30°C in CGXII minimal medium with 4% (wt/vol) glucose using a BioLector system. Induction of *eyfp* expression was triggered by adding 0 μM (■), 50 μM (), 100 μM ●(▲), or 250 μM (◊) IPTG to the cultures after 2 h.

Fig. S3. Analysis of heterologous eYFP production in the *C. glutamicum* strains MB001/pEKEx2-*eyfp* (A) and MB001(DE3)/pMKEx2-*eyfp* (B) at the single-cell level by flow cytometry. The strains were cultivated for 24 h at 30°C in CGXII minimal medium with 4% (wt/vol) glucose using a BioLector system. Induction of *eyfp* expression was triggered by adding the indicated concentrations of IPTG to the cultures after 2 h. Dot blots from FACS analysis (excitation at 488 nm, emission at 533 nm) of at least 100 000 cells of each strain displaying the eYFP fluorescence signal against the forward scatter signal (FSC). The gate used to define non-fluorescent cells was set with *C. glutamicum* MB001(DE3)/pMKEx2 with 100% of the cells falling into this gate (data not shown). The number inside the panels indicates the percentage of non-fluorescent cells inside this gate. In panels C and D, histograms of strains MB001/pEKEx2-*eyfp* (C) and MB001(DE3)/pMKEx2-*eyfp* (D) cultivated without IPTG or in the presence of 10, 25 and 250 μM IPTG are shown. The orange peaks indicate the background fluorescence set with strain MB001(DE3)/pMKEx2. The number of cells is plotted versus eYFP fluorescence.

Fig. S4. Analysis of heterologous eYFP production in *C. glutamicum* MB001(DE3)/pMKEx2-*eyfp* (A) and *E. coli* BL21(DE3)/pEKEx2-*eyfp* (B) at the single-cell level. The strains were cultivated for 24 h at 30°C in 2xTY medium using a BioLector system. Induction of *eyfp* expression was triggered by adding the indicated concentrations of IPTG to the cultures after 2 h. Dot plots from FACS analysis (excitation at 488 nm, emission at 533 nm) of at least 100 000 cells of each strain displaying the eYFP signal against the forward scatter signal (FSC) are shown. The gate used to define non-fluorescent cells was set with *C. glutamicum* MB001/pMKEx2 or *E. coli* BL21(DE3)/pMKEx2, respectively, with 100% of the cells falling into this gate (data not shown). The number inside the panels indicates the percentage of non-fluorescent cells. In panels C and D, histograms of strains *E. coli* BL21(DE3)/pMKEx2-*eyfp* (C) and *C. glutamicum* MB001(DE3)/pMKEx2-*eyfp* (D) cultivated without IPTG or in the presence of 10, 25 and 250 μM IPTG are shown. The orange peaks indicate the background fluorescence set with strain *E. coli* BL21(DE3)/pMKEx2 and *C. glutamicum* MB001(DE3)/pMKEx2. The number of cells is plotted versus eYFP fluorescence.

3.1.1   Supplementary material "A chromosomally encoded T7 RNA polymerase-dependent gene expression system for *Corynebacterium glutamicum*: construction and comparative evaluation at the single-cell level"

Kortmann M., Kuhl V., Klaffl S., Bott M.*

IBG-1: Biotechnology, Forschungszentrum Jülich, Jülich, Germany

*Corresponding author

Supplemental material to Kortmann et al. 2014

```
cg1122 <--
GGAAATAGGGGCCTTTTGTTGTCTTCTCCTGGAGGCTATTTAAGAAGTTTAAATTGTGTCCATGAGTTCG
CTCGAGAACTGCGCAACTCGTGAAAGGTAGGCGGATCCAGATCCCGGACACCATCGAATGGCGCAAAACC
TTTCGCGGTATGGCATGATAGCGCCCGGAAGAGAGTCAATTCAGGGTGGTGAATGTGAAACCAGTAACGT
TATACGATGTCGCAGAGTATGCCGGTGTCTCTTATCAGACCGTTTCCCGCGTGGTGAACCAGGCCAGCCA
CGTTTCTGCGAAAACGCGGGAAAAAGTGGAAGCGGCGATGGCGGAGCTGAATTACATTCCCAACCGCGTG
GCACAACAACTGGCGGGCAAACAGTCGTTGCTGATTGGCGTTGCCACCTCCAGTCTGGCCCTGCACGCGC
CGTCGCAAATTGTCGCGGCGATTAAATCTCGCGCCGATCAACTGGGTGCCAGCGTGGTGGTGTCGATGGT
AGAACGAAGCGGCGTCGAAGCCTGTAAAGCGGCGGTGCACAATCTTCTCGCGCAACGCGTCAGTGGGCTG
ATCATTAACTATCCGCTGGATGACCAGGATGCCATTGCTGTGGAAGCTGCCTGCACTAATGTTCCGGCGT
TATTTCTTGATGTCTCTGACCAGACACCCATCAACAGTATTATTTTCTCCCATGAAGACGGTACGCGACT
GGGCGTGGAGCATCTGGTCGCATTGGGTCACCAGCAAATCGCGCTGTTAGCGGGCCCATTAAGTTCTGTC
TCGGCGCGTCTGCGTCTGGCTGGCTGGCATAAATATCTCACTCGCAATCAAATTCAGCCGATAGCGGAAC
GGGAAGGCGACTGGAGTGCCATGTCCGGTTTTCAACAAACCATGCAAATGCTGAATGAGGGCATCGTTCC
CACTGCGATGCTGGTTGCCAACGATCAGATGGCGCTGGGCGCAATGCGCGCCATTACCGAGTCCGGGCTG
CGCGTTGGTGCGGATATCTCGGTAGTGGGATACGACGATACCGAAGACAGCTCATGTTATATCCCGCCGT
TAACCACCATCAAACAGGATTTTCGCCTGCTGGGGCAAACCAGCGTGGACCGCTTGCTGCAACTCTCTCA
GGGCCAGGCGGTGAAGGGCAATCAGCTGTTGCCCGTCTCACTGGTGAAAAGAAAAACCACCCTGGCGCCC
AATACGCAAACCGCCTCTCCCCGCGCGTTGGCCGATTCATTAATGCAGCTGGCACGACAGGTTTCCCGAC
TGGAAAGCGGGCAGTGAGCGCAACGCAATTAATGTAAGTTAGCTCACTCATTAGGCACCCCAGGCTTTAC
ACTTTATGCTTCCGGCTCGTATAATGTGTGGAATTGTGAGCGGATAACAATTTCACACAGGAAACAGCTA
TGACCATGATTACGGATTCACTGGCCGTCGTTTTACAACGTCGTGACTGGGAAAACCCTGGCGTTACCCA
ACTTAATCGCCTTGCAGCACATCCCCCTTTCGCCAGCTGGCGTAATAGCGAAGAGGCCCGCACCGATCGC
CCTTCCCAACAGTTGCGCAGCCTGAATGGCGAATGGCGCTTTGCCTGGTTTCCGGCACCAGAAGCGGTGC
CGGAAAGCTGGCTGGAGTGCGATCTTCCTGAGGCCGATACTGTCGTCGTCCCCTCAAACTGGCAGATGCA
CGGTTACGATGCGCCCATCTACACCAACGTGACCTATCCCATTACGGTCAATCCGCCGTTTGTTCCCACG
GAGAATCCGACGGGTTGTTACTCGCTCACATTTAATGTTGATGAAAGCTGGCTACAGGAAGGCCAGACGC
GAATTATTTTTGATGGCGTCGGGATCTGATCCGGATTTACTAACTGGAAGAGGCACTAAATGAACACGAT
TAACATCGCTAAGAACGACTTCTCTGACATCGAACTGGCTGCTATCCCGTTCAACACTCTGGCTGACCAT
TACGGTGAGCGTTTAGCTCGCGAACAGTTGGCCCTTGAGCATGAGTCTTACGAGATGGGTGAAGCACGCT
TCCGCAAGATGTTTGAGCGTCAACTTAAAGCTGGTGAGGTTGCGGATAACGCTGCCGCCAAGCCTCTCAT
CACTACCCTACTCCCTAAGATGATTGCACGCATCAACGACTGGTTTGAGGAAGTGAAAGCTAAGCGCGGC
AAGCGCCCGACAGCCTTCCAGTTCCTGCAAGAAATCAAGCCGGAAGCCGTAGCGTACATCACCATTAAGA
CCACTCTGGCTTGCCTAACCAGTGCTGACAATACAACCGTTCAGGCTGTAGCAAGCGCAATCGGTCGGGC
CATTGAGGACGAGGCTCGCTTCGGTCGTATCCGTGACCTTGAAGCTAAGCACTTCAAGAAAAACGTTGAG
GAACAACTCAACAAGCGCGTAGGGCACGTCTACAAGAAAGCATTTATGCAAGTTGTCGAGGCTGACATGC
TCTCTAAGGGTCTACTCGGTGGCGAGGCGTGGTCTTCGTGGCATAAGGAAGACTCTATTCATGTAGGAGT
ACGCTGCATCGAGATGCTCATTGAGTCAACCGGAATGGTTAGCTTACACCGCCAAAATGCTGGCGTAGTA
GGTCAAGACTCTGAGACTATCGAACTCGCACCTGAATACGCTGAGGCTATCGCAACCCGTGCAGGTGCGC
TGGCTGGCATCTCTCCGATGTTCCAACCTTGCGTAGTTCCTCCTAAGCCGTGGACTGGCATTACTGGTGG
TGGCTATTGGGCTAACGGTCGTCGTCCTCTGGCGCTGGTGCGTACTCACAGTAAGAAAGCACTGATGCGC
TACGAAGACGTTTACATGCCTGAGGTGTACAAAGCGATTAACATTGCGCAAAACACCGCATGGAAAATCA
ACAAGAAAGTCCTAGCGGTCGCCAACGTAATCACCAAGTGGAAGCATTGTCCGGTCGAGGACATCCCTGC
GATTGAGCGTGAAGAACTCCCGATGAAACCGGAAGACATCGACATGAATCCTGAGGCTCTCACCGCGTGG
AAACGTGCTGCCGCTGCTGTGTACCGCAAGGACAAGGCTCGCAAGTCTCGCCGTATCAGCCTTGAGTTCA
TGCTTGAGCAAGCCAATAAGTTTGCTAACCATAAGGCCATCTGGTTCCCTTACAACATGGACTGGCGCGG
TCGTGTTTACGCTGTGTCAATGTTCAACCCGCAAGGTAACGATATGACCAAAGGACTGCTTACGCTGGCG
AAAGGTAAACCAATCGGTAAGGAAGGTTACTACTGGCTGAAAATCCACGGTGCAAACTGTGCGGGTGTCG
ATAAGGTTCCGTTCCCTGAGCGCATCAAGTTCATTGAGGAAAACCACGAGAACATCATGGCTTGCGCTAA
GTCTCCACTGGAGAACACTTGGTGGGCTGAGCAAGATTCTCCGTTCTGCTTCCTTGCGTTCTGCTTTGAG
```

```
TACGCTGGGGTACAGCACCACGGCCTGAGCTATAACTGCTCCCTTCCGCTGGCGTTTGACGGGTCTTGCT
CTGGCATCCAGCACTTCTCCGCGATGCTCCGAGATGAGGTAGGTGGTCGCGCGGTTAACTTGCTTCCTAG
TGAAACCGTTCAGGACATCTACGGGATTGTTGCTAAGAAAGTCAACGAGATTCTACAAGCAGACGCAATC
AATGGGACCGATAACGAAGTAGTTACCGTGACCGATGAGAACACTGGTGAAATCTCTGAGAAAGTCAAGC
TGGGCACTAAGGCACTGGCTGGTCAATGGCTGGCTTACGGTGTTACTCGCAGTGTGACTAAGCGTTCAGT
CATGACGCTGGCTTACGGGTCCAAAGAGTTCGGCTTCCGTCAACAAGTGCTGGAAGATACCATTCAGCCA
GCTATTGATTCCGGCAAGGGTCTGATGTTCACTCAGCCGAATCAGGCTGCTGGATACATGGCTAAGCTGA
TTTGGGAATCTGTGAGCGTGACGGTGGTAGCTGCGGTTGAAGCAATGAACTGGCTTAAGTCTGCTGCTAA
GCTGCTGGCTGCTGAGGTCAAAGATAAGAAGACTGGAGAGATTCTTCGCAAGCGTTGCGCTGTGCATTGG
GTAACTCCTGATGGTTTCCCTGTGTGGCAGGAATACAAGAAGCCTATTCAGACGCGCTTGAACCTGATGT
TCCTCGGTCAGTTCCGCTTACAGCCTACCATTAACACCAACAAAGATAGCGAGATTGATGCACACAAACA
GGAGTCTGGTATCGCTCCTAACTTTGTACACAGCCAAGACGGTAGCCACCTTCGTAAGACTGTAGTGTGG
GCACACGAGAAGTACGGAATCGAATCTTTTGCACTGATTCACGACTCCTTCGGTACCATTCCGGCTGACG
CTGCGAACCTGTTCAAAGCAGTGCGCGAAACTATGGTTGACACATATGAGTCTTGTGATGTACTGGCTGA
TTTCTACGACCAGTTCGCTGACCAGTTGCACGAGTCTCAATTGGACAAAATGCCAGCACTTCCGGCTAAA
GGTAACTTGAACCTCCGTGACATCTTAGAGTCGGACTTCGCGTTCGCGTAAC**GAATTC**GCGTATGGCAAT
GACAGTTTGAGACGGCCACAGGCGATTCTGAGAAGCCATTTTCTTTGGGCGCCGTGGCAGTTTTTATTGG
--> cg1121
```

Fig. S1. Sequence of the 4,46 kb fragment amplified from the genome of *E. coli* BL21(DE3) and inserted into the intergenic region of cg1122-cg1121 of *C. glutamicum* MB001. 70 bp and 85 bp of the flanking *C. glutamicum* genome region are also shown with a grey background. The XhoI and EcoRI restriction sites used for cloning are shown in bold.

Fig. S2. Growth of *C. glutamicum* MB001/pEKEx2-*eyfp* (A) and *C. glutamicum* MB001(DE3)/pMKEx2-*eyfp* (B). The strains were inoculated to an OD_{600} of 1 and cultivated for 24 h at 30°C in CGXII minimal medium with 4% (wt/vol) glucose using a BioLector system. Induction of *eyfp* expression was triggered by adding 0 µM (■), 50 µM (●), 100 µM (▲), or 250 µM (◊) IPTG to the cultures after 2 h.

Fig. S3. Analysis of heterologous eYFP production in the *C. glutamicum* strains MB001/pEKEx2-*eyfp* (A) and MB001(DE3)/pMKEx2-*eyfp* (B) at the single cell level by flow cytometry. The strains were cultivated for 24 h at 30°C in CGXII minimal medium with 4% (wt/vol) glucose using a BioLector system. Induction of *eyfp* expression was triggered by adding the indicated concentrations of IPTG to the cultures after 2 h. Dot blots from FACS analysis (excitation at 488 nm, emission at 533 nm) of at least 100,000 cells of each strain displaying the eYFP fluorescence signal against the forward scatter signal (FSC). The gate used to define non-fluorescent cells was set with *C. glutamicum* MB001(DE3)/pMKEx2 with 100 % of the cells falling into this gate (data not shown). The number inside the panels indicates the percentage of non-fluorescent cells inside this gate. In panels C and D, histograms of strains MB001/pEKEx2-*eyfp* (C) and MB001(DE3)/pMKEx2-*eyfp* (D) cultivated without IPTG or in the presence of 10, 25, and 250 µM IPTG are shown. The orange peaks indicate the background fluorescence set with strain MB001(DE3)/pMKEx2. The number of cells is plotted vs. eYFP fluorescence.

Fig. S4. Analysis of heterologous eYFP production in *C. glutamicum* MB001(DE3)/pMKEx2-*eyfp* (A) and *E. coli* BL21(DE3)/pEKEx2-*eyfp* (B) at the single cell level. The strains were cultivated for 24 h at 30°C in 2xTY medium using a BioLector system. Induction of *eyfp* expression was triggered by adding the indicated concentrations of IPTG to the cultures after 2 h. Dot plots from FACS analysis (excitation at 488 nm, emission at 533 nm) of at least 100,000 cells of each strain displaying the eYFP signal against the forward scatter signal (FSC) are shown. The gate used to define non-fluorescent cells was set with *C. glutamicum* MB001/pMKEx2 or *E. coli* BL21(DE3)/pMKEx2, respectively, with 100 % of the cells falling into this gate (data not shown). The number inside the panels indicates the percentage of non-fluorescent cells. In panels C and D, histograms of strains *E. coli* BL21(DE3)/pMKEx2-*eyfp* (C) and *C. glutamicum* MB001(DE3)/pMKEx2-*eyfp* (D) cultivated without IPTG or in the presence of 10, 25, and 250 µM IPTG are shown. The orange peaks indicate the background fluorescence set with strain strain *E. coli* BL21(DE3)/pMKEx2 and *C. glutamicum* MB001(DE3)/pMKEx2. The number of cells is plotted vs. eYFP fluorescence.

3.2 Pyruvate carboxylase variants enabling improved lysine production from glucose identified by biosensor-based high-throughput fluorescence-activated cell sorting screening

Kortmann M., Mack C., Baumgart M., and Bott M*.

IBG-1: Biotechnology, Institute of Bio- and Geosciences, Forschungszentrum Jülich, Jülich, Germany

*Corresponding author

Author contributions

MK, MBa and MBo designed the study and planned the experiments, supervised by MBa and MBo. The experimental work was performed by MK and CM. MK performed library preparation, FACS analysis, strain and plasmid construction, cultivation experiments, analysis of lysine production, Western Blot analysis and structure modelling of PCx. CM supported the construction of strains *C. glutamicum* DM1868*pyc*[T132A] and DM1868*pyc*[T343A]. MK, MBa and MBo analyzed the data. All figures were prepared by MK. MK, MBa and MBo wrote the manuscript.

MK: Maike Kortmann, CM: Christina Mack, MBa: Meike Baumgart, MBo: Michael Bott

Overall contribution MK: 70%

Pyruvate Carboxylase Variants Enabling Improved Lysine Production from Glucose Identified by Biosensor-Based High-Throughput Fluorescence-Activated Cell Sorting Screening

Maike Kortmann, Christina Mack, Meike Baumgart, and Michael Bott*

IBG-1: Biotechnology, Institute of Bio- and Geosciences, Forschungszentrum Jülich, 52425 Jülich, Germany

S Supporting Information

ABSTRACT: Pyruvate carboxylase is an anaplerotic carbon dioxide-fixing enzyme replenishing the tricarboxylic acid cycle with oxaloacetate during growth on sugars. In this study, we applied a lysine biosensor to identify pyruvate carboxylase variants in *Corynebacterium glutamicum* that enable improved L-lysine production from glucose. A suitable reporter strain was transformed with a *pyc* gene library created by error-prone PCR and screened by fluorescence-activated cell sorting (FACS) for cells with increased fluorescence triggered by an elevated cytoplasmic lysine concentration. Two pyruvate carboxylase variants, PCx^{T343A,I1012S} and PCx^{T132A} were identified allowing 9% and 19% increased lysine titers upon plasmid-based expression. Chromosomal expression of PCx^{T132A} and PCx^{T343A} variants led to 6% and 14% higher L-lysine levels. The new PCx variants can be useful also for other microbial strains producing TCA cycle-derived metabolites. Our approach indicates that a biosensor such as pSenLys enables directed evolution of many enzymes involved in converting a carbon source into the target metabolite.

KEYWORDS: *pyruvate carboxylase, Corynebacterium glutamicum, FACS-based screening, biosensor, lysine production, transcriptional regulator, LysG, metabolic engineering*
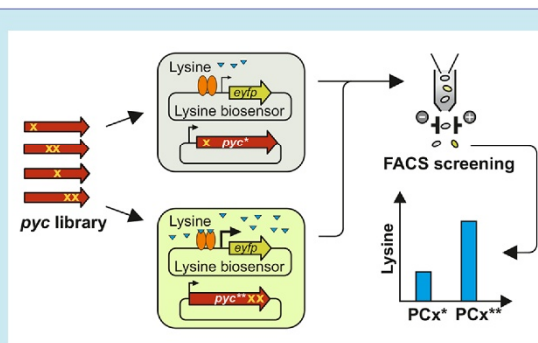
Many chemicals produced industrially with microbial cell factories as biocatalysts are intermediates or derivatives of the tricarboxylic acid (TCA) cycle, such as amino acids, organic acids, or diamines.[1] For continuous operation of the TCA cycle, anaplerotic reactions are required to replenish the deprived intermediates.[2] When sugars serve as carbon sources, the anaplerotic functions are fulfilled by pyruvate carboxylase (PCx)[3] and/or by phosphoenolpyruvate carboxylase (PEPCx).[4] Consequently, these enzymes are crucial for production of TCA cycle-derived metabolites from sugars (Figure 1A).

Corynebacterium glutamicum is the most prominent industrial amino acid producer with L-glutamate (flavor enhancer) and L-lysine (feed additive) being produced in the million tons scale per year.[5] In the past years, strains for production of many other TCA cycle-derived metabolites, such as succinate,[6,7] 1,5-diaminopentane,[8] or putrescine,[9] were constructed. Regarding anaplerosis, *C. glutamicum* is equipped with both PEPCx[10,11] and PCx.[12−14] Whereas PEPCx (encoded by the *ppc* gene) was shown to be dispensable for lysine production,[15,16] the deletion of the *pyc* gene for PCx caused a strong decrease, and its overexpression caused an increase in the synthesis of this amino acid.[17] Tween 60-induced glutamate production was lowered upon *pyc* deletion and increased by *pyc* over-expression, as well.[17] These results emphasize the importance of PCx as an anaplerotic enzyme for the production of amino acids of the glutamate and aspartate families. Overexpression of either the native *pyc* gene or of its *pyc*^{P458S} variant (see below) has often been used to improve various production strains of *C. glutamicum*, as summarized in Table S1. These examples confirm PCx as an important target to optimize sugar-based production processes for metabolites derived from the TCA cycle.

Only two studies have been reported on PCx variants of *C. glutamicum*. In the lysine-producing strain *C. glutamicum* B6, which was obtained from the type strain ATCC13032 by several rounds of random mutagenesis and selection, the amino acid exchange PCx^{P458S} was identified.[18] Introduction of the P458S mutation into the genomic *pyc* gene of strain AHD-2 (*hom*^{V59A}, *lysC*^{T311I}) caused an increase in lysine production from about 75 g/L to about 80 g/L.[18] The influence of the P458S mutation on PCx properties is unknown. In the patent US 7,300,777 B2,[19] a PCx variant was identified by genome sequence analysis of the lysine-producing *C. glutamicum* strain NRRL-B11474, which contained six amino acid exchanges (E153D, A182S, A206S, H227R, A455G, D1120E) compared to the reference sequence from *C. glutamicum* strain ATCC21253. Whereas PCx activity from ATCC21253 was
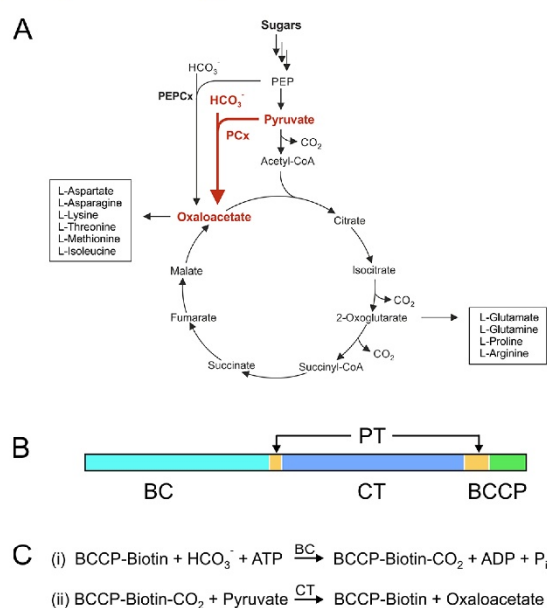
Figure 1. Function, domain organization, and partial reactions of pyruvate carboxylase. (A) Diagram highlighting the function of PCx as anaplerotic enzyme during growth on sugars and showing amino acids derived from the TCA cycle intermediates oxaloacetate and 2-oxoglutarate. (B) Domain organization of PCx. (C) Partial reactions catalyzed by PCx: BC, biotin carboxylase domains; CT, carboxyl-transferase domain; BCCP, biotin carboxyl carrier protein; PT, tetramerization or allosteric domain.

strongly inhibited by low aspartate concentrations, PCx from NRRL-B11474 was activated by aspartate concentrations up to 30 mM. Higher concentrations reduced PCx activity, but even at 100 mM aspartate 50% of the original activity was retained. It is unknown how this PCx variant affects lysine production and which of the six amino acid substitutions are responsible for the altered aspartate sensitivity.

Besides DNA sequence analysis of producer strains generated by random mutagenesis, several other strategies to identify or generate improved enzyme variants are available. If structures or structural models of the target protein are available, amino acid residues involved, for example, in allosteric regulation can be identified and exchanged by site-directed mutagenesis. This abolishes or alters regulation, as exemplified by reducing aspartate inhibition of PEPCx.[20] We recently developed a strategy to identify "productive" mutations based on genetically encoded single-cell biosensors and high-throughput (HT) screening by fluorescence-activated cell sorting (FACS).[21] The key elements are selected transcriptional regulators that serve as metabolite sensors, since their activity is dependent on the concentration of a certain metabolite within the cell that acts as coactivator, corepressor, inhibitor, or inducer. By placing a suitable target promoter in front of a reporter gene encoding a fluorescent protein, the metabolite concentration can be converted into a fluorescent output.

A prominent example for this type of biosensor is the plasmid pSenLys, which harbors the transcriptional regulator LysG of *C. glutamicum*.[21] LysG senses increased intracellular concentrations of the basic amino acids L-lysine, L-arginine, and L-histidine and activates expression of its target gene *lysE* in

complex with these coactivators.[22] In pSenLys, the *lysE* gene, encoding an exporter for L-lysine and L-arginine,[23] was replaced by *eyfp* to generate an optical output. pSenLys has successfully been employed for ultrafast screening of genome-wide, gene-specific, and site-specific mutant libraries by FACS for variants with improved L-lysine, L-arginine, or L-histidine production.[21,24,25] In this study, we tested whether pSenLys-Spc can be applied to search for novel PCx variants that enable improved production of L-lysine.

■ RESULTS AND DISCUSSION

Construction and Initial Characterization of a Reporter Strain for Screening of a *pyc* Mutant Library. The aim of the current study was to identify novel PCx variants that allow improved pyruvate carboxylation, measured as an increase in L-lysine production. For this purpose, we used the lysine biosensor pSenLys-Spc as a tool for FACS-based HT-screening of a plasmid-encoded PCx mutant library in *C. glutamicum*. This approach required a *C. glutamicum* strain already producing moderate levels of L-lysine, as PCx mutations alone are not sufficient to trigger lysine over-production in a wild-type background due to feedback inhibition of aspartate kinase by lysine and threonine.[26] Therefore, we used strain DM1868, which is an ATCC13032 derivative encoding the feedback-resistant aspartate kinase variant LysC[T311I] (Table S2). The T311I mutation is known to be sufficient to trigger lysine overproduction.[18] To avoid interference with the plasmid-encoded PCx variants, we deleted the chromosomal *pyc* gene in strain DM1868, resulting in strain DM1868Δ*pyc*. The deletion was confirmed by PCR using the oligonucleotides listed in Table S3 and by the growth defect of the strain in lactate minimal medium (Figure S1, see supplementary data for details).

To study the influence of *pyc* deletion and overexpression on L-lysine production in DM1868, the relevant strains were cultivated in CGXII minimal medium with 4% (w/v) glucose in a BioLector microcultivation system for 24 h. As shown in Table S4, the lysine titer of strain DM1868Δ*pyc*/pAN6 was reduced by 14% compared to the lysine titer of the parental strain DM1868/pAN6. In a previous study with the *C. glutamicum* strain DG52-5, deletion of *pyc* had a much stronger effect, as lysine production dropped by about 60%.[17] The reasons for this discrepancy could be the different strain background (strain DG52-5 was generated by random mutagenesis) and differences in the cultivation conditions. IPTG-induced overexpression of *pyc* via plasmid pAN6-*pyc* in strains DM1868 and DM1868Δ*pyc* caused an increase of the lysine titer by 63% compared to strain DM1868/pAN6. These results confirm that PCx activity based on chromosomal expression of *pyc* from its native promoter is a bottleneck for lysine overproduction. Similar results were obtained previously with strain DG52-5, where IPTG-induced *pyc* overexpression increased the lysine titer by 47%.[17] The results described above for strain DM1868Δ*pyc* suggested that this strain is suitable for screening a mutant library for improved PCx variants.

Testing the Reporter Strain by Comparison of Wild-Type PCx and the PCx[P458S] Variant. To test whether the biosensor pSenLys-Spc[24] allows to distinguish cells with small differences in lysine production, strain DM1868Δ*pyc* was cotransformed with pSenLys-Spc and either pAN6, pAN6-*pyc*, or pAN6-*pyc*[P458S]. The *pyc*[P458S] variant was reported to enable a 7% increase in lysine production compared to wild-type *pyc* in a strain carrying additionally the *lysC*[T311I] mutation.[18] After

Letter

cultivation, the strains were analyzed by FACS and the median fluorescence output of the cells was determined. As shown in Figure 2, cells of the strain with the PCx^{P458S} variant showed a
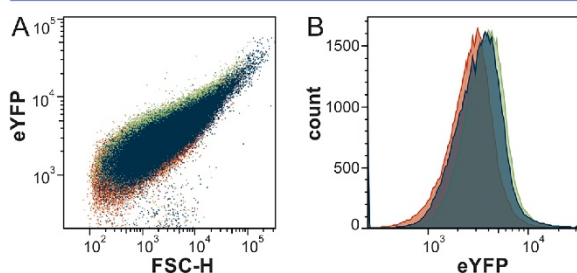
Figure 2. FACS analysis of *C. glutamicum* DM1868Δ*pyc* carrying pSenLys-Spc and different plasmid-encoded *pyc* variants. An overlay of DM1868Δ*pyc*/pSenLys-Spc transformed with either pAN6 (red), pAN6-*pyc* (blue), or pAN6-*pyc*^{P458S} (green) is shown as dot plot (A) and histogram (B). In the dot plot, the fluorescence intensity (eYFP) is plotted against cell size (FSC-H), whereas the histogram shows the cell count against the fluorescence intensity (eYFP).

median fluorescence of 3690, which is 13% higher than that of the strain with wild-type PCx and 36% higher than that of a PCx-negative strain. On the basis of these results, our reporter strain DM1868Δ*pyc*/pSenLys-Spc can be employed to distinguish between wild-type PCx and improved variants. However, due to the rather small difference in fluorescence output between the cells with wild-type PCx and optimized PCx variants, a high number of false positive cells was expected after FACS.

Construction and Screening of a *pyc* Mutant Library. A *pyc* mutant library was generated via error-prone PCR and cloned into pAN6, resulting in the library L-pAN6-*pyc*^{Mut}, which was subsequently used to transform *E. coli* NEB5α. The plasmids were isolated from about 9.6×10^4 colonies and used to transform the screening strain *C. glutamicum* DM1868Δ*pyc*/pSenLys-Spc. The resulting 1.1×10^6 transformants were pooled for further analysis. The mutant library and control strains were cultivated in glucose minimal medium until they reached on OD$_{600}$ of 2 at which *pyc* expression was induced with 1 mM IPTG, and the cultures were incubated for another 4–5 h. After suitable dilution the cultures were used for FACS analysis (Figure 3).

Gate 0 was set for all subsequent FACS experiments to exclude cell doublets and debris from screening, which made up approximately 7% of all analyzed events of each culture (Table 1). Sorting of cells with increased fluorescence compared to the reference strain with wild-type PCx was accomplished using two different approaches: gate 1 was set in a dot plot of eYFP fluorescence against FSC (forward scatter, a parameter for cell size) in such a way that both the number of cells of the positive control strain with pAN6-*pyc*^{P458S} falling within the gate and the number of cells containing either pAN6-*pyc* or only pAN6 being excluded from the gate were maximized (Figure 3). Of 100 000 analyzed cells each, 272 cells of the positive control with pAN6-*pyc*^{P458S}, 185 cells of the reference strain expressing wild-type *pyc*, and only 9 cells of the negative control with pAN6 fell within this gate (Table 1). The overall fluorescence of the *pyc* mutant library was lower compared to cells harboring exclusively pAN6-*pyc* or pAN6-*pyc*^{P458S}, presumably because random mutagenesis resulted in a large fraction of PCx variants with lowered or lost activity.
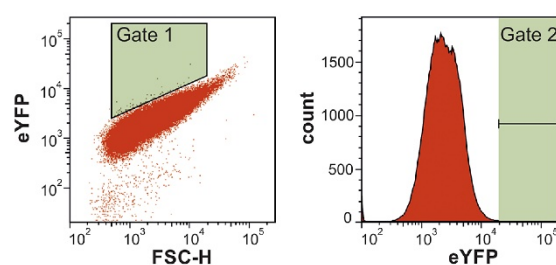
Figure 3. Sorting strategy for screening of the *pyc* mutant library in *C. glutamicum* DM1868Δ*pyc*/pSenLys-Spc. Cells were inoculated to an OD$_{600}$ of 1 in CGXII minimal medium with 4% (w/v) glucose and cultivated at 30 °C. At an OD$_{600}$ of 2, *pyc* expression was induced with 1 mM IPTG. After 5 h incubation, the cells were diluted to an OD$_{600}$ < 0.1 in sterile PBS and directly analyzed by FACS. Selection of single cells with increased fluorescence was performed by setting either gate 1 in the dot plot or gate 2 in the histogram. Cells outside the gates were not analyzed further.

Nevertheless, 80 out of 100 000 analyzed cells of the mutant library fell into gate 1 (Figure 3; Table 1).

Gate 2 for sorting highly fluorescent cells was set in the histogram showing the cell count with respect to fluorescence intensity. In this approach, only one cell out of 100 000 cells of the negative control, 63 cells of the reference strain with pAN6-*pyc*, and 115 cells of the positive control with pAN6-*pyc*^{P458S} fell into this gate. With gate 2, cells were sorted independent of their cell size and hence only bigger cells were collected (data not shown). In contrast to the approach used for gate 1, only six out of 100 000 cells of the library were sorted using gate 2 (Figure 3; Table 1).

Using the gates described above, more than 1.7×10^6 cells of the mutant library were screened and 96 clones each of gate 1 and gate 2 were sorted onto BHI agar plates with kanamycin and spectinomycin for further analysis. After cultivation for 24 h, 74 cells from gate 1 and 71 cells from gate 2 had formed colonies.

Testing of Clones Isolated from the *pyc* Mutant Library Regarding Growth and L-Lysine Production. A total of 40 clones of each gate were evaluated regarding growth and specific fluorescence by cultivation in a BioLector and measurement of the L-lysine concentration in the supernatant after 28 h (Table 2). Three clones of gate 2 did not grow and were therefore not analyzed further. Moreover, 35 clones of gate 1 and 31 clones of gate 2 were excluded from further analysis because of lower or equal lysine titers and specific fluorescences compared to the reference strain DM1828Δ*pyc*/pSenLys-Spc/pAN6-*pyc*. As mentioned before, the high number of false positive clones was expected due to the small differences in fluorescence between wild-type PCx and the improved variants. Nevertheless, five clones isolated from the *pyc* library with gate 1 and six clones isolated with gate 2 were chosen for further analysis due to their increased L-lysine titers. Sequence analysis of the 11 *pyc* variants revealed two which did not contain any mutation and were therefore not analyzed further. In the other nine *pyc* variants, 21 mutations were identified, three of which were silent, whereas 18 resulted in amino acid exchanges (Table 2). These nine PCx variants (PCx^{C1}, PCx^{C2}, etc.) contained 1–4 amino acid exchanges each.

Analysis of Isolated Clones after Reconstruction. Potential beneficial mutations identified by the screening

Table 1. FACS Analysis of *C. glutamicum* DM1868Δ*pyc*/pSenLys-Spc Carrying Either the *pyc* Mutant Library or Control Plasmids[a]

DM1868Δ*pyc*/pSenLys-Spc transformed with	Gate 0		Gate 1		Gate 2	
	events	median fluoresc.	events	median fluoresc.	events	median fluoresc.
pAN6	93 044	1 723	9	10 782	1	18 091
pAN6-*pyc*[WT]	93 145	3 287	185	7 287	63	18 737
pAN6-*pyc*[P458S]	93 031	3 504	272	7 861	115	18 862
L-pAN6-*pyc*[Mut]	92 581	2 397	80	6 861	6	18 767

[a]100 000 cells of each strain were analyzed. For all sortings, electronic gating was set in a dot plot of FSC-H against FSC-W to exclude cell doublets and cell debris (gate 0). Selection of single cells with increased fluorescence was performed by setting either a gate in a dot plot (gate 1) or in a histogram (gate 2). The number of cells falling into the respective gates as well as the median fluorescence of the population within each gate is shown.

Table 2. Genotypic and Phenotypic Characterization of *C. glutamicum* Strains Isolated by FACS from the *pyc* Mutant Library and of Control Strains

gate or control strains	clones	mutation in *pyc*[a]	amino acid exchange in PCx[a]	specific fluorescence (AU)[b]	L-lysine (mM)[b]	L-lysine (mM) of reconstructed clones (RC)[c]
1	(R)C1	A205G	K069E	0.92	59.8	36.2 ± 2.9
		A2708G	D903G			
		T3001C	F1001L			
	(R)C2	C882T	H294H	0.94	57.7	32.6 ± 1.1
		A1171G	I391V			
		C1318A	R440R			
		G1957A	D653N			
		T3254C	V1085A			
		T3302C	I1101T			
	(R)C3	G1452C	K484N	0.86	61.9	17.5 ± 2.0
		G1564A	A522N			
	(R)C4	A1027G	T343A	1.02	53.9	41.8 ± 2.5*
		T3035G	I1012S			
	(R)C5	T3245C	V1082A	0.83	50.4	37.2 ± 3.0
2	(R)C7	A394G	T132A	0.46	47.2	45.7 ± 1.7**
	(R)C8			0.41	42.9	
	(R)C9	A2104G	I702V	1.38	42.7	40.8 ± 1.0*
	(R)C11	A3355G	I1119V	0.38	47.8	38.5 ± 1.7
	(R)C12			0.39	46.4	
	(R)C13	T2422C	Y808H	0.41	55.5	38.2 ± 3.9
		A2584G	N862D			
control strains	pAN6					20.9 ± 2.3
	pAN6-*pyc*			Gate 1:0.9	Gate 1:53.0	38.4 ± 2.2
				Gate 2:0.7	Gate 2:42.1	
	pAN6-*pyc*[P458S]	C1372T	P458S			39.3 ± 3.0

[a]Positions of point mutations in *pyc* genes and the resulting amino acid exchanges in PCx are listed for 13 clones isolated by FACS (C1–C13). RC indicates the clones in which the *pyc* variants were reconstructed and transferred into *C. glutamicum* DM1868Δ*pyc*. [b]The specific fluorescence and the L-lysine titers of clones C1–C13 were determined after 28 h cultivation in a BioLector from a single experiment. [c]The *pyc* genes from clones C1–C13 were recloned into pAN6 and the resulting plasmids pAN6-*pyc*[RC1-RC13] were transferred into *C. glutamicum* DM1828Δ*pyc* without pSenLys-Spc. After cultivation for 24 h in a BioLector, the lysine concentration was determined. In this case, data represent average values and standard deviations of at least six biological replicates. Single and double asterisks indicate *p*-values of ≤0.05 and ≤0.01, respectively (*t* test).

procedure described above had to be re-evaluated in an independent strain and plasmid background in order to exclude secondary mutations on the plasmids or within the genome as causes of the improved L-lysine production. Hence, the mutated *pyc* genes of the clones C1, C2, C3, C4, C5, C7, C9, C11, and C13 were amplified by high-fidelity PCR and recloned into pAN6. *C. glutamicum* DM1868Δ*pyc* without pSenLys-Spc was transformed with the different pAN6-*pyc*[Cx] plasmids and the resulting strains RC1, RC2, etc., as well as the reference strain DM1868Δ*pyc*/pAN6-*pyc* and the negative control DM1868Δ*pyc*/pAN6, were analyzed with respect to growth and L-lysine production as described above. As shown in Table 2, three strains showed a higher lysine titer than the

reference strain after reconstruction. The best strain was RC7, which carried a single amino acid exchange (PCx[T132A]) and formed 19% more lysine (45.7 ± 1.7 mM) than the reference strain (38.4 ± 2.2 mM). Second best was strain RC4 carrying two amino acid exchanges (PCx[T343A, I1012S]) with a 9% higher lysine titer (41.8 ± 1.0 mM). The mentioned strains grew like the reference strain (data not shown).

Chromosomal Integration of Two *pyc* Mutations and Analysis of Their Impact on Growth and L-Lysine Production. For biotechnological production processes, chromosomally encoded variants of improved enzymes are often desirable. To exemplarily analyze the effects of chromosomal PCx mutations, we constructed the strains
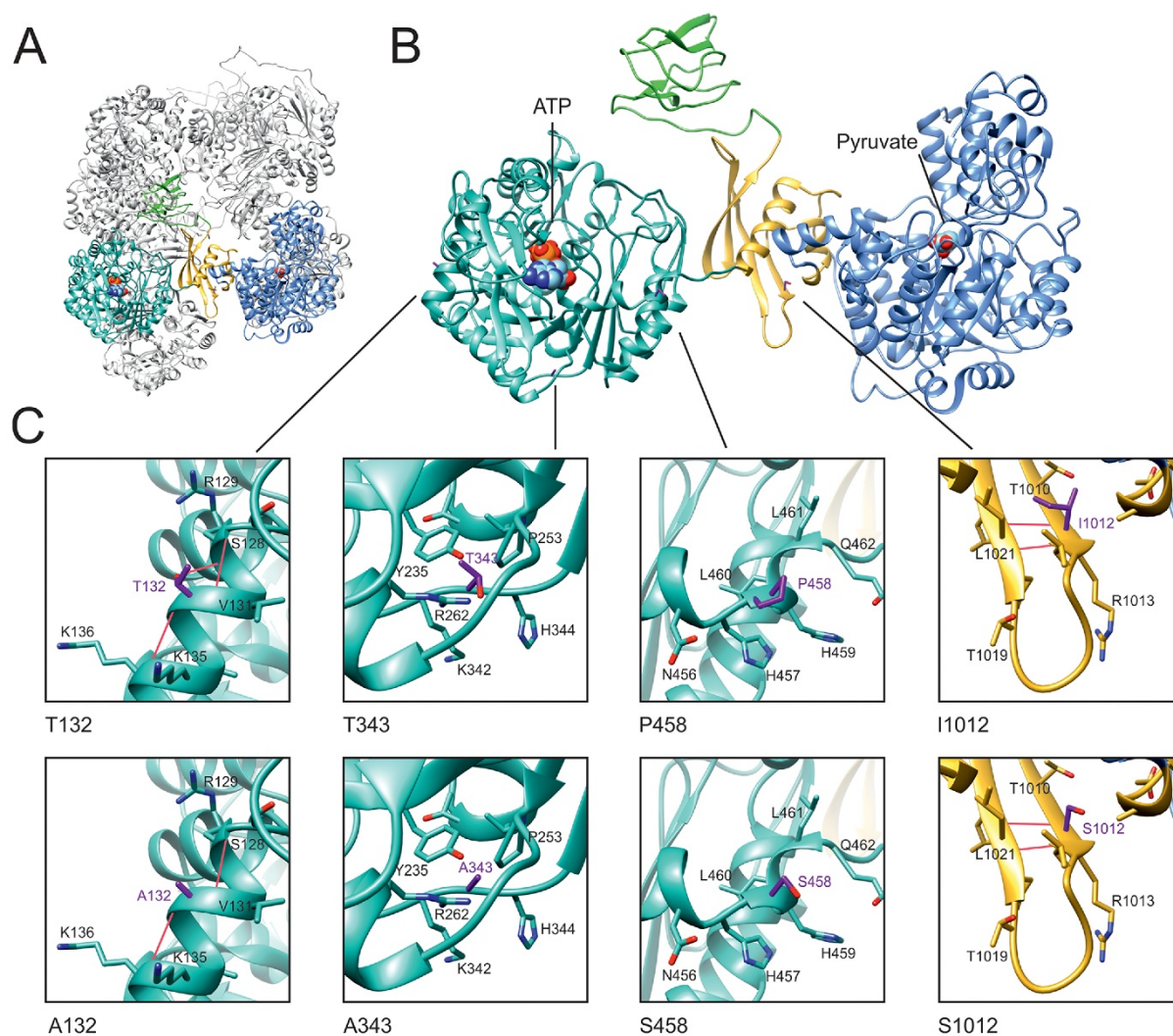
Figure 4. Structural model of PCx of *C. glutamicum* generated with SWISS-MODEL. Structure modeling was performed with SWISS-Model[28] using the crystal structure of *Staphylococcus aureus* PCx (PDB ID: 3BG5)[29] which shows 47% amino acid sequence identity to *C. glutamicum* PCx. In graphic A, the homotetrameric form of PCx is shown with one subunit colored. In graphic B, the colored monomer is shown in more detail with the biotin carboxylation domain (BC) in cyan, the PCx tetramerization domain (PT) in yellow, the biotin carboxyl carrier domain in green, and the carboxyltransferase domain (CT) in blue. Pyruvate is shown in the binding pocket of the CT domain and ATP in the binding pocket of the BC domain. In panels C, the vicinity of the four amino residues whose exchange was found to stimulate lysine synthesis is enlarged. The relevant regions with the wild-type amino acid residues (purple) and with the mutated residues (purple) are shown below each other. Oxygen atoms are marked in red, nitrogen atoms in blue, and hydrogen bonds are shown as red solid lines. The image was edited by using UCSF Chimera 1.10.2 (Resource for Biocomputing, Visualization, and Informatics at the University of California, San Francisco).

DM1868 pyc^{T132A} and DM1868 pyc^{T343A} (Figure S2). Strain DM1800 was used as positive control, since it encodes the feedback-resistant aspartate kinase LysC^{T311I} as well as PCx^{P458S}. All strains were cultivated in a BioLector and the L-lysine concentration was measured in the supernatants after 24 h. The strains showed a comparable growth behavior and reached the stationary phase after 12 h (data not shown). Strain DM1800 produced 27.5 ± 3.1 mM lysine, which corresponds to an increase of 1.2% compared to strain DM1868 (27.2 ± 1.1 mM) and was not significant in a *t* test. The newly constructed chromosomal variants PCx^{T132A} and PCx^{T343A} led to an increase of the lysine titer by 7% (29.1 ± 3.0 mM) and by 15% (31.4 ± 1.7 mM), respectively.

Alignment and Structural Modeling of PCx. A structure-based alignment of different biotin-dependent carboxylases was performed using a 3DM database[27] to check the conservation of the mutated residues (Table S5). A sequence-based alignment of several PCx proteins is shown in Figure S3. The proline residue of the previously identified PCx^{P458S} variant is highly abundant among biotin-dependent carboxylases with 21.7% of all 9901 aligned sequences showing proline at position 458. Conversely, a serine residue at this position was found in only about 1% of the aligned sequences. The threonine residues changed in variants PCx^{T132A} and PCx^{T343A} show a low degree of conservation, and alanine residues are also found at these positions. Also, the isoleucine

residue changed in the PCx[I1012S] variant has a low degree of conservation and is often replaced by other branched-chain amino acids, but rarely by serine.

A homology model of *C. glutamicum* PCx was generated to analyze the amino acid exchanges T132A, T343A, I1012S, and P458S on the structural level (Figure 4). Residues T132, T343, and P458 are located on the surface of the BC domain, whereas I1012 is present in the PT domain. None of the residues is located near the active sites of PCx and the consequences of the mutations cannot be predicted from the model. Higher affinities for pyruvate or bicarbonate or reduced inhibition by aspartate could be possible reasons for the positive effects of the identified mutations on lysine production.

Concluding Remarks. The genetically encoded single-cell biosensor pSenLys enables the detection of increased cytoplasmic lysine concentrations as increased fluorescence at the single-cell level and allows FACS-based HT-screening.[21] In a previous study, pSenLys was employed to identify feedback-resistant variants of aspartate kinase.[24] In that case, wild-type *C. glutamicum* could be used as background for the *lysC* mutant library, as amino acid exchanges causing feedback-resistance of LysC are sufficient to trigger strong overproduction of lysine and consequently a strong increase in fluorescence. Cells carrying such LysC variants could be easily distinguished by FACS from cells carrying wild-type LysC. In the present study, the prerequisites for successful screening of a PCx mutant library with pSenLys were much more intricate, as PCx mutations alone are not sufficient to trigger lysine over-production. Therefore, a strain that already overproduced lysine had to be used as a parent strain and the improved PCx variants enabled only small increases in lysine production and thus fluorescence. Nevertheless, our results demonstrate that these small differences were sufficient to identify new beneficial mutations in PCx, while also leading to a high fraction of false positive clones that had to be eliminated. For this purpose, efficient medium-throughput analysis of the originally sorted clones by microscale cultivation devices and rapid product analysis methods is inevitable.

The fact that, despite the difficult experimental setup, PCx variants enabling increased lysine production could be isolated from a relatively small library (ca. 10[5] clones) underlines the potential of the directed evolution approach used here. Particularly, it suggests that biosensors such as pSenLys can be used to screen for optimized variants of many enzymes involved in transforming the substrate, for example, glucose, into the analyzed product, for example, lysine. Thus, the approach might enable the identification of improved variants of enzymes of central metabolic pathways such as glycolysis or the pentose phosphate pathway, which in turn are expected to be useful for metabolic engineering of a large spectrum of producer strains for diverse products, all of which involve these enzymes in their biosynthesis.

◾ METHODS

Bacterial Strains, Plasmids, Growth Conditions, Recombinant DNA Techniques, and Lysine Quantification. Strains, plasmids, growth conditions, recombinant DNA techniques, and lysine quantification by HPLC are described in the Supporting Information.

Library Construction. For the construction of a *pyc* mutant library, the *C. glutamicum pyc* open reading frame (cg0791) with additionally ∼50 bp upstream and downstream regions was amplified from plasmid pUC18-*pyc* with the GeneMorph II Random Mutagenesis Kit (Agilent Technology, Santa Clara, CA, USA) and oligonucleotides EP-*pyc*-for and EP-*pyc*-rev. Conditions were adjusted in such a way that about four mutations/gene were introduced. Error prone-PCR products were purified, digested with NdeI and MfeI, and ligated with plasmid pAN6 that had been cut with NdeI and EcoRI. The ligation mixture was used to transform chemically competent *E. coli* NEB5α cells. The transformation mixture was spread onto two agar plates (Ø 260 mm) with 50 mg L^{−1} kanamycin and incubated for 24 h at 30 °C. Additional control plates were prepared for the determination of the library size. Afterward, all colonies were washed off the plate and pooled in LB medium. The L-pAN6-pyc[Mut] library was isolated with the QIAprep Spin Miniprep Kit (QIAGEN, Hilden, Germany) and used to transform *C. glutamicum* DM1868Δ*pyc* already harboring plasmid pSenLys-Spc. The cells were spread onto BHI agar plates (Ø 260 mm) with 12.5 mg L^{−1} kanamycin and 125 mg L^{−1} spectinomycin. After 24 h of incubation at 30 °C all colonies were pooled in 4 mL of BHI medium with appropriate antibiotics. Aliquots were supplemented with glycerol to a final concentration of 12.5% (v/v) and stored at −80 °C.

FACS Analysis. FACS analysis was performed using a FACS ARIA II high-speed cell sorter (BD Biosciences, Franklin Lakes, NJ, USA). *C. glutamicum* strains were first cultivated as 10 mL BHI cultures in 100 mL baffled shaking flasks at 130 rpm and 30 °C for 16 h. After these cells were washed with 0.9% (w/v) NaCl, they were used to inoculate the main cultures of 50 mL of CGXII medium with 4% (w/v) glucose in 500 mL baffled shake flasks to an OD_{600} of 1. Expression of *pyc* was induced by the addition of 1 mM IPTG at an OD_{600} of 2. After further cultivation for 4−5 h, the cells were diluted to an OD_{600} below 0.1 in sterile phosphate-buffered saline (PBS, 37 mM NaCl, 2.7 mM KCl, 10 mM Na_2HPO_4, 1.8 mM KH_2PO_4, pH 7.4) and used immediately for FACS analysis. A 488 nm blue solid state laser was used to detect eYFP fluorescence with a 502 nm long-pass and a 530/30 nm band-pass filter set. Forward-scatter (FSC) and side-scatter (SSC) were detected as a voltage pulse of height (H), weight (W), and area (A). Cells were analyzed with a threshold rate up to 6000 events s[−1] and a sample pressure of 70 psi. For cell sorting, a preselection of cells was performed to exclude doublets and debris by electronic gating using FSC-W against FSC-H. Gates in the eYFP channel were set to exclude low-fluorescent cells harboring pAN6 or pAN6-*pyc*. Clones of each gate showing an enhanced eYFP signal were sorted on BHI agar plates with 12.5 mg L^{−1} kanamycin and 125 mg L^{−1} spectinomycin, which were subsequently incubated for 24 h at 30 °C. Afterward, each colony was used to inoculate 5 mL of BHI medium supplemented with 12.5 mg L^{−1} kanamycin and 125 mg L^{−1} spectinomycin, and cells were grown overnight at 30 °C and 170 rpm. From these cultures glycerol stocks were prepared with a final glycerol concentration of 12.5% (v/v) in BHI media and stored at −80 °C until the clones were analyzed further. All FACS data were analyzed using BD DIVA 6.1.3 and FlowJo 7.6.5 software (Tree Star, Inc., Ashland, OR, USA).

■ ASSOCIATED CONTENT

Ⓢ Supporting Information

The Supporting Information is available free of charge on the ACS Publications website at DOI: 10.1021/acssynbio.8b00510.

> Bacterial strains, plasmids, and growth conditions; recombinant DNA techniques; construction of plasmid pUC18-*pyc*, strain DM1868Δ*pyc*, and strains with chromosomally encoded PCx variants; Western blot analysis; lysine quantification; relevance of PCx for growth of *C. glutamicum* DM1868 on lactate as carbon source; additional tables and figures (PDF)

■ AUTHOR INFORMATION

Corresponding Author

*Tel.: +49 2461 613294. Fax: +49 2461 612710. E-mail: m.bott@fz-juelich.de.

ORCID ⊙

Maike Kortmann: 0000-0001-9733-9569

Meike Baumgart: 0000-0002-9874-1151

Michael Bott: 0000-0002-4701-8254

Author Contributions

M.K. performed the experiments, analyzed the data and participated in the design of the research. C.M. supported some of the experimental work. M.Bo. and M.Ba. analyzed the data and designed the research. All authors participated in writing of the manuscript.

Notes

The authors declare the following competing financial interest(s): M.Bo., M.Ba. and M.K. have filed patent applications covering results described in this study.

■ REFERENCES

(1) Becker, J., and Wittmann, C. (2015) Advanced biotechnology: Metabolically engineered cells for the bio-based production of chemicals and fuels, materials, and health-care products. *Angew. Chem., Int. Ed. 54*, 3328−3350.

(2) Sauer, U., and Eikmanns, B. J. (2005) The PEP-pyruvate-oxaloacetate node as the switch point for carbon flux distribution in bacteria. *FEMS Microbiol. Rev. 29*, 765−794.

(3) Utter, M. F., and Keech, D. B. (1960) Formation of oxaloacetate from pyruvate and carbon dioxide. *J. Biol. Chem. 235*, Pc17−18.

(4) Bandurski, R. S., and Greiner, C. M. (1953) The enzymatic synthesis of oxalacetate from phosphoryl-enolpyruvate and carbon dioxide. *J. Biol. Chem. 204*, 781−786.

(5) Eggeling, L., and Bott, M. (Eds.) (2005) *Handbook of Corynebacterium glutamicum*, CRC Press, Taylor & Francis Group, Boca Raton, Florida, USA.

(6) Okino, S., Noburyu, R., Suda, M., Jojima, T., Inui, M., and Yukawa, H. (2008) An efficient succinic acid production process in a metabolically engineered *Corynebacterium glutamicum* strain. *Appl. Microbiol. Biotechnol. 81*, 459−464.

(7) Litsanov, B., Brocker, M., and Bott, M. (2012) Toward homosuccinate fermentation: metabolic engineering of *Corynebacterium glutamicum* for anaerobic production of succinate from glucose and formate. *Appl. Environ. Microbiol. 78*, 3325−3337.

(8) Kind, S., Neubauer, S., Becker, J., Yamamoto, M., Volkert, M., von Abendroth, G., Zelder, O., and Wittmann, C. (2014) From zero to hero - Production of bio-based nylon from renewable resources using engineered *Corynebacterium glutamicum*. *Metab. Eng. 25*, 113−123.

(9) Schneider, J., and Wendisch, V. F. (2010) Putrescine production by engineered *Corynebacterium glutamicum*. *Appl. Microbiol. Biotechnol. 88*, 859−868.

(10) Eikmanns, B. J., Follettie, M. T., Griot, M. U., and Sinskey, A. J. (1989) The phosphoenolpyruvate carboxylase gene of *Corynebacterium glutamicum*: Molecular cloning, nucleotide sequence, and expression. *Mol. Gen. Genet. 218*, 330−339.

(11) O'Regan, M., Thierbach, G., Bachmann, B., Villeval, D., Lepage, P., Viret, J. F., and Lemoine, Y. (1989) Cloning and nucleotide sequence of the phosphoenolpyruvate carboxylase-coding gene of *Corynebacterium glutamicum* ATCC13032. *Gene 77*, 237−251.

(12) Peters-Wendisch, P. G., Wendisch, V. F., Paul, S., Eikmanns, B. J., and Sahm, H. (1997) Pyruvate carboxylase as an anaplerotic enzyme in *Corynebacterium glutamicum*. *Microbiology 143*, 1095−1103.

(13) Peters-Wendisch, P. G., Kreutzer, C., Kalinowski, J., Patek, M., Sahm, H., and Eikmanns, B. J. (1998) Pyruvate carboxylase from *Corynebacterium glutamicum*: characterization, expression and inactivation of the *pyc* gene. *Microbiology 144*, 915−927.

(14) Koffas, M. A., Ramamoorthi, R., Pine, W. A., Sinskey, A. J., and Stephanopoulos, G. (1998) Sequence of the *Corynebacterium glutamicum* pyruvate carboxylase gene. *Appl. Microbiol. Biotechnol. 50*, 346−352.

(15) Peters-Wendisch, P. G., Eikmanns, B. J., Thierbach, G., Bachmann, B., and Sahm, H. (1993) Phosphoenolpyruvate carboxylase in *Corynebacterium glutamicum* is dispensable for growth and lysine production. *FEMS Microbiol. Lett. 112*, 269−274.

(16) Gubler, M., Park, S. M., Jetten, M., Stephanopoulos, G., and Sinskey, A. J. (1994) Effects of phosphoenol pyruvate carboxylase deficiency on metabolism and lysine production in *Corynebacterium glutamicum*. *Appl. Microbiol. Biotechnol. 40*, 857−863.

(17) Peters-Wendisch, P. G., Schiel, B., Wendisch, V. F., Katsoulidis, E., Möckel, B., Sahm, H., and Eikmanns, B. J. (2001) Pyruvate carboxylase is a major bottleneck for glutamate and lysine production by *Corynebacterium glutamicum*. *J. Mol. Microbiol. Biotechnol. 3*, 295−300.

(18) Ohnishi, J., Mitsuhashi, S., Hayashi, M., Ando, S., Yokoi, H., Ochiai, K., and Ikeda, M. (2002) A novel methodology employing *Corynebacterium glutamicum* genome information to generate a new L-lysine-producing mutant. *Appl. Microbiol. Biotechnol. 58*, 217−223.

(19) Hanke, P. D., Sinskey, A. J., Willis, L. B., and Guillouet, S. (2007) Feedback-resistant pyruvate carboxylase gene from *Corynebacterium*, US 7,300,777 B2.

(20) Chen, Z., Bommareddy, R. R., Frank, D., Rappert, S., and Zeng, A. P. (2014) Deregulation of feedback inhibition of phosphoenolpyruvate carboxylase for improved lysine production in *Corynebacterium glutamicum*. *Appl. Environ. Microbiol. 80*, 1388−1393.

(21) Binder, S., Schendzielorz, G., Stäbler, N., Krumbach, K., Hoffmann, K., Bott, M., and Eggeling, L. (2012) A high-throughput approach to identify genomic variants of bacterial metabolite producers at the single-cell level. *Genome Biol. 13*, R40.

(22) Bellmann, A., Vrljic, M., Patek, M., Sahm, H., Krämer, R., and Eggeling, L. (2001) Expression control and specificity of the basic amino acid exporter LysE of *Corynebacterium glutamicum*. *Microbiology 147*, 1765−1774.

(23) Vrljic, M., Sahm, H., and Eggeling, L. (1996) A new type of transporter with a new type of cellular function: L-lysine export from *Corynebacterium glutamicum*. *Mol. Microbiol. 22*, 815−826.

(24) Schendzielorz, G., Dippong, M., Grünberger, A., Kohlheyer, D., Yoshida, A., Binder, S., Nishiyama, C., Nishiyama, M., Bott, M., and Eggeling, L. (2014) Taking control over control: Use of product sensing in single cells to remove flux control at key enzymes in biosynthesis pathways. *ACS Synth. Biol. 3*, 21−29.

(25) Binder, S., Siedler, S., Marienhagen, J., Bott, M., and Eggeling, L. (2013) Recombineering in *Corynebacterium glutamicum* combined with optical nanosensors: a general strategy for fast producer strain generation. *Nucleic Acids Res. 41*, 6360−6369.

(26) Shiio, I., Miyajima, R., and Sano, K. (1970) Genetically desensitized aspartate kinase to the concerted feedback inhibition in *Brevibacterium flavum*. *J. Biochem. 68*, 701−710.

(27) Kuipers, R. K., Joosten, H. J., van Berkel, W. J., Leferink, N. G., Rooijen, E., Ittmann, E., van Zimmeren, F., Jochens, H., Bornscheuer,

U., Vriend, G., dos Santos, V. A., and Schaap, P. J. (2010) 3DM: systematic analysis of heterogeneous superfamily data to discover protein functionalities. *Proteins: Struct., Funct., Genet. 78*, 2101−2113.

(28) Waterhouse, A., Bertoni, M., Bienert, S., Studer, G., Tauriello, G., Gumienny, R., Heer, F. T., de Beer, T. A. P., Rempfer, C., Bordoli, L., Lepore, R., and Schwede, T. (2018) SWISS-MODEL: homology modelling of protein structures and complexes. *Nucleic Acids Res. 46*, W296−W303.

(29) Xiang, S., and Tong, L. (2008) Crystal structures of human and *Staphylococcus aureus* pyruvate carboxylase and molecular insights into the carboxyltransfer reaction. *Nat. Struct. Mol. Biol. 15*, 295−302.

3.2.1 Supplementary material "Pyruvate carboxylase variants enabling improved lysine production from glucose identified by biosensor-based high-throughput fluorescence-activated cell sorting screening"

Kortmann M., Mack C., Baumgart M., and Bott M*.

IBG-1: Biotechnology, Forschungszentrum Jülich, Jülich, Germany

*Corresponding author

Supporting information

Pyruvate carboxylase variants enabling improved lysine production identified by biosensor-based high-throughput FACS screening

Maike Kortmann, Christina Mack, Meike Baumgart, and Michael Bott

IBG-1: Biotechnology, Institute of Bio- and Geosciences, Forschungszentrum Jülich, 52425 Jülich, Germany

Supplemental methods

Bacterial strains, plasmids and growth conditions. All bacterial strains and plasmids used in this study are listed in Table S2. *Escherichia coli* DH5α was used for cloning and *E. coli* NEB5α for library construction. Both strains were cultivated at 37°C in lysogeny broth (LB).[1] If necessary, the medium was supplemented with 100 mg L^{-1} ampicillin, or 50 mg L^{-1} kanamycin. The *C. glutamicum* type strain ATCC13032 was used as wild-type. For determination of growth and specific fluorescence of *pyc* library clones and complementation experiments, 800 μL brain heart infusion (BHI) (Difco Laboratories, Detroit, MI, USA) medium with required antibiotics (25 mg L^{-1} kanamycin and/or 250 mg L^{-1} spectinomycin) was inoculated with a *C. glutamicum* colony from a fresh BHI agar plate and this first preculture was incubated for 8 h in a Microtron shaker (Infors HT, Bottmingen, Switzerland) at 900 rpm, 30°C, and 75% humidity. After washing with 0.9% (wt/vol) NaCl and centrifugation (10 min, 15,000 g, 4°C), the cells of the first preculture were used to inoculate 800 μL CGXII minimal medium[2] with 4% (wt/vol) glucose and 0.03 g^{L-1} 3,4-dihydroxybenzoate as iron chelator to an optical density at 600 nm (OD$_{600}$) of 0.05. This second preculture was incubated for 16 h in the Microtron shaker. The cells of the second preculture were washed as described above and used to inoculate 800 μL CGXII medium with 4% (wt/vol) glucose or 2% (wt/vol) lactate to an OD$_{600}$ of 0.5. These main cultures were incubated at 1200 rpm, 30°C, and 80% humidity in a BioLector (m2p-labs, Baesweiler, Germany), which allows online measurement of growth as backscattered light of 620 nm and of eYFP fluorescence (excitation/emission 510 nm/532 nm). All cultivations were performed in 48-well microtiter Flowerplates (m2p-labs, Baesweiler, Germany). The expression of target genes was induced by addition of 0 – 1 mM isopropyl β-D-1-thiogalactopyranoside (IPTG).

Recombinant DNA techniques. Oligonucleotides were purchased from Eurofins MWG Operon (Ebersberg, Germany) and are listed in Table S3. Standard DNA and cloning techniques were performed as described.[3] FastDigest restriction enzymes were used according to the recommendations of the supplier (Thermo Fisher Scientific, Waltham, MA, USA). Plasmid DNA of *E. coli* was isolated using the QIAprep Spin Miniprep Kit and PCR fragments were purified from agarose gels using the QIAex gel elution kit (both QIAGEN, Hilden, Germany). PCR fragments were cloned into plasmids using either the Rapid DNA Ligation Kit (Roche Diagnostics GmbH, Mannheim, Germany) or a self-prepared Gibson Assembly master mix.[4] Transformation of RbCl-competent *E. coli* cells with plasmid DNA was done by heat-shock.[5] Competent *C. glutamicum* cells were prepared and transformed with plasmid DNA by electroporation as described previously.[6] All plasmids were checked for the correct insert by sequencing (Eurofins MWG Operon, Ebersberg, Germany). The construction of plasmids and strains is described in the supporting information.

Construction of plasmid pUC18-*pyc*. For the construction of plasmid pUC18-*pyc*, *pyc* was amplified using Phusion Green High-Fidelity DNA Polymerase (Thermo Fisher Scientific, Waltham, MA, USA) and oligonucleotides Pyc-XbaI-NdeI-for and Pyc-MfeI-HindIII-rev with genomic DNA of *C. glutamicum* ATCC13032 as template. Afterwards, digestion of the PCR product and plasmid pUC18 was done with enzymes XbaI and HindIII

and both fragments were ligated using the rapid ligation kit and used to transform *E. coli* DH5α.

Construction of strain DM1868Δ*pyc*. For the construction of the deletion mutant DM1868Δ*pyc*, plasmid pK19*mobsacB*-Δ*pyc* was constructed. The flanking regions of the *pyc* gene were amplified using Phusion Green High-Fidelity DNA Polymerase (Thermo Fisher Scientific, Waltham, MA, USA) and the oligonucleotide pairs dpyc-1-BamHI-for/dpyc-1-ov-rev and dpyc-2-ov-for/dpyc-2-EcoRI-rev with genomic DNA of *C. glutamicum* ATCC13032 as template. The resulting PCR products had a size of 468 bp and 431 bp, respectively. With an overlap-extension PCR both fragments were fused, resulting in an 868 bp-PCR product, encoding the up- and downstream regions of *pyc* linked by 21 bp. Afterwards, digestion of the generated DNA fragment and plasmid pK19*mobsacB* was done with enzymes BamHI and EcoRI and both fragments were ligated using the DNA rapid ligation kit. The deletion of *pyc* in *C. glutamicum* DM1868 was done by two-step homologous recombination with pK19*mobsacB*-Δ*pyc* as described before.[7] Finally, the correct deletion of *pyc* in the genome was verified by PCR using the oligonucleotides c-dpyc-for/rev.

Construction of strains with chromosomally encoded PCx variants. For the integration of the mutations T132A and T343A into the chromosomal *pyc* gene of *C. glutamicum* DM1868 the plasmids pK19*mobsacB*-*pyc*^T132A and pK19*mobsacB*-*pyc*^T343A were constructed (Fig. S2). First, ~500 bp fragments of wild-type *pyc* were amplified with the oligonucleotide pairs T132A-Ex-for/rev or T343A-Ex-for/rev from genomic DNA of strain ATCC13032 and cloned into pK19*mobsacB* cut with BamHI and EcoRI by Gibson assembly. In the next step, the point mutations T132A and T343A were introduced into the corresponding pK19*mobsacB* derivatives using the oligonucleotide pairs T132A-mut-BglI-for/rev and T343A-mut-BglI-for/rev with the QuikChange II Site-Directed Mutagenesis Kit (Agilent Technologies, Waldbronn, Germany). To allow screening for the correct insertion of the point mutation by restriction, a second, silent point mutation was introduced close to the desired mutation leading to the formation of a new restriction site. The plasmids were checked by sequencing using the oligonucleotides c-pK19-for/rev. Introduction of the *pyc* mutations into the genome of *C. glutamicum* DM1868 was performed by two-step homologous recombination.[7] The recombinants were analyzed by digesting a PCR-amplified *pyc* fragment from the genome with BglI and positive clones were rechecked by sequencing with the oligonucleotides c-Ins-T132A-for/rev and c-Ins-T343A-for/rev.

Western blot analysis. To verify that increased IPTG concentrations led to an increased production of biotinylated PCx in *C. glutamicum* DM1868Δ*pyc*/pAN6-*pyc* when cells were grown on lactate as sole carbon source, Western blotting with a biotin-detecting antibody was performed. A first preculture of 10 mL BHI-medium was inoculated with a fresh colony from a BHI agar plate and cultivated in a 100 mL baffled shaking flask at 130 rpm and 30°C. The second preculture in CGXII medium supplemented with 4% (wt/vol) glucose was inoculated to an OD_{600} of 0.5 and cultivated for 16 h at 30°C. Subsequently, the cells were washed once with 0.9% (wt/vol) NaCl and used to inoculate 50 mL CGXII medium supplemented with 2% (wt/vol) Na-D,L-lactate to an OD_{600} of 1. After 24 h the cells were harvested by centrifugation

3

(4°C, 15 min, 5200 g), washed once with 10 mM Tris-HCl pH 8.3, 400 mM NaCl and 2 mM EDTA and suspended in 800 µL of the same buffer. The cells were disrupted by beat-beating with about 200 mg glass beads using a Precellys 24 device (Peqlab Biotechnologie, Erlangen, Germany). Cell debris was removed by centrifugation (4°C, 15 min, 16,000 g) and the protein concentration in the cell-free supernatant was determined with the BCA assay (BC Assay Protein Quantitation Kit, Uptima, Interchim, Montlucon, France). Proteins of the crude extract were separated by SDS-polyacrylamide gel electrophoresis.[8] Gels were electroblotted for 1 h with 15 V onto a nitrocellulose membrane (GE Healthcare Bio-Sciences, Uppsala, Sweden) using a transblot semidry transfer cell (Bio-Rad, München, Germany) and buffer containing 25 mM Tris, 192 mM glycine, and 20% (vol/vol) methanol. To avoid unspecific binding, the membrane was blocked for at least 4 h with 5% (wt/vol) skim milk powder in TBST buffer (10 mM Tris-HCl pH 7.5, 150 mM NaCl, 0.1% (vol/vol) Tween-20) at room temperature. Biotinylated proteins were detected using a Strepavidin-alkaline phosphatase conjugate (Amersham), diluted 1:4000 in TBST buffer and Novex® AP Chemiluminescent Substrate (Thermo Scientific, Waltham, MA, USA). A Fuji LAS-3000 Mini CCD camera (Fujifilm Life Science; Tokyo, Japan) was used for visualization of chemiluminescent bands.

Lysine quantification by HPLC. L-Lysine concentrations were determined in the supernatant of *C. glutamicum* clones cultivated in a BioLector for 24 h. Cells were separated by centrifugation (15 min, 13,000 g, 4°C) and amino acids were quantified as their *o*-phthaldialdehyde derivatives via high-pressure liquid chromatography using a Agilent LC 1100 HPLC system (Agilent Technologies, Waldbronn, Germany) as described equipped with an ODS Hypersil 120 x 4 mm column (CS Chromatographie Service GmbH, Langerwehe, Germany) and a fluorescence detector. As eluent, a gradient of 80% (vol/vol) solvent A (0.1 M sodium acetate buffer (pH 7.2)) and 20% solvent B (100% methanol) to 20% solvent A and 80% solvent B was used. Substances were eluted based on their hydrophobicity with a flow rate of 0.6 mL/min at 40°C. Fluorescence was detected at 540 nm with excitation at 230 nm and the amino acid concentrations were determined using an external amino acid standard (AAS18; Sigma Aldrich, St. Louis, MO, USA) with defined concentrations.

Supplemental results

Relevance of PCx for growth of *C. glutamicum* DM1868 on lactate as sole carbon source. The deletion of *pyc* is known to cause a strong growth defect with lactate as sole carbon source.[9] We therefore checked our strain DM1868Δ*pyc* with respect to growth in CGXII minimal medium with lactate and tested complementation with plasmid pAN6-*pyc* or pAN6 as negative control. As shown in Fig. S1A, DM1868Δ*pyc*/pAN6 had the expected growth defect (µ = 0.06 ± 0.02 h^{-1}), whereas strain DM1868/pAN6 showed a growth rate of µ = 0.24 ± 0.01 h^{-1}. In the presence of pAN6-*pyc*, but without IPTG addition, growth of DM1868Δ*pyc* was already slightly improved due to the leakiness of the P$_{tac}$ promoter driving *pyc* expression. With increasing IPTG concentrations, growth of DM1868Δ*pyc*/pAN6-*pyc* continuously improved, reaching a growth rate of µ = 0.34 ± 0.01 h^{-1} at 250 µM IPTG, even better than strain DM1868/pAN6 carrying only the chromosomal *pyc* gene. IPTG-induced

overexpression of *pyc* in strain DM1868/pAN6-*pyc* also improved growth and the strain reached a growth rate of 0.35 ± 0.03 h^{-1} at 250 µM IPTG. Western blotting confirmed that the production of PCx in *C. glutamicum* DM1868/pAN6-*pyc* and DM1868Δ*pyc*/pAN6-*pyc* increased with higher IPTG concentrations (Figure S1B). These results confirm that PCx is a limiting factor for growth of *C. glutamicum* on lactate. Higher PCx concentrations allow a higher carbon flux into the TCA cycle and probably also improve gluconeogenesis, which is dependent on PEP carboxykinase and thus on OAA as substrate.

Supplemental tables

Table S1. Selected examples of *C. glutamicum* producer strains for various products where PCx was a target of metabolic engineering.[a]

Product	Strain	PCx modification	Ref.
Amino acids			
L-Lysine	B-6	Chromosomal expression of *pyc*[P458S]	10
	AHP-3	Chromosomal expression of *pyc*[P458S]	11
	AGM-5	Chromosomal expression of *pyc*[P458S]	12
	Lys-12	Chromosomal expression of *pyc*[P458S] under control of P_{sod}	13
	Lys5-9	Chromosomal expression of *pyc*[P458S], with a start codon exchange from GTG to ATG	14
	BS87Δ*sucCD*	Chromosomal expression of *pyc*[P458S] under control of P_{sod}	15
	DM1933Δ*ilvB*	Chromosomal expression of *pyc*[P458S]	16
	DG52-5/ pVWEx1-*pyc*	Plasmid-based expression of *pyc* under control of P_{tac}	17
L-Glutamate	ATCC13032/ pVWEx1-*pyc*	Plasmid-based expression of *pyc* under control of P_{tac}	17
	SJ8145/pEK-*pyc*	Plasmid-based expression of *pyc* under control of P_{araBAD}	18
L-Homo-serine	DM368-3/ pVWEx1-*pyc*	Plasmid-based expression of *pyc* under control of P_{tac}	17
L-Threonine	DM368-3/ pVWEx1-*pyc*	Plasmid-based expression of *pyc* under control of P_{tac}	17
L-Methionine	LY-5	Chromosomal expression of *pyc*[P458S], with a start codon exchange from GTG to ATG	19
L-Pipecolic acid	PIPE4	Chromosomal expression of *pyc*[P458S]	20
5-Amino-valerate	5AVA3	Chromosomal expression of *pyc*[P458S]	21
Diamines			
Cadaverine	DAP-16	Chromosomal expression of *pyc*[P458S] under control of P_{sod}	22
	DM1945 Δ*act3-ldcC*[opt]	Chromosomal expression of *pyc*[P458S]	23
Putrescine	NA6/ pVWEx1-*speC-gapA-pyc-argB*[A49V/M54V]-*argF21*	Plasmid-based expression of *pyc* under control of P_{tac}	24
Organic acids			
Succinate	ATCC13032 Δ*ldhA/* pCRA717	Plasmid-based expression of *pyc* under control of P_{lac}	25, 26
	BOL2 and BOL3	Chromosomal expression of *pyc*[P458S] under control of P_{tuf}	27

	SA5	Chromosomal expression of *pyc* under control of P*trc*	[28]
	NC-6	Chromosomal expression of an additional *pyc* copy under control of P*ldh*	[29]
Glutarate	AVA2	Chromosomal expression of *pyc*^{P458S} under control of P*sod*	[30]

[a] Unless otherwise stated, *pyc* expression is controlled by its native promoter P*pyc*.

Table S2. Bacterial strains and plasmids used in this study.

Strains and plasmids	Relevant characteristics	Source or reference
Strains		
E. coli DH5α	Strain used for cloning procedures; F⁻ φ80*lacZ* ΔM15 Δ(*lacZYA-argF*) U169 *recA*1 *endA*1 *hsdR*17(rk⁻, mk⁺) *phoA supE44 thi*-1 *gyrA*96 *relA*1 λ⁻	[5]
E. coli NEB5α	*E. coli* DH5α derivative with high transformation efficiency; *fhuA2* Δ(*argF-lacZ*) U169 *phoA glnV44 Φ80* Δ(*lacZ*)M15 *gyrA96 recA1 relA1 endA1 thi-1 hsdR17*	New England Biolabs, Frankfurt, Germany
C. glutamicum ATCC13032	Biotin-auxotrophic wild-type	[31]
C. glutamicum DM1868	ATCC13032 with a point mutation in *lysC* (cg0306) resulting in *lysC*^T311I	Evonik Industries AG, Halle (Westf.), Germany
C. glutamicum DM1800	ATCC13032 with point mutations in *lysC* (cg0306) and *pyc* (cg0791) resulting in *lysC*^T311I and *pyc*^P458S	Evonik Industries AG, Halle (Westf.), Germany
C. glutamicum DM1868Δ*pyc*	*C. glutamicum* DM1868 with an in-frame deletion of *pyc* (cg0791)	This work
C. glutamicum DM1868 *pyc*^T132A	*C. glutamicum* DM1868 with a nucleotide exchange in *pyc* resulting in *pyc*^T132A	This work
C. glutamicum DM1868 *pyc*^T343A	*C. glutamicum* DM1868 with a nucleotide exchange in *pyc* resulting *pyc*^T343A	This work
Plasmids		
pUC18	Amp^R; *E. coli* expression plasmid (P_lac, *lacI*_q, pMB1 *oriV*_Ec)	[32]
pUC18-*pyc*	Amp^R; pUC18 derivative containing the *C. glutamicum pyc* gene (cg0791)	This work
pAN6	Kan^R; *C. glutamicum*/*E. coli* shuttle vector for regulated gene expression using P_*tac* (P_*tac* *lacI*^q pBL1 *oriV*_Cg pUC18 *oriV*_Ec)	[33]
pAN6-*pyc*	Kan^R; pAN6 derivative for expression of *pyc* (cg0791) under control of P_*tac*	This work
pAN6-*pyc*^P458S	Kan^R; pAN6 derivative for expression of *pyc*^P458S under control of P_*tac*	[34]
pAN6-*pyc*^RCx	Kan^R; pAN6 derivatives for expression of *pyc* variants encoding PCx variants with the following amino acid exchanges[a]: *pyc*^RC1: K069E, D903G, F1001L *pyc*^RC2: H294H, I391V, R440R, D653N, V1085A, I1101T	This work

	pyc^{RC3}: K484N, A522N	
	pyc^{RC4}: T343A, I1012S	
	pyc^{RC5}: V1082A	
	pyc^{RC6}: E734K, V883V, K1034R	
	pyc^{RC7}: T132A	
	pyc^{RC9}: I702V	
	pyc^{RC10}: M323V, W578R, I644V, K713R	
	pyc^{RC11}: I1119V	
	pyc^{RC13}: Y808H, N862D	
pSenLys-Spc	Spc^R; sensor plasmid encoding LysG and its target promoter P$_{lysE}$ fused to *eyfp*	[35]
pK19*mobsacB*	Kan^R, vector for allelic exchange in *C. glutamicum* (*oriV*$_{E.c.}$ *sacB lacZα*)	[36]
pK19*mobsacB*-Δ*pyc*	Kan^R, pK19*mobsacB* derivative containing two homologous regions of about 400 bp up- and downstream of *pyc* (cg0791) for deletion of *pyc*	This work
pK19*mobsacB*-*pyc*^{T132A}	Kan^R, pK19*mobsacB* derivative containing a 568 bp *pyc* fragment with T132A mutation	This work
pK19*mobsacB*-*pyc*^{T343A}	Kan^R, pK19*mobsacB* derivative containing a 556 bp *pyc* fragment with T343A mutation	This work

[a]A detailed description of the individual PCx variants can be found in Table 5.

Table S3. Oligonucleotides used in this study.

Oligoname	Sequence (5'→ 3')[a]
Construction of pUC18-*pyc*	
Pyc-XbaI-NdeI-for	GC<u>TCTAGA</u>CG<u>CATATG</u>TCGACTCACACATCTTC
Pyc-HindIII-MunI-rev	CTT<u>AAGCTT</u>C<u>AATTG</u>AAAGCCCCGCCTCCTCC
Construction of L-pAN6-*pyc*^{Mut}	
EP-*pyc*-for	GGAAACAGCTATGACCATGATTAC
EP-*pyc*-rev	GATGTGCTGCAAGGCGATTAAG
Oligonucleotides for sequencing L-pAN6-*pyc*^{Mut}	
PCxCg-Seq-1	AGCATCTCGTGAAGCTGAAG
PCxCg-Seq-2	TCACCGCACACTTTGACTCC
PCxCg-Seq-3	TTTGAGGATCCGTGGGACAG
PCxCg-Seq-4	CGTCGCGATACCGGTTTGAG
PCxCg-Seq-5	TCACACAGGAAACAGAATTA
PCxCg-Seq-6-rev	ACGGCCAGTGAATTGAAAGC
Construction of pK19*mobsacB*-Δ*pyc* and PCR analysis of *C. glutamicum* DM1868Δ*pyc*	
dpyc-1-BamHI-for	TATA<u>GGATCC</u>AAGCAGCACGTCAGCTGGTTC
dpyc-1-ov-rev	*CCCATCCACTAAACTTAAACA*TAGAGTAATTATTCCTTTC
dpyc-2-ov-for	*TGTTTAAGTTTAGTGGATGGG*ACCTTTCTGTAAAAGC
dpyc-2-EcoRI-rev	TATA<u>GAATTC</u>CACCACCACCTCCTTAG
c-dpyc-for	GTTGCTGATCTGGCTGATAC
c-dpyc-rev	ATCGCCCTTTATTACCTGCC
Construction of pK19*mobsacB*-*pyc*^{T132A} and PCR analysis of *C. glutamicum* DM1868 *pyc*^{T132A}	
T132A-Ex-for	**TCGACTCTAGAGGAT**CGCCACGGTAGCTATTTAC
T132A-Ex-rev	**GACGGCCAGTGAATT**TCGCCAAGGATCTGC
T132A-mut-BgLI-for	CTCACCGGTGATAAGTCTCGCGCGGTAgCCGCC<u>GCCAAGA</u> <u>AGGC</u>TGGTCTGCCAGTTTTG (BglI)
T132A-mut-BgLI-rev	CAAAACTGGCAGACCA<u>GCCTTCTTGGC</u>GGCGGcTACCGCG CGAGACTTATCACCGGTGAG (BglI)
c-Ins-T132A-for	GCTCTAGACGTGTCGACTCACACATCTTC
c-Ins-T132A-rev	TGTCCCACGGATCCTCAAAG
Construction of pK19*mobsacB*-*pyc*^{T343A} and PCR analysis of *C. glutamicum* DM1868 *pyc*^{T343A}	
T343A-Ex-for	**TCGACTCTAGAGGAT**CGCCAGCACAGCATTTG
T343A-Ex-rev	**GACGGCCAGTGAATT**ACGCACGCAAGAAACCAATG
T343A-mut-BgLI-for	TGACCCAAGATAAGATCAAGg<u>CCCACGGGGC</u>AGCACTGC AGTGCCGCATCACCACGGAAG

10

T343A-mut-BgLI-rev	CTTCCGTGGTGATGCGGCACTGCAGTGCT<u>GCCCCGTGGG</u>c CTTGATCTTATCTTGGGTCA
c-Ins-T343A-for	AGCATCTCGTGAAGCTGAAG
c-Ins-T343A-rev	TGTCCCACGGATCCTCAAAG

Analysis of pK19*mobsacB-pyc*^{T132A} and pK19*mobsacB-pyc*^{T343A}

c-pK19-for	TACCGCCTTTGAGTGAGCTG
c-pK19-rev	CTGCGCAACTGTTGGGAAGG

^a Restriction sites are underlined, overlaps for Gibson assembly are in bold and for overlap-extension PCRs are with bold and italic letters. Point mutations causing amino acid exchanges are indicated with lower case letters.

Table S4. Influence of *pyc* deletion and overexpression on L-lysine production of *C.glutamicum* DM1868.[a]

C. glutamicum strain	L-Lysine (mM) 0 µM IPTG	L-lysine (mM) 250 µM IPTG
DM1868/pAN6	25.7 ± 0.9	24.3 ± 1.7
DM1868Δ*pyc*/pAN6	21.5 ± 0.5	20.9 ± 0.6
DM1868/pAN6-*pyc*	28.2 ± 0.5	39.7 ± 0.7
DM1868Δ*pyc*/pAN6-*pyc*	24.3 ± 0.7	39.6 ± 1.1

[a] Strains were cultivated for 24 h in CGXII minimal medium with 4% (wt/vol) glucose either in the absence of IPTG or in the presence of 250 µM IPTG in a BioLector. Afterwards, the L-lysine concentrations in the supernatant were determined by HPLC. The data represent mean values and standard deviations of three biological replicates.

Table S5. Conservation of the amino acids at positions 132, 343 and 1012 of *C. glutamicum* PCx among other biotin-dependent carboxylases.

Amino acid position[a]	Frequency of amino acids in aligned sequences (%)			
	132[b]	343[c]	1012[d]	458[e]
Alanine	18.5	1.4	2.1	1.5
Arginine	11.4	2.2		1.9
Asparagine	7.0			
Aspartic Acid	5.0			3.7
Cysteine		1.8		
Glutamine	8.7	2.8		2.7
Glutamic Acid	14.8			4.5
Glycine				1.1
Histidine	5.2	2.3		1.9
Isoleucine	2.8	25.4	41.5	11.8
Leucine	1.2	25.0	2.1	22.5
Lysine	11.6	1.0		2.0
Methionine		2.6	1.1	3.4
Phenylalanine		8.6		9.2
Proline		9.1		21.7
Serine	4.5		1.1	1.0
Threonine	8.0	8.3	1.1	1.4
Tyrosine		1.7		5.6
Tryptophan				1.0
Valine		7.0	51.1	2.0

[a] The frequency (in %) of different amino acids at the indicated positions of *C. glutamicum* PCx was derived from a 3D-model database[37] containing an alignment of related biotin-dependent carboxylases based on their structure.

[b] Data of 8869 sequences.

[c] Data of 5942 sequences.

[d] Data of 94 sequences.

[e] Data of 9901 sequences.

Supplemental figures
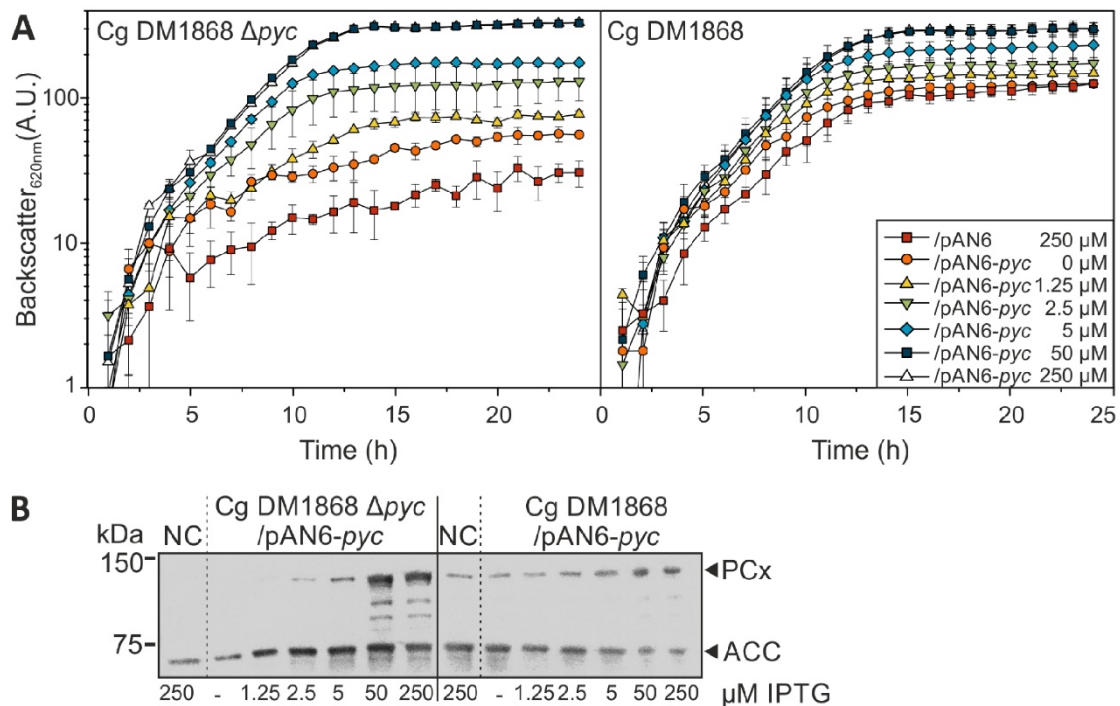
Figure S1. Effects of *pyc* deletion and overexpression in *C. glutamicum* DM1868 on growth with lactate as sole carbon source. (A) The strains DM1868Δ*pyc* and DM1868 carrying either pAN6-*pyc* or as negative control pAN6 were cultivated at 30°C for 24 h in a BioLector in CGXII medium with 2% (wt/vol) lactate. Expression of plasmid-borne *pyc* was induced by addition of the indicated IPTG concentrations at the start of the cultivation. (B) To check the expression of *pyc*, biotinylated PCx was analyzed by Western blotting using StrepTactin-AP conjugate for detection. Equivalent protein amounts (120 µg) of cell-free extracts of lactate-grown cells were subjected to SDS-PAGE and blotted onto a nitrocellulose membrane. Biotinylated proteins are indicated by arrows and represent PCx (123 kDa) and acetyl-CoA carboxylase (ACC, 65 kDa). Strains harboring pAN6 were used as negative control (NC). To estimate the size of the proteins, Precision Plus Protein™ All Blue Prestained Protein Standard marker (M) was used (Bio-Rad Laboratories, Inc., Hercules, California, US).
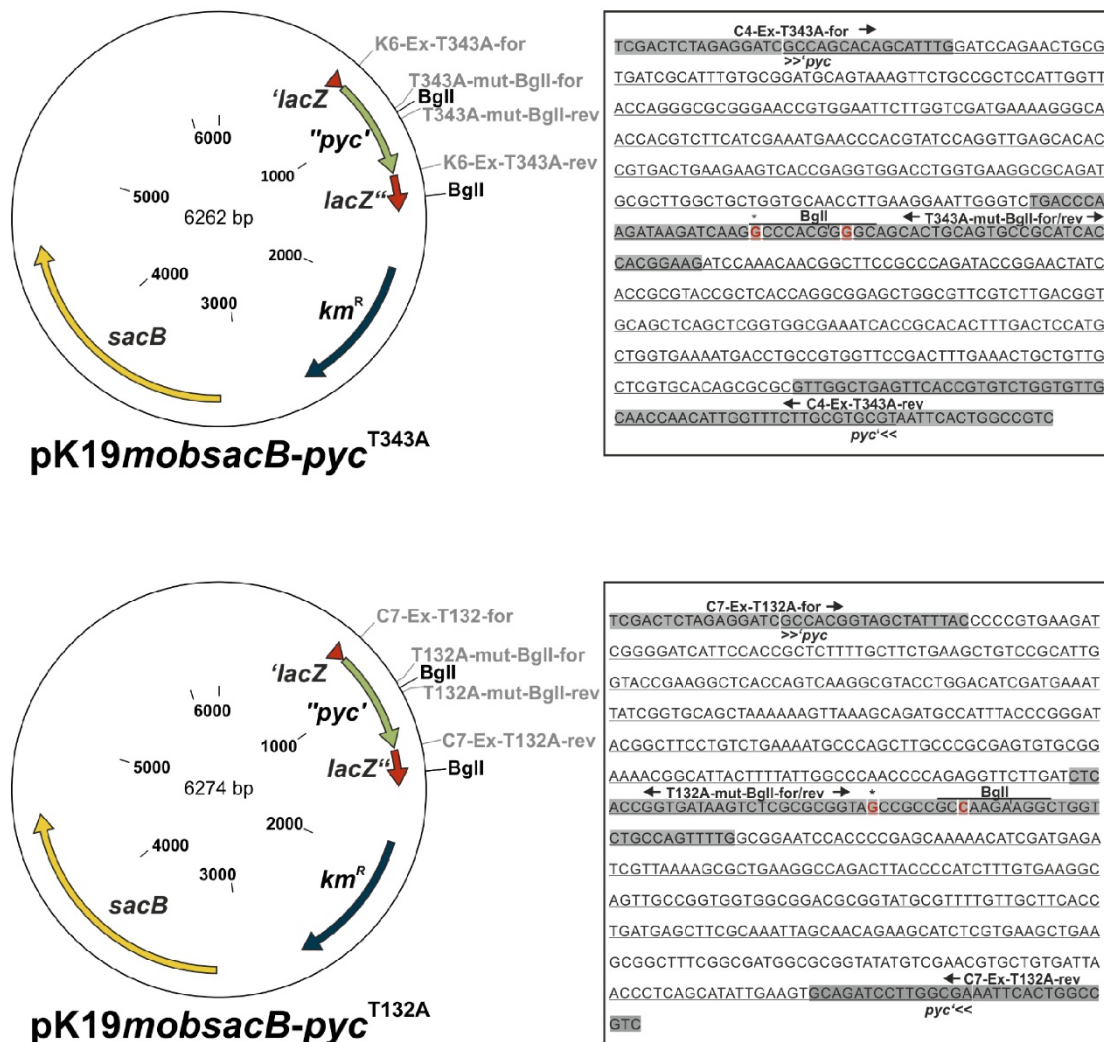
Figure S2. Maps and partial sequences of plasmids pK19*mobsacB-pyc*[T132A] and pK19*mobsacB-pyc*[T343A]. The *pyc* gene fragments carrying the mutations are marked green and the sequences are shown on the right. Oligonucleotides are indicated in grey, the PCx-encoding sequence is underlined, and point mutations are marked in red. Asterisks indicate the mutation causing the amino acid exchange.
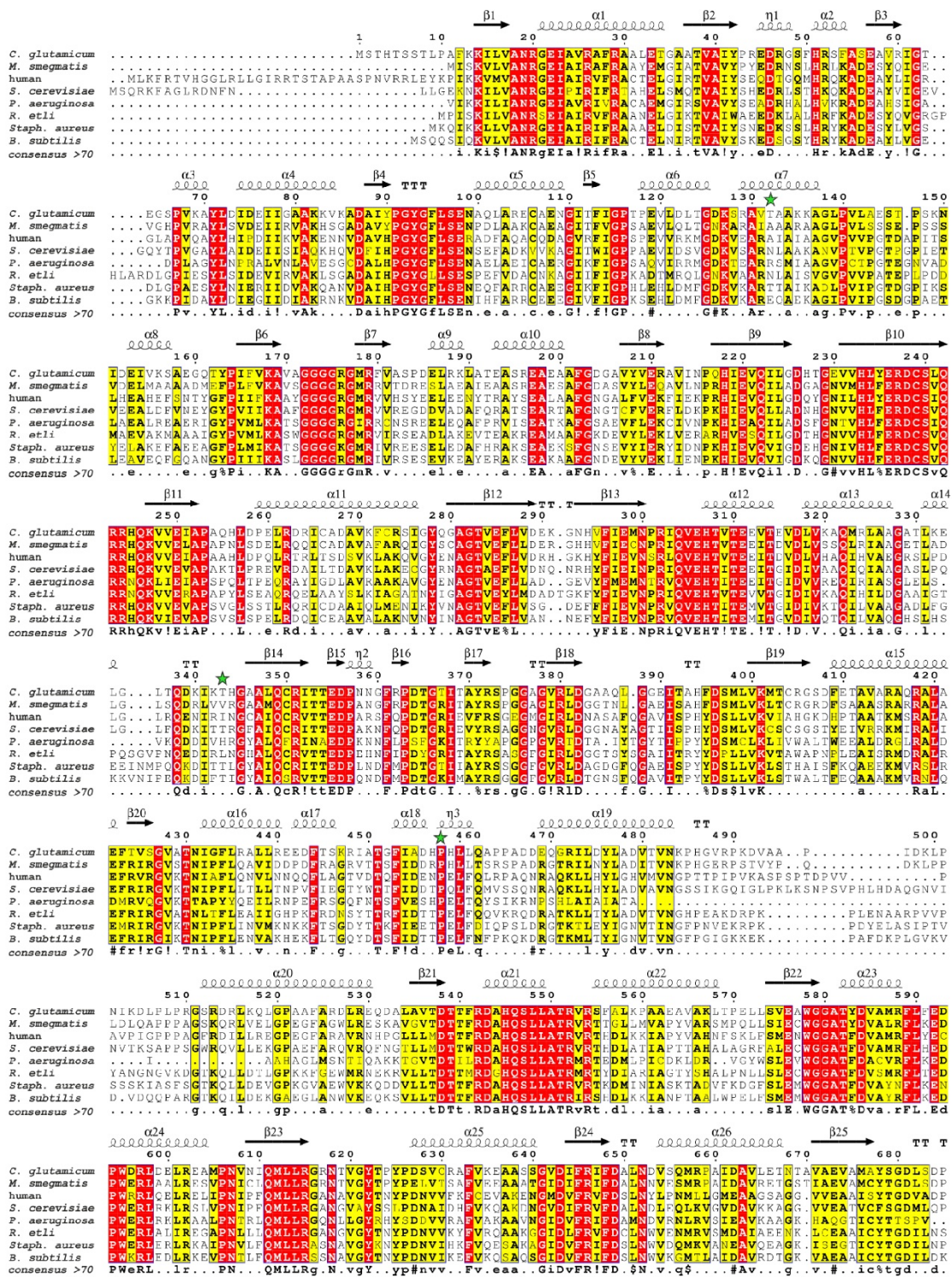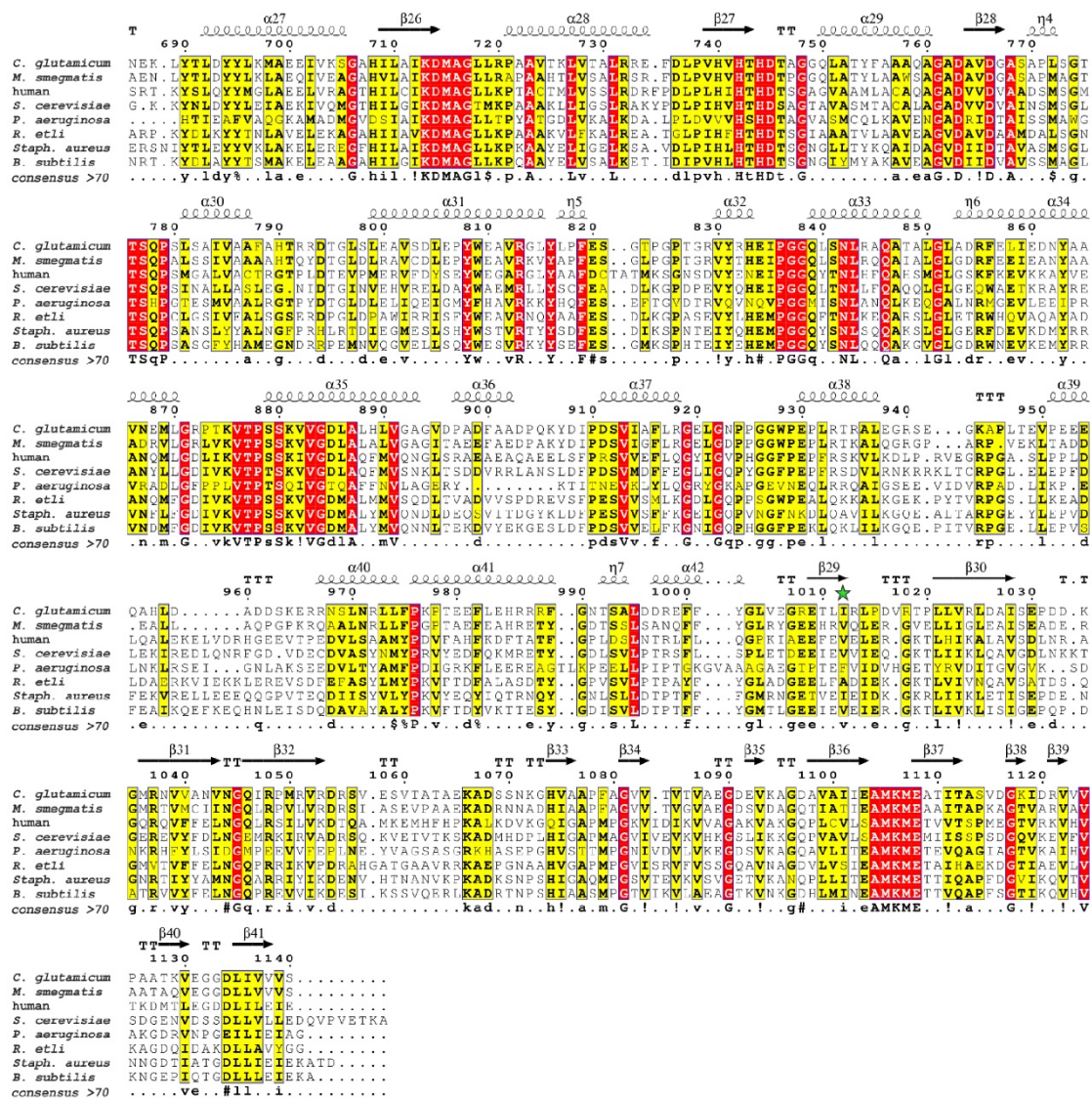
Figure S3. Amino acid sequence alignment of PCx proteins. The PCx sequences were derived from *C. glutamicum* ATCC13032 (CGTRNA_RS03450; cg0791), *Mycobacterium smegmatis* NCTC8159 (ERS451418_02426), *Homo sapiens* (NP_071504), *Saccharomyces cerevisiae* S288c (PCx isoenzyme 1: YGL062W), *Pseudomonas aeruginosa* NBRC12689 (PCxA: PA50071_28335; PCxB: PA50071_28330); *Rhizobium etli* CFN42 (RHE_CH04002), *Staphylococcus aureus* DSM20231 (AA076_05500); *Bacillus subtilis* NCIB3610 (B4U62_08180). Note that PCx of *P. aeruginosa* is actually composed of subunit A (471 amino acids, C-terminus AAHAGL) and subunit B (607 amino acids, N-terminus MSNTIQ) and the fusion is located at position 524/525 of the alignment. The sequences were aligned with Clustal Omega[38] and edited with Esprit 3.0.[39] Positions with 100% identical amino acids in all aligned proteins are shaded in red, whereas positions in which amino acids are found in at least 70% of the aligned proteins are marked in yellow. Mutations described in this study are marked with a green star. The secondary structure shown above the alignment is

17

based on a model of *C. glutamicum* PCx, which was constructed with SWISS-MODEL[40] using the PCx structure of *S. aureus* as template (PDB: 3bg5). Additionally, the consensus sequence is shown beneath the alignment, based on an amino acid identity for ≥70% of the aligned PCx sequences. Uppercase letters indicate an identity of 100%, lowercase letters represent conservation in >50% of the aligned sequences. "!" stands for either isoleucine or valine, "$" for leucine or methionine, "%" for phenylalanine or tyrosine, and "#" for asparagine, aspartic acid, glutamine, or glutamic acid. Predicted secondary structures are marked as follows: helices represent α-helices, the symbol η refers to a 3_{10}-helix, arrows represent β-strands, "TT" indicates strict β-turns, and "TTT" strict α-turns.

Supplemental references

[1] Bertani, G. (1951) Studies on lysogenesis. I. The mode of phage liberation by lysogenic *Escherichia coli*, *J. Bacteriol. 62*, 293-300.

[2] Keilhauer, C., Eggeling, L., and Sahm, H. (1993) Isoleucine synthesis in *Corynebacterium glutamicum*: molecular analysis of the *ilvB-ilvN-ilvC* operon, *J. Bacteriol. 175*, 5595-5603.

[3] Sambrook, J., and Russell, D. (2001) *Molecular Cloning. A Laboratory Manual*, 3rd ed., Cold Spring Harbor Laboratory Press, Cold Spring Harbor, New York.

[4] Gibson, D. G. (2011) Enzymatic assembly of overlapping DNA fragments, *Methods Enzymol 498*, 349-361.

[5] Hanahan, D. (1983) Studies on transformation of *Escherichia coli* with plasmids, *J. Mol. Biol. 166*, 557-580.

[6] Tauch, A., Kirchner, O., Löffler, B., Gotker, S., Pühler, A., and Kalinowski, J. (2002) Efficient electrotransformation of *Corynebacterium diphtheriae* with a mini-replicon derived from the *Corynebacterium glutamicum* plasmid pGA1, *Curr. Microbiol. 45*, 362-367.

[7] Niebisch, A., and Bott, M. (2001) Molecular analysis of the cytochrome bc_1-aa_3 branch of the *Corynebacterium glutamicum* respiratory chain containing an unusual diheme cytochrome c_1, *Arch. Microbiol. 175*, 282-294.

[8] Laemmli, U. K. (1970) Cleavage of structural proteins during the assembly of the head of bacteriophage T4, *Nature 227*, 680-685.

[9] Peters-Wendisch, P. G., Kreutzer, C., Kalinowski, J., Patek, M., Sahm, H., and Eikmanns, B. J. (1998) Pyruvate carboxylase from *Corynebacterium glutamicum*: characterization, expression and inactivation of the *pyc* gene, *Microbiology 144*, 915-927.

[10] Hirao, T., Nakano, T., Azuma, T., Sugimoto, M., and Nakanishi, T. (1989) L-Lysine production in continuous culture of an L-lysine hyperproducing mutant of *Corynebacterium glutamicum*, *Appl. Microbiol. Biotechnol. 32*, 269-273.

[11] Ohnishi, J., Mitsuhashi, S., Hayashi, M., Ando, S., Yokoi, H., Ochiai, K., and Ikeda, M. (2002) A novel methodology employing *Corynebacterium glutamicum* genome information to generate a new L-lysine-producing mutant, *Appl. Microbiol. Biotechnol. 58*, 217-223.

[12] Ikeda, M., Ohnishi, J., Hayashi, M., and Mitsuhashi, S. (2006) A genome-based approach to create a minimally mutated *Corynebacterium glutamicum* strain for efficient L-lysine production, *J. Ind. Microbiol. Biotechnol. 33*, 610-615.

[13] Becker, J., Zelder, O., Hafner, S., Schröder, H., and Wittmann, C. (2011) From zero to hero - design-based systems metabolic engineering of *Corynebacterium glutamicum* for L-lysine production, *Metab. Eng. 13*, 159-168.

[14] Xu, J., Han, M., Zhang, J., Guo, Y., and Zhang, W. (2014) Metabolic engineering *Corynebacterium glutamicum* for the L-lysine production by increasing the flux into L-lysine biosynthetic pathway, *Amino Acids 46*, 2165-2175.

[15] Kind, S., Becker, J., and Wittmann, C. (2013) Increased lysine production by flux coupling of the tricarboxylic acid cycle and the lysine biosynthetic pathway - metabolic engineering of the availability of succinyl-CoA in *Corynebacterium glutamicum*, *Metab. Eng. 15*, 184-195.

[16] Blombach, B., Hans, S., Bathe, B., and Eikmanns, B. J. (2009) Acetohydroxyacid synthase, a novel target for improvement of L-lysine production by *Corynebacterium glutamicum*, *Appl. Environ. Microbiol. 75*, 419-427.

[17] Peters-Wendisch, P. G., Schiel, B., Wendisch, V. F., Katsoulidis, E., Möckel, B., Sahm, H., and Eikmanns, B. J. (2001) Pyruvate carboxylase is a major bottleneck for glutamate

and lysine production by *Corynebacterium glutamicum*, *J. Mol. Microbiol. Biotechnol. 3*, 295-300.

[18] Hwang, J. H., Hwang, G. H., and Cho, J. Y. (2008) Effect of increased glutamate availability on L-ornithine production in *Corynebacterium glutamicum*, *J. Microbiol. Biotechnol. 18*, 704-710.

[19] Li, Y., Cong, H., Liu, B., Song, J., Sun, X., Zhang, J., and Yang, Q. (2016) Metabolic engineering of *Corynebacterium glutamicum* for methionine production by removing feedback inhibition and increasing NADPH level, *Antonie Van Leeuwenhoek 109*, 1185-1197.

[20] Perez-Garcia, F., Max Risse, J., Friehs, K., and Wendisch, V. F. (2017) Fermentative production of L-pipecolic acid from glucose and alternative carbon sources, *Biotechnol. J. 12*.

[21] Jorge, J. M. P., Perez-Garcia, F., and Wendisch, V. F. (2017) A new metabolic route for the fermentative production of 5-aminovalerate from glucose and alternative carbon sources, *Bioresour. Technol.*

[22] Kind, S., Neubauer, S., Becker, J., Yamamoto, M., Volkert, M., von Abendroth, G., Zelder, O., and Wittmann, C. (2014) From zero to hero - Production of bio-based nylon from renewable resources using engineered *Corynebacterium glutamicum*, *Metab. Eng. 25*, 113-123.

[23] Limberg, M. H., Schulte, J., Aryani, T., Mahr, R., Baumgart, M., Bott, M., Wiechert, W., and Oldiges, M. (2017) Metabolic profile of 1,5-diaminopentane producing *Corynebacterium glutamicum* under scale-down conditions: blueprint for robustness to bioreactor inhomogeneities, *Biotechnol. Bioeng. 114*, 560-575.

[24] Nguyen, A. Q., Schneider, J., Reddy, G. K., and Wendisch, V. F. (2015) Fermentative production of the diamine putrescine: system metabolic engineering of *Corynebacterium glutamicum*, *Metabolites 5*, 211-231.

[25] Inui, M., Murakami, S., Okino, S., Kawaguchi, H., Vertes, A. A., and Yukawa, H. (2004) Metabolic analysis of *Corynebacterium glutamicum* during lactate and succinate productions under oxygen deprivation conditions, *J. Mol. Microbiol. Biotechnol. 7*, 182-196.

[26] Okino, S., Noburyu, R., Suda, M., Jojima, T., Inui, M., and Yukawa, H. (2008) An efficient succinic acid production process in a metabolically engineered *Corynebacterium glutamicum* strain, *Appl. Microbiol. Biotechnol. 81*, 459-464.

[27] Litsanov, B., Brocker, M., and Bott, M. (2012) Toward homosuccinate fermentation: metabolic engineering of *Corynebacterium glutamicum* for anaerobic production of succinate from glucose and formate, *Appl. Environm. Microbiol. 78*, 3325-3337.

[28] Zhu, N., Xia, H., Yang, J., Zhao, X., and Chen, T. (2014) Improved succinate production in *Corynebacterium glutamicum* by engineering glyoxylate pathway and succinate export system, *Biotechnol. Lett. 36*, 553-560.

[29] Wang, C., Zhou, Z., Cai, H., Chen, Z., and Xu, H. (2017) Redirecting carbon flux through *pgi*-deficient and heterologous transhydrogenase toward efficient succinate production in *Corynebacterium glutamicum*, *J. Ind. Microbiol. Biotechnol. 44*, 1115-1126.

[30] Rohles, C. M., Giesselmann, G., Kohlstedt, M., Wittmann, C., and Becker, J. (2016) Systems metabolic engineering of *Corynebacterium glutamicum* for the production of the carbon-5 platform chemicals 5-aminovalerate and glutarate, *Microbial cell factories 15*, 154.

[31] Kinoshita, S., Udaka, S., and Shimono, M. (1957) Studies on amino acid fermentation. Part I. Production of L-glutamic acid by various microorganisms., *J. Gen. Appl. Microbiol. 3*, 193-205.

[32] Yanisch-Perron, C., Vieira, J., and Messing, J. (1985) Improved M13 phage cloning vectors and host strains: nucleotide sequence of the M13mp18 and pUC19 vectors, *Gene 33*, 103-119.

[33] Frunzke, J., Engels, V., Hasenbein, S., Gätgens, C., and Bott, M. (2008) Co-ordinated regulation of gluconate catabolism and glucose uptake in *Corynebacterium glutamicum* by two functionally equivalent transcriptional regulators, GntR1 and GntR2, *Mol. Microbiol. 67*, 305-322.

[34] Litsanov, B., Kabus, A., Brocker, M., and Bott, M. (2012) Efficient aerobic succinate production from glucose in minimal medium with *Corynebacterium glutamicum*, *Microb. Biotechnol. 5*, 116-128.

[35] Schendzielorz, G., Dippong, M., Grünberger, A., Kohlheyer, D., Yoshida, A., Binder, S., Nishiyama, C., Nishiyama, M., Bott, M., and Eggeling, L. (2014) Taking control over control: Use of product sensing in single cells to remove flux control at key enzymes in biosynthesis pathways, *ACS Synth. Biol. 3*, 21-29.

[36] Schäfer, A., Tauch, A., Jäger, W., Kalinowski, J., Thierbach, G., and Pühler, A. (1994) Small mobilizable multipurpose cloning vectors derived from the *Escherichia coli* plasmids pK18 and pK19 - Selection of defined deletions in the chromosome of *Corynebacterium glutamicum*, *Gene 145*, 69-73.

[37] Kuipers, R. K., Joosten, H. J., van Berkel, W. J., Leferink, N. G., Rooijen, E., Ittmann, E., van Zimmeren, F., Jochens, H., Bornscheuer, U., Vriend, G., dos Santos, V. A., and Schaap, P. J. (2010) 3DM: systematic analysis of heterogeneous superfamily data to discover protein functionalities, *Proteins 78*, 2101-2113.

[38] Sievers, F., Wilm, A., Dineen, D., Gibson, T. J., Karplus, K., Li, W., Lopez, R., McWilliam, H., Remmert, M., Soding, J., Thompson, J. D., and Higgins, D. G. (2011) Fast, scalable generation of high-quality protein multiple sequence alignments using Clustal Omega, *Mol. Syst. Biol. 7*, 539.

[39] Robert, X., and Gouet, P. (2014) Deciphering key features in protein structures with the new ENDscript server, *Nucleic Acids Res. 42*, W320-324.

[40] Arnold, K., Bordoli, L., Kopp, J., and Schwede, T. (2006) The SWISS-MODEL workspace: a web-based environment for protein structure homology modelling, *Bioinformatics 22*, 195-201.

3.3 Pyruvate carboxylase from *Corynebacterium glutamicum*: purification and characterization.

Kortmann M., Baumgart M., and Bott M*.

IBG-1: Biotechnology, Institute of Bio- and Geosciences, Forschungszentrum Jülich, Jülich, Germany

*Corresponding author

Author contributions

The project was planned by MK, MBa and MBo and supervised by MBa and MBo. MK performed all experimental work (construction of plasmids, strain cultivation, protein purification, determination of PCx kinetics in enzyme assays, streptavidin gel shift assays) and data were analysed by MK, MBa and MBo. All figures were prepared by MK, the manuscript was written by MK and MBo. MK, MBa and MBo edited the manuscript.

MK: Maike Kortmann, MBa: Meike Baumgart, MBo: Michael Bott

Overall contribution MK: 80%

BIOTECHNOLOGICALLY RELEVANT ENZYMES AND PROTEINS

Pyruvate carboxylase from *Corynebacterium glutamicum*: purification and characterization

Maike Kortmann[1] · Meike Baumgart[1] · Michael Bott[1] (iD)

Abstract

Pyruvate carboxylase of *Corynebacterium glutamicum* serves as anaplerotic enzyme when cells are growing on carbohydrates and plays an important role in the industrial production of metabolites derived from the tricarboxylic acid cycle, such as L-glutamate or L-lysine. Previous studies suggested that the enzyme from *C. glutamicum* is very labile, as activity could only be measured in permeabilized cells, but not in cell-free extracts. In this study, we established conditions allowing activity measurements in cell-free extracts of *C. glutamicum* and purification of the enzyme by avidin affinity chromatography and gel filtration. Using a coupled enzymatic assay with malate dehydrogenase, V_{max} values between 20 and 25 μmol min^{-1} mg^{-1} were measured for purified pyruvate carboxylase corresponding to turnover numbers of $160 - 200$ s^{-1} for the tetrameric enzyme. The concentration dependency for pyruvate and ATP followed Michaelis-Menten kinetics with K_m values of 3.76 ± 0.72 mM and 0.61 ± 0.13 mM, respectively. For bicarbonate, concentrations $\geq$5 mM were required to obtain activity and half-maximal rates were found at 13.25 ± 4.88 mM. ADP and aspartate inhibited PCx activity with apparent K_i values of 1.5 mM and 9.3 mM, respectively. Acetyl-CoA had a weak inhibitory effect, but only at low concentrations up to 50 μM. The results presented here enable further detailed biochemical and structural studies of this enzyme.

Keywords Pyruvate carboxylase · *Corynebacterium glutamicum* · Anaplerotic reactions · Enzyme purification · Enzyme assay · Enzyme kinetics · Kinetic parameters · Inhibitors

Introduction

Strains of the Gram-positive soil bacterium *Corynebacterium glutamicum* are important microbial cell factories for the industrial production of amino acids, major products being L-glutamate and L-lysine (Becker and Wittmann 2012; Eggeling and Bott 2015; Wendisch et al. 2016). For the sugar-based overproduction of these amino acids and a variety of other metabolites derived from the tricarboxylic acid (TCA) cycle, anaplerotic reactions replenishing oxaloacetate by carboxylation of either phosphoenolpyruvate or pyruvate are essential. *C. glutamicum* possesses both phosphoenolpyruvate carboxylase (PEPCx) and pyruvate carboxylase (PCx) (for review, see Sauer and Eikmanns 2005)

✉ Michael Bott
    m.bott@fz-juelich.de

[1]   IBG-1: Biotechnology, Institute of Bio- and Geosciences,
     Forschungszentrum Jülich, 52425 Jülich, Germany

Whereas PEPCx encoded by the *ppc* gene was shown to be dispensable for lysine production (Gubler et al. 1994; Peters-Wendisch et al. 1993), deletion of the *pyc* gene encoding PCx caused a strong decrease in lysine production and—vice versa—*pyc* overexpression increased the synthesis of this amino acid (Peters-Wendisch et al. 2001). Tween 60–induced glutamate production was also lowered upon *pyc* deletion and increased by *pyc* overexpression (Peters-Wendisch et al. 2001). PCx was shown to be important for growth on lactate, and absence of both PCx and PEPCx led to the inability to grow in glucose minimal medium, indicating the absence of further anaplerotic enzymes for growth on carbohydrates (Peters-Wendisch et al. 1998). A ^{13}C-based carbon flux study by NMR revealed that both PEPCx and PCx were active in cells growing with glucose, but PCx was calculated to contribute about 90% of the C_3 carboxylation flux (Petersen et al. 2000).

Whereas in an early study describing PEPCx activity in cell-free extracts of *C. glutamicum* subspecies *flavum* PCx could not be detected (Ozaki and Shiio 1969), the simultaneous presence of PEPCx activity and PCx activity was later found in cell-free extracts of *C. glutamicum* subspecies *lactofermentum* (Tosaka

et al. 1979). In this study, PCx was shown to be inhibited by avidin and independent of acetyl-CoA (Tosaka et al. 1979). However, subsequent attempts to detect PCx activity in cell extracts of *C. glutamicum* failed (Cocaign-Bousquet et al. 1996; Cocaign-Bousquet and Lindley 1995; Gubler et al. 1994; Jetten et al. 1994; Peters-Wendisch et al. 1993). Only the use of cells permeabilized with CTAB (*N*-cetyl-*N,N,N*-trimethylammonium bromide) allowed reliable measurement of PCx activity using a discontinuous glutamate-oxaloacetate transaminase-coupled assay (Peters-Wendisch et al. 1997) or, alternatively, a discontinuous assay measuring the remaining pyruvate by NADH-dependent conversion to lactate with lactate dehydrogenase (Koffas et al. 2002; Uy et al. 1999).

C. glutamicum PCx, encoded by the *pyc* gene, is a biotin-dependent enzyme composed of 1140 amino acids (123 kDa) (Koffas et al. 1998; Peters-Wendisch et al. 1998). Based on its sequence similarity to other PCx enzymes with known crystal structure (Jitrapakdee et al. 2008; St Maurice et al. 2007), it is presumed to form a homotetramer with each monomer composed of four domains, an N-terminal biotin carboxylase domain (BC), a central carboxyl transferase domain (CT), a C-terminal biotin carboxyl carrier protein (BCCP), and a protein tetramerization domain (PT) composed of two amino acid stretches located between the BC and CT domains and between the CT and BCCP domains (Kortmann et al. 2019). PCx activity involves two partial reactions: first, the BC domain catalyzes the ATP-dependent carboxylation of biotin linked covalently to K^{1106} within the BCCP domain of *C. glutamicum* PCx; then the CT domain transfers the activated CO_2 group from carboxybiotin to pyruvate forming oxaloacetate. Cryo-electron microscopy of the tetrameric PCx of *Staphylococcus aureus* revealed the structural transitions that are accompanied with the catalysis of the two partial reactions (Lasso et al. 2014).

The inability to measure PCx activity in cell-free extracts of *C. glutamicum*, except for the very first report (Tosaka et al. 1979), suggested that the enzyme is very labile and becomes rapidly inactive upon cell disruption. Alternatively, a metabolite essential for PCx activity might be lost during the preparation of the extracts. As PCx activity measurements with permeabilized cells require the presence of a detergent and might include interfering enzymatic activities, this study aimed at finding experimental conditions allowing the measurement of PCx activity in *C. glutamicum* cell extracts, purification of the enzyme in its active state, and determination of the kinetic parameters with the purified enzyme.

Methods

Bacterial strains and cultivation conditions

All bacterial strains and plasmids used in this study are listed in Table 1. For cloning procedures, *Escherichia coli* DH5α was used. The strain was grown at 37 °C in LB medium (Bertani 1951) supplemented with kanamycin (50 mg l^{-1}). The strain *C. glutamicum* DM1868Δ*pyc*, transformed with the plasmid pAN6-*pyc* (Kortmann et al. 2019), was used for overproduction of the *C. glutamicum* PCx protein. For that purpose, a colony from a fresh BHI agar plate was used to inoculate 10-ml brain heart infusion (BHI) medium (Difco Laboratories, Detroit, MI, USA) with kanamycin (25 mg l^{-1}) in a 100-ml shaking flask with baffles and the culture was incubated at 130 rpm and 30 °C for 8 h. Cells of this first preculture were washed with 0.9% (wt/vol) NaCl and used to inoculate a second preculture in 50 ml CGXII medium (Keilhauer et al. 1993) containing glucose (40 g l^{-1}) and protocatechuate (0.03 g l^{-1}) to an optical density of 0.5 at 600 nm (OD_{600}). This preculture was incubated for 16 h at 30 °C and 120 rpm in a 500-ml shaking flask with baffles. Afterwards, the cells were washed with 0.9% (wt/vol) NaCl and used to inoculate 500 ml CGXII medium with glucose (20 g l^{-1}) and protocatechuate (0.03 g l^{-1}) to an OD_{600} of 1. This culture was incubated at 30 °C and 100 rpm in a 2-l shaking flask with baffles. The expression of the *pyc* gene was induced by addition of 1 mM isopropyl β-ᴅ-1-thio-galactopyranoside (IPTG) at an OD_{600} of 2 and the cultures

Table 1 Bacterial strains and plasmids used in this study

Strain or plasmid	Relevant characteristics	Reference
Strains		
E. coli DH5α	Strain used for cloning procedures; F⁻ φ80*lacZ* ΔM15 Δ(*lacZYA-argF*) U169 *recA*1 *endA*1 *hsdR*17(rk⁻, mk⁺) *phoA supE44 thi*-1 *gyrA*96 *relA*1 λ⁻	(Hanahan 1983)
C. glutamicum ATCC13032	Biotin-auxotrophic wild type	(Abe et al. 1967)
C. glutamicum DM1868	ATCC13032 with a point mutation in *lysC* (cg0306) resulting in *lysC*^T311I (feedback-resistant aspartate kinase)	Evonik Industries AG
C. glutamicum DM1868Δ*pyc*	DM1868 with a deletion of the *pyc* gene (cg0791)	(Kortmann et al. 2019)
Plasmids		
pAN6	Kan^R; *C. glutamicum*/*E. coli* shuttle vector for regulated gene expression using P*tac* (P*tac* *lacI*^q pBL1 *oriV*_{Cg} pUC18 *oriV*_{Ec})	(Frunzke et al. 2008)
pAN6-*pyc*	Kan^R; pAN6 derivative for expression of *pyc* (cg0791) under control of P*tac*	(Kortmann et al. 2019)

were incubated for another approx. 5 h until they reached an OD_{600} of 7. Afterwards, cells were harvested by centrifugation (4 °C, 10 min, 6000g), resuspended in 200 ml PCx buffer (50 mM Tris-HCl, pH 7.2, 1 M KCl, 0.278 M *myo*-inositol, 5 mM $MgCl_2$, 2 mM DTT), and centrifuged at 4 °C for 15 min at 5000g. The cell pellets were stored at − 80 °C until use.

Preparation of cell-free extracts and purification of pyruvate carboxylase

For the purification of PCx from *C. glutamicum*, PCx buffer (described above) was supplemented with cOmplete™ ULTRA Protease Inhibitor Cocktail (Roche Diagnostics, Mannheim, Germany) for all steps described in the following chapter. Cell pellets of *C. glutamicum* DM1868Δ*pyc* carrying pAN6-*pyc* were thawed on ice and resuspended in PCx buffer to obtain a concentration of about 0.3 mg wet cells per milliliter. Cells were disrupted by five passages through a HTU-Digi French Press (G. Heinemann, Schwaebisch Gmuend, Germany). After removal of intact cells and cell debris by centrifugation (4 °C, 20 min, 5100g), the cell extract was subjected to ultracentrifugation (4 °C, 1 h, 100,000g) to sediment membranes. The resulting supernatant was used as cell-free extract for PCx activity measurements and for PCx purification.

For the purification of PCx, the cell-free extract was supplemented with 3 mM ATP, 10 mM pyruvate, and 10 mM $KHCO_3$ to improve the accessibility of protein-bound biotin (Purcell and Wallace [1996]). The biotinylated proteins were then purified by affinity chromatography with monomeric avidin-agarose (Pierce™ Thermo Scientific, Waltham, MA, USA) using a column with 2-ml bed volume. Before use, the avidin agarose was regenerated by washing with 0.1 M glycine, pH 2.8, and then equilibrated with PCx buffer. The cell-free extract was passed twice through the column, which subsequently was washed with 14 ml PCx buffer to remove unbound proteins. To elute bound proteins, 4 ml PCx buffer supplemented with 4 mM D-biotin was added to the avidin agarose column and the column was incubated in the elution buffer for 30 min at 4 °C. Afterwards, the eluate was collected and concentrated 10-fold with Amicon® Ultra Centrifugal Filters (30 kDa cutoff) as described by the manufacturer (Merck Millipore, Darmstadt, Germany). The concentrated eluate (0.4 ml) was used for size exclusion chromatography and loaded onto a Superdex 200 Increase 10/300 GL column integrated into an Äkta Pure™ system (GE Healthcare Bio-Sciences, Uppsala, Sweden) and equilibrated with PCx buffer. Elution was performed with PCx buffer at flow rate of 0.5 ml min^{-1} and monitored by following the absorption at 280 nm. PCx-containing fractions were pooled and directly used further. Protein concentrations were determined with the Bradford assay (Bradford [1976]) using an Infinite M1000Pro plate reader (Tecan, Männedorf, Switzerland) and a commercial staining solution (AppliChem GmbH, Darmstadt, Germany).

Measurement of PCx activity

PCx activity was measured using a coupled enzyme assay with malate dehydrogenase, which catalyzes the NADH-dependent reduction of oxaloacetate formed by PCx to malate (Milrad de Forchetti and Cazzulo [1976]). The oxidation of NADH was followed spectrophotometrically at 340 nm with an Ultrospec™ 2100 Pro UV spectrophotometer (GE Healthcare, Freiburg, Germany). PCx activity was assayed at 30 °C in 1 ml 50 mM Tris-HCl buffer pH 7.2 containing 8 mM $MgCl_2$, 40 mM $KHCO_3$, 6 mM ATP, 0.2 mM NADH, 1 U/ml malate dehydrogenase from porcine heart (Sigma, St. Louis, MO, USA), and 0.5 to 5 μg protein (cell-free extract or purified PCx). After preincubation for 1 min to determine the background rate of NADH oxidation in the absence of PCx activity, the reaction was started by adding 20 mM sodium pyruvate. The decrease in absorbance at 340 nm was measured for 2 min and corrected for NADH oxidation in the absence of pyruvate. An extinction coefficient of 6.2 mM^{-1} cm^{-1} at 340 nm was used for NADH in the calculation of reaction rates. For the determination of K_m values, the concentrations of pyruvate, ATP, or $KHCO_3$ were varied, whereas all other substrates were held constant at saturating concentrations. To test the effects of ADP, aspartate, and acetyl-CoA on PCx activity, different concentrations of these metabolites were added to the assay mixture. One unit (U) of PCx activity is defined as 1 μmol of NADH oxidized per minute.

K_m and V_{max} values were determined with a non-linear regression fit using the OriginPro 8.5 software (OriginLab, Northampton, MA, USA). A plot of velocity (v) vs. varying substrate concentration (S) was fitted to the Hill equation:

$$v = V_{max} \frac{(S^n)}{K_m{}^n + (S^n)} \qquad (1)$$

When the Hill coefficient n is set to 1, Eq. [1] is equal to Michaelis-Menten equation, which was used for the determination of K_m and V_{max} values for pyruvate and ATP. For the calculation of half maximal inhibition, a dose response curve was used to fit a plot of velocity (v) vs. varying inhibitor concentrations (I) with the following equation:

$$v = B + \frac{T-B}{1 + 10^{logI0-I}*p} \qquad (2)$$

T is the maximal velocity observed in the absence of an inhibitor, B is the minimal velocity observed at high inhibitor concentrations, log I_0 is the center point of the S-shaped curve halfway between T and B, and p is the Hill slope.

Protein analysis by SDS-PAGE and streptavidin gel shift assay

The purification of PCx was analyzed by sodium dodecyl sulfate-polyacrylamide gel electrophoresis (SDS-PAGE) (Laemmli 1970). A trichloroacetic acid precipitation of all samples to be analyzed by SDS-PAGE was performed in advance. For this purpose, 1 volume of sample was mixed with 1/4 volume of ice-cold 100% (wt/vol) trichloroacetic and incubated at 4 °C for 10 min. Afterwards, the sample was centrifuged for 15 min at 15,000g and 4 °C. The supernatant was removed and the pellet was washed twice with 200 μl ice-cold acetone. After centrifugation for 15 min at 15,000g and 4 °C, the pellet was dried at 95 °C for 5 min and dissolved in H_2O to a concentration of 0.1 mg protein per milliliter. Finally, the samples were mixed with an appropriate volume of 5× sample buffer (250 mM Tris-HCl, pH 6.8, 5% (wt/vol) SDS, 250 mM DTT, 0.5% (wt/vol) bromophenol blue, 50% (vol/vol) glycerin) and incubated for 5 min at 95 °C. A volume corresponding to 1.5 μg protein was loaded onto the gel (4% stacking gel, 8% separating gel). After electrophoresis at 140 V, the gel was stained with GelCode™ Blue Stain Reagent (Thermo Scientific, Waltham, MA, USA).

To quantify the extent of PCx biotinylation, a streptavidin gel shift assay with the purified enzyme was performed as described (Fairhead and Howarth 2015). As mentioned above, TCA precipitation of protein samples was performed prior to SDS-PAGE. The protein pellet containing 6 μg purified PCx was dissolved in 5 μl H_2O and mixed with a 4-fold molar excess of streptavidin (AppliChem GmbH, Darmstadt, Germany). As a negative control, a PCx sample was treated exactly the same way as described above, but streptavidin was replaced by water. The samples were subjected to SDS-PAGE (4% stacking gel, 8% separating gel) at 120 V. To avoid warming of the gel, the electrophoresis chamber was placed in an ice bath.

Results

Identification of conditions allowing measurement of *C. glutamicum* PCx activity in cell-free extracts

PCx is an important anaplerotic enzyme in *C. glutamicum*. However, in almost all studies on PCx of *C. glutamicum* published until now, enzyme activity could only be measured in permeabilized cells, but not in cell-free extracts, indicating that the enzyme is very labile. In order to characterize the enzyme in the purified form, we searched for conditions that might stabilize it in an active state. For this purpose, we used strain *C. glutamicum* DM1868Δ*pyc* carrying the expression plasmid pAN6-*pyc*, which allows IPTG-inducible overexpression of the *pyc* gene. Based on a study reporting the purification and

characterization of a PCx enzyme of *Mycobacterium smegmatis* (Mukhopadhyay and Purwantini 2000), which shows 65% amino acid sequence identity to *C. glutamicum* PCx, we prepared cell extracts using a PCx buffer composed of 50 mM Tris-HCl pH 7.2, 5 mM $MgCl_2$, 2 mM DTT, 0.278 M *myo*-inositol, and 1 M KCl. *Myo*-inositol had been reported to stabilize PCx activity and the high KCl concentration improved purification of PCx from *M. smegmatis* by avidin affinity chromatography (Mukhopadhyay and Purwantini 2000). For the determination of PCx activity in *C. glutamicum*, a coupled enzymatic assay with malate dehydrogenase was used (Milrad de Forchetti and Cazzulo 1976).

After cell disruption, intact cells and cell debris were removed by low-speed centrifugation and membranes by ultracentrifugation. The resulting cell-free extract was used for the enzymatic assay. Indeed, a specific PCx activity of 0.17 ± 0.02 μmol min^{-1} (mg protein)$^{-1}$ was measured for *C. glutamicum* DM1868Δ*pyc*/pAN6-*pyc*, indicating that the buffer conditions used were able to stabilize *C. glutamicum* PCx. In a control experiment with cell-free extract of the negative control strain *C. glutamicum* DM1868Δ*pyc*/pAN6, no PCx activity was detectable. The PCx activity was strictly dependent on the presence of ATP, bicarbonate (supplied as $KHCO_3$), Mg^{2+} (supplied as $MgCl_2$), and pyruvate (data not shown). Without NADH, no activity was detectable. In the absence of malate dehydrogenase from porcine heart, 41% of the PCx activity of the complete assay mixture could still be measured, which is due to the endogenous malate dehydrogenase of *C. glutamicum* (Molenaar et al. 2000) present in the cell-free extracts.

Purification of PCx from *C. glutamicum*

The cell-free extract of strain *C. glutamicum* DM1868Δ*pyc*/pAN6-*pyc* was used for affinity chromatography with monomeric avidin agarose to specifically purify biotinylated proteins. After washing the column with PCx buffer, biotinylated proteins were eluted with PCx buffer supplemented with 4 mM D-biotin and the protein-containing elution fractions were analyzed by SDS-PAGE and Coomassie straining. Two protein bands were detected, a dominant one with an apparent mass of about 125 kDa and a minor one with an apparent mass of about 65 kDa (Fig. 1a), which corresponded to PCx (Cg0791, calculated mass 123.3 kDa with biotin) and to the biotin-containing α-subunit of acetyl-CoA/propionyl-CoA carboxylase (AccBC, Cg0802, calculated mass 63.6 kDa with biotin), respectively (Jäger et al. 1996; Peters-Wendisch et al. 1998).

To purify PCx to homogeneity and get rid of AccBC, size exclusion chromatography was performed in a next step. For this purpose, the eluate of the avidin affinity
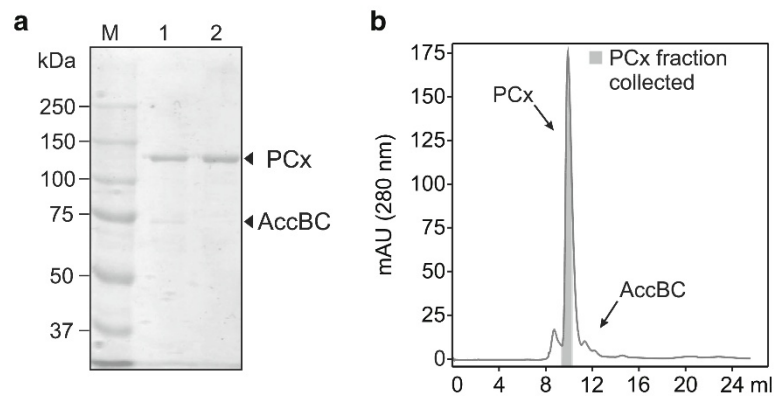
Fig. 1 Purification of PCx from *C. glutamicum*. *a* Coomassie-stained SDS-polyacrylamide gel showing the elution fraction of the avidin agarose affinity chromatography (lane 1) and the PCx fraction collected during size-exclusion chromatography (lane 2). Lane M contains Precision Plus Protein™ All Blue Prestained Protein Standard (Bio-Rad Laboratories, Hercules, California, USA). *b* Chromatogram of the size exclusion chromatography of the concentrated elution fraction of avidin-agarose chromatography. Peaks representing PCx and AccBC are indicated. The PCx fraction collected for biochemical studies is marked in grey. mAU, absorbance units at 280 nm

chromatography was concentrated to a total volume of about 0.4 ml and then subjected to gel filtration using a Superdex 200 Increase 10/300 GL column (GE Healthcare) and PCx buffer. PCx eluted as a sharp peak before AccBC (Fig. 1b). Because of some overlap, the collection of the PCx peak was terminated prematurely to avoid contamination with AccBC. As shown by SDS-PAGE, the collected fraction contained a single protein band with an apparent size of about 125 kDa (Fig. 1a), whose identity as PCx was confirmed by peptide mass fingerprinting (data not shown). From a 500-ml culture of *C. glutamicum* DM1868Δ*pyc*/pAN6-*pyc*, about 0.5 mg purified PCx was obtained.

Estimation of the extent of biotinylation of purified PCx from C. glutamicum

To determine the extent of biotinylation of purified PCx, a streptavidin gel shift assay was performed, which is based on the observation that streptavidin (monomeric form 16.81 kDa) will retain its native tetramer structure (67.24 kDa) and remain bound to biotin conjugates during SDS-PAGE if the gel does not get excessively warm during electrophoresis (Fairhead and Howarth 2015). Purified PCx from *C. glutamicum* was denatured by incubation for 5 min at 95 °C to obtain monomeric PCx, mixed with a 4-fold molar excess of streptavidin (apparent mass after SDS-PAGE approx. 60 kDa; calculated mass 75.34 kDa) and separated by SDS-PAGE. As controls, PCx alone and streptavidin alone were loaded next to the mixed sample. As shown in Fig. 2, incubation of PCx with streptavidin caused a shift of the band from 125 kDa to about 150 kDa and only a very small fraction of about 5% appeared not be shifted. This indicated that the vast majority of purified PCx was biotinylated.

Kinetic parameters of purified PCx of C. glutamicum

The kinetic parameters of purified PCx from *C. glutamicum* were measured using the coupled enzymatic assay with malate dehydrogenase immediately after the purification. The activity remained stable over several hours as checked by measurements at the start and at the end of an assay series. However, storage of the purified PCx overnight at 4 °C or at − 20 °C caused a complete inactivation of the enzyme. Therefore, all enzyme activity measurements had to be performed on the same day as PCx was purified. In initial experiments with the complete
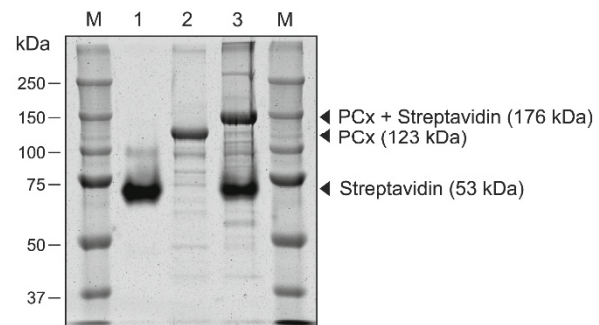
Fig. 2 Quantification of PCx biotinylation by a streptavidin gel shift assay. Lane 1 contains 15 μg streptavidin, lane 2 contains 6 μg PCx, and lane 3 a mixture of 6 μg PCx and 12 μg streptavidin. Before electrophoresis, the PCx-streptavidin mixture was incubated for 5 min at room temperature to enable the binding of streptavidin to biotin of PCx. The samples were separated by SDS-PAGE at 120 V with the electrophoresis chamber cooled in an ice bath. Subsequently, the gel was stained with GelCode™ Blue Stain Reagent (Thermo Scientific, Waltham, MA, USA) and scanned with a Typhoon scanner (GE Healthcare). Precision Plus Protein™ All Blue Prestained Protein Standard (Bio-Rad Laboratories, Hercules, California, US) was used to estimate the apparent molecular mass of the proteins

assay mixture, specific activities between 20 and 25 μmol min^{-1} (mg protein)$^{-1}$ were determined for purified PCx preparations, corresponding to a 118-fold to 147-fold enrichment compared to the cell-free extract. The turnover number calculated for a PCx monomer is 41–51 s^{-1}. Control experiments in which individual components were omitted from the assay mixture confirmed that PCx activity was dependent on the presence of pyruvate, ATP, bicarbonate, Mg^{2+}, NADH, and malate dehydrogenase. The fact that no activity of purified PCx was found without the addition of malate dehydrogenase to the assay mixture confirmed that the residual activity observed in cell-free extracts was due to the endogenous malate dehydrogenase activity of *C. glutamicum*.

For the determination of the K_m values for the substrates pyruvate, ATP, and bicarbonate, the concentrations in the assay mixture were varied from 0 to 20 mM for pyruvate, from 0 to 6 mM for ATP, and from 0 to 50 mM for KHCO$_3$. Plots of initial velocities vs. substrate concentrations are shown in Fig. 3. In the case of pyruvate, the data could be fitted with non-linear regression to Michaelis-Menten kinetics resulting in a K_m value of 3.76 ± 0.71 mM and a V_{max} of 24.89 ± 2.54 μmol min^{-1} (mg protein)$^{-1}$ (Fig. 3a). For ATP, a K_m of 0.61 ± 0.13 mM and a V_{max} of 19.05 ± 1.93 μmol min^{-1} (mg protein)$^{-1}$ were determined (Fig. 3b). The dependency of PCx activity for the bicarbonate concentration did not follow Michaelis-Menten kinetics (Fig. 3c). No activity was observed at KHCO$_3$ concentrations below 5 mM. When the data were fitted to the Hill equation, a K_m of 13.25 ± 4.88 mM and a V_{max} of 20.88 ± 1.62 μmol min^{-1} (mg protein)$^{-1}$ were calculated. The Hill coefficient was determined as $n = 4.3$, indicating positive cooperativity towards bicarbonate.

Influence of effector molecules on the activity of purified PCx of *C. glutamicum*

Previous studies with permeabilized cells had shown that ADP, acetyl-CoA, and aspartate inhibited PCx activity (Koffas et al. 2002; Peters-Wendisch et al. 1997). We now tested the effects of these metabolites on purified PCx. ADP inhibited PCx activity (100% corresponded to 20.77 ± 2.34 μmol min^{-1} (mg protein)$^{-1}$) and fitting of the data to a dose-response equation resulted in an apparent K_i of 1.5 mM (Fig. 4a). Complete inhibition of PCx activity was observed at 10–20 mM ADP. Acetyl-CoA usually acts as an activator of PCx enzymes of the α_4 type (Adina-Zada et al. 2012), but in previous studies with permeabilized cells, acetyl-CoA was found to act as inhibitor of PCx of *C. glutamicum* with a K_i of 110 μM (Peters-Wendisch et al. 1997). In our studies with the purified enzyme, acetyl-CoA at concentrations below 50 μM had a slightly
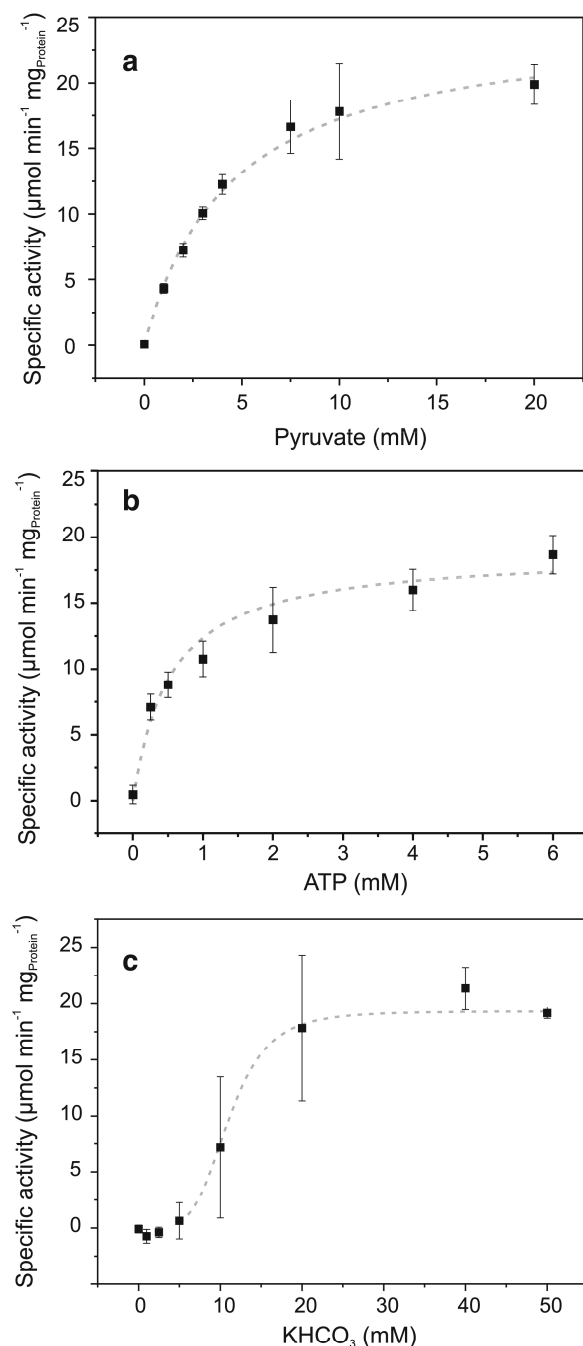
Fig. 3 Activity of purified PCx from *C. glutamicum* at different concentrations of the substrates pyruvate (*a*), ATP (*b*), and HCO$_3^-$ (*c*). Dashed lines indicate the fit to the Hill equation with fixed $n = 1$ for pyruvate and ATP, whereas n was not fixed for HCO$_3^-$. Mean values and standard deviations of at least three independent enzyme preparations are shown

inhibitory effect, reducing PCx activity by 20% at most, whereas higher acetyl-CoA concentrations were less

inhibitory (Fig. 4b). In the case of aspartate, an apparent K_i of 9.3 mM was calculated and complete inhibition was obtained at concentrations above 20 mM (Fig. 4c).
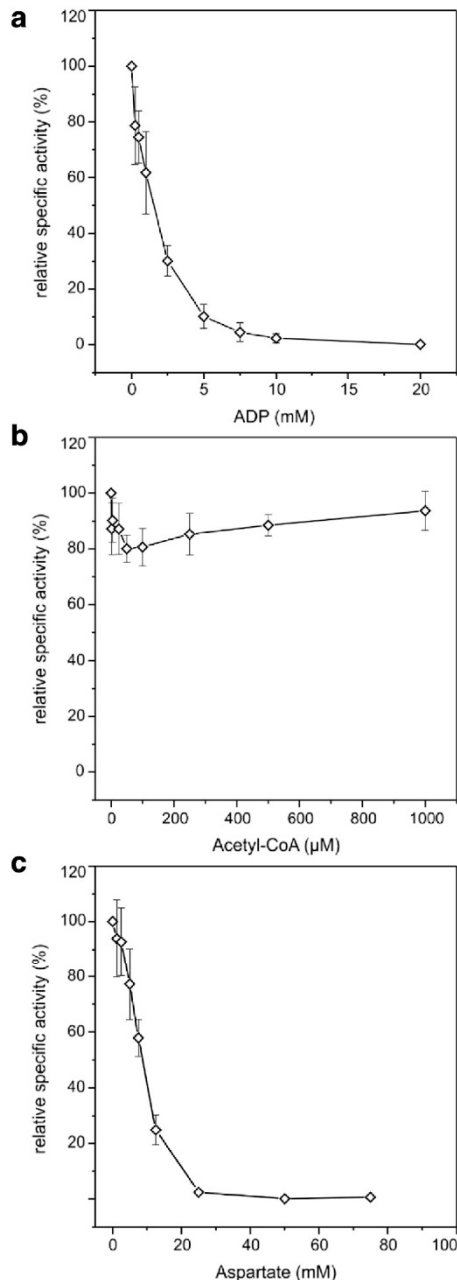
Fig. 4 Influence of ADP, acetyl-CoA, and L-aspartate on the activity of purified PCx of *C. glutamicum*. Activity was measured using the standard assay mixture supplemented with the indicated concentrations of ADP, aspartate, and acetyl-CoA. The activities were plotted as percentage of PCx activity measured in the absence of these metabolites, which was set as 100%. Mean values of at least three independent enzyme preparations with standard deviations are shown

Discussion

PCx is an important anaplerotic enzyme for the sugar-based production of amino acids like L-lysine and L-glutamate with *C. glutamicum*. In previous studies, PCx activity could only be detected in permeabilized cells, but not in cell-free extracts of *C. glutamicum* (Koffas et al. 2002; Peters-Wendisch et al. 1997; Uy et al. 1999). In this study, we identified experimental conditions allowing the measurement of PCx activity in cell-free extracts of *C. glutamicum* and report on the purification and characterization of PCx from *C. glutamicum*.

In general, two types of PCx enzymes have been described, those with an $\alpha_4\beta_4$ quaternary structure, where the α subunits contain the BC domain, while the β subunits contain the CT and BCCP domains, and those with an α_4 quaternary structure. The $\alpha_4\beta_4$-type PCs are found in archaea, such as *Methanobacterium thermoautotrophicum* (Mukhopadhyay et al. 1998), but also in some bacteria, such as *Pseudomonas aeruginosa* (Lai et al. 2006). The α_4-type PCs are more common and have been found in fungi, invertebrates, vertebrates, and most bacteria, including *C. glutamicum* (Adina-Zada et al. 2012). They are composed of four identical subunits having a size of 120–130 kDa and the tetrameric structure is essential for activity, as the BC domain carboxylates the biotin group of the BCCP domain of the same subunit, but the activated CO_2 is used by the CT domain of the neighboring subunit to carboxylate pyruvate to oxaloacetate (Lasso et al. 2014).

The failure to measure PCx activity in cell-free extracts of *C. glutamicum* could be due to an intrinsic lability of the enzyme, causing dissociation and thus inactivation upon cell disruption. In this study, we used a buffer containing 0.278 M *myo*-inositol and 1 M KCl. Similar conditions had previously been used to purify PCx of *Methanobacterium thermoautotrophicum* (Mukhopadhyay et al. 1998) and *Mycobacterium smegmatis* (Mukhopadhyay and Purwantini 2000), where the inclusion of *myo*-inositol was crucial to obtain active protein. *Myo*-inositol was reported to promote the thermal and structural stability of different proteins, as shown by an increase of the melting temperature (Ortbauer and Popp 2008). The positive impact of high salt concentrations on enzyme stability or activity was shown for various enzymes, like PCx from *M. thermoautotrophicum* (Mukhopadhyay et al. 1998) or mammalian adipocyte lipid-binding protein (Schoeffler et al. 2003). A high KCl concentration was also reported to be important to obtain good yield and purity of PCx after avidin affinity chromatography (Mukhopadhyay et al. 1998). Since avidin has a pI of about 10.5, it is positively charged at the lower pH values used for affinity chromatography, allowing negatively charged proteins in the cell extracts to bind unspecifically to the avidin matrix. High concentrations of K^+ probably help to avoid this unspecific binding.

When using the buffer with *myo*-inositol and KCl, a specific PCx activity of 170 nmol min^{-1} (mg protein)$^{-1}$ was measured

in cell-free extracts of glucose-grown *C. glutamicum* DM1868Δ*pyc*/pAN6-*pyc*, which is comparable to the value obtained with permeabilized cells for a strain overexpressing the *pyc* gene (Peters-Wendisch et al. 1998). The eluate obtained after avidin-agarose affinity chromatography of cell-free extract of *C. glutamicum* DM1868Δ*pyc*/pAN6-*pyc* contained only the two known biotinylated proteins present in this organism, PCx and AccBC, confirming that the experimental conditions prevented unspecific binding of proteins to the avidin matrix. The AccBC protein could be separated from PCx by gel filtration, leading to a highly pure PCx preparation from *C. glutamicum* (Fig. 1). Unfortunately, the activity of this PCx preparation was lost after incubation overnight at 4 °C or at − 20 °C, supporting the assumed lability of the protein. Further studies are required to identify conditions allowing long-term stability of PCx activity. Purified PCx of *C. glutamicum* revealed a specific activity of 20–25 μmol min^{-1} (mg protein)$^{-1}$ corresponding to turnover numbers of 160–200 s^{-1} for the tetrameric enzyme. For purified PCx of *M. smegmatis*, specific activities up to 150 μmol min^{-1} (mg protein)$^{-1}$ were reported, but these were measured at 45 °C and not at 30 °C as in our experiments with PCx of *C. glutamicum*.

The apparent K_m value determined for pyruvate (3.76 mM) with purified PCx of *C. glutamicum* was about 3-fold higher than the apparent K_m value measured with permeabilized cells (1.3 mM). This discrepancy is presumably caused by the different experimental conditions used in these determinations. The K_m values for pyruvate reported for PCx enzymes of other organisms are typically lower with values around or below 0.5 mM (Table 2). A possible explanation for the high K_m value of *C. glutamicum* PCx could be that the pyruvate dehydrogenase complex of this species, which forms a unique supercomplex with 2-oxoglutarate dehydrogenase (Niebisch et al. 2006), was reported to have a K_m value of 1.7 mM for pyruvate (Schreiner et al. 2005). As pyruvate dehydrogenase competes with PCx for the substrate, a higher affinity of PCx for pyruvate might have negative consequences for carbon metabolism. The apparent K_m value of purified PCx for ATP

(0.61 mM) was also about 3-fold higher than the K_m measured with permeabilized cells, but is within the range reported for PCx enzymes of other species (Table 2) and within the range of the intracellular ATP concentration (Bennett et al. 2009). In contrast to pyruvate and ATP, the concentration dependency of purified PCx for HCO$_3^-$ did not follow Michaelis-Menten kinetics, but showed an allosteric behavior with half-maximal activity at 13 mM HCO$_3^-$. An allosteric behavior was also reported for PCx of *M. thermoautotrophicum* (Mukhopadhyay et al. 1998). PEPCx of *C. glutamicum* was reported to have a K_m value of 2.8 mM for HCO$_3^-$ (Chen et al. 2014) and it might be speculated that PEPCx is more important at low bicarbonate concentrations and PCx at higher bicarbonate concentrations.

Purified PCx of *C. glutamicum* was inhibited by ADP and aspartate with apparent K_i values of 1.5 mM and 9.3 mM, respectively. These values are in good agreement with the ones measured with permeabilized cells, which were 2.6 mM for ADP (Peters-Wendisch et al. 1997) and about 10 mM for aspartate (Koffas et al. 2002). Acetyl-CoA usually acts as an allosteric activator of PCx enzymes of the α$_4$-type (Adina-Zada et al. 2012), but was reported to be an inhibitor of PCx of *C. glutamicum* with a K_i of 110 μM (Peters-Wendisch et al. 1997). In our studies with purified PCx, an unusual response towards acetyl-CoA was observed, with maximally 20% inhibition at about 50 μM acetyl-CoA and less inhibition at higher concentrations. An explanation for this behavior and the difference between the results with permeabilized cells and purified PCx cannot be provided.

In a previous study, we employed the genetically encoded lysine biosensor pSenLys to identify PCx variants that enabled an increased lysine production from glucose (Kortmann et al. 2019). These PCx variants contained the amino acid exchanges T132A, T343A, and I1012S. In order to get hints on the effects of these mutations, we performed a number of preliminary studies. We purified the variants PCx^{T132A}, PCx^{T343A}, and PCx^{I1012S} as described above for wild-type PCx using *C. glutamicum* DM1868Δ*pyc* transformed with

Table 2 Subunit composition and K_m values of PCx enzymes from different organisms

Species	PCx type	K_m (mM) Pyruvate	K_m (mM) ATP	K_m (mM) HCO$_3^-$	Reference
C. glutamicum	α$_4$	3.76 ± 0.71	0.61 ± 0.13	13.3 ± 4.9	This study
C. glutamicum (permeabilized cells)	α$_4$	1.3	0.2	n.d.	(Peters-Wendisch et al. 1997)
Rhizobium etli	α$_4$	0.15 ± 0.01	0.15 ± 0.01	10.8 ± 0.4	(Zeczycki et al. 2011)
Mycobacterium smegmatis PCx1 (MSMEG_2412)	α$_4$	0.3 ± 0.04	1.26 ± 0.24	3 ± 0.5	(Mukhopadhyay and Purwantini 2000)
Saccharomyces cerevisiae PCx1	α$_4$	0.50 ± 0.06	0.07 ± 0.01	1.36 ± 0.12	(Jitrapakdee et al. 2007)
Saccharomyces cerevisiae PCx2	α$_4$	0.17 ± 0.02	0.79 ± 0.04	21.5 ± 1.8	(Jitrapakdee et al. 2007)
Methanobacterium thermoautotrophicum	α$_4$β$_4$	0.5 ± 0.026	2.5 ± 0.43	5.3 ± 0.59	(Mukhopadhyay et al. 1998)
Methanococcus jannaschii	α$_4$β$_4$	0.53 ± 0.002	0.37 ± 0.04	0.22 ± 0.00	(Mukhopadhyay et al. 2000)

the expression plasmids pAN6-*pyc*^{T132A}, pAN6-*pyc*^{T343A}, and pAN6-*pyc*^{I1012S}, respectively. With around 20 μmol min^{-1} (mg protein)$^{-1}$, the specific activity of the purified PCx variants was in a similar range as that of wild-type PCx. The influence of ADP and acetyl-CoA on the three PCx variants was comparable to wild-type PCx. In the case of aspartate, the PCx^{I1012S} variant showed a similar inhibition as wild-type PCx, but PCx^{T132A} and PCx^{T343A} displayed a different pattern. These variants appeared to be less sensitive to aspartate at low concentrations, as their activity was not inhibited up to 7.5 mM aspartate. The apparent K_i values were 13.16 mM for PCx^{T132A} and 10.80 mM for PCx^{T343A} and thus higher compared to wild-type PCx with an apparent K_i value of 8.94 mM aspartate. Full inhibition was observed with 50 mM aspartate for all mutated PCx variants. These results, although preliminary, suggest that the positive effects of PCx^{T132A} and PCx^{T343A} on lysine production might be due at least in part to a reduced inhibition of activity by aspartate.

In summary, our study has revealed conditions allowing the measurement of PCx activity in cell-free extracts of *C. glutamicum* and purification of the enzyme in an active form. This provides the basis for more detailed analysis of the biochemical and structural properties of this enzyme and mutated variants.

Compliance with ethical standards

Conflict of interest   The authors declare that they have no conflict of interest.

Ethical approval   This article does not contain any studies with human participants or animals performed by any of the authors.

References

Abe S, Takayama K, Kinoshita S (1967) Taxonomical studies on glutamic acid producing bacteria. J Gen Appl Microbiol 13:279–301

Adina-Zada A, Zeczycki TN, Attwood PV (2012) Regulation of the structure and activity of pyruvate carboxylase by acetyl CoA. Arch Biochem Biophys 519(2):118–130. https://doi.org/10.1016/j.abb.2011.11.015

Becker J, Wittmann C (2012) Bio-based production of chemicals, materials and fuels -*Corynebacterium glutamicum* as versatile cell factory. Curr Opin Biotechnol 23(4):631–640. https://doi.org/10.1016/j.copbio.2011.11.012

Bennett BD, Kimball EH, Gao M, Osterhout R, Van Dien SJ, Rabinowitz JD (2009) Absolute metabolite concentrations and implied enzyme active site occupancy in *Escherichia coli*. Nat Chem Biol 5(8):593–599

Bertani G (1951) Studies on lysogenesis. I. The mode of phage liberation by lysogenic *Escherichia coli*. J Bacteriol 62(3):293–300

Bradford MM (1976) A rapid and sensitive method for the quantitation of microgram quantities of protein utilizing the principle of protein-dye binding. Anal Biochem 72:248–254

Chen Z, Bommareddy RR, Frank D, Rappert S, Zeng AP (2014) Deregulation of feedback inhibition of phosphoenolpyruvate carboxylase for improved lysine production in *Corynebacterium*

glutamicum. Appl Environ Microbiol 80(4):1388–1393. https://doi.org/10.1128/aem.03535-13

Cocaign-Bousquet M, Guyonvarch A, Lindley ND (1996) Growth rate-dependent modulation of carbon flux through central metabolism and the kinetic consequences for glucose-limited chemostat cultures of *Corynebacterium glutamicum*. Appl Environ Microbiol 62(2):429–436

Cocaign-Bousquet M, Lindley ND (1995) Pyruvate overflow and carbon flux within the central metabolic pathways of *Corynebacterium glutamicum* during growth on lactate. Enzym Microb Technol 17(3):260–267

Eggeling L, Bott M (2015) A giant market and a powerful metabolism: L-lysine provided by *Corynebacterium glutamicum*. Appl Microbiol Biotechnol 99(8):3387–3394. https://doi.org/10.1007/s00253-015-6508-2

Fairhead M, Howarth M (2015) Site-specific biotinylation of purified proteins using BirA. In: Gautier A, Hinner MJ (eds) Site-specific protein labeling: methods and protocols. Methods in Molecular Biology. Springer Science+Business Media, New York, pp 171–184

Frunzke J, Engels V, Hasenbein S, Gätgens C, Bott M (2008) Co-ordinated regulation of gluconate catabolism and glucose uptake in *Corynebacterium glutamicum* by two functionally equivalent transcriptional regulators, GntR1 and GntR2. Mol Microbiol 67(2):305–322

Gubler M, Park SM, Jetten M, Stephanopoulos G, Sinskey AJ (1994) Effects of phosphoenol pyruvate carboxylase deficiency on metabolism and lysine production in *Corynebacterium glutamicum*. Appl Microbiol Biotechnol 40:857–863

Hanahan D (1983) Studies on transformation of *Escherichia coli* with plasmids. J Mol Biol 166(4):557–580

Jäger W, Peters-Wendisch PG, Kalinowski J, Pühler A (1996) A *Corynebacterium glutamicum* gene encoding a two-domain protein similar to biotin carboxylases and biotin-carboxyl-carrier proteins. Arch Microbiol 166:76–82

Jetten MSM, Pitoc GA, Follettie MT, Sinskey AJ (1994) Regulation of phospho(enol)-pyruvate and oxaloacetate-converting enzymes in *Corynebacterium glutamicum*. Appl Microbiol Biotechnol 41(1):47–52

Jitrapakdee S, Adina-Zada A, Besant PG, Surinya KH, Cleland WW, Wallace JC, Attwood PV (2007) Differential regulation of the yeast isozymes of pyruvate carboxylase and the locus of action of acetyl CoA. Int J Biochem Cell Biol 39(6):1211–1223. https://doi.org/10.1016/j.biocel.2007.03.016

Jitrapakdee S, St Maurice M, Rayment I, Cleland WW, Wallace JC, Attwood PV (2008) Structure, mechanism and regulation of pyruvate carboxylase. Biochem J 413(3):369–387. https://doi.org/10.1042/BJ20080709

Keilhauer C, Eggeling L, Sahm H (1993) Isoleucine synthesis in *Corynebacterium glutamicum*: molecular analysis of the *ilvB-ilvN-ilvC* operon. J Bacteriol 175(17):5595–5603

Koffas MA, Jung GY, Aon JC, Stephanopoulos G (2002) Effect of pyruvate carboxylase overexpression on the physiology of *Corynebacterium glutamicum*. Appl Environ Microbiol 68(11):5422–5428

Koffas MA, Ramamoorthi R, Pine WA, Sinskey AJ, Stephanopoulos G (1998) Sequence of the *Corynebacterium glutamicum* pyruvate carboxylase gene. Appl Microbiol Biotechnol 50(3):346–352

Kortmann M, Mack C, Baumgart M, Bott M (2019) Pyruvate carboxylase variants enabling improved lysine production from glucose identified by biosensor-based high-throughput fluorescence-activated cell sorting screening. ACS Synth Biol 8(2):274–281. https://doi.org/10.1021/acssynbio.8b00510

Laemmli UK (1970) Cleavage of structural proteins during the assembly of the head of bacteriophage T4. Nature 227:680–685

Lai H, Kraszewski JL, Purwantini E, Mukhopadhyay B (2006) Identification of pyruvate carboxylase genes in *Pseudomonas*

aeruginosa PAO1 and development of a *P. aeruginosa*-based over-expression system for a$_4$- and a$_4$b$_4$-type pyruvate carboxylases. Appl Environ Microbiol 72(12):7785–7792. https://doi.org/10.1128/AEM.01564-06

Lasso G, Yu LP, Gil D, Lazaro M, Tong L, Valle M (2014) Functional conformations for pyruvate carboxylase during catalysis explored by cryoelectron microscopy. Structure 22(6):911–922. https://doi.org/10.1016/j.str.2014.04.011

Milrad de Forchetti SR, Cazzulo JJ (1976) Some properties of the pyruvate carboxylase from *Pseudomonas fluorescens*. J Gen Microbiol 93(1):75–81. https://doi.org/10.1099/00221287-93-1-75

Molenaar D, van der Rest ME, Drysch A, Yücel R (2000) Functions of the membrane-associated and cytoplasmic malate dehydrogenases in the citric acid cycle of *Corynebacterium glutamicum*. J Bacteriol 182:6884–6891

Mukhopadhyay B, Patel VJ, Wolfe RS (2000) A stable archaeal pyruvate carboxylase from the hyperthermophile *Methanococcus jannaschii*. Arch Microbiol 174(6):406–414

Mukhopadhyay B, Purwantini E (2000) Pyruvate carboxylase from *Mycobacterium smegmatis*: stabilization, rapid purification, molecular and biochemical characterization and regulation of the cellular level. Biochim Biophys Acta 1475:191–206

Mukhopadhyay B, Stoddard SF, Wolfe RS (1998) Purification, regulation, and molecular and biochemical characterization of pyruvate carboxylase from *Methanobacterium thermoautotrophicum* strain DH. J Biol Chem 273(9):5155–5166

Niebisch A, Kabus A, Schultz C, Weil B, Bott M (2006) Corynebacterial protein kinase G controls 2-oxoglutarate dehydrogenase activity via the phosphorylation status of the OdhI protein. J Biol Chem 281:12300–12307

Ortbauer M, Popp M (2008) Functional role of polyhydroxy compounds on protein structure and thermal stability studied by circular dichroism spectroscopy. Plant Physiol Biochem 46(4):428–434. https://doi.org/10.1016/j.plaphy.2008.02.002

Ozaki H, Shiio I (1969) Regulation of the TCA and glyoxylate cycles in *Brevibacterium flavum*. II. Regulation of phosphoenolpyruvate carboxylase and pyruvate kinase. J Biochem 66(3):297–311

Peters-Wendisch PG, Eikmanns BJ, Thierbach G, Bachmann B, Sahm H (1993) Phosphoenolpyruvate carboxylase in *Corynebacterium glutamicum* is dispensable for growth and lysine production. FEMS Microbiol Lett 112(3):269–274

Peters-Wendisch PG, Kreutzer C, Kalinowski J, Patek M, Sahm H, Eikmanns BJ (1998) Pyruvate carboxylase from *Corynebacterium glutamicum*: characterization, expression and inactivation of the *pyc* gene. Microbiology 144:915–927

Peters-Wendisch PG, Schiel B, Wendisch VF, Katsoulidis E, Möckel B, Sahm H, Eikmanns BJ (2001) Pyruvate carboxylase is a major bottleneck for glutamate and lysine production by *Corynebacterium glutamicum*. J Mol Microbiol Biotechnol 3(2):295–300

Peters-Wendisch PG, Wendisch VF, Paul S, Eikmanns BJ, Sahm H (1997) Pyruvate carboxylase as an anaplerotic enzyme in *Corynebacterium glutamicum*. Microbiology 143(4):1095–1103

Petersen S, de Graaf AA, Eggeling L, Möllney M, Wiechert W, Sahm H (2000) *In vivo* quantification of parallel and bidirectional fluxes in the anaplerosis of *Corynebacterium glutamicum*. J Biol Chem 275(46):35932–35941

Purcell AW, Wallace JC (1996) The accessibility of the prosthetic group biotin during monomeric avidin affinity chromatography. Anal Biochem 238(2):213–216. https://doi.org/10.1006/abio.1996.0280

Sauer U, Eikmanns BJ (2005) The PEP-pyruvate-oxaloacetate node as the switch point for carbon flux distribution in bacteria. FEMS Microbiol Rev 29(4):765–794

Schoeffler AJ, Ruiz CR, Joubert AM, Yang X, LiCata VJ (2003) Salt modulates the stability and lipid binding affinity of the adipocyte lipid-binding proteins. J Biol Chem 278(35):33268–33275. https://doi.org/10.1074/jbc.M304955200

Schreiner ME, Fiur D, Holatko J, Patek M, Eikmanns B (2005) E1 enzyme of the pyruvate dehydrogenase complex in *Corynebacterium glutamicum*: molecular analysis of the gene and phylogenetic aspects. J Bacteriol 187:6005–6018

St Maurice M, Reinhardt L, Surinya KH, Attwood PV, Wallace JC, Cleland WW, Rayment I (2007) Domain architecture of pyruvate carboxylase, a biotin-dependent multifunctional enzyme. Science 317(5841):1076–1079. https://doi.org/10.1126/science.1144504

Tosaka O, Morioka H, Takinami K (1979) Role of biotin-dependent pyruvate-carboxylase in L-lysine production. Agric Biol Chem 43(7):1513–1519. https://doi.org/10.1080/00021369.1979.10863663

Uy D, Delaunay S, Engasser JM, Goergen JL (1999) A method for the determination of pyruvate carboxylase activity during the glutamic acid fermentation with *Corynebacterium glutamicum*. J Microbiol Methods 39(1):91–96

Wendisch VF, Jorge JMP, Perez-Garcia F, Sgobba E (2016) Updates on industrial production of amino acids using *Corynebacterium glutamicum*. World J Microbiol Biotechnol 32(6):105. https://doi.org/10.1007/s11274-016-2060-1

Zeczycki TN, Menefee AL, Jitrapakdee S, Wallace JC, Attwood PV, St Maurice M, Cleland WW (2011) Activation and inhibition of pyruvate carboxylase from *Rhizobium etli*. Biochemistry 50(45):9694–9707. https://doi.org/10.1021/bi201276r

4   Discussion

4.1 Establishing a T7 RNA polymerase-dependent gene expression system in *Coryne-bacterium glutamicum*

In biotechnology it is of great importance to be able to overproduce proteins in large amounts. On the one hand, the proteins itself can be the product of interest for the industry and therefore an efficient overexpression of the corresponding gene is necessary. One example is the re-combinant production of insulin, which is nowadays almost exclusively produced in recombinant *E. coli* or *Saccharomyces cerevisiae* strains (Landgraf and Sandow, 2016; Wong, 2018). On the other hand, gene expression systems are needed for the characterization of proteins to allow the efficient synthesis of the respective protein in order to study its structures and physiological functions. Because of the low costs and easy handling, in many cases bacteria are preferred as expression host, like *E. coli* or *Bacillus subtillis* (Georgiou and Valax, 1996). Even though *C. glutamicum* seems to be very suitable as an expression host as well, no strong and at the same time tightly regulated system for the expression of heterologous proteins has been constructed so far. The plasmid-based pEKEx2 system, in which the target gene is cloned under the control of the IPTG-inducible promoter P_{tac}, is one of the most frequently used systems to date for *C. glutamicum* (Eikmanns et al., 1991). Nevertheless, the system shows basal expression in the absence of the inducer and the promoter only allows a moderate ex-pression rate after induction (Patek et al., 2003). Other systems, such as pCLTON2, show a reduced basal expression compared to the pEKEx2 system, but the expression level of the target gene is after induction by anhydrotetracycline (ATc) even lower than for pEKEx2 (Lausberg et al., 2012).

Therefore, we established the widely used T7 RNA polymerase-dependent expression system (Studier and Moffatt, 1986) in *C. glutamicum*. The corynebacterial system was con-structed analogously to the T7 expression system of *E. coli* BL21(DE3) and allows expression of the target gene after induction via IPTG. Therefore, a 4.5 kb DNA fragment was amplified from the genome of *E. coli* BL21(DE3) containing the repressor gene *lacI* under the control of its native promoter, *lacZα*, and T7 gene *1*, the latter two under the control of the *lac*UV5 pro-moter, including three LacI operator sites. This DNA fragment was integrated into the genome of the prophage-free strain *C. glutamicum* MB001 (Baumgart et al., 2013) resulting in the strain *C. glutamicum* MB001(DE3). In strain MB001, the prophages CGP1-3 and by that also the restriction modification (RM)-system located within CGP3, are deleted (Baumgart et al., 2013). It was shown that this genome reduction enabled up to 40% higher expression of *eyfp* with the plasmid pEKEx2-*eyfp* compared to the wild-type ATCC13032 (Baumgart et al., 2013), which made this strain particularly suitable as a platform strain for the T7 expression system. Addi-tionally, the plasmid pMKEx2 was constructed, in which the desired gene can easily be cloned

under control of the strong T7 promoter. For the construction of this plasmid, the expression cassette of the vector pET52b(+) with an N-terminal Strep-tag II and a C-terminal His-tag was cloned into the backbone of the corynebacterial pJC1 vector. In order to extend the range of options for easy purification of the desired protein, the expression plasmid pMKEx1 was also constructed, but not further characterized in this work. Here, the expression cassette of pET-TEV1 with an N-terminal His-tag was inserted into the pJC1 backbone. Construction and application of this vector are described in a paper by Schulte *et al.* (Schulte et al., 2017). In the course of this work, the newly constructed system in *C. glutamicum* was characterized by the expression of different genes and compared with other existing systems.

4.1.1   Potentials and limitations of the T7 RNA polymerase-dependent gene expression system in *C. glutamicum*

In order to characterize the usability and potential of the newly constructed T7 expression system, first, the expression of the reporter gene *eyfp* was characterized. The amount of the produced eYFP and at the same time the maximal specific fluorescence, i.e. maximal fluorescence per cell density after growth for 24 h, of eYFP increased proportionally to the added quantity of the inducer IPTG. The specific fluorescence increased up to 450-fold and its maximum was observed after addition of 250 µM IPTG, which is far below the previously added standard quantity of 1 mM used e.g. for pEKEx2-based expression. Moreover, the results also showed that P_{T7} is not recognized by the corynebacterial RNAP, thus allowing a tightly controllable expression with the T7 system in *C. glutamicum*.

Compared to the well-established pEKEx2 system, in which eYFP was cloned under the control of the IPTG-inducible P_{tac}, the maximal specific fluorescence of eYFP was about 3.5-fold higher. Reasons for the higher expression level can be explained by several beneficial characteristics of the T7 RNAP over the native polymerase of *C. glutamicum*, which is used for expression in the pEKEx2 system but also other expression systems like the pCLTON2 system (Eikmanns et al., 1991; Lausberg et al., 2012). One probable explanation is the high transcription rate of T7 RNAP, which elongates RNA strands up to 5 times faster than bacterial RNAP (Chamberlin and Ring, 1973; Golomb and Chamberlin, 1977). In addition, the corynebacterial polymerase is dependent on cofactors such as $MgCl_2$ to enable the recognition of promoter sequences (Patek and Nesvera, 2011), whereas the T7 RNAP does not require any further cofactors in the cell (Studier and Moffatt, 1986). Since the corynebacterial RNAP recognizes all native promoters of the host genome and not only the one of the target gene, less RNAP is available for the target promoter (Nesvera et al., 2012), leading to lower expression levels compared to T7 RNAP, which binds only to the promoter of the target gene. In addition to differences of both polymerases, the vectors on which the target gene is encoded can also be decisive for the expression level. While pEKEx2 has a replication origin of the cryptic plasmid

pBL1 (Santamaría et al., 1984), in pMKEx2 the replication is regulated by genes of the plasmid pCG1 (Ozaki et al., 1984). Although both plasmids are replicated via a rolling circle mechanism, the copy numbers differ from 10-30 copies for pBL1 to 30 copies for pCG1 (Nesvera et al., 1997; Santamaría et al., 1984). To investigate the influence of both origins on the expression level, the expression cassette of the pEKEx2 vector should also be cloned into the pJC1 vector (Cremer et al., 1991), the backbone of pMKEx2, and subsequently expression of a target gene should be compared with pMKEx2.

At the same time, a lower basal expression in the absence of the inducer IPTG was measured with the T7 system compared to the pEKEx2 system. This can be explained by the double repression of LacI, blocking both, the expression of the *lac*UV5 promoter, which is responsible for the expression of chromosomally encoded T7 RNA polymerase, and P_{T7lac} itself. For this purpose, three *lac* operator sequences O_1-O_3 can be found on the chromosomally encoded DE3 fragment to which the repressor LacI is able to bind. As a result, loop structures can be formed between O_1 and O_2 or O_3, thus preventing the bacterial polymerase from binding to P_{lacUV5} (Oehler et al., 1990), and by that effectively preventing the expression of T7 RNAP in the non-induced state. In order to further repress the expression of the target gene in the non-induced state, additional operator sequences O_1 and O_3 are also encoded on the expression plasmid pMKEx2, which also prevents the T7 RNAP from binding to P_{T7} in the non-induced state. These operator sequences, O_1 and O_3, are also encoded on pEKEx2, being solely responsible for repression of this system. However, it was shown that the absence of the operator sequence O_2 decreases the repression of LacI about 3- to 6-fold (Eismann et al., 1987; Oehler et al., 1990). Both factors, the simple repression and the absence of the operator sequence O_2, can therefore explain the increased basal expression of the pEKEx2 system. More recently, however, another reason for the high basal expression observed with pEKEx2 was recognized. The pEKEx2-encoded repressor LacI harbours a modified C-terminus, which presumably causes a weakened functionality. After repair of this defect and another one responsible for population heterogeneity, tight repression of target genes could be observed with the improved pEKEx2 derivatives (Bakkes et al. 2020, in preparation).

Low basal expression is particularly important for the expression of genes that have a toxic effect on the cell, like causing cell death or significant growth defects and by that decreasing the production titers. Therefore, tight control of expression enables the culture to grow to high cell densities before the expression of the target gene is induced (Saida et al., 2006). Nevertheless, although the basal expression with the T7 system was lower than with the pEKEx2 system, it could still be measured in the absence of inducer (chapter 3.1). For the T7 system in *E. coli*, it was shown that basal expression in the non-induced state could be reduced by additional expression of the *lysY* gene for T7 lysozyme (Studier, 1991). The T7 lysozyme binds the T7 RNA polymerase formed in the non-induced state of the cell, whereupon genes

under the control of the P_{T7} can no longer be expressed by the T7 RNAP. In first attempts we also tried to further reduce basal expression in *C. glutamicum* by expression of *lysY* encoded on a second plasmid. However, since basal expression of the T7 system in previous measurements was at the lower detection limit when measured with the Biolector®, a more sensitive system for the detection of changes in basal expression had to be found. This failed in the present work (data not shown) and further studies will be necessary in the future to enable a further reduced basal expression of the T7 system in *C. glutamicum*.

4.1.2   Recombinant gene expression in *Corynebacterium glutamicum* with the T7 system

To further characterize the T7 system in *C. glutamicum* for recombinant gene expression, the production of further proteins was analyzed in this work. For this purpose, the *pyk* gene encoding the native pyruvate kinase was expressed and the activity of this enzyme in whole cell extracts was determined. The convincing results obtained for *eyfp* expression with the T7 system were further confirmed. A nearly 40-fold higher activity of pyruvate kinase was measured in *C. glutamicum* MB001(DE3) cells carrying pMKEx2-*pyk* after induction with IPTG compared to cells without IPTG induction (chapter 3.1), showing that pyruvate kinase was functionally overproduced.

As it was possible to use the T7 system in *C. glutamicum* successfully for functional production of the cytoplasmic proteins eYFP and pyruvate kinase, the applicability of the system for the expression of genes for secreted proteins was examined in a next step. The secretion of proteins into the extracellular medium has the considerable advantage of a simpler isolation and purification of the product in the downstream process as fewer other cellular components and proteins are present (Quax, 1997). Since *C. glutamicum* also possesses only low extracellular protease activity, secretional protein production seems to be particularly suitable in this organism (Suzuki et al., 2009). In this work, we analyzed if expression via the T7 system could also enhance the yield of a secreted protein in the extracellular medium of *C. glutamicum* compared to expression via pEKEx2 (see chapter 6.1.1). For this purpose, secretion via the twin-arginine translocation pathway (Tat pathway) was chosen, since the Tat pathway offers the advantage of secreting already folded proteins, even in an oligomeric state (Lee et al., 2006). For secretion, GFP was fused to three different Tat signal peptides, namely TorA of *E. coli*, PhoD of *B. subtilis*, and PhoD (Cg2485) of *C. glutamicum* itself. Successful secretion of these fusion proteins by *C. glutamicum* had already been analyzed previously after expression of the corresponding genes via the pEKEx2 system (Meissner et al., 2007). The results obtained in this thesis showed that the T7 expression system can be used to express genes efficiently and subsequently secrete them into the extracellular medium of *C. glutamicum*. The amount of secreted protein strongly depends on the signal sequence that is used. Moreover,

in comparison to the pEKEx2 system, an overall higher expression of the fusion proteins of the T7 system was observed in Western Blot analysis, with the exception of PhoD$_{Bs}$-GFP. However, a large part of the synthesized target protein could not be transported out of the cell and remained in the cytosol or membrane fraction. Especially with the homologous Tat sequence of PhoD$_{Cg}$ most of the GFP remained in the cell and the lowest GFP fluorescence compared to the other GFP variants could be measured in the supernatant. The results indicate that the Tat system might be overloaded by the high expression rate of the T7 system and the proteins cannot be secreted as fast as they are produced within the cell. This hypothesis is also supported by the observation that the pEKEx2 system produces less protein compared to the T7 system, but shows a higher secretion efficiency. Thereupon, a first attempt was made to overexpress the genes of the Tat system, *tatABC*. The genes were cloned into the expression plasmid pCLTON2 under control of P$_{tet}$, allowing the expression of *tatABC* after adding the inducer ATc. However, the strong growth defect after induction of *tatABC* expression already indicated stress for the cell, which also affected *gfp* expression. Thus, the optimal conditions for the overexpression of the secretion system should be determined in further approaches. Moreover, it was not examined in which ratio the three components are best expressed in order to provide the cell with a functional secretion system. That the secretion of proteins can be increased by the overexpression of the Tat system in *C. glutamicum* has been successfully demonstrated in previous studies (Kikuchi et al., 2009). Here, secretion of a pro-protein glutaminase fused to the TorA signal peptide could be increased about 10-fold after overexpression of *tatABC*. In contrast to this thesis, however, the coding regions of the genes *tatAC* as well as *tatB* were cloned under their respective native promoters P$_{tatAC}$ and P$_{tatB}$ in plasmid pVC7. Overexpression of *tatABC* is therefore only achieved by the higher copy number of the plasmid and expression is not further regulated, e.g. by induction of the expression at a defined time point. Plasmid pVC7 is derived from pAM330, for which a copy number of 10-14 is described (Miwa et al., 1984). The fact that *C. glutamicum* can be used for the efficient expression of proteins, which are secreted via the Tat system, has been demonstrated by the production of an α-amylase or a sorbitol-xylitol oxidase, for example (Lee et al., 2014; Scheele et al., 2013). Moreover, a comparison with the alternative expression hosts *B. subtilis* and *S. carnosus* revealed that *C. glutamicum* was able to secrete the highest amount of functional GFP into the extracellular medium via the Tat system (Meissner et al., 2007). In summary, it can therefore be said that *C. glutamicum* seems suitable for the expression and subsequent secretion of proteins via the Tat system. For the efficient use of the T7 system, however, the expression strain should be optimized to enable also a higher secretion rate, e.g. by balanced overexpression of the Tat system according to Kikuchi et al. (Kikuchi et al., 2009). Furthermore, for the optimization of the expression and secretion efficiency of the desired protein, the optimal Tat signal sequence seems to be of major importance.

Due to its easy handling and the demonstrated ability to strongly overexpress genes, the T7 system in *C. glutamicum* has already been used in numerous other applications in the last years: For the production of plant polyphenols like stilbenes and flavonoids, different *C. glutamicum* platform strains were constructed. These platform strains are based on the strain MB001(DE3) and heterologous genes for polyphenol production were cloned under control of the T7 promoter in the pMKEx2-plasmid (Kallscheuer et al., 2016). In first attempts stilbene concentrations of up to 158 mg l^{-1} and (2S)-flavanone concentrations of 37 mg l^{-1} could be reached (Kallscheuer et al., 2016). Another application of the T7 system was the successful overexpression of the phosphodiesterase gene *cpdA* for subsequent purification and characterization of the protein (Schulte et al., 2017). Moreover, operons of *Citrobacter freundii* encoding propanediol utilization compartment shell genes could be expressed efficaciously via the T7 system in *C. glutamicum* (Huber et al., 2017).

All these results clearly show the power of the T7 RNA polymerase-dependent gene expression system in *C. glutamicum* to produce active proteins in large quantities, whether they are homologous or heterologous proteins. Furthermore, the aforementioned wide range of applications shows that the system is an ideal tool for strain optimization of *C. glutamicum* and perfectly complements existing expression systems.

4.2 Strategies for strain optimization in *Corynebacterium glutamicum*

Since the discovery of *C. glutamicum* and its ability to secrete L-glutamate, strain optimization has been intensively pursued so that the organism is now one of the most important amino acid producers in white biotechnology, especially for the production of L-glutamate or L-lysine. In the past, strains were generated by undirected mutagenesis using UV light and/or chemicals to improve the production of a desired substance (Kelle et al., 2005). This method is very time-consuming due to the necessary multiple rounds of mutagenesis and subsequent screening for suitable strains. Moreover, the generated strains contain numerous mutations in the genome, some of which may have no or even a negative effect. As a result, metabolic burden such as a low stress tolerance or slow growth is often observed for these strains (Ohnishi et al., 2002). Only some of the mutations are actually beneficial for production, but often they have not been identified or insufficiently characterized and consequently their impact on production is largely unknown. As an example, the observed differences in the L-lysine production of the two strains *C. glutamicum* DG52-5 and DM1868 in this work can be used: whereas in strain DG52-5 overexpression of *pyc* leads to a 50% increase in L-lysine accumulation and *pyc* deletion causes a 60% decrease (Peters-Wendisch et al., 2001), in strain DM1868 overexpression of *pyc* caused an increase in lysine production of 63% and *pyc* deletion a 14% decrease (see chapter 3.2). Both strains, DG52-5 (Cremer et al., 1988) and DM1868 (Evonik, Halle-Künsebeck) contain a feedback-resistant aspartate kinase (LysC). However, in contrast to strain DM1868 the strain DG52-5 was generated by undirected mutagenesis. A re-sequencing of the genome of strain DG52-5 in this work revealed 104 SNPs as well as 8 insertions or deletions, and 7 MNPs, whereby the latter are characterized by several consecutive nucleotide alterations causing an amino acid exchange (see chapter 6.2). It was discovered that the feedback resistance of LysC is caused by different mutations in both strains. In addition, mutations were found in genes that might have an effect on lysine production in strain DG52-5 as well, like the genes encoding the inositol permeases IolT2 and the regulators SigA or OxyR. This example demonstrates the problematic nature of these strains, since without further analysis, it remains unknown which mutations are actually affecting L-lysine biosynthesis. Within the last decades, a deeper understanding of the metabolic pathways and their regulation was obtained. One of the most important milestones in this regard was the sequencing of the complete genome of *C. glutamicum* in 2003 (Ikeda and Nakagawa, 2003; Kalinowski et al., 2003). This opened the door to progress the development and application of genetic engineering tools, systems biology and global analysis methods, like transcriptome or metbolom anaylsis (Kim et al. 2013). Nowadays, rational approaches are increasingly used for strain optimization e.g. by overcoming feedback resistances of specific enzymes or minimizing by-product formation. As a result, production strains with a defined genome, e.g. for L-lysine production, have been constructed, like the strain LYS-12, encoding 12 defined mutations in the genome (Becker et

al., 2011). For the construction of this strain, mutations known from classically derived production strains were used and combined. However, since the number of such known mutations is limited, there is a lack of alternatives to be able to further improve L-lysine production with *C. glutamicum*. Therefore, a major aim of this work was to find gene variants that enable improved L-lysine production in *C. glutamicum* to offer novel options for rational strain optimization.

4.2.1 Use of biosensors for screening of PCx muteins enabling improved L-lysine production

The progress of rational strain engineering is often still limited by the predictability of mutations with an anticipated positive effect on product synthesis. In order to combine the advantages of the rational, targeted approach with those of undirected mutagenesis, transcription factor-based biosensors have been developed in recent years as a new tool for strain optimization (Binder et al., 2012; Mustafi et al., 2012; Siedler et al., 2014). With this method, the concentration of a certain metabolite within a single cell is converted to a measurable optical output, i.e. fluorescence. When combined with FACS, transcription factor-based biosensors allow screening of libraries composed of millions of variants within minutes or hours for those single cells that show increased fluorescence.

In this work the transcription factor-based biosensor pSenLys-Spec (Binder et al., 2012; Schendzielorz et al., 2014) was used to screen a mutant library of the corynebacterial PCx generated by error-prone PCR. The sensor is based on the transcriptional regulator LysG, which senses increased concentrations of the basic amino acids L-arginine, L-histidine and L-lysine in *C. glutamicum*, whereupon its target gene *lysE* encoding an exporter for L-lysine and L-arginine is transcribed (Bellmann et al., 2001). In case of pSenLys-Spec, *lysE* has been replaced by *eyfp*, with the purpose to couple increased concentrations of the named amino acids to an increased fluorescence output, which can be measured for example by FACS. The sensor has been successfully used in previous studies, e. g. to find variants of feedback-inhibited enzymes of lysine, arginine and histidine biosynthesis that show feedback resistance towards the respective amino acid (Schendzielorz et al., 2014). For example, 11 variants of the aspartate kinase LysC were identified due to the fact that they allowed increased lysine production in *C. glutamicum* compared to the strain with wild-type LysC. Further analysis of three of these LysC variants showed that they exhibited significantly reduced feedback inhibition by L-lysine. Variants of ATP phosphoribosyltransferase (HisG) and N-acetyl-L-glutamate kinase (ArgB) resistant to inhibition by histidine and arginine, respectively, were also discovered with pSenLys-Spec (Schendzielorz et al. 2014).

In this thesis, we used the pSenLys-Spec to screen a PCx mutant library for enzyme variants that enable a higher lysine production in strain *C. glutamicum* DM1868. For this purpose, more than 1.7×10^6 cells of a *pyc*-mutant library generated by error-prone PCR with about 9.6×10^4 individual transformants were analyzed in one FACS screening step (chapter 3.2). Since PCx has a size of 1140 amino acids, the coverage of all possible PCx variants within this library is impractical. If only a single amino acid residue would be mutated per protein, $\binom{1140}{1} \times 19 = 2.3 \times 10^4$ PCx variants are possible, calculated as the binominal coefficient, which could still be covered by the generated library if variants do not appear several times and all variants contain exactly one mutation. But in this study conditions were chosen to introduce about four amino acid exchanges per protein and consequently the number of possible PCx variants exponentially increases up to $\sum_{k=1}^{4} \binom{1140}{k} \times 19^k = 9.1 \times 10^{15}$ (Bosley et al., 2004). In turn, this means that less than $1 \times 10^{-9}\%$ of all possible muteins were included in the screened library, without consideration of PCx variants which do not fit the criteria of one to four mutations. It seems highly impossible to be able to prepare a library of this size for the screening of all possible variants with this approach. So further strategies can be combined in the future to increase the number of positive variants, like preparing saturation libraries of found mutations (Schendzielorz et al., 2014) or sequence saturation mutagenesis (Wong et al., 2004). Likewise, only defined parts of PCx, like the binding sites of effectors like ADP, aspartate or acetyl CoA could be randomly mutagenized to find further mutations leading to a higher L-lysine production.

Moreover, mutations in the PCx alone are not sufficient to trigger increased L-lysine production in the wild-type background of *C. glutamicum*, because the lysine biosynthesis is still strongly feedback-inhibited by LysC. Therefore, the strain DM1868Δ*pyc* encoding the feedback resistant aspartate kinase LysC^{T311I} was chosen for the screening of PCx variants since it is already capable of producing moderate amounts of lysine. As a result, only small differences in fluorescence output were observed between strains harboring the wild-type PCx and mutant variants and many false positive clones were isolated in the FACS analysis (chapter 3.2). Consequently, a good validation system of sorted clones was inevitable. In this work, isolated clones were grown in in a microscale cultivation system (Biolector®) and subsequent amino acid quantification was performed via HPLC, which allowed a throughput of about 50 clones per day. To increase this throughput, alternative assays might be performed, like a ninhydrin assay to determine the lysine concentration of more than 100 clones within minutes (Unthan et al., 2015).

However, despite the fact that only a tiny fraction of the theoretically possible PCx variants was screened in this work and the differences in fluorescence output were only marginal, three mutations allowing an increased lysine production were identified in only one screening round, i.e. T132A, T343A and I1012S. Because PCx activity is not regulated by the end product

L-lysine, it can be assumed that the use of pSenLys or other biosensors is also suitable for screening of other enzymes of central metabolism, such as glycolysis or the pentose phosphate pathway, thus extending the application possibilities of biosensors in strain optimization of *C. glutamicum*. Furthermore, the applied screening procedure revealed PCx mutations that were previously completely unknown and whose influence on L-lysine production could not be predicted, since the mutated residues were not located within functionally characterized regions of PCx, like the ATP- or pyruvate-binding site.

4.2.2   Engineering PCx to overcome the bottleneck of precursor supply in the TCA cycle

Many of the products for which *C. glutamicum* producer strains have been developed are intermediates or derivatives of the TCA cycle (see chapter 3.2.1, Table S1). Of particular economic importance is L-lysine, which is derived from oxaloacetate (OAA). It was found that this precursor can be a limiting factor for optimal lysine production (Menkel et al., 1989) and therefore the supply of OAA is of great interest for strain optimization. Its production is ensured by two anaplerotic enzymes in *C. glutamicum:* PEPCx and PCx catalyze the carboxylation of PEP and pyruvate towards OAA, respectively (Eikmanns et al., 1989; O'Regan et al., 1989; Peters-Wendisch et al., 1996; Peters-Wendisch et al., 1997). It could be shown that under glycolytic conditions PCx is contributing about 90% of the total OAA synthesis (Petersen et al., 2000). Moreover, overproduction of *pyc* resulted in an approximately 50% higher L-lysine production, whereas overexpression of the PEPCx gene had no effect (Peters-Wendisch et al., 1993; Peters-Wendisch et al., 2001). These results underline the major role of PCx in anaplerosis and the associated possibilities to improve the production of various substances with OAA as precursor, like L-lysine. Nevertheless, so far only one mutation has been described for corynebacterial PCx, P458S, which led to an increase in L-lysine production of about 7% (Ohnishi et al., 2002), but which has not been characterized any further. In addition, a second PCx variant was described in a patent of Hanke et al., which showed a feedback-resistance towards aspartic acid and harbors seven mutations: M001V, E153D, A182S, A206S, H227R, A455G and D1120E (Hanke et al., 2005). However, the impact of this enzyme variant on L-lysine production has not been reported.

In order to further exploit the potential of PCx for OAA supply, this thesis involved screening for PCx variants that enable an increased production of L-lysine. Two PCx variants were found, one containing the single mutation T132A and the other one with the double mutation T343A and I1012S. Plasmid-based overexpression of the corresponding genes caused an increase of 19% and 9% in L-lysine production in strain DM1868Δ*pyc*/pSenLys-Spec (chapter 3.2). Integration of the mutations T132A and T343A into the genome of strain DM1868, which also encodes a feedback-resistant aspartate kinase, also led to increased L-lysine production by 7% and 15%, respectively, compared to the parental strain with wild-type PCx.

Since these mutations have not been described so far, they offer new possibilities in combination with other advantageous mutations in the optimization of corynebacterial production strains with a defined genome. Moreover, the newly identified mutations also appear to be a good alternative to the known mutation P458S, which in the same set of experiments caused only an increase in lysine production of only 1.2% compared to wild-type PCx. Due to the described role of PCx in precursor supply, a beneficial effect of the PCx variants can be assumed not only on lysine production but also on other substances such as glutamate.

Until now, the kinetic characterization of PCx of *C. glutamicum* could only be performed with permeabilized cells using discontinuous coupled enzymatic assays with glutamate-oxaloacetate transaminase or lactate dehydrogenase (Peters-Wendisch et al., 1997; Uy et al., 1999). Since other enzymes or metabolites can influence the activity of PCx in assays with permeabilized cells, conditions were established in this work which enabled the determination of PCx activity in cell-free extracts in a continuous coupled assay with malate dehydrogenase and the purification of PCx in an active form (chapter 3.3). These advances allowed a more detailed characterization of new identified PCx variants and, more generally, an in-depth characterization of the enzyme in the future to enable targeted optimization. Kinetic characterization of corynebacterial PCx with the new established assay confirmed that it is strongly inhibited by its product ADP with a K_i of 1.5 mM. A similar effect has also been determined for PCx from *Mycobacterium smegmatis* (Mukhopadhyay and Purwantini, 2000), where the addition of 8 mM ADP led to an 83% reduction in PCx activity, or organisms like *Rhodobacter capsulatus* (Modak and Kelly, 1995) and *Pseudomonas fluorescens* (Milrad de Forchetti and Cazzulo, 1976), for example. Moreover, a K_i for aspartate of 9.3 mM was determined for *C. glutamicum* PCx. Under physiological conditions, aspartate provides regulatory feedback inhibition in response to increased OAA production (Koffas et al., 2002). It is therefore all the more surprising that the activity of corynebacterial PCx is not activated by acetyl-CoA, since an antagonistic effect of aspartate and acetyl-CoA at the same binding site has been described for the PCx of different organisms such as *Staphylococcus aureus* or *Rhizobium etlii* (Sirithanakorn et al., 2014; Xiang and Tong, 2008). In *C. glutamicum*, acetyl-CoA concentrations up to 50 µM lead to an inhibition of PCx by approx. 20%. If acetyl-CoA concentrations were further increased up to 1000 µM, this inhibition is overcome and the PCx is almost completely active again (chapter 3.3). On the other hand, other PCx enzymes are known whose activity is also not strictly dependent on acetyl-CoA or on which the molecule has no influence at all (Adina-Zada et al., 2012). One example for a PCx, which is insensitive towards acetyl-CoA, is the enzyme from *Lactococcus lactis*, although the crystal structure of this enzyme showed a conserved acetyl-CoA binding site (Choi et al., 2017). Structural analysis revealed that *L. lactis* PCx mimics the acetyl-CoA-bound conformation of acetyl-CoA-dependent PCx like the one of *S. aureus* (Choi et al., 2017). This observation gives a first hint for differences in activation of PCx. However,

since the response of PCx activity of *C. glutamicum* to increasing acetyl-CoA concentrations is quite unusual, further investigations should be made to study this effect in more detail.

When the newly established procedure for the purification and assay of corynebacterial PCx was applied to the three enzyme variants PCx^{T132A}, PCx^{T343A} and PCx^{I1012S}, no differences of the specific activities compared to wild-type PCx could be observed under standard conditions (chapter 6.3). Further preliminary studies with these PCx variants indicated that the mutations T132A and T343A cause an apparently higher resistance towards aspartate. For both PCx^{T132A} and PCx^{T343A}, no inhibition up to 7.5 mM aspartate was found, whereas wild-type PCx was inhibited by 42% at this concentration. The K_i values of 13.2 mM and 10.8 mM of PCx^{T132A} and PCx^{T343A}, respectively, were higher compared to the K_i of wild-type PCx (9.3 mM). In contrast, the mutation I1012S caused no changes with respect to aspartate inhibition compared to the wild-type PCx. Since this mutation did also not show any changes towards ADP and acetyl-CoA, other factors must allow the increased L-lysine production with PCx^{I1012S} variant. Even a structural model and alignment with heterologous PCxs did not provide any explanation for the increased lysine production. This result shows that the screening approach chosen in this work enables the identification of useful mutations that would not have been found by a rational approach.

The specific activity of purified PCx of *C. glutamicum* was in the range of 20 - 25 µmol min^{-1} (mg protein)$^{-1}$ and thus lower than the activity of PCx from other sources, such as the enzyme of *M. smegmatis* with a reported activity of up to 150 µmol min^{-1} (mg protein)$^{-1}$ (Mukhopadhyay and Purwantini, 2000). Therefore, the possibility to improve L-lysine production by replacing the native corynebacterial PCx by heterologous variants with higher activity was also examined (chapter 6.4). Three variants were analyzed: PCx from *M. smegmatis* and *S. aureus* both have the same α_4 structure like PCx from *C. glutamicum* (Mukhopadhyay and Purwantini, 2000; Xiang and Tong, 2008). In contrast, the third variant, PCx from *Pseudomonas aeruginosa*, has an $\alpha_4\beta_4$ structure, i.e. the PCx is encoded on two genes (Lai et al., 2006). Growth experiments in minimal medium supplemented either with 4% (wt/vol) glucose or 2% (wt/vol) lactate showed that PCx from *S. aureus* was not able to replace the homologous PCx of *C. glutamicum* in strain DM1868Δ*pyc*. The strain was neither able to grow on lactate nor produce lysine with this carbon source. Furthermore, no increased L-lysine production could be observed compared to the negative mutant without PCx when the cells grew on glucose. Contrary to this observation, the PCx variants of *M. smegmatis* and *P. aeruginosa* were both able to functionally replace corynebacterial PCx and enabled growth on lactate. The lysine production of the strain encoding PCx^{Pa} was similar to the strain with PCx^{Cg}. However, this strain showed a significantly slower growth rate than with PCx^{Cg} when cells were grown on glucose, which probably explains the lower lysine accumulation after 24 hours as well. Expression of *pyc*^{Ms} enabled the strain DM1868Δ*pyc* to produce about the same amount of lysine in

comparison to *pyc*^{Cg} when cells were grown on glucose, and about 1.2-fold more after growth on lactate. This offers interesting possibilities for strain optimization in *C. glutamicum*, especially considering the different regulation of the analyzed enzymes. For instance, the activity of PCx from *M. smegmatis* is, in contrast to corynebacterial PCx, strongly dependent on acetyl-CoA (Mukhopadhyay and Purwantini, 2000). Therefore, further characterization of the expression of heterologous PCx variants for higher L-lysine production in *C. glutamicum* might be interesting to avoid bottlenecks at various growth conditions.

5   References

Adina-Zada, A., Zeczycki, T.N., and Attwood, P.V. (2012). Regulation of the structure and activity of pyruvate carboxylase by acetyl CoA. Arch Biochem Biophys *519*, 118-130.

Ajinomoto Co., (2016). FY2015 Market and other information. https://www.ajinomoto.com/en/ir/event/presentation/main/09/teaserItems1/00/linkList/02/link/FY15_Data_E.pdf

Archer, J.A., and Sinskey, A.J. (1993). The DNA sequence and minimal replicon of the *Corynebacterium glutamicum* plasmid pSR1: evidence of a common ancestry with plasmids from *C. diphtheriae*. J Gen Microbiol *139*, 1753-1759.

Arndt, A., Auchter, M., Ishige, T., Wendisch, V.F., and Eikmanns, B.J. (2008). Ethanol catabolism in *Corynebacterium glutamicum*. J Mol Microbiol Biotechnol *15*, 222-233.

Attwood, P.V. (1995). The structure and the mechanism of action of pyruvate carboxylase. Int J Biochem Cell Biol *27*, 231-249.

Bakkes, P.J., Rama, P., Bida, A., Dohmen-Olma, D., Bott, M., and Freudl, R. (2020) Improved pEKEx2-derived expression vectors for tightly controlled production of recombinant proteins with or without affinity tag in *Corynebacterium glutamicum*. In preparation.

Baritugo, K.A., Kim, H.T., David, Y., Choi, J.I., Hong, S.H., Jeong, K.J., Choi, J.H., Joo, J.C., and Park, S.J. (2018). Metabolic engineering of *Corynebacterium glutamicum* for fermentative production of chemicals in biorefinery. Appl Microbiol Biotechnol *102*, 3915-3937.

Bathe, B., Hans, S., Kreutzer, C., and Pfefferle, W. (2003). Alleles of the SigA gene from coryneform bacteria. Pub. No. WO2003054179A1.

Bäumchen, C., Knoll, A., Husemann, B., Seletzky, J., Maier, B., Dietrich, C., Amoabediny, G., and Büchs, J. (2007). Effect of elevated dissolved carbon dioxide concentrations on growth of *Corynebacterium glutamicum* on D-glucose and L-lactate. J Biotechnol *128*, 868-874.

Baumgart, M., Unthan, S., Ruckert, C., Sivalingam, J., Grunberger, A., Kalinowski, J., Bott, M., Noack, S., and Frunzke, J. (2013). Construction of a prophage-free variant of *Corynebacterium glutamicum* ATCC 13032 - a platform strain for basic research and industrial biotechnology. Appl Environ Microbiol *79*, 6006-6015.

Becker, J., Klopprogge, C., Zelder, O., Heinzle, E., and Wittmann, C. (2005). Amplified expression of fructose 1,6-bisphosphatase in *Corynebacterium glutamicum* increases in vivo flux through the pentose phosphate pathway and lysine production on different carbon sources. Appl Environ Microbiol *71*, 8587–8596.

Becker, J., and Wittmann, C. (2012). Systems and synthetic metabolic engineering for amino acid production - the heartbeat of industrial strain development. Curr Opin Biotechnol *23*, 718-723.

Becker, J., and Wittmann, C. (2015). Advanced biotechnology: metabolically engineered cells for the bio-based production of chemicals and fuels, materials, and health-care products. Angew Chem Int Ed Engl *54*, 3328-3350.

Becker, J., Zelder, O., Hafner, S., Schroder, H., and Wittmann, C. (2011). From zero to hero - - design-based systems metabolic engineering of *Corynebacterium glutamicum* for L-lysine production. Metab Eng *13*, 159-168.

Bell, C.E., and Lewis, M. (2000). A closer view of the conformation of the Lac repressor bound to operator. Nat Struct Biol *7*, 209-214.

Bellmann, A., Vrljic, M., Patek, M., Sahm, H., Krämer, R., and Eggeling, L. (2001). Expression control and specificity of the basic amino acid exporter LysE of *Corynebacterium glutamicum*. Microbiology *147*, 1765-1774.

Berens, C., and Suess, B. (2015). Riboswitch engineering - making the all-important second and third steps. Curr Opin Biotechnol *31*, 10-15.

Bermejo, C., Ewald, J.C., Lanquar, V., Jones, A.M., and Frommer, W.B. (2011). In vivo biochemistry: quantifying ion and metabolite levels in individual cells or cultures of yeast. Biochem J *438*, 1-10.

Billman-Jacobe, H., Wang, L., Kortt, A., Stewart, D., and Radford, A. (1995). Expression and secretion of heterologous proteases by *Corynebacterium glutamicum*. Appl Environ Microbiol *61*, 1610-1613.

Binder, S., Schendzielorz, G., Stäbler, N., Krumbach, K., Hoffmann, K., Bott, M., and Eggeling, L. (2012). A high-throughput approach to identify genomic variants of bacterial metabolite producers at the single-cell level. Genome Biol *13*, R40.

Blombach, B., and Eikmanns, B.J. (2011). Current knowledge on isobutanol production with *Escherichia coli*, *Bacillus subtilis* and *Corynebacterium glutamicum*. Bioeng Bugs. *2*, 346-350.

Blombach, B., and Seibold, G.M. (2010). Carbohydrate metabolism in *Corynebacterium glutamicum* and applications for the metabolic engineering of L-lysine production strains. Appl Microbiol Biotechnol *86*, 1313-1322.

Bolhuis, A., Tjalsma, H., Smith, H.E., de Jong, A., Meima, R., Venema, G., Bron, S., and van Dijl, J.M. (1999). Evaluation of bottlenecks in the late stages of protein secretion in *Bacillus subtilis*. Appl Environ Microbiol *65*, 2934-2941.

Bolten, C.J., Kiefer, P., Letisse, F., Portais, J.C., and Wittmann, C. (2007). Sampling for metabolome analysis of microorganisms. Anal Chem *79*, 3843-3849.

Bosley, A.D., and Ostermeier, M. (2004). Mathematical expressions useful in the construction, description and evaluation of protein libraries. Biomol Eng *22*, 57-61.

Bott, M. (2007). Offering surprises: TCA cycle regulation in *Corynebacterium glutamicum*. Trends Microbiol *15*, 417-425.

Buschke, N., Becker, J., Schafer, R., Kiefer, P., Biedendieck, R., and Wittmann, C. (2013). Systems metabolic engineering of xylose-utilizing *Corynebacterium glutamicum* for production of 1,5-diaminopentane. Biotechnol J *8*, 557-570.

Calos, M.P. (1978). DNA sequence for a low-level promoter of the *lac* repressor gene and an 'up' promoter mutation. Nature *274*, 762-765.

Cavalieri, D., McGovern, P.E., Hartl, D.L., Mortimer, R., and Polsinelli, M. (2003). Evidence for *S. cerevisiae* fermentation in ancient wine. J Mol Evol *57 Suppl 1*, S226-232.

Chamberlin, M., and Ring, J. (1973). Characterization of T7-specific ribonucleic acid polymerase. 1. General properties of the enzymatic reaction and the template specificity of the enzyme. J Biol Chem *248*, 2235-2244.

Chen, Z., Bommareddy, R.R., Frank, D., Rappert, S., and Zeng, A.P. (2014). Deregulation of feedback inhibition of phosphoenolpyruvate carboxylase for improved lysine production in *Corynebacterium glutamicum*. Appl Environ Microbiol *80*, 1388-1393.

Chen, Z., Meyer, W., Rappert, S., Sun, J., and Zeng, A.P. (2011). Coevolutionary analysis enabled rational deregulation of allosteric enzyme inhibition in *Corynebacterium glutamicum* for lysine production. Appl Environ Microbiol *77*, 4352-4360.

Choi, P.H., Vu, T.M.N., Pham, H.T., Woodward, J.J., Turner, M.S., and Tong, L. (2017). Structural and functional studies of pyruvate carboxylase regulation by cyclic di-AMP in lactic acid bacteria. Proc Natl Acad Sci U S A *114*, E7226-e7235.

Cremer, J., Eggeling, L., and Sahm, H. (1991). Control of the lysine biosynthesis sequence in *Corynebacterium glutamicum* as analyzed by overexpression of the individual corresponding genes. Appl Environ Microbiol *57*, 1746-1752.

Cremer, J., Treptow, C., Eggeling, L., and Sahm, H. (1988). Regulation of enzymes of lysine biosynthesis in *Corynebacterium glutamicum*. J Gen Microbiol *134*, 3221-3229.

Daber, R., Stayrook, S., Rosenberg, A., and Lewis, M. (2007). Structural analysis of lac repressor bound to allosteric effectors. J Mol Biol *370*, 609-619.

Date, M., Itaya, H., Matsui, H., and Kikuchi, Y. (2006). Secretion of human epidermal growth factor by *Corynebacterium glutamicum*. Lett Appl Microbiol *42*, 66-70.

Delaunay, S., Uy, D., Baucher, M.F., Engasser, J.M., Guyonvarch, A., and Goergen, J.L. (1999). Importance of phosphoenolpyruvate carboxylase of *Corynebacterium glutamicum* during the temperature triggered glutamic acid fermentation. Metab Eng *1*, 334-343.

Demain, A.L., and Adrio, J.L. (2008). Contributions of microorganisms to industrial biology. Mol Biotechnol *38*, 41-55.

Dietrich, J.A., McKee, A.E., and Keasling, J.D. (2010). High-throughput metabolic engineering: advances in small-molecule screening and selection. Annu Rev Biochem *79*, 563-590.

Dubendorff, J.W., and Studier, F.W. (1991). Controlling basal expression in an inducible T7 expression system by blocking the target T7 promoter with Lac repressor. J Mol Biol *219*, 45-59.

Drysch, A., El Massaoudi, M., Mack, C., Takors, R., de Graaf, AA., and Sahm H. (2003). Production process monitoring by serial mapping of microbial carbon flux distributions using a

novel Sensor Reactor approach: II-^{13}C-labeling-based metabolic flux analysis and L-lysine production. Metab Eng *5*, 96-107.

Eggeling, L., and Bott, M. (2015). A giant market and a powerful metabolism: L-lysine provided by *Corynebacterium glutamicum*. Appl Microbiol Biotechnol *99*, 3387-3394.

Eggeling, L., and Sahm, H. (1999). L-Glutamate and L-lysine: traditional products with impetuous developments. Appl Microbiol Biotechnol *52*, 146–153.

Eikmanns, B.J., and Blombach, B. (2014). The pyruvate dehydrogenase complex of *Corynebacterium glutamicum*: an attractive target for metabolic engineering. J Biotechnol *192 Pt B*, 339-345.

Eikmanns, B.J., Follettie, M.T., Griot, M.U., and Sinskey, A.J. (1989). The phosphoenolpyruvate carboxylase gene of *Corynebacterium glutamicum*: molecular cloning, nucleotide sequence, and expression. Mol Gen Genet *218*, 330-339.

Eikmanns, B.J., Kleinertz, E., Liebl, W., and Sahm, H. (1991). A family of *Corynebacterium glutamicum*/*Escherichia coli* shuttle vectors for cloning, controlled gene expression, and promoter probing. Gene *102*, 93-98.

Eismann, E., von Wilcken-Bergmann, B., and Muller-Hill, B. (1987). Specific destruction of the second lac operator decreases repression of the lac operon in *Escherichia coli* fivefold. J Mol Biol *195*, 949-952.

Erickson, B., Nelson, and Winters, P. (2012). Perspective on opportunities in industrial biotechnology in renewable chemicals. Biotechnol J *7*, 176-185.

Feilmeier, B.J., Iseminger, G., Schroeder, D., Webber, H., and Phillips, G.J. (2000). Green fluorescent protein functions as a reporter for protein localization in *Escherichia coli*. J Bacteriol *182*, 4068-4076.

Fernandez-Gonzalez, C., Cadenas, R.F., Noirot-Gros, M.F., Martin, J.F., and Gil, J.A. (1994). Characterization of a region of plasmid pBL1 of *Brevibacterium lactofermentum* involved in replication via the rolling circle model. J Bacteriol *176*, 3154-3161.

Freudl, R. (2017). Beyond amino acids: Use of the *Corynebacterium glutamicum* cell factory for the secretion of heterologous proteins. J Biotechnol *258*, 101-109.

Freudl, R. (2018). Signal peptides for recombinant protein secretion in bacterial expression systems. Microb Cell Fact *17*, 52.

Fried, M., and Crothers, D.M. (1981). Equilibria and kinetics of lac repressor-operator interactions by polyacrylamide gel electrophoresis. Nucleic Acids Res *9*, 6505-6525.

Gamer, M., Frode, D., Biedendieck, R., Stammen, S., and Jahn, D. (2009). A T7 RNA polymerase-dependent gene expression system for *Bacillus megaterium*. Appl Microbiol Biotechnol *82*, 1195-1203.

Gao, B., and Gupta, R.S. (2012). Phylogenetic framework and molecular signatures for the main clades of the phylum *Actinobacteria*. Microbiol Mol Biol Rev *76*, 66-112.

Georgiou, G., and Valax, P. (1996). Expression of correctly folded proteins in *Escherichia coli*. Curr Opin Biotechnol *7*, 190-197.

Gibson, D.G. (2011). Enzymatic Assembly of Overlapping DNA Fragments. Method Enzymol *498*, 349-361.

Golomb, M., and Chamberlin, M.J. (1977). T7- and T3-specific RNA polymerases: characterization and mapping of the in vitro transcripts read from T3 DNA. J Virol *21*, 743-752.

Gourdon, P., Baucher, M.F., Lindley, N.D., and Guyonvarch, A. (2000). Cloning of the malic enzyme gene from *Corynebacterium glutamicum* and role of the enzyme in lactate metabolism. Appl Environ Microbiol *66*, 2981-2987.

Graf, M., Haas, T., Muller, F., Buchmann, A., Harm-Bekbenbetova, J., Freund, A., Niess, A., Persicke, M., Kalinowski, J., Blombach, B*., et al.* (2019). Continuous adaptive evolution of a fast-growing *Corynebacterium glutamicum* strain independent of protocatechuate. Front Microbiol *10*, 1648.

Gubler, M., and et al. (1994). Effects of phosphoenol pyruvate carboxylase deficiency on metabolism and lysine production in *Corynebacterium glutamicum*. Appl Microbiol Biot *40*, 857-863.

Hanke, P., Sinskey, A., and Willis, L. (2005). Feedback-resistant pyruvate carboxylase gene from *Corynebacterium*. In US Patent No 6,965,021 B2.

Hirao, T., Nakano, T., Azuma, T., Sugimoto, M., and Nakanishi, T. (1989). L-Lysine production in continuous culture of an L-lysine hyperproducing mutant of *Corynebacterium glutamicum*. Appl Microbiol Biotechnol *32*, 269-273.

Huber, I., Palmer, D.J., Ludwig, K.N., Brown, I.R., Warren, M.J., and Frunzke, J. (2017). Construction of recombinant Pdu metabolosome shells for small molecule production in *Corynebacterium glutamicum*. ACS Synth Biol *6*, 2145-2156.

Huh, L., Lee, K.H., Kim, H.J., Moon, J.O., and Ryu, S.G. (2016). Microorganism with improved L-lysine productivity, and method for producing L-lysine by using same. Pub. No. WO2016036191A1.

Ikeda, M. (2003). Amino acid production processes. Adv Biochem Eng Biotechnol *79*, 1-35.

Ikeda, M., and Nakagawa, S. (2003). The *Corynebacterium glutamicum* genome: features and impacts on biotechnological processes. Appl Microbiol Biotechnol *62*, 99-109.

Ikeda, M., Ohnishi, J., Hayashi, M., and Mitsuhashi, S. (2006). A genome-based approach to create a minimally mutated *Corynebacterium glutamicum* strain for efficient L-lysine production. J Ind Microbiol Biotechnol *33*, 610-615.

Jang, Y.S., Kim, B., Shin, J.H., Choi, Y.J., Choi, S., Song, C.W., Lee, J., Park, H.G., and Lee, S.Y. (2012). Bio-based production of C2-C6 platform chemicals. Biotechnol Bioeng *109*, 2437-2459.

Jetten, M.M., Pitoc, G., Follettie, M., and Sinskey, A. (1994). Regulation of phospho(enol)-pyruvate-and oxaloacetate-converting enzymes in *Corynebacterium glutamicum*. Appl Microbiol Biotechnol *41*, 47-52.

Jetten, M.S., and Sinskey, A.J. (1995). Purification and properties of oxaloacetate decarboxylase from *Corynebacterium glutamicum*. Antonie Van Leeuwenhoek *67*, 221-227.

Jitrapakdee, S., St Maurice, M., Rayment, I., Cleland, W.W., Wallace, J.C., and Attwood, P.V. (2008). Structure, mechanism and regulation of pyruvate carboxylase. Biochem J *413*, 369-387.

Kalinowski, J., Bathe, B., Bartels, D., Bischoff, N., Bott, M., Burkovski, A., Dusch, N., Eggeling, L., Eikmanns, B.J., Gaigalat, L.*, et al.* (2003). The complete *Corynebacterium glutamicum* ATCC 13032 genome sequence and its impact on the production of L-aspartate-derived amino acids and vitamins. J Biotechnol *104*, 5-25.

Kallscheuer, N., Vogt, M., Stenzel, A., Gatgens, J., Bott, M., and Marienhagen, J. (2016). Construction of a *Corynebacterium glutamicum* platform strain for the production of stilbenes and (2S)-flavanones. Metab Eng *38*, 47-55.

Kamionka, A., Majewski, M., Roth, K., Bertram, R., Kraft, C., and Hillen, W. (2006). Induction of single chain tetracycline repressor requires the binding of two inducers. Nucleic Acids Res *34*, 3834-3841.

Kania, J., and Brown, D.T. (1976). The functional repressor parts of a tetrameric *lac* repressor-β-galactosidase chimaera are organized as dimers. Proc Natl Acad Sci USA *73*, 3529-3533.

Käß, F., Hariskos, I., Michel, A., Brandt, H.J., Spann, R., Junne, S., Wiechert, W., Neubauer, P., and Oldiges, M. (2014). Assessment of robustness against dissolved oxygen/substrate oscillations for *C. glutamicum* DM1933 in two-compartment bioreactor. Bioprocess Biosyst Eng *37*, 1151-1162.

Katzke, N., Arvani, S., Bergmann, R., Circolone, F., Markert, A., Svensson, V., Jaeger, K.E., Heck, A., and Drepper, T. (2010). A novel T7 RNA polymerase dependent expression system for high-level protein production in the phototrophic bacterium *Rhodobacter capsulatus*. Protein Expr Purif *69*, 137-146.

Keilhauer, C., Eggeling, L., and Sahm, H. (1993). Isoleucine synthesis in *Corynebacterium glutamicum* - Molecular analysis of the Ilvb-Ilvn-Ilvc Operon. J Bacteriol *175*, 5595 - 5603.

Kelle, R., Hermann, T., and Bathe, B. (2005). L-lysine production. In Handbook of *Corynebacterium glutamicum*, L. Eggeling, and M. Bott, eds. (CRC Press, Boca Raton), pp. 465–488.

Kikuchi, Y., Date, M., Itaya, H., Matsui, K., and Wu, L.F. (2006). Functional analysis of the twin-arginine translocation pathway in *Corynebacterium glutamicum* ATCC 13869. Appl Environ Microbiol *72*, 7183-7192.

Kikuchi, Y., Itaya, H., Date, M., Matsui, K., and Wu, L.-F. (2009). TatABC overexpression improves *Corynebacterium glutamicum* Tat-Dependent protein secretion. Appl Environ Microbiol *75*, 603-607.

Kim, H.I., Nam, J.Y., Cho, J.Y., Lee, C.S., and Park, Y.J. (2013). Nextgeneration sequencing-based ranscriptome analysis of L-lysine-producing *Corynebacterium glutamicum* ATCC 21300 strain. J Microbiol *51*, 877-880.

Kinoshita, S., Nakayama, K., and Kitada, S. (1961). Method of producing L-lysine by fermentation. In US Patent No 2,979,439.

Kinoshita, S., Udaka, S., and Shimono, M. (1957). Studies on amino acid fermentation. Part I. Production of L-glutamic acid by various microorganisms. J Gen Appl Microbiol *3*, 193-205.

Klaffl, S., and Eikmanns, B.J. (2010). Genetic and functional analysis of the soluble oxaloacetate decarboxylase from *Corynebacterium glutamicum*. J Bacteriol *192*, 2604-2612.

Koffas, M.A., Jung, G.Y., Aon, J.C., and Stephanopoulos, G. (2002). Effect of pyruvate carboxylase overexpression on the physiology of *Corynebacterium glutamicum*. Appl Environ Microbiol *68*, 5422-5428.

Kogure, T., and Inui, M. (2018). Recent advances in metabolic engineering of *Corynebacterium glutamicum* for bioproduction of value-added aromatic chemicals and natural products. Appl Microbiol Biotechnol *102*, 8685-8705.

Kortmann, M., Baumgart, M., Bott, M. (2019). Pyruvate carboxylase from *Corynebacterium glutamicum*: purification and characterization. Appl Microbiol Biotechnol *103*, 6571-6580.

Kortmann, M., Kuhl, V., Klaffl, S., Bott, M. (2015). A chromosomally encoded T7 RNA polymerase-dependent gene expression system for *Corynebacterium glutamicum*: construction and comparative evaluation at the single-cell level. Microb Biotechnol *8,* 253–265.

Kortmann M., Mack C., Baumgart M., Bott M. (2019) Pyruvate carboxylase variants enabling improved lysine production from glucose identified by biosensor-based high-throughput fluorescence-activated cell sorting screening. ACS Synth Biol *8*, 274-281.

Kotrba, P., Inui, M., and Yukawa, H. (2003). A single V317A or V317M substitution in Enzyme II of a newly identified beta-glucoside phosphotransferase and utilization system of *Corynebacterium glutamicum* R extends its specificity towards cellobiose. Microbiology *149*, 1569-1580.

Krause, F.S., Henrich, A., Blombach, B., Kramer, R., Eikmanns, B.J., and Seibold, G.M. (2010). Increased glucose utilization in *Corynebacterium glutamicum* by use of maltose, and its application for the improvement of L-valine productivity. Appl Environ Microbiol *76*, 370-374.

Krings, E., Krumbach, K., Bathe, B., Kelle, R., Wendisch, V.F., Sahm, H., and Eggeling, L. (2006). Characterization of myo-inositol utilization by *Corynebacterium glutamicum*: the stimulon, identification of transporters, and influence on L-lysine formation. J Bacteriol *188*, 8054-8061.

Laemmli, U.K. (1970). Cleavage of structural proteins during the assembly of the head of bacteriophage T4. Nature *227*, 680-685.

Lai, H., Kraszewski, J.L., Purwantini, E., and Mukhopadhyay, B. (2006). Identification of pyruvate carboxylase genes in *Pseudomonas aeruginosa* PAO1 and development of a *P.*

aeruginosa-based overexpression system for α_4- and $\alpha_4\beta_4$-type pyruvate carboxylases. Appl Environ Microbiol *72*, 7785-7792.

Landgraf, W., and Sandow, J. (2016). Recombinant human insulins - Clinical efficacy and safety in diabetes therapy. Eur Endocrinol *12*, 12-17.

Lausberg, F., Chattopadhyay, A.R., Heyer, A., Eggeling, L., and Freudl, R. (2012). A tetracycline inducible expression vector for C*orynebacterium glutamicum* allowing tightly regulable gene expression. Plasmid *68*, 142-147.

Lee, J., Sim, S.J., Bott, M., Um, Y., Oh, M.K., and Woo, H.M. (2014). Succinate production from CO_2-grown microalgal biomass as carbon source using engineered *Corynebacterium glutamicum* through consolidated bioprocessing. Sci Rep *4*, 5819.

Lee, M.J., and Kim, P. (2018). Recombinant protein expression system in *Corynebacterium glutamicum* and its application. Front Microbiol *9*, 2523.

Lee, P.A., Tullman-Ercek, D., and Georgiou, G. (2006). The bacterial twin-arginine translocation pathway. Annu Rev Microbiol *60*, 373-395.

Lei, C., Ren, Z., Yang, W., Chen, Y., Chen, D., Liu, M., Yan, W., and Zheng, Z. (2002). Characterization of a novel plasmid pXZ608 from *Corynebacterium glutamicum*. FEMS Microbiol Lett *216*, 71-75.

Leuchtenberger, W. (1996). Amino Acids – Technical Production and Use. In Biotechnology, pp. 465-502.

Liebl, W., Sinskey, A.J., and Schleifer, K.H. (1992). Expression, secretion, and processing of staphylococcal nuclease by *Corynebacterium glutamicum*. J Bacteriol *174*, 1854-1861.

Lindner, S.N., Seibold, G.M., Henrich, A., Kramer, R., and Wendisch, V.F. (2011). Phosphotransferase system-independent glucose utilization in *Corynebacterium glutamicum* by inositol permeases and glucokinases. Appl Environ Microbiol *77*, 3571-3581.

Litsanov, B., Kabus, A., Brocker, M., and Bott, M. (2012). Efficient aerobic succinate production from glucose in minimal medium with *Corynebacterium glutamicum*. Microb Biotechnol *5*, 116-128.

Mahr, R., and Frunzke, J. (2016). Transcription factor-based biosensors in biotechnology: current state and future prospects. Appl Microbiol Biotechnol *100*, 79-90.

Mahr, R., Gatgens, C., Gatgens, J., Polen, T., Kalinowski, J., and Frunzke, J. (2015). Biosensor-driven adaptive laboratory evolution of L-valine production in *Corynebacterium glutamicum*. Metabol Eng *32*, 184-194.

Meissner, D., Vollstedt, A., van Dijl, J., and Freudl, R. (2007). Comparative analysis of twin-arginine (Tat)-dependent protein secretion of a heterologous model protein (GFP) in three different Gram-positive bacteria. Appl Microbiol Biotechnol *76*, 633-642.

Menefee, A.L., and Zeczycki, T.N. (2014). Nearly 50 years in the making: defining the catalytic mechanism of the multifunctional enzyme, pyruvate carboxylase. FEBS J *281*, 1333-1354.

Menkel, E., Thierbach, G., Eggeling, L., and Sahm, H. (1989). Influence of increased aspartate availability on lysine formation by a recombinant strain of *Corynebacterium glutamicum* and utilization of fumarate. Appl Environ Microbiol *55*, 684-688.

Michel, A., Koch-Koerfges, A., Krumbach, K., Brocker M., and Bott M. (2015). Anaerobic growth of *Corynebacterium glutamicum* via mixed-acid fermentation. Appl Environ Microbiol *81*, 7496-7508.

Milrad de Forchetti, S.R., and Cazzulo, J.J. (1976). Some properties of the pyruvate carboxylase from *Pseudomonas fluorescens*. J Gen Microbiol *93*, 75-81.

Milse, J., Petri, K., Ruckert, C., and Kalinowski, J. (2014). Transcriptional response of *Corynebacterium glutamicum* ATCC 13032 to hydrogen peroxide stress and characterization of the OxyR regulon. J Biotechnol *190*, 40-54.

Miwa, K., Matsui, K., Terabe, M., Ito, K., Ishida, M., Takagi, H., Nakamori, S., and Sano, K. (1985). Construction of novel shuttle vectors and a cosmid vector for the glutamic acid-producing bacteria *Brevibacterium lactofermentum* and *Corynebacterium glutamicum*. Gene *39*, 281-286.

Miwa, K., Matsui, H., Terabe, M., Nakamori, S., Sano, K., and Momose, H. (1984). Cryptic plasmids in glutamic acid-producing bacteria. Agric Biol Chem *48*, 2901-2903.

Modak, H.V., and Kelly, D.J. (1995). Acetyl-CoA-dependent pyruvate carboxylase from the photosynthetic bacterium *Rhodobacter capsulatus*: rapid and efficient purification using dye-ligand affinity chromatography. Microbiology *141 (Pt 10)*, 2619-2628.

Mori, M., and Shiio, I. (1985). Synergistic inhibition of phosphoenolpyruvate carboxylase by aspartate and 2-oxoglutarate in *Brevibacterium flavum*. J Biochem *98,* 1621-1630.

Mukhopadhyay, B., and Purwantini, E. (2000). Pyruvate carboxylase from *Mycobacterium smegmatis*: stabilization, rapid purification, molecular and biochemical characterization and regulation of the cellular level. Biochim Biophys Acta *1475*, 191-206.

Mussatto, S.I., Ballesteros, L.F., Teixeira, S.M. and Teixeira, J.A. (2012). Use of agro-industrial wastes in solid-state fermentation processes. In Industrial Waste, Show, K.Y. and Guo, X. ed. (IntechOpen), pp. 121-140.

Mustafi, N., Bott, M., and Frunzke, J. (2015). Genetically encoded biosensors for strain development and single-cell analysis of *Corynebacterium glutamicum*. In *Corynebacterium glutamicum* - From Systems Biology to Biotechnological Applications, A. Burkovski, ed. (Norfolk, UK: Caister Academic Press), pp. 179-196.

Mustafi, N., Grunberger, A., Kohlheyer, D., Bott, M., and Frunzke, J. (2012). The development and application of a single-cell biosensor for the detection of L-methionine and branched-chain amino acids. Metabol Eng *14*, 449-457.

Mustafi, N., Grunberger, A., Mahr, R., Helfrich, S., Noh, K., Blombach, B., Kohlheyer, D., and Frunzke, J. (2014). Application of a genetically encoded biosensor for live cell imaging of L-valine production in pyruvate dehydrogenase complex-deficient *Corynebacterium glutamicum* strains. PLoS One *9*, e85731.

Nakayama, K., Araki, K., and Kase, H. (1978). Microbial production of essential amino acid with *Corynebacterium glutamicum* mutants. Adv Exp Med Biol *105*, 649-661.

Nesvera, J., Holatko, J., and Patek, M. (2012). Analysis of *Corynebacterium glutamicum* promoters and their applications. Subcell Biochem *64*, 203-221.

Nesvera, J., and Patek, M. (2011). Tools for genetic manipulations in *Corynebacterium glutamicum* and their applications. Appl Microbiol Biotechnol *90*, 1641-1654.

Nesvera, J., Patek, M., Hochmannova, J., Abrhamova, Z., Becvarova, V., Jelinkova, M., and Vohradsky, J. (1997). Plasmid pGA1 from *Corynebacterium glutamicum* codes for a gene product that positively influences plasmid copy number. J Bacteriol *179*, 1525-1532.

Nguyen, A.Q., Schneider, J., Reddy, G.K., and Wendisch, V.F. (2015). Fermentative production of the diamine putrescine: system metabolic engineering of *Corynebacterium glutamicum*. Metabolites *5*, 211-231.

Niimi, S., Suzuki, N., Inui, M., and Yukawa, H. (2011). Metabolic engineering of 1,2-propanediol pathways in *Corynebacterium glutamicum*. Appl Microbiol Biotechnol *90*, 1721-1729.

Nishimura, T., Vertes, A.A., Shinoda, Y., Inui, M., and Yukawa, H. (2007). Anaerobic growth of *Corynebacterium glutamicum* using nitrate as a terminal electron acceptor. Appl Microbiol Biotechnol *75*, 889-897.

O'Regan, M., Thierbach, G., Bachmann, B., Villeval, D., Lepage, P., Viret, J.F., and Lemoine, Y. (1989). Cloning and nucleotide sequence of the phosphoenolpyruvate carboxylase-coding gene of *Corynebacterium glutamicum* ATCC13032. Gene *77*, 237-251.

Oehler, S., Eismann, E.R., Kramer, H., and Muller-Hill, B. (1990). The three operators of the Lac operon cooperate in repression. EMBO J *9*, 973-979.

Oertel, D., Schmitz, S., and Freudl, R. (2015) A TatABC-type Tat translocase is required for unimpaired aerobic growth of *Corynebacterium glutamicum* ATCC13032. PLoS ONE *10*, e0123413.

Ohnishi, J., Katahira, R., Mitsuhashi, S., Kakita, S., and Ikeda, M. (2005). A novel *gnd* mutation leading to increased L-lysine production in *Corynebacterium glutamicum*. FEMS Microbiol Lett *242*, 265–274.

Ohnishi, J., Mitsuhashi, S., Hayashi, M., Ando, S., Yokoi, H., Ochiai, K., and Ikeda, M. (2002). A novel methodology employing *Corynebacterium glutamicum* genome information to generate a new L-lysine-producing mutant. Appl Microbiol Biotechnol *58*, 217-223.

Ozaki, A., Katsumata, R., Oka, T., and Furuya, A. (1984). Functional expression of the genes of *Escherichia coli* in gram-positive *Corynebacterium glutamicum*. Mol Gen Genet *196*, 175-178.

Park, S.M., Shaw-Reid, C., Sinskey, A.J., and Stephanopoulos, G. (1997). Elucidation of anaplerotic pathways in *Corynebacterium glutamicum* via ^{13}C-NMR spectroscopy and GC-MS. Appl Microbiol Biotechnol *47*, 430-440.

Patek, M., and Nesvera, J. (2011). Sigma factors and promoters in *Corynebacterium glutamicum*. J Biotechnol *154*, 101-113.

Patek, M., Nesvera, J., Guyonvarch, A., Reyes, O., and Leblon, G. (2003). Promoters of *Corynebacterium glutamicum*. J Biotechnol *104*, 311-323.

Peralta-Yahya, P.P., Zhang, F., del Cardayre, S.B., and Keasling, J.D. (2012). Microbial engineering for the production of advanced biofuels. Nature *488*, 320-328.

Perez-Garcia, F., Peters-Wendisch, P., and Wendisch, V.F. (2016). Engineering *Corynebacterium glutamicum* for fast production of L-lysine and L-pipecolic acid. Appl Microbiol Biotechnol *100*, 8075-8090.

Peters-Wendisch, P.G., Eikmanns, B.J., Thierbach, G., Bachmann, B., and Sahm, H. (1993). Phosphoenolpyruvate carboxylase in *Corynebacterium glutamicum* is dispensable for growth and lysine production. FEMS Microbiol Lett *112*, 269-274.

Peters-Wendisch, P.G., Kreutzer, C., Kalinowski, J., Patek, M., Sahm, H., and Eikmanns, B.J. (1998). Pyruvate carboxylase from *Corynebacterium glutamicum*: characterization, expression and inactivation of the *pyc* gene. Microbiology *144 (Pt 4)*, 915-927.

Peters-Wendisch, P.G., Schiel, B., Wendisch, V.F., Katsoulidis, E., Mockel, B., Sahm, H., and Eikmanns, B.J. (2001). Pyruvate carboxylase is a major bottleneck for glutamate and lysine production by *Corynebacterium glutamicum*. J Mol Microbiol Biotechnol *3*, 295-300.

Peters-Wendisch, P.G., Wendisch, V.F., de Graaf, A.A., Eikmanns, B.J., and Sahm, H. (1996). C3-carboxylation as an anaplerotic reaction in phosphoenolpyruvate carboxylase-deficient *Corynebacterium glutamicum*. Arch Microbiol *165*, 387-396.

Peters-Wendisch, P.G., Wendisch, V.F., Paul, S., Eikmanns, B.J., and Sahm, H. (1997). Pyruvate carboxylase as an anaplerotic enzyme in *Corynebacterium glutamicum*. Microbiology *143*, 1095-1103.

Petersen, S., de Graaf, A.A., Eggeling, L., Mollney, M., Wiechert, W., and Sahm, H. (2000). In vivo quantification of parallel and bidirectional fluxes in the anaplerosis of *Corynebacterium glutamicum*. J Biol Chem *275*, 35932-35941.

Petersen, S., Mack, C., De Graaf, A.A., Riedel, C., Eikmanns, B.J., and Sahm, H. (2001). Metabolic consequences of altered phosphoenolpyruvate carboxykinase activity in *Corynebacterium glutamicum* reveal anaplerotic regulation mechanisms in vivo. Metab Eng *3*, 3344–3461.

Pfahl, M., Gulde, V., and Bourgeois, S. (1979). "Second" and "third operator" of the *lac* operon: An investigation of their role in the regulatory mechanism. J Mol Biol *127*, 339-344.

Pfefferle, W., Möckel, B., Bathe, B., and Marx, A. (2003). Biotechnological manufacture of lysine. In Microbial production of L-amino acids, R. Faurie, and J. Thommel, eds. (Heidelberg: Springer), pp. 59-112.

Pickens, L.B., Tang, Y., and Chooi, Y.H. (2011). Metabolic engineering for the production of natural products. Annu Rev Chem Biomol Eng *2*, 211-236.

Quax, W.J. (1997). Merits of secretion of heterologous proteins from industrial microorganisms. Folia microbiologica *42*, 99-103.

Riedel, C., Rittmann, D., Dangel, P., Mockel, B., Petersen, S., Sahm, H., and Eikmanns, B.J. (2001). Characterization of the phosphoenolpyruvate carboxykinase gene from *Corynebacterium glutamicum* and significance of the enzyme for growth and amino acid production. J Mol Microbiol Biotechnol *3*, 573-583.

Rittmann, D., Lindner, S.N., and Wendisch, V.F. (2008). Engineering of a glycerol utilization pathway for amino acid production by *Corynebacterium glutamicum*. Appl Environ Microbiol *74*, 6216-6222.

Rowlands, R.T. (1984). Industrial strain improvement: mutagenesis and random screening procedures. Enzyme Microb Technol *6*, 3-10.

Sahm, H., Eggeling, L., and de Graaf, A.A. (2000). Pathway analysis and metabolic engineering in *Corynebacterium glutamicum*. Biol Chem *381*, 899-910.

Saida, F., Uzan, M., Odaert, B., and Bontems, F. (2006). Expression of highly toxic genes in *E. coli*: special strategies and genetic tools. Curr Protein Pept Sci 7, 47-56.

Sambrook, J., Fritsch, E.F., and Maniatis, T. (1989). Molecular cloning. A laboratory manual., N. Cold Spring Habor Laboratory Press, ed.

Sanchez, S., Rodríguez-Sanoja, R., Ramos, A., and Demain, A.L. (2018). Our microbes not only produce antibiotics, they also overproduce amino acids. J Antibiot *71*, 26–36.

Santamaría, R., Gil, J.A., Mesas, J.M., and Martín, J.F. (1984). Characterization of an Endogenous Plasmid and Development of Cloning Vectors and a Transformation System in *Brevibacterium lactofermentum*. Microbiology *130*, 2237-2246.

Santini, C.L., Bernadac, A., Zhang, M., Chanal, A., Ize, B., Blanco, C., and Wu, L.F. (2001). Translocation of jellyfish green fluorescent protein via the Tat system of *Escherichia coli* and change of its periplasmic localization in response to osmotic up-shock. J Biol Chem *276*, 8159-8164.

Sauer, U., and Eikmanns, B.J. (2005). The PEP-pyruvate-oxaloacetate node as the switch point for carbon flux distribution in bacteria. FEMS Microbiol Rev *29*, 765-794.

Schaffer, S., Weil, B., Nguyen, V.D., Dongmann, G., Gunther, K., Nickolaus, M., Hermann, T., and Bott, M. (2001). A high-resolution reference map for cytoplasmic and membrane-associated proteins of *Corynebacterium glutamicum*. Electrophoresis *22*, 4404-4422.

Scheele, S., Oertel, D., Bongaerts, J., Evers, S., Hellmuth, H., Maurer, K.H., Bott, M., and Freudl, R. (2013). Secretory production of an FAD cofactor-containing cytosolic enzyme (sorbitol-xylitol oxidase from *Streptomyces coelicolor*) using the twin-arginine translocation (Tat) pathway of *Corynebacterium glutamicum*. Microb Biotechnol *6*, 202-206.

Schendzielorz, G., Dippong, M., Grunberger, A., Kohlheyer, D., Yoshida, A., Binder, S., Nishiyama, C., Nishiyama, M., Bott, M., and Eggeling, L. (2014). Taking control over control:

use of product sensing in single cells to remove flux control at key enzymes in biosynthesis pathways. ACS Synth Biol *3*, 21-29.

Schulte, J., Baumgart, M., and Bott, M. (2017). Identification of the cAMP phosphodiesterase CpdA as novel key player in cAMP-dependent regulation in *Corynebacterium glutamicum*. Mol Microbiol *103*, 534-552.

Shiio, I., Miyajima, R., and Sano, K. (1970). Genetically desensitized aspartate kinase to the concerted feedback inhibition in *Brevibacterium flavum*. J Biochem *68*, 701-710.

Siebert, D., and Wendisch, V.F. (2015). Metabolic pathway engineering for production of 1,2-propanediol and 1-propanol by *Corynebacterium glutamicum*. Biotechnol Biofuels *8*, 91.

Siedler, S., Schendzielorz, G., Binder, S., Eggeling, L., Bringer, S., and Bott, M. (2014). SoxR as a single-cell biosensor for NADPH-consuming enzymes in *Escherichia coli*. ACS Synth Biol *3*, 41-47.

Sindelar, G., and Wendisch, V.F. (2007). Improving lysine production by *Corynebacterium glutamicum* through DNA microarray-based identification of novel target genes. Appl Microbiol Biotechnol *76*, 677-689.

Sirithanakorn, C., Adina-Zada, A., Wallace, J.C., Jitrapakdee, S., and Attwood, P.V. (2014). Mechanisms of Inhibition of *Rhizobium etli* Pyruvate Carboxylase by L-Aspartate. Biochem *53*, 7100-7106.

Sonnen, H., Thierbach, G., Kautz, S., Kalinowski, J., Schneider, J., Puhler, A., and Kutzner, H.J. (1991). Characterization of pGA1, a new plasmid from *Corynebacterium glutamicum* LP-6. Gene *107*, 69-74.

Stäbler, N., Oikawa, T., Bott, M., and Eggeling, L. (2011). *Corynebacterium glutamicum* as a host for synthesis and export of D-Amino Acids. J Bacteriol *193*, 1702-1709.

Stansen, C., Uy, D., Delaunay, S., Eggeling, L., Goergen, J.L., and Wendisch, V.F. (2005). Characterization of a *Corynebacterium glutamicum* lactate utilization operon induced during temperature-triggered glutamate production. Appl Environ Microbiol *71*, 5920-5928.

Studier, F.W. (1991). Use of bacteriophage T7 lysozyme to improve an inducible T7 expression system. J Mol Biol *219*, 37-44.

Studier, F.W., and Moffatt, B.A. (1986). Use of bacteriophage T7 RNA polymerase to direct selective high-level expression of cloned genes. J Mol Biol *189*, 113-130.

Suzuki, N., Watanabe, K., Okibe, N., Tsuchida, Y., Inui, M., and Yukawa, H. (2009). Identification of new secreted proteins and secretion of heterologous amylase by *C. glutamicum*. Appl Microbiol Biotechnol *82*, 491-500.

Tabor, S., and Richardson, C.C. (1985). A bacteriophage T7 RNA polymerase/promoter system for controlled exclusive expression of specific genes. Proc Natl Acad Sci USA *82*, 1074-1078.

Takamura, Y., and Nomura, G. (1988). Changes in the intracellular concentration of acetyl-CoA and malonyl-CoA in relation to the carbon and energy metabolism of *Escherichia coli* K12. J Gen Microbiol *134*, 2249-2253.

Taniguchi, H., Henke, N.A., Heider, S.A.E., and Wendisch, V.F. (2017). Overexpression of the primary sigma factor gene *sigA* improved carotenoid production by *Corynebacterium glutamicum*: Application to production of β-carotene and the non-native linear C50 carotenoid bisanhydrobacterioruberin. Metab Eng Commun *4*, 1-11.

Tauch, A., Puhler, A., Kalinowski, J., and Thierbach, G. (2003). Plasmids in *Corynebacterium glutamicum* and their molecular classification by comparative genomics. J Biotechnol *104*, 27-40.

Teramoto, H., Inui, M., and Yukawa, H. (2013). OxyR acts as a transcriptional repressor of hydrogen peroxide-inducible antioxidant genes in *Corynebacterium glutamicum* R. FEBS J *280*, 3298-3312.

Thomas, J.D., Daniel, R.A., Errington, J., and Robinson, C. (2001). Export of active green fluorescent protein to the periplasm by the twin-arginine translocase (Tat) pathway in *Escherichia coli*. Mol Microbiol *39*, 47-53.

Tosaka, O., Morioka, H., and Takinami, K. (1979). The role of biotin-dependent pyruvate carboxylase in L-lysine production. Agric Biol Chem *43*, 1513-1519.

Tsirigotaki, A., De Geyter, J., Sostaric, N., Economou, A., and Karamanou, S. (2017). Protein export through the bacterial Sec pathway. Nat Rev Microbiol *15*, 21-36.

Unthan, S., Grunberger, A., van Ooyen, J., Gatgens, J., Heinrich, J., Paczia, N., Wiechert, W., Kohlheyer, D., and Noack, S. (2014). Beyond growth rate 0.6: What drives *Corynebacterium glutamicum* to higher growth rates in defined medium. Biotechnol Bioeng *111*, 359-371.

Unthan, S., Radek, A., Wiechert, W., Oldiges, M., and Noack, S. (2015). Bioprocess automation on a Mini Pilot Plant enables fast quantitative microbial phenotyping. Microb Cell Fact *14*, 32.

Uy, D., Delaunay, S., Engasser, J., and Goergen, J. (1999). A method for the determination of pyruvate carboxylase activity during the glutamic acid fermentation with *Corynebacterium glutamicum*. J Microbiol Methods *39*, 91-96.

Venkova, T., Patek, M., and Nesvera, J. (2001). Identification of a novel gene involved in stable maintenance of plasmid pGA1 from *Corynebacterium glutamicum*. Plasmid *46*, 153-162.

Ventura, M., Canchaya, C., Tauch, A., Chandra, G., Fitzgerald, G.F., Chater, K.F., and van Sinderen, D. (2007). Genomics of *Actinobacteria*: tracing the evolutionary history of an ancient phylum. Microbiol Mol Biol Rev *71*, 495-548.

Vitorino, L.C., and Bessa, L.A. (2017). Technological Microbiology: Development and Applications. Front Microbiol *8*, 827.

Vogt, M., Haas, S., Klaffl, S., Polen, T., Eggeling, L., van Ooyen, J., and Bott, M. (2014). Pushing product formation to its limit: metabolic engineering of *Corynebacterium glutamicum* for L-leucine overproduction. Metab Eng *22*, 40-52.

Vogt, M., Krumbach, K., Bang, W.G., van Ooyen, J., Noack, S., Klein, B., Bott, M., and Eggeling, L. (2015). The contest for precursors: channelling L-isoleucine synthesis in *Corynebacterium glutamicum* without byproduct formation. Appl Microbiol Biotechnol *99*, 791-800.

Walsh, G. (2018). Biopharmaceutical benchmarks 2018. Nature Biotechnol *36*, 1136-1145.

Wang, C., Zhou, Z., Cai, H., Chen, Z., and Xu, H. (2017). Redirecting carbon flux through *pgi*-deficient and heterologous transhydrogenase toward efficient succinate production in *Corynebacterium glutamicum*. J Ind Microbiol Biotechnol *44*, 1115-1126.

Watanabe, K., Tsuchida, Y., Okibe, N., Teramoto, H., Suzuki, N., Inui, M., and Yukawa, H. (2009). Scanning the *Corynebacterium glutamicum* R genome for high-efficiency secretion signal sequences. Microbiology *155*, 741-750.

Wells, J.M., Wilson, P.W., Norton, P.M., Gasson, M.J., and Le Page, R.W. (1993). *Lactococcus lactis*: high-level expression of tetanus toxin fragment C and protection against lethal challenge. Mol Microbiol *8*, 1155-1162.

Wendisch, V.F. (2003). Genome-wide expression analysis in *Corynebacterium glutamicum* using DNA microarrays. J Biotechnol *104*, 273-285.

Wendisch, V.F., Jorge, J.M.P., Perez-Garcia, F., and Sgobba, E. (2016). Updates on industrial production of amino acids using *Corynebacterium glutamicum*. World J Microbiol Biotechnol *32*, 105.

Wendisch, V.F., Spies, M., Reinscheid, D.J., Schnicke, S., Sahm, H., and Eikmanns, B.J. (1997). Regulation of acetate metabolism in *Corynebacterium glutamicum*: transcriptional control of the isocitrate lyase and malate synthase genes. Arch Microbiol *168*, 262-269.

Wieschalka, S., Blombach, B., Bott, M., and Eikmanns, B.J. (2013). Bio-based production of organic acids with *Corynebacterium glutamicum*. Microb Biotechnol *6*, 87-102.

Wittmann, C., Kiefer, P., and Zelder, O. (2004). Metabolic fluxes in *Corynebacterium glutamicum* during lysine production with sucrose as carbon source. Appl Environ Microbiol *70*, 7277-7287.

Wong, D. (2018). Microbial Production of Recombinant Human Insulin. In The ABCs of Gene Cloning (Springer, Cham).

Wong, T.S., Tee, K.L., Hauer, B., and Schwaneberg, U. (2004). Sequence saturation mutagenesis (SeSaM): a novel method for directed evolution. Nucleic Acids Res *32*, e26.

Xiang, S., and Tong, L. (2008). Crystal structures of human and *Staphylococcus aureus* pyruvate carboxylase and molecular insights into the carboxyltransfer reaction. Nat Struct Mol Biol *15*, 295-302.

Yoshida, A., Tomita, T., Kuzuyama, T., and Nishiyama, M. (2010). Mechanism of concerted inhibition of alpha2beta2-type hetero-oligomeric aspartate kinase from *Corynebacterium glutamicum*. J Biol Chem *285*, 27477-27486.

Yukawa, H., Omumasaba, C.A., Nonaka, H., Kos, P., Okai, N., Suzuki, N., Suda, M., Tsuge, Y., Watanabe, J., Ikeda, Y.*, et al.* (2007). Comparative analysis of the *Corynebacterium glutamicum* group and complete genome sequence of strain R. Microbiology *153*, 1042-1058.

Zhang, J., Jensen, M.K., and Keasling, J.D. (2015). Development of biosensors and their application in metabolic engineering. Curr Opin Chem Biol *28*, 1-8.

Zhang, X., Zhang, X., Xu, G., Zhang, X., Shi, J., and Xu, Z. (2018). Integration of ARTP mutagenesis with biosensor-mediated high-throughput screening to improve L-serine yield in *Corynebacterium glutamicum*. Appl Microbiol Biotechnol *102*, 5939-5951.

6 Appendix

## 6.1 Production of secretional proteins with *Corynebacterium glutamicum* MB001(DE3)

The newly developed T7 RNA polymerase-dependent gene expression system for *C. glutamicum* has already been characterized by the successful overproduction of the cytosolic proteins eYFP and pyruvate kinase (see chapter 3.1). Since the purification of cytosolic proteins is much more laborious than the isolation of secreted ones, the T7 system was also evaluated for the production of secretory proteins. Two different systems exist in *C. glutamicum* for the translocation across the cytoplasmic membrane: in the general secretion pathway (Sec pathway), proteins are secreted across the cytoplasmic membrane in an unfolded conformation and folding occurs only on the extracytoplasmic side of the membrane after cleavage of the signal peptide by a type I signal peptidase (Tsirigotaki et al., 2017). If heterologous proteins are secreted via the Sec system, this folding mechanism is often insufficient, since proper chaperones are missing in the cell envelope. Moreover, unfolded proteins are more susceptible to degradation by proteases, which in turn can reduce the overall yield of the produced proteins (Bolhuis et al., 1999). In contrast to the Sec system, the twin-arginine translocation pathway (Tat pathway) actively translocates completely folded and even oligomeric proteins across the cytoplasmic membrane (Lee et al., 2006). Proteins transported via this system have in common that their N-terminal signal peptide contains a highly conserved twin-arginine-containing sequence motif ((S/T)RRxFLK). After the proteins have been secreted via the Tat system, the signal peptide is cleaved from the precursor protein by a type I signal peptidase similar to the Sec system. Several examples show that the Tat system seems to be particularly advantageous for the secretion of heterologous proteins. In *E.coli* for example, it was possible to secrete GFP via the Sec system, but it was non-fluorescent due to inappropriate folding outside the cell (Feilmeier et al., 2000; Santini et al., 2001; Thomas et al., 2001). For this reason, Meissner and coworkers investigated the secretion of GFP via the Tat system in *C. glutamicum* (Meissner et al., 2007). The reporter protein GFP was fused with three different Tat signal peptides, which originated from a phosphodiesterase of *B. subtilis* (PhoD$_{Bs}$) and of *C. glutamicum* (PhoD$_{Cg}$), and in addition from the oxidoreductase TorA of *E. coli*. After expression of the corresponding genes via the pEKEx2 system in *C. glutamicum*, all three signal peptides enabled Tat-dependent secretion into the supernatant of the cells, as fluorescent GFP was detected in this fraction. The highest fluorescence was observed in the supernatant of samples containing the fusion protein PhoD$_{Bs}$-GFP, while the lowest fluorescence was detected in samples in which GFP was secreted via the signal peptide TorA (Meissner et al., 2007). In order to characterize the T7 system of *C. glutamicum* with respect to the production of secretory proteins, the production of the GFP variants via the pEKEx2 system was compared with that of the T7 system.

6.1.1 T7 RNA polymerase-dependent synthesis of GFP and subsequent secretion into the extracellular medium with *C. glutamicum*

The T7 system established in *C. glutamicum* was characterized with regard to the synthesis of secretory proteins and compared with the established pEKEx2 system. As mentioned above, Meissner et al. (2007) was able to show that GFP, fused to three different Tat signal peptides, could be successfully secreted into the extracellular medium by *C. glutamicum* after expression of the corresponding genes with the pEKEx2 system. The *gfp* genes were first amplified from the respective pEKEx2 plasmids using a specific forward primer for each fusion product (PhoD$_{Bs}$-GFP-for: GCATACGACAGTCGTTTTG, PhoDC$_g$-GFP-for: CCACAGTTAAGCAGAC-GCCAGTTC or TorA-GFP-for: AACAATAACGATCTCTTTCAGG) and a common reverse primer for all three products (GFP-rev: AACAATAACGATCTCTTTCAGG). The plasmid pMKEx2 was used as expression vector for the T7 system and was cut with the restriction enzymes NcoI/BamHI (both New England Biolabs, Frankfurt, Germany). Subsequently, 5' overhangs were filled by using the Klenow fragment of DNA polymerase I (New England Biolabs, Frankfurt, Germany) and then dephosphorylated (rAPid Alkaline Phosphatase, Roche Diagnostics, Mannheim, Germany). The PCR fragments were phosphorylated with ATP and T4 polynucleotide kinase (Thermo Fisher Scientific, Waltham, MA, USA) prior to ligation with cut pMKEx2 vector. Finally, the T7 expression strain *C. glutamicum* MB001(DE3) was transformed with the resulting plasmids pMKEx2-*phoD*$_{Cg}$-*gfp*, pMKEx2-*phoD*$_{Bs}$-*gfp* or pMKEx2-*torA*-*gfp.* For comparison, C*. glutamicum* MB001 was transformed with the three already existing pEKEx2 plasmids carrying the respective *gfp* fusion constructs. As a negative control strain MB001(DE3) with the empty vector pMKEx2 was used. For the expression of *gfp*, precultures of the respective strains were used to inoculate 50 ml of 2xTY medium (Sambrook et al., 1989) to an OD$_{600}$ of 0.5 and incubated at 30 °C and 120 rpm until cells reached an OD$_{600}$ of 1. At this time point, expression of the *gfp* genes was induced with 250 µM IPTG and the cultures were incubated for another 4 hours under the same conditions. Afterwards, cells were fractionated into a membrane fraction and a soluble fraction containing cytosolic proteins and soluble proteins from the periplasm. These fractions and the cell-free culture supernatants were analyzed for GFP. Fractionation was carried out by sedimentation of the cells (4000 x *g*, 4 °C, 20 min) in a first step. The supernatant was concentrated from 50 ml to 1 ml using centrifugal filters (Amicon Ultra-15 Centrifugal Filter Units, 10 NMWL) to analyze the amount of secreted GFP. To separate the membrane fraction from the soluble fraction, cell pellets were washed with 50 mM Tris-HCl, pH 8.0 and then disrupted by beat beating using a Precellys 24 device (Peqlab Biotechnologie, Erlangen, Germany). In a next step, cell debris was removed by centrifugation (4000 x *g*, 4 °C, 20 min) and the gained supernatant was fractionated by ultracentrifugation (35,000 x *g*, 4 °C, 1 h). Proteins of the membrane fraction were sedimented and subsequently suspended in 50 mM Tris-HCl, pH 7.5. To localize and quantify the synthesized GFP fusion

proteins, Western Blot analyses was performed. Therefore, proteins of each fraction were separated by SDS polyacrylamide gel electrophoresis using 10% separating gels (Laemmli, 1970). Subsequently, gels were electroblotted (1 h, 15 V) onto a nitrocellulose membrane (GE Healthcare Bio-Sciences, Uppsala, Sweden) and detection of GFP was performed by using polyclonal anti-GFP antibodies (BioGenes GmbH, Berlin, Germany) and Goat Anti-Rabbit IgG(H+L)-Cy5 (Bio-Rad Laboratories, Inc., Hercules, California, US). Visualization of GFP fluorescence was performed with a Typhoon Trio Scanner (GE Healthcare Bio-Sciences, Uppsala, Sweden). Finally, fluorescence in all three fractions was measured with a Tecan Reader Infinite 200 (Tecan Group, Männedorf, Switzerland). GFP was excited at a wavelength of 385 nm and the emission was measured at 510 nm to quantify the amount in the respective fraction. Measurements of fluorescence were blanked to the respective medium of the sample, which was treated in the same way as the other samples after cultivation. In order to consider the influence of different ODs after cultivation of all strains, the specific fluorescence (fluorescence divided by the end-OD_{600} of a culture) is given in the following.

It could be shown that with the pEKEx2 system as well as with the T7 system all of the three fusion proteins could be produced and subsequently secreted into the culture supernatant of the respective *C. glutamicum* strain (Figure 5). However, clear differences were apparent for the secretion efficiency. For the secretion of the protein $PhoD_{Bs}$-GFP into the extracellular medium, no difference in the band intensity in Western Blot analysis could be detected for both expression systems (Figure 5A). However, the specific fluorescence of $PhoD_{Bs}$-GFP is higher after *gfp* expression via the pEKEx2 system (420.9 ± 46.3 for the T7 system and 585.0 ± 102.2 for the pEKEx2 system; Figure 5B). Moreover, the specific GFP fluorescence in the soluble and in the membrane fractions is more than 1.5 times higher for the pEKEx2 system compared to the T7 system, respectively (Figure 5B). In the soluble fraction of strain MB001/pEKEx2-*phoD_{Bs}*-*gfp*, a band with a size of about 33 kDa could be detected, which probably indicates the GFP fusion protein with the uncleaved Tat signal peptide of $PhoD_{Bs}$ (Figure 5A). On the other hand, a band with a size of 26 kDa was visible in the membrane fraction of the same strain, thus corresponding to the size of the mature protein in which the signal peptide has been split off. Compared to these results, in the soluble and membrane fractions of strain MB001(DE3)/pMKEx2-*phoD_{Bs}*-*gfp* much thicker bands could be detected in Western Blot analysis, despite a lower measured specific GFP fluorescence in both fractions. It can therefore be assumed that the protein was not folded correctly and is therefore inactive and not suitable for secretion anymore. Reasons for this could be the high expression rate of the T7 system.
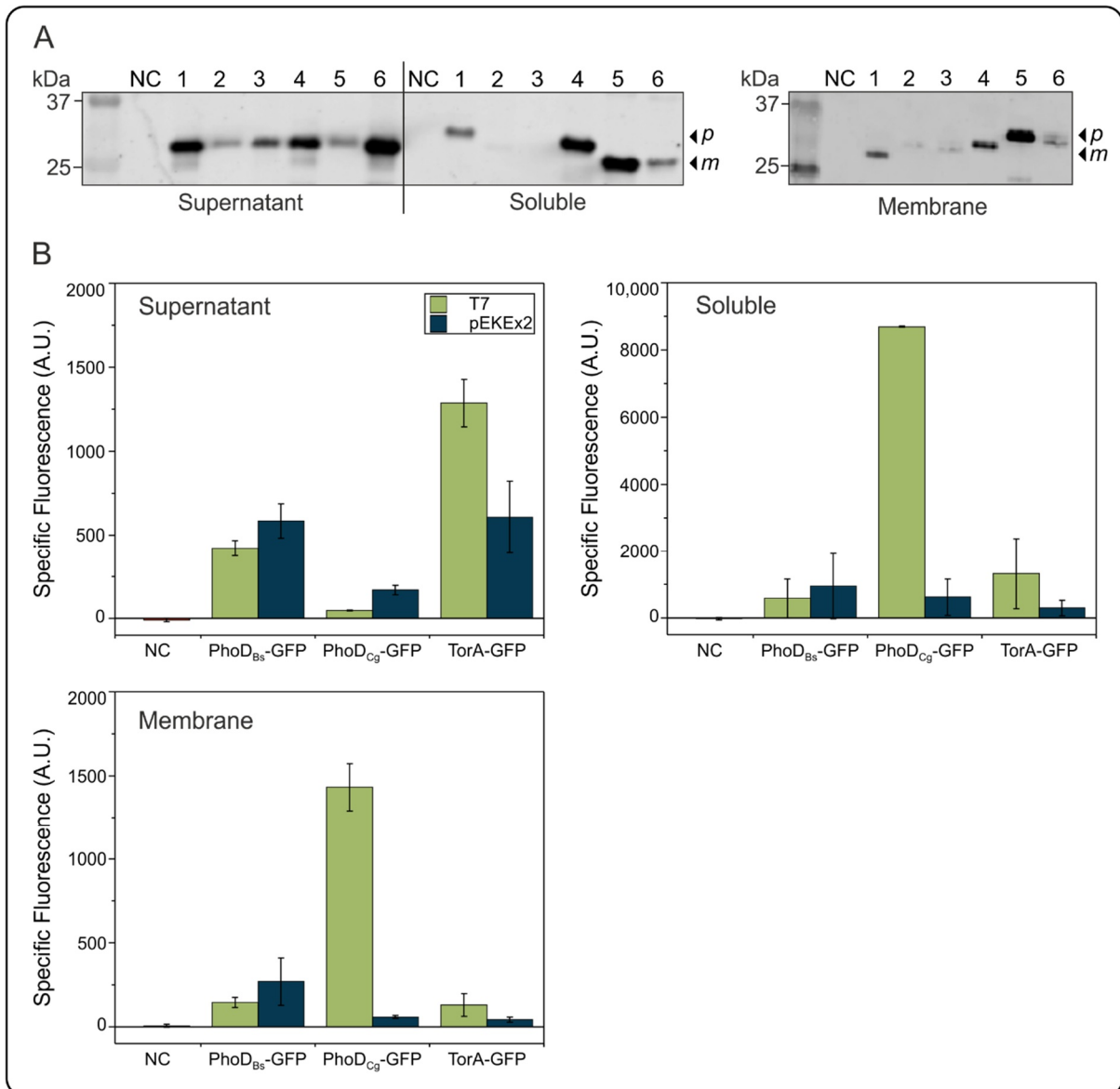
Figure 5 Analysis of PhoD$_{Bs}$-GFP, PhoD$_{Cg}$-GFP and TorA-GFP production with the T7 and the pEKEx2 system and subsequent secretion via the Tat system in *C. glutamicum*. The amount of the fusion protein in the soluble fraction, the membrane fraction and the supernatant of each strain was analyzed. (A) Western Blot analysis was performed to check the presence of GFP by using polyclonal anti-GFP antibodies (BioGenes GmbH, Berlin, Germany) and Goat Anti-Rabbit IgG(H+L)-Cy5 (Bio-Rad Laboratories, Inc., Hercules, California, US). Precision Plus Protein™ All Blue Prestained Protein Standard marker (Bio-Rad Laboratories, Inc., Hercules, California, US) was used to estimate the size of GFP. Mature GFP (*m*) without the signal peptide has a size of 26 kDa, precursor GFP (*p*) with Tat signal peptide not cleaved off has a size of 30 kDa for PhoD$_{Cg}$-GFP and TorA-GFP and of 33 kDa, for PhoD$_{Bs}$-GFP. NC – negative control (*C. glutamicum* MB001(DE3)/pMKEx2); 1 – MB001/pEKEx2-*phoD$_{Bs}$-gfp*; 2 – MB001/pEKEx2-*phoD$_{Cg}$-gfp*; 3 – MB001/pEKEx2-*torA-gfp*; 4 – MB001(DE3)/ pMKEx2-*phoD$_{Bs}$-gfp*; 5 – MB001(DE3)/pMKEx2-*phoD$_{Cg}$-gfp*; 6 – MB001(DE3)/pMKEx2-*torA-gfp*. (B) Specific fluorescence was analyzed in all three fractions with a Tecan Reader Infinite 200 (Tecan Group, Männedorf, Switzerland). GFP was excited at a wavelength of 385 nm and the emission was measured at 510 nm to quantify the amount in the respective fraction. Mean values of three independent experiments and standard deviations are shown.

Analyzing the production and subsequent secretion of GFP fused with the signal peptide PhoD$_{Cg}$ in a Western Blot showed that this fusion protein was secreted into the supernatant in

the lowest amount compared to the other two signal peptides, independent of the used expression system (Figure 5A). When *phoD$_{Cg}$-gfp* was expressed via the pEKEx2 system, only weak bands could be detected in the membrane fraction and in the soluble fraction. In comparison, a higher amount of GFP was synthesized with the T7 system as indicated by Western Blot analysis, but apparently could not be secreted, as strong bands were observed both in the soluble and the membrane fraction. Moreover, the apparent size of approximately 26 kDa observed in the soluble fraction indicates that the accumulated GFP is misfolded and/or the signal peptide is already cleaved off in the cell, thus preventing the secretion of the protein via the Tat signaling pathway. The measured specific fluorescence of PhoD$_{Cg}$-GFP shown in Figure 5B confirmed that GFP accumulates for the most part in the soluble fraction as it was about 188 times higher than in the supernatant (8,687.8 ± 21.0 and 46.1 ± 2.1, respectively) and about 6 times higher than in the membrane fraction (1431.2 ± 141.0). When *phoD$_{Cg}$-gfp* was expressed via the pEKEx2 system, active GFP was also detected in the cytosolic and membrane fractions (Figure 5B). Here, however, the specific fluorescence measured in the supernatant was only 4 times lower than in the cytosol (615.9 ± 538.5 and 168.3 ± 29.0) and 3 times higher than in the membrane fraction (57.3 ± 9.1). In summary, the accumulated specific fluorescence of all three fractions was more than 12 times higher after expression via the T7 system than via the pEKEx2 system. However, due to the strong fluorescence in the soluble and membrane fraction, it can be assumed that a large part of the PhoD$_{Cg}$-GFP produced by the T7 system was not secreted. In contrast, the specific fluorescence in the supernatant in relation to the total specific fluorescence of all three fractions is significantly higher after expression with the pEKEx2 system, and a better secretion efficiency of PhoD$_{Cg}$-GFP can be assumed after production with the pEKEx2 system.

For the third fusion protein TorA-GFP, the strongest band in the supernatant was detected in Western Blot analysis when *torA-gfp* was expressed via the T7 system (Figure 5A). This band also appears more intensive in comparison to the other bands of the fusion proteins PhoD$_{Cg}$-GFP and PhoD$_{Bs}$-GFP, independent of the respective expression system. Analyzing the specific fluorescence in the supernatant confirmed this result: while a value of 1285.8 ± 141.5 was measured in the supernatant of strain MB001(DE3)/pMKEx2-*torA-gfp*, a twofold lower value of 607.1 ± 214.5 was observed in the supernatant of the strain using the pEKEx2 system for overexpression of *torA-gfp* (Figure 5B). In contrast to this, almost no bands could be detected in the soluble and membrane fractions in Western Blots analysis when *torA-gfp* was expressed via the pEKEx2 system. After expression with the T7 system, a band with a size of approx. 30 kDa was visible for TorA-GFP in the membrane fraction, which corresponds to the protein with non-cleaved signal peptide, and a band with a size of about 26 kDa, corresponding to the mature protein without the signal peptide, was visible in the cytosolic fraction of strain MB001(DE3)/pMKEx2-*torA-gfp*. Measurements of the specific fluorescence in both fractions

confirmed the results of the Western Blot: the specific fluorescence in the soluble fraction was more than four times higher for *gfp* expressed with the T7 system (1325.7 ± 1052.2) compared to the pEKEx2 system (293.3 ± 233.2). Additionally, a higher specific fluorescence was also found in the membrane fraction of the strain with the T7 system (128.4 ± 67.7 for the T7 system and 42.1 ± 14.0 for the pEKEx2 system, Figure 5B). These results show that the secretion of GFP apparently works best with TorA among the three signal peptides chosen for this experiment, since the highest specific fluorescence in the supernatant was measured for both systems and the bands in Western Blot seem to be most intense. In contrast only weak bands in the Western Blot and a low specific fluorescence could be detected in the membrane and cytosolic fractions, indicating that the largest part of the protein seems to be actually secreted and even in an active form. The higher amount of expressed *gfp* observed for the T7 system based on Western Blot analysis, but also the higher specific fluorescence in all three fractions of this strain underlines the capacity of the newly established expression system.

6.1.2   Influence of *tatABC* overexpression on the secretion of the heterologous protein PhoD$_{Bs}$-GFP in *C. glutamicum*

Production of secretory proteins via the T7 system in *C. glutamicum* MB001(DE3) showed that a large fraction of the protein was not secreted but remained in the cytosol or membrane fraction of the cell (see chapter 6.1.1). One possible explanation for this result is that the Tat system is the bottleneck for protein export due to overload in these strains. Therefore, in another approach, the Tat system was also overproduced in order to enlarge the secretion capacity and avoid accumulation within the cell. In *C. glutamicum*, the Tat system is encoded by *tatA*, *tatB* and *tatC* (Oertel et al., 2015). To be able to overexpress and induce *tatABC* expression independently of the T7 system, the *tatABC* genes were cloned into pCLTON2 under the control of the *tet* promoter (P$_{tet}$), which can be induced with anhydrotetracycline (ATc) (Lausberg et al., 2012). The construction is described in Figure 6 in more detail. To analyze the secretion efficiency, *phoD$_{Bs}$-gfp* was chosen to be expressed under control of the T7 promoter using the plasmid pMKEx2-*phod$_{Bs}$-gfp*, since previous experiments showed an equivalent distribution of the corresponding protein among the supernatant and cytosolic and membrane fraction. For the expression of *gfp*, precultures of *C. glutamicum* MB001(DE3)/pCLTON2-*tatABC*/pMKEx2-*phoD$_{Bs}$-gfp* were used to inoculate 50 ml CGXII minimal medium supplemented with 4% (wt/vol) glucose (Keilhauer et al., 1993) to an OD$_{600}$ of 0.5 and incubated at 30 °C and 120 rpm. After 2.5 h, the T7 system was induced with 250 µM IPTG and the culture was incubated for another 4 h.
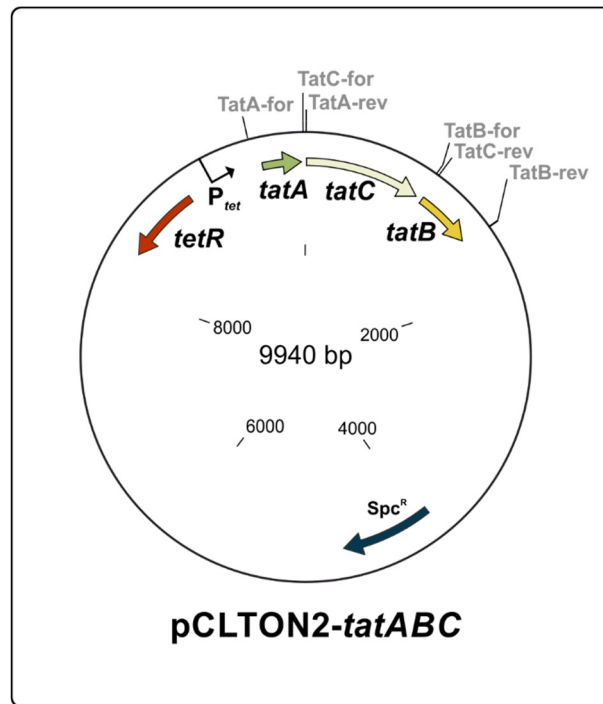
Figure 6 Construction of pCLTON2-*tatABC*. The genes *tatABC* were amplified from *C. glutamicum* ATCC 13032 with the following primers: *tatA* - TatA-for (CTTTAAGAAGGAGATATACAATGCCCACTCTCGGACCA) and TatA-rev (ATATCTCCTTCATTTTTTAGATGCAAACTGCCCAAC); *tatB* – TatB-for (ATTTTTCTGGAAGGA-GATATACAATGTTTTCTAGCGTGGGTTGG) and TatB-rev (GTCGACGGAGCTCGAATTCGAAACGCTT-GGGCTTGGCG); *tatC* – TatC-for (ATCTAAAAAATGAAGGAGATATACAATGTCCATTGTTGAGCAC) and TatC-rev (ATATCTCCTTCCAGAAAAACTCATGCCCTC). The vector pCLTON2 was cut with FastDigest restriction enzymes SacI/PstI (both Thermo Fisher Scientific, Waltham, MA, USA) and subsequently ligated with the amplified PCR fragments via a self-prepared Gibson assembly master mix (Gibson, 2011).

Moreover, the timing of induction of the *tet* system (before (0 h), with (2.5 h) or after induction (3.5 h) of the T7 system with IPTG) as well as the concentration of the inducer ATc (25 ng/ml or 250 ng/ml ATc) were varied and analyzed in this experiment. As a control, the strains *C. glutamicum* MB001(DE3)/pCLTON2/pMKEx2-*phoD_{Bs}*-*gfp* (250 ng/ml ATc; 250 µM IPTG) and MB001(DE3)/pCLTON2-*tatABC*/pMKEx2-*phoD_{Bs}*-*gfp* (0 ng/ml ATc; 0 µM IPTG) were used. After growth, cells were harvested by centrifugation (4000 x *g*, 4 °C, 20 min) and the supernatant was used for further analysis. Sedimented cells were washed with 50 mM Tris-HCl, pH 8.0 and then disrupted by beat beating using a Precellys 24 device and glass beads (Peqlab Biotechnologie, Erlangen, Germany). Finally, total cell extract (TCE) was obtained after centrifugation (16,000 x *g*, 4 °C, 20 min) using the obtained supernatant. Localization and quantification of the synthesized GFP fusion proteins in Western Blot analysis and determination of specific fluorescence was performed as described in chapter 6.1.1. Measurements of fluorescence were blanked to the respective medium of the sample, which was treated in the same way as the other samples after cultivation.

A comparison of the growth behavior of all strains showed that the growth deteriorates the earlier the *tet* system was induced, whereas the added amount of ATc had only a minor

effect (Figure 7A). Only for strain MB001(DE3)/pCLTON2-*tatABC*/pMKEx2-*phoD$_{Bs}$-gfp* a negative effect of higher ATc concentration was detected when the *tet* system was induced directly after the start of cultivation (OD$_{600}$ after 6 h of growth - 25 ng/ml ATc: 1.48; 250 ng/ml ATc: 1.32). 3.5 h after induction, the cells were harvested and the amount of produced and secreted GFP was analysed in the supernatant and in TCEs by Western Blot analysis and measurement of specific fluorescence. As expected, no band for GFP was visible in the supernatant or in TCE for the non-induced control strain MB001(DE3)/pMKEx2- *phoD$_{Bs}$-gfp*/pCLTON2-*tatABC* (Figure 7B). Moreover, no GFP band was detected in the Western Blot when *tatABC* expression was induced directly at the beginning of the cultivation. If, on the other hand, the *tet* system was induced at a later time point, bands at the height of the mature GFP with a size of 26 kDa could be detected in the supernatant. Here, the intensity of the bands increased the later the system was induced and when 25 ng/ml ATc instead of 250 ng/ml ATc was used. However, if the Tat system was not overexpressed in strain MB001(DE3)/pMKEx2-*phoD$_{Bs}$-gfp*/pCLTON2, the band with the highest intensity for PhoD$_{Bs}$-GFP was visible. There are no clear differences in the intensity of the bands in the supernatant or TCE. The band in the supernatant apparently shows a size which equals the size of the mature GFP with the signal sequence already cleaved off, whereas in the TCE, a band with a size of about 33 kDa could be detected. This equals the size of GFP protein including the signal peptide. Here, again, the band with the most intensive staining was found in the control strain, which does not overexpress the *tatABC* genes.

The measurements of the specific fluorescence correspond to the results of the Western Blot analysis (Figure 7B,C). For overexpression of the *tatABC* genes, the highest specific fluorescence of 195 was measured in the supernatant of strain MB001(DE3)/pMKEx2-*phoD$_{Bs}$-gfp*/pCLTON2-*tatABC*, in which the *tet* system was induced with 25 ng/ml ATc after induction of the T7 system. However, this fluorescence is 2.6 times lower than in the control strain MB001(DE3)/pMKEx2-*phoD$_{Bs}$-gfp*/pCLTON2 (508). If the *tet* system was induced to an earlier time point, only negative values were determined after subtraction of the blank value. This could have been caused by the low fluorescence of GFP in these samples. In the TCE the highest specific fluorescence (3205) in strain MB001(DE3)/pMKEx2-*phoD$_{Bs}$-gfp*/pCLTON2-*tatABC* was measured with 25 ng/ml ATc, added after induction of the T7 system. In comparison, the specific fluorescence in strain MB001(DE3)/pMKEx2-*phoD$_{Bs}$-gfp*/pCLTON2 was 2729 and thus 1.2 times lower. If the expression of the *tat* genes was induced with a higher concentration of ATc and/or at an earlier time point, the specific fluorescence was comparatively lower.
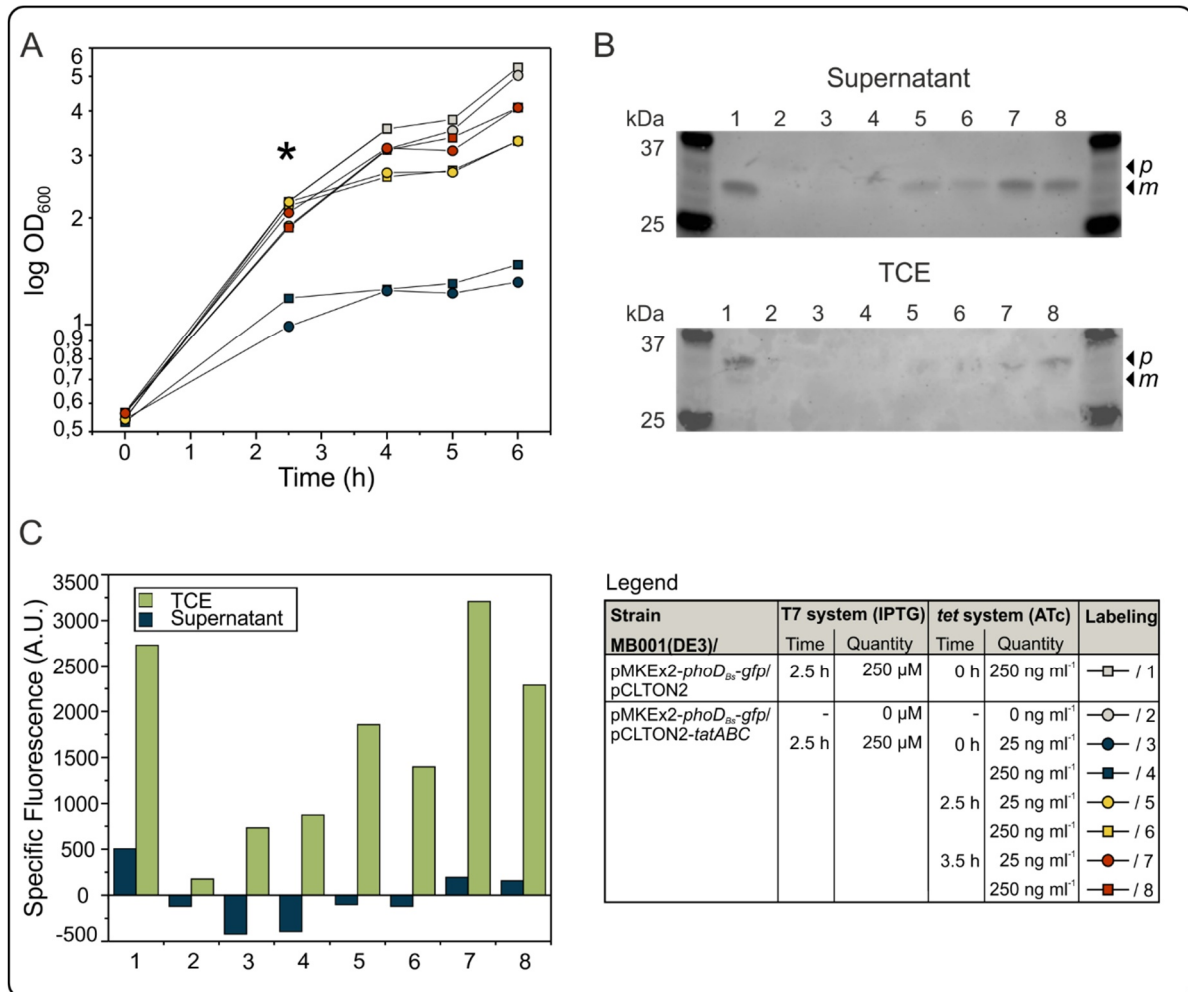
Figure 7 Analysis of *tatABC* overexpression on production and secretion of PhoD_Bs-GFP by *C. glutamicum* MB001(DE3)/pMKEx2-*phoD_Bs*-*gfp*/pCLTON2-*tatABC*. (**A**) Comparison of the growth of MB001(DE3)/pMKEx2-*phoD_Bs*-*gfp*/pCLTON2-*tatABC* strains, in which the *tet* system was induced at given time points with two different concentrations of the inducer ATc as described in the legend of the figure. MB001(DE3)/pMKEx2-*phoD_Bs*-*gfp*/pCLTON2 and MB001(DE3)/pMKEx2-*phoD_Bs*-*gfp*/pCLTON2-*tatABC* were used as control strains. The cells were grown as described in the text in CGXII minimal medium containing 4% (wt/vol) glucose. After 2.5 h the T7 system was induced with 250 µM IPTG (indicated with an asterisk) and the cells were further incubated for 4 h. (**B**) Western Blot analysis was performed to check the expression of GFP by using polyclonal anti-GFP antibody (BioGenes GmbH, Berlin, Germany) and Goat Anti-Rabbit IgG(H+L)-Cy5 (Bio-Rad Laboratories, Inc., Hercules, California, US). Precision Plus Protein™ All Blue Prestained Protein Standard marker (Bio-Rad Laboratories, Inc., Hercules, California, US) was used to estimate the size of GFP. Mature GFP (*m*) has a size of 26 kDa, precursor GFP (*p*) with Tat-signal peptide not cleaved off has a size of 33 kDa. (**C**) Specific fluorescence was analyzed in the supernatant and TCE with a Tecan Reader Infinite 200 (Tecan Group, Männedorf, Switzerland). GFP was excited at a wavelength of 385 nm and the emission was measured at 510 nm to quantify the amount in the respective fraction. Time of induction for both the T7 system (*gfp* expression) and *tet* system (*tatABC* expression) as well as the quantity of the respective inducer IPTG or ATc used for each strain are also shown in the legend of the figure.

From these results it can be concluded that overexpression of the *tatABC* genes causes stress for the cell, which in turn has a negative effect on the expression of *gfp*. The more the expression of the *tat* genes was induced, the less GFP was produced and eventually secreted. However, Kikuchi et al. were able to show that the overexpression of *tatABC* in *C. glutamicum* could increase the secretion of a glutaminase protein by a factor of almost 10 (Kikuchi et al., 2009). In contrast to our experiment, the native promoters and ribosome binding sites were used for

the overexpression of the *tat* genes. This indicates a too strong overproduction of the Tat system in our work. Moreover, since the stoichiometric ratio of the three *tat* genes should be maintained after overexpression, this may be another factor that could have had a negative effect on GFP production and could be optimized in future experiments.

6.2 Genome-sequencing of the lysine-producing strain *Corynebacterium glutamicum* DG52-5

For the characterization of pyruvate carboxylase (PCx) with regard to its role in L-lysine production in *C. glutamicum*, the PCx gene (*pyc*) was deleted or overexpressed in strain *C. glutamicum* DG52-5 (Peters-Wendisch et al., 2001). Subsequent measurements of the lysine concentration in the supernatant of this strain revealed that deletion of *pyc* caused a reduction of the lysine titer by almost 60% in comparison to strain DG52-5 encoding the wild-type PCx and an increased production by almost 50% after overexpression of *pyc*. L-lysine production in this strain is possible due to a feedback-resistance of the aspartate kinase LysC towards its end-product lysine, caused by a non-characterized mutation in the gene (Menkel et al., 1989). Moreover, since this strain was generated by classical mutagenesis, effects on lysine production by additional mutations in the genome cannot be excluded. To omit these possible side effects of other, unknown mutations, a different strain than DG52-5 with a defined genomic background was used for the screening of PCx muteins in this work, named DM1868 (see chapter 3.2; Evonik Industries AG, Halle (Westf.), Germany). In this strain, the feedback resistance towards lysine is due to the mutation T311I in LysC. However, a deletion of *pyc* in DM1868 caused only a 14% decrease in L-lysine production, whereas overexpression of *pyc* resulted in a 60% higher L-lysine titer (see chapter 3.2). A possible explanation for these deviations in lysine production might be the different strain backgrounds of DG52-5 and DM1868. In order to be able to compare the genomes of both strains and to find further mutations in the background of DG52-5 that could influence lysine production as well, the genome of strain DG52-5 was sequenced in this work. Therefore, genomic DNA of *C. glutamicum* DG52-5 was isolated by ethanol precipitation of a 5 ml overnight-culture. For this purpose, cells were harvested by centrifugation (4000 x *g*, 4 °C, 15 min) and re-suspended in 5 ml lysis buffer (20 mM Tris-HCl, pH 8; 0.2 mM EDTA; 1.2% Triton X-100) containing 20 mg ml^{-1} lysozyme. After incubation for 1 h at room temperature, 80 µl of 10% SDS and 25 µl proteinase K (20 mg ml^{-1} solved in TE) were added and cells were incubated for another 30 min at 70 °C. For precipitation of genomic DNA, 200 µl 6 M NaCl were added and the lysate was centrifuged for 10 min at 16 000 x *g*. The supernatant was mixed with 2.5 volumes of ice cold 100% EtOH and incubated for 1 h at -20 °C. In the next step, DNA was sedimented by centrifugation (16 000 x *g*, 4 °C, 30 min) and the obtained pellet was washed once with 0.5 ml ice cold 75% EtOH. Afterwards, EtOh was removed and the pellet was air dried and suspended in 100 µl 10 mM l^{-1} Tris-HCl. Finally, Illumina sequencing was performed by Dr. Tino Polen and Doris Rittmann (IBG-1, Forschungszentrum Jülich). *C. glutamicum* ATCC 13032 (GenBank ID: BX927147) was used as reference genome. In comparison to the wild-type strain ATCC 13032, 104 single nucleotide polymorphisms (SNPs) were identified in DG52-5. 53 of them resulted in amino acid exchanges, 24 in silent mutations, and another 3 in stop codons in the corresponding coding

region. Furthermore, 25 mutations were found in intergenic regions. In addition to these SNPs, 8 insertions or deletions and 7 multiple nucleotide polymorphisms (MNPs) were found, whereby MNPs are defined as multiple, consecutive nucleotide alterations to the wild-type gene.

SNPs and MNPs found in DG52-5, which cause either amino acid exchanges in proteins or nucleotide exchanges in rRNAs are summarized in Table 1. As expected, an amino acid exchange (S301F) was identified in LysC causing the feedback resistance of aspartate kinase towards lysine. The S301F exchange is located 10 amino acid residues apart from the L311I exchange in LysC of strain DM1868 (Table 1) and both named mutations have already been characterized in more detail (Ohnishi et al., 2002; Yoshida et al., 2010). Analysis of the crystal structure of LysC^{S301F} showed that the enzyme is able to bind the inhibitors lysine and threonine despite the mutation (Yoshida et al., 2010). Deregulation is therefore probably based on allosteric signal transduction between the individual domains of this enzyme (Chen et al., 2011; Yoshida et al., 2010). Due to the position of L311I and S301F, a similar effect on the regulation of aspartate kinase can be assumed, but a direct comparison of deregulation was not performed. An altered impact of the two aspartate kinase mutations on lysine production can therefore not be excluded.

Another mutation to be noted was found in the inositol permease IolT2. This permease catalyzes not only the uptake of *myo*-inositol in *C. glutamicum* (Krings et al., 2006), but also transports glucose, which then is phosphorylated either by the ATP-dependent glucokinase (Cg2399) or by the polyphosphate/ATP-dependent glucokinase PpgK (Cg2091) (Lindner et al. 2011). With these reactions, the phosphoenolpyruvate-dependent phosphotransferase system (PTS) can be bypassed. Moreover, it was shown that the combined overexpression of *iolT2* and *ppgk* caused an increased L-lysine production whereas by-product formation of lactate and L-alanine was reduced (Lindner et al., 2011; Perez-Garcia et al., 2016). An effect on glucose uptake and thus on L-lysine production in strain DG52-5 caused by the mutation G190R in IolT2 might therefore be possible. Another mutated transporter protein in *C. glutamicum* DG52-5 was the sucrose-specific component PtsS of the PTS. In contrast to IolT2, the influence of this enzyme on L-lysine production in *C. glutamicum* has not been investigated any further to our knowledge.

SNPs have also been found in genes of different regulators, including *sigA*, encoding the house-keeping RNA polymerase σ70 factor A (Table 1). According to CoryneRegNet (http://coryneregnet.compbio.sdu.dk/ v6/index.html) this sigma factor acts as an activator for at least 251 genes in *C. glutamicum*, including *pyc* and other genes of the PEP-pyruvate-OAA node and of lysine biosynthesis (Patek and Nesvera, 2011). An increased activity of the sigma factor can therefore presumably also change the expression of the aforementioned genes and

thus enable an increased lysine biosynthesis. Indeed, SigA variants for increased lysine production have already been discovered, like the variant $SigA^{A414V}$, which led to an increased lysine production of about 12% in *C. glutamicum* (Bathe et al., 2003). Furthermore, another SigA variant was reported with an amino acid exchange at position 447 from leucine to histidine, which also enables increased lysine production of the respective *C. glutamicum* strain (Huh et al., 2016). This described mutation is at the same position as the newly identified amino acid exchange in SigA of strain DG52-5, in which a leucine is also exchanged for a basic amino acid, in this case arginine. Therefore, an influence of the SigA variant seems very likely and should be investigated in more detail. Another regulator which is mutated in strain DG52-5 is the repressor OxyR (Q210P) (Milse et al., 2014; Teramoto et al., 2013). The importance of this regulator for the lysine producer *C. glutamicum* MH20-22B has already been determined in various DNA microarrays (Sindelar and Wendisch, 2007). Lysine production in this strain seems to trigger redox stress in the cell, which leads to an increased expression of the repressor. A deletion of this regulator in turn led to a higher resistance of *C. glutamicum* towards H_2O_2 (Milse et al., 2014). By structural alignment of 186 related sequences using the 3DM database (Bio-Prodict BV, Nijmegen, Netherlands), it was shown that the mutated glutamine-residue of OxyR in strain DG52-5 is highly conserved (100% Q, 0% P) and an alteration of its activity is therefore very likely. Nevertheless, more information is required to characterize the influence of the mutation in the regulator OxyR on L-lysine production in this strain.

Further mutations have been found for example in transporters (e.g. AbgT), enzymes of the peptidoglycan biosynthesis (e.g. MurA and PbpA) or in various hypothetical proteins. However, since all mutations were introduced into the genome of DG52-5 by chance, it is not possible to make a definite statement about which genes really have an effect on lysine biosynthesis. Further experiments such as DNA microarrays can be carried out in order to gain more insight into the expression of these genes under different conditions. Nevertheless, a definite conclusion as to whether the mutation has a positive effect on lysine production in *C. glutamicum* is only possible if the mutations are introduced one by one into a lysine producing strain such as DM1868 and changes in lysine production are analyzed.

Table 1 List of SNPs and MNPs found in *C. glutamicum* DG52-5, which cause an amino acid exchange in the corresponding protein when compared to the genome sequence of the type strain ATCC 13032. If more than one nucleotide alteration caused the specified amino acid exchange (i.e. MNP), the amino acid exchange is marked with an *.

Locus tag	Gene name	Amino Acid Exchange	Gene Annotation
cg0046		L215F	putative ABC transport protein, ATP-binding component
cg0060	*pbpA*	G473E	D-alanyl-D-alanine carboxypeptidase (EC:3.4.16.4)
cg0060	*pbpA*	A227T	D-alanyl-D-alanine carboxypeptidase (EC:3.4.16.4)

Locus tag	Gene name	Amino Acid Exchange	Gene Annotation
cg0122		G663D	putative glycerol 3-phosphate dehydrogenase
cg0122		G56D	putative glycerol 3-phosphate dehydrogenase
cg0133	*abgT*	T251I	p-aminobenzoyl-glutamate transporter
cg0216		P52S	putative membrane protein
cg0246		A66T	glycosyl transferase
cg0284		A533V	putative drug exporter of the RND-superfamily
cg0300		G317S	putative tripeptide synthase involved in murein formation
cg0306	*lysC*	S301F	aspartate kinase (EC:2.7.2.4); deletion causes lysine-auxotrophy in *C. glutamicum*
cg0336	*ponA*	G736S	penicillin-binding protein 1B (EC:2.4.2.-)
cg0340		S225N	putative sugar/metabolite permease, MFS-type
cg0370		A356T	putative ATP-dependent RNA helicase, DEAD/DEAH box-family
cg0409		E356K	putative metallopeptidase
cg0422	*murA*	I430N	UDP-N-acetylglucosamine 1-carboxyvinyltransferase (EC:2.5.1.7)
cg0485		R103C	hypothetical protein
cg0501	*qsuA*	P19L	putative shikimate permease, MFS-type
cg0507		G78S	permease subunit of ABC-type spermidine/putrescine/ironIII transporter
cg0565	*gabR*	E475K	transcriptional regulator of *gabTDP* genes
cg0634	*rplO*	T146I	50S ribosomal protein L15
cg0629	*rplF*	G82I*	50S ribosomal protein L6
cg0794	*yciC*	A239V	putative P-loop GTPase of the COG0523-family, involved in zinc metabolism
cg0843		E977K	putative helicase
cg0877	*rshA*	G11D	putative anti-sigma factor
cg1149		P27S	hypothetical protein
cg1782	*tnp13b*	M416V	transposase
cg2031		P301L	hypothetical protein, conserved CGP3 region
cg2049		I14T*	hypothetical protein, conserved CGP3 region
cg2049		L91T*	hypothetical protein, conserved CGP3 region
cg2066		D243N*	putative low-complexity protein
cg2066		H245E*	putative low-complexity protein
cg2092	*sigA (rpoD)*	L447R	RNA polymerase sigma factor A
cg2109	*oxyR*	Q210P	hydrogen peroxide sensing regulator, LysR family
cg2262	*ftsY*	V169I	signal recognition particle GTPase
cg2262	*ftsY*	A170V*	signal recognition particle GTPase
cg2353		P75S	putative protein disrupted by insertion of ISCg2e
cg2353		L76I*	putative protein disrupted by insertion of ISCg2e

Locus tag	Gene name	Amino Acid Exchange	Gene Annotation
cg2354	*tnp2e*	G314R	transposase
cg2384	*idsA*	V17I	putative geranylgeranyl pyrophosphate synthase (EC:2.5.1.30)
cg2711		S93N	putative secreted protein
cg2776	*dinG*	G20D	putative ATP-dependent DNA helicase-related protein
cg2914	*tnp5b*	I339F	transposase
cg2925	*ptsS*	L463F	sucrose-specific EIIABC component EIISuc of PTS, fructose-specific enzyme II BC (EIIFru) component of PTS (EC:2.7.1.69)
cg3151	*tnp2b*	V168I	transposase
cg3247	*hrrA*	S201F	response regulator of HrrAS two component system involved in heme homeostasis
cg3316		P306S	putative universal stress protein UspA no. 4 or related nucleotide-binding protein
cg3322		D82N	putative secreted membrane-fusion protein
cg3352	*nagR (genR)*	G258E	transcriptional regulator of gentisate pathway, IclR family
cg3363	*trpB*	A39V	tryptophan synthase subunit ß (EC:4.2.1.20)
cg3387	*iolT2*	G190R	*myo*-inositol transporter 2, MFS-type
cg3393	*phoC*	H71R	putative secreted phosphoesterase
cg3393	*phoC*	T1212I	putative secreted phosphoesterase
cg3397		D283N	hypothetical protein
cg3404		A53T	putative ABC-type putative ironIII dicitrate transporter
cgr01		-	16S ribosomal RNA; nucleotide exchange A1438T
cgr03		-	5S ribosomal RNA; nucleotide exchange C115T
cgr15		-	16S ribosomal RNA; nucleotide exchange G404A
cgr17		-	23S ribosomal RNA; nucleotide exchange G2914A

6.3 Characterization of corynebacterial PCx muteins with PCx-Assay

As described in chapter 3.2, we identified PCx variants of *C. glutamicum* that enabled an increased L-lysine production from glucose. These variants carry the amino acid exchanges T132A, T343A, and I1012S. Since it has not yet been possible to clarify why these mutations lead to an increased L-lysine production in *C. glutamicum*, the individual mutations were characterized in more detail with the PCx assay presented in chapter 3.3. Initial results have already been described in the publication reported in chapter 3.3, but are explained in more detail in the following.

For kinetic characterization of PCx variants, *C. glutamicum* DM1868Δ*pyc* was transformed with either pAN6-*pyc*[T132A], pAN6-*pyc*[T343A], or pAN6-*pyc*[I1012S]. Plasmids were constructed by amplifying the corresponding *pyc* gene from genomic DNA of strains DM1868 *pyc*[T132A], DM1868 *pyc*[T343A] or DM1868 *pyc*[I1012S], respectively, with the primers Pyc-NdeI-for (GCTCTAGACGCATATGTCGACTCACACATCTTC) and Pyc-MfeI-rev (CTTAA-GCTTCAATTGAAAGCCCCGCCTCCTCC) purchased from Eurofins MWG Operon (Ebersberg, Germany). The generated PCR fragments were cut with NdeI/MfeI (FastDigest restriction enzymes, Thermo Fisher Scientific, Waltham, MA, USA) and cloned into pAN6 that was cut with NdeI/EcoRI (Thermo Fisher Scientific, Waltham, MA, USA). Afterwards, plasmids were transferred into *C. glutamicum* DM1868Δ*pyc*. Strain cultivation, purification and enzyme assays are performed as described in chapter 3.3.

In all purifications and activity assays, wild-type PCx (PCx[wt]) was included in parallel as an internal control to exclude differences in the experimental settings. During the purification process of the three PCx variants, no differences to wild-type PCx were observed with respect to purity or protein yield, indicating that the PCx variants show comparable stability as the wild-type protein. The activity of the three purified PCx variants was compared to PCx[wt] under standard conditions with 40 mM $KHCO_3$ and 6 mM ATP. The maximal specific activities at saturating pyruvate concentrations were 23.8 ± 2.1, 20.7 ± 0.0, and 30.5 ± 2.0 µmol min^{-1} (mg protein)$^{-1}$) for PCx[T132A], PCx[T343A], and PCx[I1012S] and thus within the same range as PCx[wt] (24.9 ± 2.5 µmol min^{-1} (mg protein)$^{-1}$). The higher activity observed for PCx[I1012S] might be relevant for increased lysine production. The K_m values for pyruvate of the three PCx variants were also in a similar range as the one of PCx[wt] (3.8 ± 0.7 mM) with 3.2 ± 0.6 mM, 2.4 ± 0.0 mM, and 4.2 ± 0.4 mM for PCx[T132A], PCx[T343A], and PCx[I1012S], respectively. The somewhat lower value determined for PCx[T343A] might be of relevance for the positive influence of this variant on lysine production.

In further experiments, the effects of ADP, aspartate, and acetyl-CoA on the activity of the three PCx variants were determined (Figure 8). All variants showed strong inhibition by ADP, but no significant changes with respect to the K_i values compared to PCx[wt] (Figure 8A). The response of the PCx variants towards acetyl-CoA was quite unusual and similar to the response of PCx[wt]: Up to 50 µM, acetyl-CoA had a slight inhibitory effect on all PCx variants, which was reversed at higher concentrations (Figure 8B). At concentrations of about 250 µM acetyl-CoA and above, about the same activity was measured as in the absence of acetyl-CoA, except for PCx[T343A], for which the activity at 1000 µM acetyl-CoA was only about 85% of the activity of PCx[wt]. When intracellular concentrations of acetyl-CoA were determined in the wild-type strain *C. glutamicum* ATCC 13032, about 24 µM were measured in cells grown on minimal medium supplemented with glucose and about 155 µM in cells grown with glucose and acetate (Wendisch et al., 1997). For *E. coli* K12, cytosolic concentrations between 20 and

600 µM acetyl-CoA were reported (Takamura and Nomura, 1988). The small inhibitory effect detected at 500-1000 µM acetyl-CoA for PCx^T343A therefore seems to be at the upper limit of the physiological range of this effector and a significance for L-lysine production is therefore unlikely.
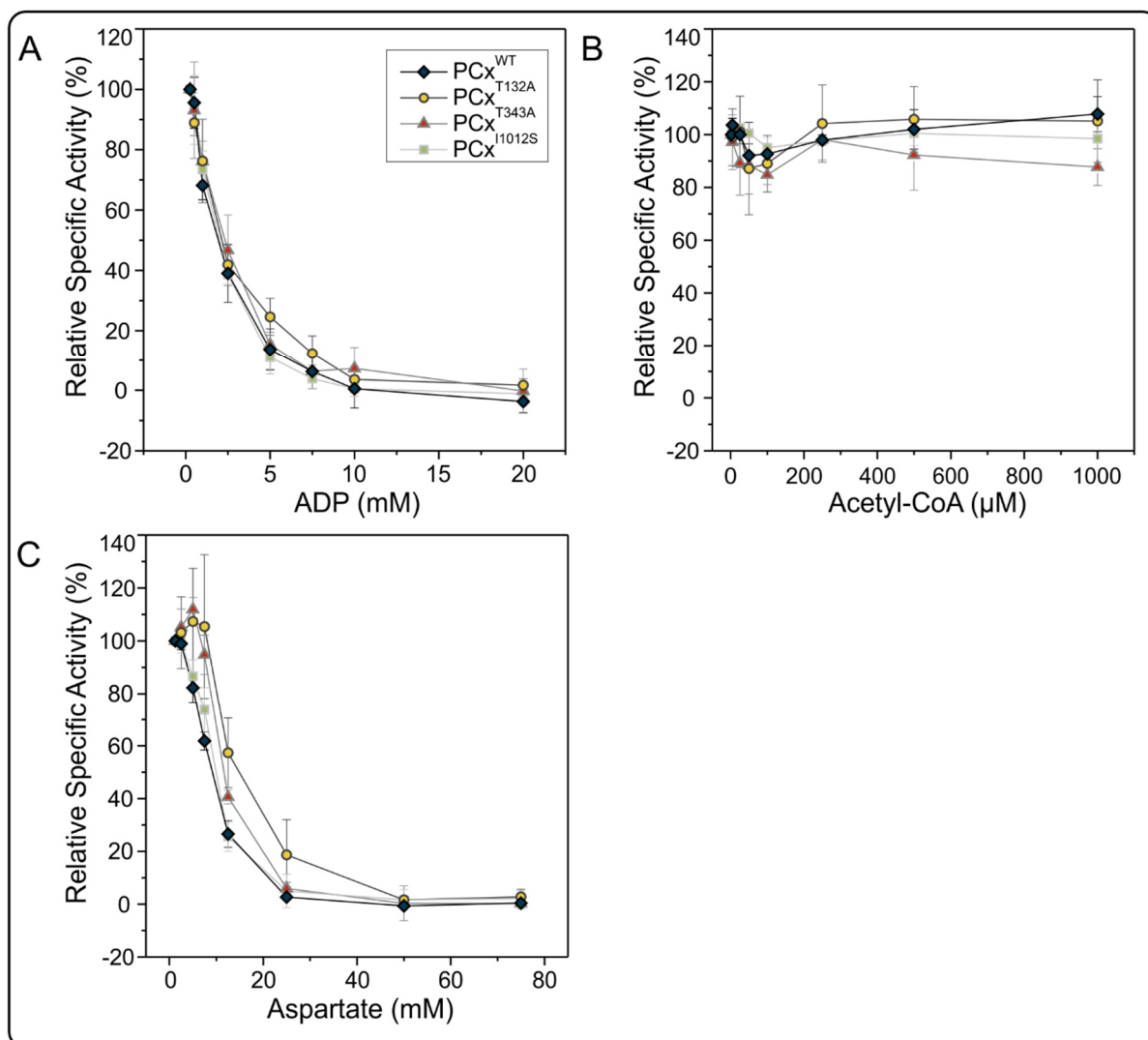

Figure 8 Influence of ADP (A), acetyl-CoA (B), and aspartate (C) on the activity of purified PCx^wt and the variants PCx^T132A, PCx^T343A, and PCx^I1012S. Activities were measured in the standard assay mixture supplemented with the indicated concentration of ADP, aspartate, and acetyl-CoA. The activities were plotted as percentage of PCx activity measured in the absence of these metabolites, which was set as 100%. Mean values of at least two independent enzyme preparations of two biological replicates with standard deviations are shown for the mutated PCx variants. For wild-type PCx mean values of at least three independent enzyme preparations with standard deviations are shown.

In the case of aspartate, PCx^{I1012S} showed a similar response as PCx^{wt}, however, PCx^{T132A} and PCx^{T343A} displayed a different pattern, as already described in chapter 3.3. These variants were less sensitive to aspartate at low concentrations ($\leq$ 5 mM) and their activity was not inhibited at all up to 7.5 mM aspartate (Figure 8C). The apparent K_i values for aspartate were 13.2 mM for PCx^{T132A} and 10.8 mM for PCx^{T343A} and thus higher compared to the K_i value of PCx^{wt} (9.3 mM). The weakened feedback inhibition by aspartate could be a possible explanation for increased L-lysine production in strains expressing *pyc*^{T343A} and *pyc*^{T132A}.

6.4 Expression of heterologous *pyc* variants in *Corynebacterium glutamicum*

In order to test whether the function of native PCx in *C. glutamicum* (PCx^{Cg}) can be replaced by heterologous enzymes and whether these might have a positive effect on L-lysine production, *pyc* genes of three different bacteria were selected for overexpression in *C. glutamicum*. PCx from *Staphylococcus aureus* (*pyc*^{Sa}) was chosen since it is well characterized and its crystal structure is known (Xiang and Tong, 2008). Due to its close phylogenetic relationship to *C. glutamicum*, PCx of *Mycobacterium smegmatis* (*pyc*^{Ms}) was picked as the second enzyme to be evaluated. Both, PCx^{Sa} and PCx^{Ms}, consist of four identical subunits and therefore belong structurally to the α_4-type PCx proteins, like PCx^{Cg}. In order to additionally examine a PCx with an $\alpha_4\beta_4$ structure, PCx of *Pseudomonas aeruginosa* was also selected for expression in *C. glutamicum.* In PCx of the $\alpha_4\beta_4$ type, the enzyme is composed of two polypeptide chains, which in the case of *P. aeruginosa* are encoded by the genes *pycA* and *pycB* (Lai et al., 2006). Sequence alignment of all enzymes revealed a 66% identity between PCx^{Cg} and PCx^{Ms}, whereas PCx^{Sa} and PCx^{Pa} show 46% and 37% sequence identity to the enzyme of *C. glutamicum*, respectively (an alignment is shown in chapter 3.2.1). For overexpression, the heterologous genes were amplified from genomic DNA of the strains mentioned in the legend of Figure 9 and cloned into the vector pAN6. Subsequently, the deletion mutant *C. glutamicum* DM1868Δ*pyc* harboring the lysine sensor plasmid pSenLys-Spec (Schendzielorz et al., 2014) was transformed with the generated plasmids or pAN6-*pyc*^{Cg} (construction described in chapter 3.2). Additionally, strain DM1868Δ*pyc*/pSenLys-Spec/pAN6 devoid of any *pyc* gene was created as negative control. First, complementation experiments of all strains were performed in CGXII minimal medium (Keilhauer et al., 1993) with either 4% (wt/vol) glucose or 2% (wt/vol) Na-D,L-lactate as sole carbon source. For this purpose, all strains were cultivated in a Bio-lector® system (m2p-labs, Baesweiler, Germany) using 48-well microtiter plates (Flowerplates, m2p-labs, Baesweiler, Germany) at 30 °C for 24 h, with 0 or 1 mM IPTG added to the medium. After 24 h, cells were harvested by centrifugation and the L-lysine concentration was determined in the culture supernatants via HPLC.
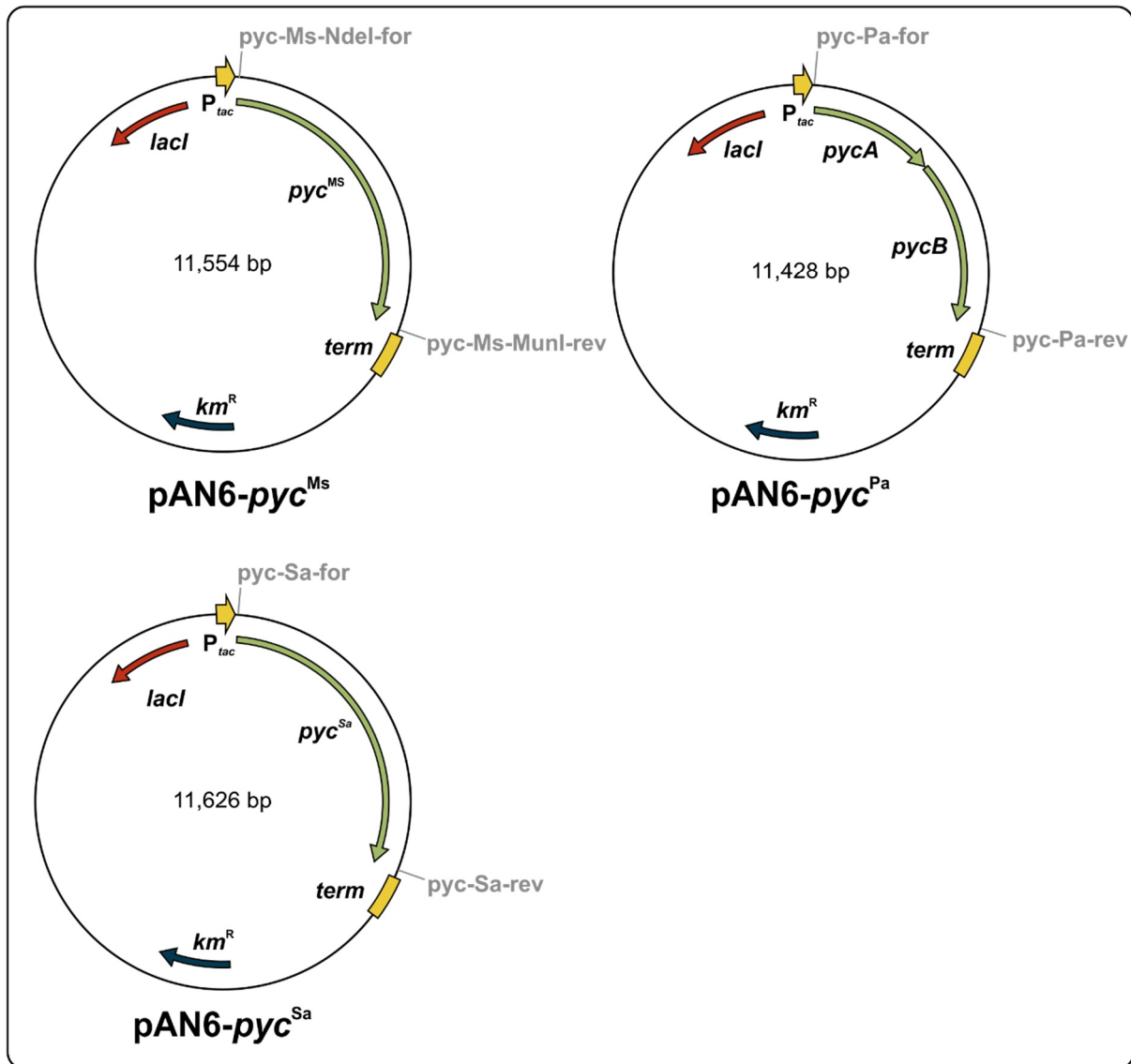
Figure 9 Plasmid maps of pAN6-*pyc*Ms, pAN6-*pyc*Pa and pAN6-*pyc*Sa. The *pyc*Ms gene was amplified from *M. smegmatis* NCTC8159 (ERS451418_02426) with primers pyc-MS-for (CAGAAGGAGA-TATACAATGATCTCCAAGGTGCTCGTCGC) and pyc-MS-rev (GGTGGGACCAGCTAGTGACCACCACCAG-CAGATCG) resulting in a PCR product of 3410 bp. The *pyc*Sa gene was amplified from *S. aureus* NCTC 8325 (SAOUHSC_01064) with primers pyc-SA-for (CAGAAGGAGATATACAATGAAACAAATAAAAAAGTTAC) and pyc-SA-rev (GGTGGGACCAGCTAGAGTCAGTTGCTTTTTCAAT) resulting in a 3451 bp PCR-fragment. The *pycA* (PA5436) and *pycB* (PA5436) genes were amplified as one PCR product of 3284 bp from genome of *P. aeruginosa* PA01 with primers pyc-PA-for (CAGAAGGAGATATACAATGATCAAGAAGATCCTGATCG) and pyc-PA-rev (GTGGGACCAGCTAGAGCCCGCAATCTCGATCAGG). All PCR products were cloned into an empty pAN6 vector, which was cut with NdeI and EcoRI, by self-prepared Gibson assembly master mix (Gibson, 2011).

When cultured on glucose in the absence of IPTG, all strains had about the same growth rate of μ = 0.29 h^{-1} (Figure 10A). The lysine production of strains with heterologous PCx was slightly increased by 3-9% compared to the negative control without *pyc*, whereas the strain with homologous *pyc*Cg showed an increase of about 20% (Table 2). This observation can be explained by the basal expression of the respective *pyc* gene in the absence of the inducer IPTG. The considerably higher lysine production with homologous PCx can be due to a more efficient gene expression of the *pyc* gene or due to a higher activity of PCx^{Cg} in *C. glutamicum*.
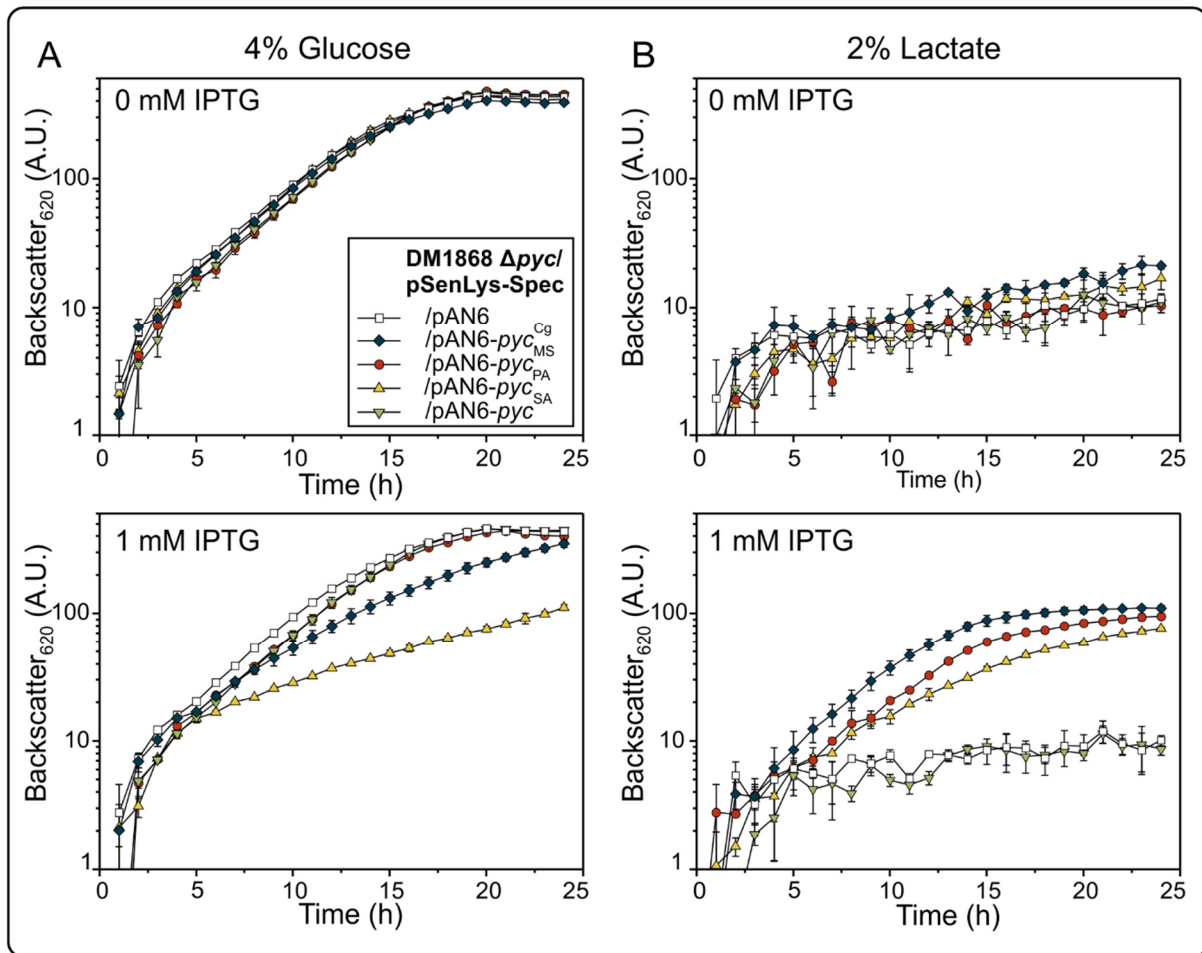
Figure 10 Growth analysis of strains DM1868Δ*pyc*/pSenLys-Spec harboring either pAN6, pAN6-*pyc*^{Cg}, pAN6-*pyc*^{Ms}, pAN6-*pyc*^{Pa} or pAN6-*pyc*^{Sa}. For cultivation, first a preculture in 5 ml BHI was cultivated for 8 h at 30 °C, which was subsequently used to inoculate a second preculture in CGXII minimal medium supplemented with 4% (wt/vol) glucose, which was incubated overnight at 30 °C. The main cultures were finally inoculated to an OD_{600} of 1 in 800 µl CGXII minimal medium containing 4% (wt/vol) glucose (**A**) or 2% (wt/vol) Na-D,L-lactate (**B**) as sole carbon source and cultivated for 24 h at 30 °C in a Biolector® system (m2p-labs, Baesweiler, Germany). Additionally, 0 or 1 mM IPTG were added at the beginning of the cultivation. All media mentioned above were supplemented with required antibiotics (25 mg l^{-1} kanamycin and 250 mg l^{-1} spectinomycin). Mean values of three biological replicates with corresponding standard deviations are shown.

When cultured on glucose with 1 mM IPTG, a growth defect was observed for strain DM1868Δ*pyc*/pSenLys-Spec/pAN6-*pyc*^{Pa} (µ = 0.11 ± 0.00 h^{-1}) (Figure 10A). The L-lysine titer of this strain was decreased by about 28% compared to the culture without IPTG (Table 2). These effects suggest that strong expression of *pycA* and *pycB* stress the cells. Induction of overexpression of *pyc*^{Sa} with 1 mM IPTG had neither an effect on the growth rate nor on L-lysine production (Figure 10A, Table 2). Consequently, the L-lysine concentration was almost 33% lower compared to the strain encoding PCx^{Cg}. For the strain with PCx^{Ms} the L-lysine concentration increased after induction with IPTG up to 28.5 ± 0.2 mM, while the growth rate remained essentially unchanged (0 mM IPTG: 0.29 ± 0.02 h^{-1}; 1 mM IPTG: 0.28 ± 0.00 h^{-1}).

Table 2 L-Lysine production of *C. glutamicum* DM1868Δ*pyc*/pSenLys-Spec harboring either pAN6, pAN6-*pyc*^Cg, pAN6-*pyc*^Ms, pAN6-*pyc*^Pa or pAN6-*pyc*^Sa. All strains were grown as 800 µl cultures in a Biolector® system (m2p-labs, Baesweiler, Germany) with either 4% (wt/vol) glucose or 2% (wt/vol) Na-D,L-lactate. After 24 h, cells were harvested by centrifugation and the L-lysine concentration in the supernatant was determined via HPLC. Mean values of three biological replicates with corresponding standard deviations are shown.

Strain	4% (wt/vol) glucose			
DM1868Δ*pyc*/ pSenLys-Spec	0 mM IPTG	L-lysine in-/ decrease[1]	1 mM IPTG	L-lysine in-/ decrease[1]
/pAN6	21.0 ± 1.0	-	22.7 ± 0.2	-
/pAN6-*pyc*^Cg	25.2 ± 0.6	20.0%	33.6 ± 5.7	48.0%
/pAN6-*pyc*^Ms	22.5 ± 0.2	7.1%	28.5 ± 0.2	25.6%
/pAN6-*pyc*^Pa	22.9 ± 0.5	9.0%	16.5 ± 1.0	-27.3%
/pAN6-*pyc*^Sa	21.7 ± 1.0	3.3%	22.6 ± 1.8	-0.4%
Strain	**2% (wt/vol) lactate**			
DM1868Δ*pyc*/ pSenLys-Spec	0 mM IPTG	L-lysine in-/ decrease[1]	1 mM IPTG	L-lysine in-/ decrease[1]
/pAN6	1.1 ± 0.1	-	1.1 ± 0.2	-
/pAN6-*pyc*^Cg	2.6 ± 0.1	136.4%	7.1 ± 0.2	545.5%
/pAN6-*pyc*^Ms	1.3 ± 0.1	18.2%	8.2 ± 0.2	645.5%
/pAN6-*pyc*^Pa	2.2 ± 0.1	100.0%	7.3 ± 0.1	563.6%
/pAN6-*pyc*^Sa	0.9 ± 0.1	-18.2%	0.9 ± 0.2	-18.2%

[1] in comparison to the strain DM1868Δ*pyc*/ pSenLys-Spec/ pAN6

Comparing the results of the strain expressing *pyc*^Ms to the strain expressing the native *pyc*^Cg gene, it becomes apparent that the highest L-lysine titer was obtained with PCx^Cg. Here an increase of about 48% after induction with 1 mM IPTG up to 33.6 ± 5.7 mM could be observed, which is about 1.2-fold higher compared to the strain expressing *pyc*^Ms.

Furthermore, it was tested whether heterologous *pyc* genes enable the deletion mutant DM1868Δ*pyc* to grow on lactate as sole carbon source, which requires PCx activity (Peters-Wendisch et al., 1997). As expected, almost no growth could be detected for all strains without the induction of *pyc* expression (Figure 10B, Table 2). Nevertheless, especially in strains with PCx^Cg and PCx^Pa, lysine concentrations were observed to be 2.6 or 2 times higher compared to the negative control with empty plasmid, respectively, due to basal expression. When 1 mM IPTG was added to the media, the strain with PCx^Cg was able to grow (µ ~ 0.19 ± 0.03 h^{-1}) and the L-lysine concentration in the supernatant increased up to 7.1 ± 0.2 mM. The heterologous

enzymes PCx^{Pa} and PCx^{Ms} were able to take over the function of the native PCx at least partially after induction and enabled growth on lactate as the sole carbon source of the deletion mutant DM1868Δ*pyc* (Figure 10B). Strain DM1868Δ*pyc*/pSenLys-Spec/pAN6-*pyc*^{Pa} showed a growth rate of 0.13 ± 0.00 h^{-1}, whereas the strain harboring pAN6-*pyc*^{Ms} had a growth rate of 0.22 ± 0.02 h^{-1}. The fact that these enzymes are functionally expressed in *C. glutamicum* was also shown by the L-lysine titers: the concentration in the supernatant of the strain harboring PCx^{Pa} increased from 2.2 ± 0.1 mM up to 7.3 ± 0.1 mM, which is about the same concentration as detected with PCx^{Cg}. After induction of the strain with PCx^{Ms} with 1 mM IPTG, an even higher L-lysine titer was determined: here the concentration increased about 6-fold from 1.3 ± 0.1 mM to 8.2 ± 0.2 mM. An explanation for this increased titer could be a higher activity of the PCx^{Ms}, since a maximal specific activity of up to 150 µmol min^{-1} (mg protein)$^{-1}$ was reported for this enzyme (Mukhopadhyay and Purwantini, 2000), whereas PCx from *C. glutamicum* showed a maximal specific activity of about 20–25 µmol min^{-1} (mg protein)$^{-1}$ (chapter 3.3). Nevertheless, the conditions used for the determination of the mentioned specific activities were not the same and measurements under identical conditions are required for a reliable comparison. In contrast to expression of *pyc*^{Ms}, no growth of the strain DM1868Δ*pyc*/pSenLys-Spec/pAN6-*pyc*^{Sa} on lactate was observed, even after the addition of IPTG (Figure 10B). Moreover, the lysine concentration in this strain did not increase after induction, as it was already observed for the production on glucose. These results indicate that this enzyme cannot take over the function of the homologous PCx in *C. glutamicum*.

Danksagung

Die vorliegende Arbeit hätte ohne die Unterstützung zahlreicher Personen sicherlich nicht realisiert werden können. An dieser Stelle möchte ich mich daher sehr herzlich bedanken.

Ganz besonders möchte ich mich bei Professor Dr. Michael Bott für die Überlassung des spannenden Themas, für das stetige Interesse am Fortgang meiner Arbeit sowie die immerwährende Unterstützung und die hilfreichen Diskussionen bedanken.

Herr Professor Dr. Karl-Erich Jaeger danke ich für die freundliche Übernahme des Zweitgutachtens meiner Arbeit.

Bei Dr. Meike Baumgart möchte ich mich für die gute Betreuung, auch nach der Zeit im Labor, bedanken. Ich danke Dir für die zahlreichen kritischen Durchsichten meiner Arbeiten und Deine fachliche Unterstützung.

Allen jetzigen und ehemaligen Mitgliedern der AG Bott/Baumgart danke ich für die zahlreichen Tipps im Labor, geborgten Puffer und die schöne Zeit. Besonders möchte ich mich bei meinen Bürokollegen Julia und Andi bedanken, die immer ein offenes Ohr hatten und mich sehr im Fortgang meiner Arbeit unterstützt haben. Auch Tina gilt ein großes Dankeschön für ihre Unterstützung im Labor!

Ein riesiger Dank geht an Kim. Mit Dir zusammen habe ich alle Hochs und Tiefs meiner Promotion überstanden. Ich danke Dir für das gemeinsame Freuen, Ärgern, Motivieren und die zahlreichen Gespräche egal zu welcher Tages- oder Nachtzeit.

Bei allen Mitarbeitern des IBG-1 möchte ich mich für die tolle Arbeitsatmosphäre, die stetige Hilfsbereitschaft, die spannenden Diskussionen und die schöne Zeit (auch nach Feierabend) bedanken. Ganz herzlich bedanke ich mich bei Eugen für seine Unterstützung am FACS und zahlreiche Tipps im Labor und Micha für seine Hilfe bei HPLC-Messungen.

Ein besonderer Dank gilt meiner Familie und meinen Freunden für ihren unendlichen Rückhalt und alle motivierenden Worte. Insbesondere danke ich meinen Eltern, dass sie mich immer meinen Weg haben gehen lassen und mich darin unermüdlich unterstützt haben!

Willi danke ich, dass er im Gegensatz zu mir immer die Nerven behalten hat, mich aufgebaut und in den Arm genommen hat und mir täglich gesagt hat, dass ich doch mal fertig werden soll.

Erklärung

Ich versichere an Eides Statt, dass die vorgelegte Dissertation von mir selbständig und ohne unzulässige fremde Hilfe unter Beachtung der „Grundsätze zur Sicherung guter wissenschaftlicher Praxis an der Heinrich-Heine-Universität Düsseldorf" erstellt worden ist.

Die Dissertation wurde in der vorgelegten oder in ähnlicher Form noch bei keiner anderen Institution eingereicht. Ich habe bisher keine erfolglosen Promotionsversuche unternommen.

_____

Jülich, den 02.06.2020